The Pennsylvania State University

The Graduate School

Intercollege Graduate Program in Physiology

ROLE OF PRAS40 AND DEPTOR – TWO mTOR BINDING PROTEINS IN C2C12 MYOCYTES

A Dissertation in

Physiology

by

Abid A. Kazi

Submitted in Partial Fulfillment
of the Requirements
for the Degree of

Doctor of Philosophy

Aug 2011

The dissertation of Abid Kazi was reviewed and approved* by the following:

Charles H. Lang
Distinguished Professor and Vice Chair of Cellular and Molecular Physiology
Professor of Surgery
Dissertation Advisor
Chair of Committee

Scot R. Kimball
Professor of Cellular and Molecular Physiology

Lisa M. Shantz
Associate Professor of Cellular and Molecular Physiology

Timothy M. Ritty
Assistant Professor of Orthopaedics

Leonard S. Jefferson
Evan Pugh Professor of Cellular and Molecular Physiology
Head of the Department of Cellular and Molecular Physiology

*Signatures are on file in the Graduate School

ABSTRACT

PRAS40 and DEPTOR are mTOR binding proteins that affect cell metabolism. Under catabolic conditions such as sepsis and glucocorticoid excess, there is an increase in total DEPTOR protein and a reduction in phosphorylation of PRAS40, suggesting that these proteins may modulate the mTOR-mediated protein synthetic response under normal and diseased conditions. The hypothesis of the present study was that knock down (KD) of PRAS40 or DEPTOR in C2C12 myocytes will increase protein synthesis via stimulating mTOR-S6K1 signaling. PRAS40 and DEPTOR KD was achieved using lentiviral particles containing shRNA to target the mouse PRAS40 and DEPTOR mRNA sequence, whereas control cells were transfected with a scrambled control shRNA. KD reduced PRAS40 and DEPTOR mRNA and protein content by 90%. PRAS40 KD did not result in increased phosphorylation of mTOR substrates or increased protein synthesis, whereas, DEPTOR KD increased both phosphorylation of mTOR kinase substrates, 4E-BP1 and S6K1, and protein synthesis. The responsiveness of PRAS40 and DEPTOR KD myocytes to anabolic (IGF-I) and catabolic (AICAR) stimuli was unaltered. Both PRAS40 and DEPTOR KD myoblasts were larger in diameter and exhibited an increased mean cell volume compared to scramble control. PRAS40 KD cells had decreased phosphorylation (S807/S811) of pRb protein. In contrast, DEPTOR KD cells had an increased phosphorylation (S807/S811) of pRb protein which is critical for the G_1-S phase transition, coincident with an increased percentage of cells in the S phase. Neither PRAS40 nor DEPTOR KD altered myoblast apoptosis as evidenced by the lack of change for cleaved caspase-3. Although DEPTOR KD myoblasts did not alter

autophagy as determined by a lack of change in the ratio of LC3BII/LC3BI, PRAS40 KD myoblasts had a reduced ratio of LC3BII/LC3BI. While PRAS40 KD delayed myotube formation concurrent with delayed proliferation, DEPTOR KD had the opposite effect on myogenesis and proliferation. Finally, while *in vivo* DEPTOR KD (~50% reduction) by electroporation into the muscle of C57/BL6 mice did not alter weight or protein synthesis in the control muscle, it prevented atrophy produced by 3 days of hindlimb immobilization, at least in part by increasing protein synthesis. Thus, our data support the hypothesis that PRAS40 and DEPTOR are important regulators of protein metabolism in myocytes and demonstrate that, while PRAS40 is required for normal myoblast growth and function, decreasing DEPTOR expression is sufficient to ameliorate the atrophic response produced by immobilization.

TABLE OF CONTENTS

LIST OF FIGURES

Figures for Chapter 1

Figures for Chapter 3

Figures for Chapter 4

Figures for Chapter 5

Figure for Chapter 6

LIST OF TABLES

ACKNOWLEDGEMENTS

I owe my deepest gratitude to my advisor and mentor Dr. Charles H. Lang for giving me the opportunity to be a graduate student in his laboratory. Dr. Lang, I am heartily thankful to you for your encouragement and guidance throughout this endeavor that has enabled me to develop an understanding of the subject. Thank you for providing all the funding support necessary to pursue my interests in this field and care for my family as well. Thank you for sponsoring me at professional meetings, and for allowing me to learn and incorporate new techniques. Thank you for your vision and for being open to new ideas and allowing me to explore new areas of research and for finding new collaborators in the areas I was inexperienced. I am indeed indebted to you for keeping me focused and giving me a second opportunity in life to pursue my research interests. Thanks for all the help with the animal experiments and the numerous critiques and corrections of the manuscripts. Without your support and encouragement I would surely have been lost. It is my pleasure to thank all my committee members Drs. Scot R. Kimball, Lisa M. Shantz, Timothy M. Ritty and late Dr. Thomas Vary, who made all this possible with their support, suggestions, advice and for taking their valuable time to discuss my research progress and their help in trouble shooting and offering their expertise in interpretation of the data which has all greatly helped me in the pursuit of my doctoral degree.

I am indeed indebted to all the members of the Lang Laboratory that I had the privilege of working with – you are more than just work colleagues – you are family! I want to thank Jay Nystrom for teaching me RPA and being a friend. I miss going out for

our “coffee breaks” ever since you moved. Danuta Huber, for all your help with protein assays and radio-active counts but moreso for the “motherly” coercion to get the work done and keep my work area clean. Anne Pruznak, you are the “Westerns queen” thanks for all the blots and thanks for double-checking and verifying the data independently, as it just makes the science so much better. Maithili Navaratnarajah, thank you for all the work with the real-time PCR. I also want to thank Drs. Ly Hong-Brown, Robert Frost and Margaret Shumate for all the encouragement, ideas, help, guidance, and critical readings of the manuscripts. I want to thank all my lab members for your support in the laboratory, as well as for your friendship. Also, I greatly appreciate my senior graduate student Brian’s support and encouragement over the years – I wish we had more overlap! I want to thank my good friend and confidante Alexander Tuckow for sharing his notes in the first year, for our numerous scientific and “I-am tired-of-being-a-graduate-student” discussions and for sharing reagents, and knowing that we could count on each other.

I would be thoughtless if I didn't thank all the faculty and staff I have had the opportunity to work with at the many other laboratories and facilities of the Penn State College of Medicine. My special thanks also to Dr. David Spector for spending over four months teaching me viral purification, and to Dr. Samina Alam for sharing reagents, protocols and your guidance with the PRAS40 paper. Many thanks to our office staff: Lisa, Beth, Shanda, Ciatlin, Michele—you were all awesome to work with and made being a graduate student in the department fun and enjoyable – thank you! I want to thank Sujata, Anne, and Bruce from the core facility for the oligos and iTRAQ, David Stanford from the flow cytometry, Kang Li from Histology, the late Ms. Rhona Elise from the Confocal Core, and Bridgette, our floor housekeeper. I want to thank Ms. Kathy Simon

and Dr. Michael Verderame for all that they do for graduate students in the College of Medicine.

Finally, I am forever grateful for the undying support of all of my family, my parents-in-law who provide the most devoted childcare in the world for my son, and for all the home made food! Also for my friends at the COM, you know who you are, and my pets (Fubu, Phoebe, Whity, Shafty, Goldy, Ruben and Pinchy) who truly made a difference in my life by bringing so much joy! I owe my parents a lifetime of thanks for their motivation and support in all my endeavors. You lived a frugal life and sacrificed beyond words so that I could someday get an excellent education and achieve a better life. I wish you were here. My wife, Sangita, is the most loving and incredible person and friend. Sangita deserves recognition for her support, perseverance and unconditional devotion during the many stressful times, and for the most precious gift of all, our wonderful bundle of joy – Arman! Last, but not least, I want to thank my son Arman, who was born during these years as a graduate student in the sweetest place on earth – Hershey – and who gave more meaning to graduate life.

This work was supported in part by grants from the National Institutes of Health (GM38032 and AA11290) to CH Lang and Pennsylvania Department of Health using Tobacco Settlement Funds (AA Kazi).

Chapter 1

Introduction

While the primary function of muscle is to generate force or movement in response to a physiological stimulus, skeletal muscle also serves as the largest reservoir of protein and amino acids in the body, and as such, it represents a major component of whole body protein synthesis and degradation (1). Skeletal muscle is composed of individual components known as muscle fibers. During development, these fibers are formed from the fusion of myoblasts which are a progenitor cell capable of giving rise to muscle cells. One prominent characteristic of skeletal muscle is its ability to alter size (form) in response to a wide range of external stimuli (2). The inherent ability of skeletal muscle to change size in comparison to other tissue types is substantial. Changes in size, proliferation rate and myogenesis are usually multifactorial and these alterations make muscle a plastic and dynamic tissue. These adaptive alterations and the resulting phenotype are produced by regulating metabolic processes such as protein synthesis and degradation, autophagy and apoptosis in response to various external stimuli, and are dependent on the intrinsic and inherent ability of muscle to respond to the external cues based on current energy status and regenerative ability. While the underlying molecular interactions and causal relationships of these processes in response to a wide array of cues are not completely understood, the emerging consensus in the general area of muscle physiology is that the principal factors in determining a change in adult muscle size are an increase (hypertrophy) or decrease (atrophy) in the cross-sectional area of existing muscle fibers (3-6). This change in cross-sectional area is largely influenced by the balance in protein synthesis and degradation processes (5-8).

Muscle protein reserves in the body can be and are often used as an energy source when the physiological need arises. Protein stores in muscle are maintained by the ingestion of protein/ amino acid - containing meals which stimulate protein synthesis and suppress protein breakdown (2, 8-12). Conversely, during periods of starvation or disuse, muscle protein breakdown (proteolysis) exceeds protein synthesis (13), providing amino acids to support hepatic gluconeogenesis and acute phase protein synthesis (14). Increased proteolysis contributes to muscle atrophy that is manifested in many diseases with different etiologies (sepsis, glucocorticoid excess, cachexia, disuse atrophy and alcohol abuse), but it also occurs during normal physiological conditions such as cell senescence and aging (15-17). While understanding the regulation of muscle mass under normal physiological parameters is undoubtedly important, it is perhaps more important to understand the mechanisms which lead to dysregulation of muscle mass as demonstrated in conditions of catabolic skeletal muscle wasting. In extreme conditions which promote prolonged muscle wasting, atrophy is often associated with a loss of functional capacity of the muscle, along with marked reduction of lean body mass leading to increased morbidity (18). Uncontrolled loss of skeletal muscle is not only debilitating, but it is also a risk factor for death (19). Elucidating the signal transduction pathways responsible for regulating protein synthesis and degradation is, therefore, both important and clinically relevant. Identifying the underlying mechanisms can potentially help investigators devise prophylactic and therapeutic strategies in combating or lessening the adverse long-term consequences of these catabolic insults on myopathy.

Amino acids in general are derived from dietary sources or from cellular recycling following protein degradation. As amino acids and proteins are not generally stored for the life-span of the organism, there is rapid protein turnover resulting in a constant amino acid flux. For normal cellular functioning, it is essential that a balance be maintained between processes producing ATP and those consuming ATP. Protein synthesis is an energy demanding process.

Conversely, when amino acids are used for cellular energy their carbon skeletons are first converted to acetyl CoA, which enters the Krebs cycle for oxidation, resulting in the production of ATP. The final products of protein degradation include carbon dioxide, water, ATP, urea, and ammonia. In health, nitrogen equilibrium is achieved when the dietary intake is balanced by the removal of urea (nitrogen containing waste compound). To restate, protein balance exists, when rates of synthesis and degradation are matched so that there is no net protein gain or loss. A state of protein balance is likely to exist only transiently because of the constant interaction between the cell (organism) and its changing environment. Organismal proteomes have evolved mechanisms to provide a metabolic buffer by regulating these changes to achieve protein (nitrogen) balance. If nitrogen excretion is greater than the nitrogen intake from diet, negative nitrogen balance exists which impairs the ability to repair and recover from catabolic insults (19). Such stressors disturb the homeostatic state and shift the balance in favor of atrophy. Conversely, if nitrogen excretion is less than the dietary intake, a positive nitrogen balance exists in which sufficient proteins are available for repair and recovery. Sustained positive balance leads to accretion of proteins resulting in muscle hypertrophy. As stated above, perturbation in protein balance changes skeletal muscle mass in response to some stress; this change is associated with adaptations of the skeletal muscle by modifying its proteome. Therefore, in summary, alterations in global protein balance affect both form and function of skeletal muscle.

Protein synthesis and the regulatory role of mTOR

Understanding the regulatory control of protein synthesis is an evolving and expanding area. Based on the discovery of new protein members and their role in controlling the various steps of translation initiation, available models of these processes are constantly under revision. As an exhaustive review of all the temporal and spatial events that affect protein synthesis in

general and translation initiation in particular is beyond the scope of this thesis, we will only briefly describe the well established models and touch upon known key regulators of translation to provide the reader with a primer to better understand the research presented herein.

Protein synthesis is a high energy requiring process; by some estimates nearly 50-75% the total energy (ATP/GTP) produced is utilized to support protein synthesis (20). Given its high metabolic cost, protein synthesis is tightly regulated. In general, protein synthesis requires amino acid which are synthesized or absorbed from diet and form the amino acid precursors that are then associated with transfer-RNA (t-RNA) to form "aminoacyl-tRNA" pool which are added to the growing polypeptides. Protein synthesis also requires transcription of nuclear DNA into messenger RNA (mRNA), which is then used as a template for protein synthesis. Translation is a multistep process primarily occurring in the cytoplasm in association with the ribosomes, the cellular machines on which new peptides are synthesized. Each mammalian ribosome is composed of a small (40S) and a large (60S) subunit, and each subunit in-turn is composed of many proteins surrounding the catalytic RNA core which surrounds the mRNA. During translation, individual mRNAs produce specific polypeptides using the mRNA sequence as a template to guide the synthesis of a chain of amino acids that form a protein. Multiple ribosomes can be associated with a single mRNA in a spatial order, thus increasing the production of its protein product.

Translation proceeds in three steps: initiation, elongation, and termination (or release) (14). Most eukaryotic mRNA have a 5'cap which protects the mRNA from enzymatic degradation and also helps in the assembly of the translational machinery. In cap-dependent translation (as described in detail later), initiation involves the small subunit of the ribosome binding to the 5' end of mRNA with the help of initiation factors (IF). Elongation occurs when the next aminoacyl-tRNA ("charged" tRNA) (determined by the tri-nucleotide codon), in line binds to the ribosome along with a GTP molecule and an elongation factor (EF), adding to the

growing chain of the polypeptide. Finally, termination (or release) of the polypeptide occurs when the "A" site of the ribosome faces a stop codon (in eukaryotes encoded as UAA, UAG or UGA) which cannot be recognized by any of the many tRNAs in the eukaryotic cell. When this occurs, releasing factors (RF), which are capable of recognizing nonsense codons mediate the release of the polypeptide chain by hydrolysis. A protein thus synthesized undergoes further modifications which affect its half-life, cellular location and function.

The coordinated steps of protein synthesis involving the assembly of the mRNA - ribosome complex in association with the various protein factors are regulated by mainly by the upstream kinase – mammalian target of rapamycin (mTOR; now also known as mechanistic target of rapamycin in higher eukaryotes). Activation of mTOR not only affects protein translation initiation but its activity also positively regulates ribosome biogenesis (Figure 1-1) (21). mTOR (also known as FRAP; RAFT1) is a large ~300 kDa, multi-domain serine (S)/threonine (T) protein kinase that belongs to the phosphatidylinositol kinase related kinase (PIKK) family (21, 22). TOR is a highly conserved protein found in all eukaryotes including plants, worms, flies and mammals, and has been described as a target protein of Rapamycin (22-24). Rapamycin is an anti-fungal, lipophilic, immunosuppressant macrolide agent, originally isolated from the soil bacterium *Streptomyces hygroscopicus* (25, 26). This drug is a potent mTOR inhibitor and is approved by the FDA as an immunosuppressant for organ transplant patients (26, 27). The mechanism of mTOR inhibition involves the association of rapamycin with its ligand – intracellular receptor FK506-binding protein of 12 kDa (FKBP12) (28, 29). The FKBP12 receptor -rapamycin complex can directly bind to the FKBP12-rapamycin binding (FRB) domain of mTOR and inhibit its kinase activity (Figure 1-2).

Numerous studies have revealed the many important functions of TOR in yeast and higher eukaryotes, thus increasing our understanding and appreciation of this kinase in regulating cell growth (30). As a central controller of cell growth, mTOR plays a key role in development

(global $mTOR^{-/-}$ knockout is developmentally lethal in mice) and aging (the mTOR inhibitor rapamycin slows the aging process and increases life span). Furthermore, mTOR is dysregulated in many human diseases such as cancer, cardiovascular disease, obesity, sepsis, disuse atrophy, and diabetes (14, 21, 31-35). The increased interest in mTOR and its role in regulating cancer, longevity, neurodegenerative disease, and metabolism have been a subject of many recent studies. However, it is a well established that mTOR does not function in isolation, and its activity and function is in part regulated by the binding of other proteins. Based on proteins associated with mTOR at any given instant, mTOR is contained within two well recognized multimeric protein complexes in the cells: mTOR Complex 1 (mTORC1) and mTOR Complex 2 (mTORC2) (Figure 1-2) (33). As the predominance of the literature supports the role of mTORC1 in regulating protein synthesis and muscle protein balance, the primary thrust of the thesis and the remainder of the introduction will focus on mTORC1.

mTORC1

mTORC1 is composed of mTOR, regulatory associated protein of mTOR (Raptor), mammalian Lethal with SEC13 protein 8 /G-protein β-subunit like protein (mLST8/GβL) and the recently identified partners proline-rich Akt substrate-40 (PRAS40) and DEPTOR (DEP-domain containing partner of mTOR) (21, 36-38). mTORC1 activity is regulated in a rapamycin-sensitive manner (21). It is well established that mTORC1 regulates protein translation, metabolism, and transcription in response to nutrients (particularly the branch chain amino acid leucine), energy (e.g., ATP/AMP ratio), growth factors (e.g., insulin-like growth factor (IGF)-I), and environmental stresses (e.g., redox status) (39-43). The activity of this complex is stimulated by the addition of insulin, growth factors, serum, phosphatidic acid, and amino acids (44-46). Conversely, mTORC1 is inhibited by low nutrient levels, growth factor deprivation, oxidative

stress, and mTOR inhibitors (e.g. rapamycin, torin, etc.) (44, 47-49). It is also inhibited by inflammatory cytokines, glucocorticoids and sepsis (50-52). mTOR-heterozygous mice have decreased lean body mass and a lower rate of basal muscle protein synthesis (53).

Raptor, a second key component of the mTORC1, is a scaffolding protein that recruits mTOR substrates and regulates mTOR activity through a dynamic interaction between mTOR and its substrates (54-56). The ability of raptor to interact and recruit mTOR substrates involves the presence of a "TOS" motif found in p70-S6 Kinase 1 (S6K1), eukaryotic initiation factor 4E (eIF4E) binding protein 1 (4E-BP1) and PRAS40 (57). Raptor and mTOR share a strong N-terminal interaction and a weaker C-terminal interaction near the kinase domain of mTOR. When stimulatory signals are sensed, such as high nutrient/energy levels, the mTOR-raptor C-terminal interaction is weakened and possibly completely lost (depending on the detergent and the ionic strength of the lysis buffer), allowing mTOR kinase to be activated (54). Conversely, when stimulatory signals are withdrawn, such as low nutrient levels, the mTOR-raptor C-terminal interaction is strengthened and this favors raptor-mediated inhibition of mTOR, effectively inhibiting the kinase function of mTOR (Figure 1-4) (54). The two best characterized targets of mTORC1 are S6K1 and 4E-BP1 (Figure 1-3) (58, 59). Subsequently, the mechanism by which mTOR regulates the activity of these two substrates and thereby regulates protein synthesis/translation initiation will be described.

S6 kinase belongs to the family of AGC kinases (30, 60). S6K1 knockdown mice have a small phenotype compared to wild type (WT) mice, and such a phenotype has also been reported in other evolutionarily diverse organisms such as *Drosophila* (34, 61-63). A decrease in protein synthesis has also been attributed to decreased phosphorylation of S6K1 by mTOR, when mTOR kinase is inhibited (64-66). In mammals, there are two similar S6 kinases which are encoded by different genes. Although, S6K1 and S6K2 differ in length and the number of amino acids, all the phosphorylation sites common to these two isoforms are conserved (30, 60). S6K1 is a 70

kDa protein which is phosphorylated by mTORC1 on amino acid residue T389 present in the hydrophobic motif of the C-terminal regulatory domain of the kinase (21, 67-69). This post-translational modification is considered by some as the rate-limiting step in the activation of S6 kinase (70). The T389 phosphorylation event is followed by the phosphorylation of S6K1 by phosphoinositide-dependent kinase-1 (PDK1) at T229 present in the activation loop of the catalytic domain, resulting in the complete activation of S6K1 (71). Fully activated S6K1, in turn, stimulates the initiation of protein synthesis and proliferation through phosphorylation of multiple substrates, including ribosomal subunit protein S6, eIF4B, and other components of the translational machinery. S6K1 can also positively regulate mTORC1 by phosphorylating mTOR (on T2446 and S2448), thereby further stimulating the mTOR kinase activity (72). Since S6K2 was discovered later, most of the studies utilize S6K1 as a surrogate marker and substrate of mTOR kinase activity (73, 74). However, recent studies show that S6K2 may be a more active kinase in some cancer cells or tumor tissues as compared to S6K1 (67-69). Although it is named as the kinase that phosphorylates the substrate S6 (a component of the ribosomal protein), recent reports emphasize that S6 is perhaps not the only physiologically relevant substrate. As an alternative to S6, eIF4B is also considered to be a physiologically relevant target of S6K1 and this could explain the effect of S6K1 activation on translation and cell growth (75). eIF4B assists in efficient recruitment and binding of ribosomes to mRNA, as evidenced by the presence of a RNA binding domain. It enhances the ATPase and RNA helicase activity of eIF4A when phosphorylated at S422 by S6 kinase (21). Ribosome footprinting demonstrates that eIF4B is required for ribosome binding on mRNAs containing secondary structure, suggesting this initiation factor might also have an important role in cap-independent translation initiation (76, 77) .

The mTORC1 also activates 4E-BP1, a comparatively small phosphoprotein with at least seven known phosphorylation sites (T37, T46, S65, T70, S83, S101, S112) (78). A two-step

regulatory mechanism of 4E-BP1 phosphorylation has been proposed, wherein T37 and T46 are first phosphorylated which then facilitates the phosphorylation on S65 and T70 (79). Of these, the first five phosphorylation sites are conserved in all three 4E-BP1 isoforms (4EBP1, BP2 and BP3) (80). These isoforms are differently expressed in different tissues. For example, 4E-BP1 is abundant in muscle, whereas 4E-BP2 is highly enriched in brain (81). Phosphorylation of the first 4 residues by mTOR in a hierarchical manner is believed to be necessary for the complete activation and release of 4E-BP1 from the cap binding protein eIF4E (82, 83). These four residues (modulated via phosphorylation) are in close proximity to some of the acidic amino acids in eIF4E. Thus, one can conceptualize that adding a negatively charged phosphate group causes an electrostatic repulsion towards the acidic amino acids of eIF4E, thereby promoting the dissociation of 4E-BP1 from eIF4E. It has been demonstrated that hypo-phosphorylated 4E-BP1 binds tightly to the translation initiation factor eIF4E, preventing the binding of translational machinery to the 5'-capped mRNAs and recruiting them to the ribosome (83). Increased (overexpressed) 4E-BP1 binds to eIF4E and inhibits translation initiation (84, 85). Upon phosphorylation by mTORC1, 4E-BP1 releases eIF4E, thus allowing the scaffolding protein eIF4G to bind to eIF4E and along with eIF4A forms the active eIF4F complex (Figure 1-3).

The multimeric eIF4F complex is composed of several proteins including: eIF4E, which directly binds the m^7GTP-cap structure; eIF4A, which together with eIF4B unwinds secondary structure via its ATP-dependent RNA helicase activity; and eIF4G, which serves as the large scaffolding-adaptor protein. eIF4G serves as the nucleus for the formation of the initiation complex, as evidenced by its binding sites not only for eIF4E, but also for eIF4A and eIF3 (4). As a result, eIF4G recruits the 40S subunit to the 5' end of mRNA and coordinates the circularization of mRNA via its interactions with eIF4E, poly (A)-binding protein (PABP), and eukaryotic initiation factor 3 (eIF3) (25, 85, 86).

The eIF3 is a large and complex scaffolding protein composed of at least 13 different protein subunits. eIF3 associates with the small 40S ribosomal subunit and plays a role in restraining the large ribosomal subunit from prematurely binding the small subunit. eIF3 also interacts with the eIF4B and eIF4F complex (87). Through a series of elegant experiments, Holz *et al* showed a synchronized-coordinated protein-protein interaction between S6K1-eIF3-mTOR. According to the authors, the binding of S6K1- eIF3 and eIF3 - mTOR are mutually exclusive. Under basal or unstimulated conditions, inactive S6K1 interacts with the non-polysome-associated eIF3 complex, and under such conditions the mTOR-raptor complex does not interact with eIF3 (72). Stimulation of the PI3K-mTOR pathway promotes the recruitment and binding of the mTOR-raptor complex to the eIF3 complex. Raptor recruits mTOR to S6K1 via its interaction with the TOS motif on S6K1, thereby bringing the two proteins into close proximity and permitting activated mTOR to phosphorylate S6K1 on T389. This phosphorylation event causes a conformational change and dissociation of S6K1 from the eIF3-mTOR complex (Figure 1-3) (88). Extending this model further, one can assume in the inactive eIF3-bound state that S6K1 is not accessible to PDK1 which is required to fully activate the S6 kinase. As a result, only after mTOR activates S6K1 does it "become available" to PDK1. The activation of S6K1 and subsequent phosphorylation of the S6K1 substrate eIF4B ensures the unwinding of secondary structure on the mRNA and promotes the RNA helicase activity of eIF4A. These subtle yet important "on-off" dynamic interactions involving eIF3 are critical to the process of translation initiation and efficient protein synthesis (Figure 1-3) (72).

Another component present in the eIF4F complex is eIF4A. This initiation factor is an ATP-dependent RNA helicase, which aids the ribosome in resolving certain secondary structures formed by the mRNA transcript in collaboration with phosphorylated eIF4B. As described above, eIF4B is phosphorylated by S6K1 at S422, thereby initiating its recruitment to the eIF4A-eIF4F complex (89). eIF4A also binds to the tumor suppressor protein Programmed Cell Death 4

(PDCD4) which inhibits protein translation initiation and requires phosphorylation by S6K1 before it can be ubiquitinated and degraded by the ubiquitin proteasome system (90-93).

Approximately half of the naturally occurring mRNAs have some type of secondary structure in the form of loops and hairpins (94-96). While some of these hairpins are transient structures that do not affect the kinetics of translation initiation, other hairpins often found in the 5' UTR regions of mRNA are unusually long and have been shown to slow translation efficiency. Recruitment of the preinitiation complex at the 5' capped end requires this stretch of RNA to be somewhat open or "linear" so that it is accessible to the 40S ribosome and other translational cofactors. The unwinding of these long hairpins is accomplished by eIF4A, which has some intrinsic basal RNA helicase activity. However, as mentioned earlier, the helicase activity of eIF4A is stimulated many-fold by the presence of eIF4B (77, 89, 97).

eIF4E is the m^7GTP (methylated guanosine) cap-binding protein (reviewed in (98)). Based on its protein content, eIF4E is likely to be the least abundant of all initiation factors and functions as the rate-limiting step of cap-dependent initiation. eIF4E is often cleaved from the mRNA complex by specific viral proteases to limit the cell's ability to translate its own transcripts. This hijacking of the host machinery favors translation of viral (cap-independent) messages. eIF4E over-expression increases cell growth and transforms cells (99), and it is over-expressed in many cancers (100-102).

The eukaryotic initiation factor 4G (eIF4G) is a large (~220 kDa) modular scaffolding protein that plays a key role in assembly of the ribosome initiation complex (103-106). eIF4G directly binds with eIF3, eIF4E and eIF4A. eIF4G consist of 3 functional and structural domains connected by hinge regions and these 3 domains interact with different initiation factors (92). eIF4G is a phosphoprotein and mTOR-dependent (sensitive) phosphorylation of eIF4G on S1108 increases in response to serum, insulin and growth factors (25, 107-109). eIF4G also interacts with eIF4B and the PABP (104). PDCD4 is a tumor suppressor protein that inhibits translation

initiation by competing with eIF4G to bind with eIF4A (93, 110). In an unstimulated or basal state, PDCD4 is bound to eIF4A and inhibits the binding of eIF4G and the mRNA from binding to eIF4A (91, 92, 110).

As previously mentioned, PABP is another protein associated with the eIF4F complex. The PABP directly interacts with eIF4G of the eIF4F complex (104). As its name suggests, the protein binds the long poly (A) tail at the 3' end of the mRNA. This protein has been implicated in playing a role in circularization of the mRNA during translation. The circularization of mRNA brings the ribosome physically close to the 5' cap, thereby increasing the chance of the same protein being synthesized again via recycling (111). Recent research has revealed that the main components of the translation machinery dissociate after each round of protein biosynthesis, but there is no dissociation of the ribosome into its individual subunits. This type of mechanism favors recycling, not reinitiation, since the components are pre-assembled and ready for another round of protein biosynthesis (111, 112).

For the most part, these protein-protein interactions have been investigated *in vitro* where the stoichiometry of the various proteins has been disrupted by knockdown (KD) or over-expression. In contrast, there is limited information pertaining to these mTOR protein-protein interactions *in vivo*, in general, and in skeletal muscle, in particular. Our studies in Chapter 3 address this gap in knowledge by examining skeletal muscle under control conditions and in response to a catabolic state produced by bacterial infection.

mTOR: new partners

PRAS40 is an Akt substrate that forms part of the mTOR complex 1 (37, 113, 114). While it was originally characterized in 3T3L1, H4IIE and HeLa cells, it is now accepted that PRAS40 is present in all tissues (21). Vander Haar *et al* showed that the interaction of PRAS40

with mTOR was induced by conditions that inhibit mTOR signaling (Figure 1-4) (114). This study also established that PRAS40 regulated mTOR in cells in a tuberous sclerosis complex (TSC) independent manner and that knockdown of PRAS40 inactivates insulin-receptor substrate (IRS) and Akt, thus uncoupling the response of mTOR to Akt (114). PRAS40 is considered a putative negative regulator of mTOR via substrate inhibition, implying that when PRAS40 is bound to mTOR it obstructs the binding of other mTOR substrates, namely S6K1 and 4E-BP1 (115). Such a phenomenon of competitive substrate inhibition has been previously reported for other mTOR substrates (116, 117).

PRAS40 is phosphorylated by Akt on T246. This was the first phosphorylation site identified and since then other phosphorylation sites, (i.e., S183, S212 and S221) have been identified. Of the aforementioned sites, phosphorylation of S221 was shown to be as important as the phosphorylation of T246 for regulating PRAS40 (118). Phosphorylation is believed to play a critical role in the regulation of PRAS40-mTOR binding and the subsequent regulation of mTOR kinase activity. It is largely established that activation of the PI3K-Akt pathway, upon stimulation by insulin, results in PRAS40 being phosphorylated by Akt on T246 and by mTOR on S183. This multi-site phosphorylation of PRAS40 leads to its dissociation from the mTORC1 and enhances the subsequent binding of PRAS40 to the cytosolic anchor protein 14-3-3. Binding of PRAS40 to 14-3-3 prevents mTORC1-PRAS40 interaction and facilitates the binding of mTOR to its other known substrates. The removal of the inhibitory PRAS40 from mTORC1 activates the mTOR kinase. The binding of PRAS40 to raptor appears to be mediated by an altered TOS motif (Figure 1-4) (115).

PRAS40 binds to the 14-3-3 proteins and this requires both amino acids and insulin. Binding of PRAS40 to 14-3-3 proteins is inhibited by TSC1/2 (negative regulators of mTORC1) and stimulated by Rheb in a rapamycin-sensitive manner (48, 119). Small interfering (si)RNA-mediated knockdown of PRAS40 impairs both the amino acid and insulin-stimulated

phosphorylation of 4E-BP1 and S6K1 (119). However, this has no effect on the phosphorylation of Akt or TSC2 (an Akt substrate). Collectively, these data place PRAS40 downstream of mTORC1 but upstream of its effectors, such as S6K1 and 4E-BP1 (119). While Sancak *et al* showed that PRAS40 functions as a negative regulator of mTOR, Fonseca *et al* showed that PRAS40 is required for mTOR signaling (37, 119). These opposing data have given rise to the controversy regarding the role of PRAS40 in regulating mTOR-mediated protein translation initiation. Of particular note is the finding in *Drosophila* demonstrating that Lobe (a PRAS40 ortholog) is necessary for activation of mTOR kinase. Reduction of Lobe using siRNA decreased mTOR signaling (120). It has also been reported that nutrient starvation has a dominant effect on mTOR-PRAS40 interaction over growth factor stimulation since PRAS40 was only modestly released from mTOR under leucine-deprived conditions, compared to leucine supplemented conditions (121, 122). Despite the numerous reports implicating PRAS40 as a regulator of protein translation in`itiation in a variety of cells, a complete understanding of its role in skeletal muscle physiology is lacking. Given the pivotal role mTOR plays in response to environmental cues in regulating protein translation initiation, cell cycle and proliferation, it is reasonable to suspect that these mTOR functions would be affected by altering PRAS40 expression in myocytes. Therefore, the purpose of the studies addressed in Chapter 4 was to examine changes in C2C12 myocyte protein synthesis, cell proliferation and cell cycle in response to PRAS40 knockdown (KD) using shRNA-based *in vitro* experimental approaches.

DEPTOR is an mTOR substrate that is part of both mTORC1 and mTORC2, and it interacts with mTOR directly via its PDZ domain. Current literature, although sparse, places DEPTOR immediately downstream of mTOR (47, 123). While the DEPTOR protein negatively regulates mTOR kinase activity, the exact inhibitory mechanism is not clear. Although mTOR phosphorylates DEPTOR at multiple sites *in vitro*, the significance of these sites in regulating DEPTOR half-life or various mTOR functions is also not known (21, 47). As DEPTOR is part of

both the mTOR-containing complexes, it is possible that the differential regulation of the two mTOR complexes is one important role of DEPTOR. Whereas DEPTOR may occupy a central position in cell survival in certain types of cancers such as melanoma, its role in regulating cell survival in non-malignant tissue types is not known (47). Expression of DEPTOR in these cancers is strongly correlated in predicting the outcome of therapy by modulating mTOR mediated events (124, 125). Therefore, in Chapter 5 we performed experiments to determine whether DEPTOR KD would affect changes in myocytes. Finally, in addition to mTORC1-mediated regulation of mRNA translation and protein synthesis, mTOR is also recognized to control cell growth, cell cycle and autophagy; each of these processes will be briefly discussed in subsequent sections.

Cell growth and proliferation

Most mammalian cells have a genetically predetermined cell size. An increase in cell size over what is the "physiologically normal" is referred to as hypertrophy. Conversely, a decrease in cell size is termed atrophy. Hypertrophy in myocytes occurs in response to various physiological and pathological stimuli and results from accretion of protein following either increased protein synthesis and/or reduced protein degradation. In contrast, muscle atrophy can result from either decreased protein synthesis or increased degradation which results in tipping the homeostatic balance. IGF – I is a well-established, potent mitogenic and myogenic agent [see (126) for review]. Over expression of the IGF – I receptor results in muscle hypertrophy (127, 128) and rescues muscle loss in older animals (129-131). The ability of IGF – I to induce hypertrophy in muscle is largely attributed to its anabolic effects on protein synthesis mediated by mTORC1 (4, 7, 131, 132). Binding of IGF—I to its tyrosine kinase receptor leads to the

activation of the PI3K pathway. The PI3K signaling pathway stimulates mitogenesis and inhibition of the PI3K pathway via its regulation of mTORC1 results in G1 cell cycle arrest.

For sustained cellular proliferation to occur, coordination between cell cycle progression and cell growth (defined as an increase in cell size and cell mass) is critically important. However, the molecular signals controlling cell growth remain poorly defined. Cell growth and cell cycle almost always occur simultaneously in mammalian cells and require mTOR- and PI3K-dependent signals. Fingar *et al* showed that S6K1 and 4E-BP1 function in the translational control to regulate mammalian cell size (59, 133). The role of S6K1 in regulating cell growth and proliferation is well establish (65). Other studies in vascular smooth muscle cells and cardiomyocytes suggest the induction of hypertrophy activates signaling pathways that are also associated with cell cycle and proliferation (134). In lower eukaryotes, regulation of cyclin-dependent kinase (Cdk)-cyclin activities play an important role in controlling cell size, yet the role of these cell cycle modulators in regulation of muscle cell size is not clearly understood. Hlaing *et al*, using C2C12 skeletal myoblasts, showed that induction of hypertrophy involves transient activation of Cdk4 and increased phosphorylation of Retinoblatoma protein (pRb), resulting in the release of histone deacetylase (HDAC1) from the pRb inhibitory complex (135). In this cell type, E2F-1 becomes transcriptionally active, even when it remains associated with pRb. Furthermore, it has been suggested that even partial or perhaps selective inactivation of the pRb complex leads to activation of a subset of E2F-1 targets that are necessary for cell growth during hypertrophy (135). In addition, IGF – I induces cyclin D1 and cdk4 gene expression, enhancing the hyper-phosphorylation of pRb which encourages cellular proliferation in muscle cells (130, 136, 137). Finally, inhibition of mTORC1 is associated with hypo-phosphorylation of pRb in muscle cells isolated from transgenic mice with a muscle-specific overexpression of IGF – I, thus suggesting a role of pRb in myocytes cell cycle (128).

Cell cycle and the role of pRb

Retinoblastoma tumor suppressor protein is ubiquitously expressed and functions as a negative regulator of cell cycle progression in many eukaryotic cells where it functions as the checkpoint for regulating proliferation (Figure 1-5) (138, 139). One of the hallmarks of a low proliferating cell is the presence of the active, sub-nuclear, hypo-phosphorylated form of pRb during the G0 and G1 phases (138). pRb exerts its inhibitory influence through complex protein-protein interactions involving its pocket domain (139). In its active form, pRb functions as a transcriptional repressor by sequestering specific factors required for transcription of genes necessary for DNA synthesis (140). For cell cycle to progress, pRb must be inactivated and this is accomplished primarily by its post-translational modification, i.e., phosphorylation (141, 142).

Phosphorylation of pRb causes a steric change in its physical structure, resulting in the release of at least some E2F transcription factors (139, 143). In various cell types and under different physiological states, this hierarchical series of phosphorylation events are mediated by a family of molecules referred to as "cyclins" and cdks which coalesce to form a complete and functional holoenzyme during specific stages of the cell cycle. Mitogens such as IGF-I stimulate the activity of these cyclin-cdk proteins, thus enhancing cell cycle progression (137, 144-146). Insulin can stimulate hyper-phosphorylation of pRb and adipocyte proliferation in 3T3-L1 cells in a PI3K - and mTOR-dependent manner, connecting mitogen – mediated activation via PI3K-mTOR signaling to its effector-pRb (147). Conversely, mTOR inhibition results in the upregulation of the cdk inhibitor p27 (mRNA and protein levels). Increased concentration of p27 facilitates the interaction of p27 and cdk/cyclins which in turn affects pRb phosphorylation and cell cycle progression (Figure 1-5) (148, 149). Recently, the direct binding of some specific cyclins (145) and stimulation of other regulatory pathways independent of cell cycle protein are shown to alter pRb phosphorylation (150, 151). The phosphorylation state of pRb in proliferating

versus arrested and differentiated myotubes is consistent with the above mentioned modulations, with actively replicating cells expressing both hypo- and hyper-phosphorylated pRb (138, 150, 152, 153), while arrested (128, 154-157) and differentiated (150, 152) cells predominantly show hypo-phosphorylated pRb. If pRb is sufficiently phosphorylated, cells progress to the S phase of the cell cycle, thus implying the need for some threshold level of pRb phosphorylation.

Autophagy

Autophagy or "self-eating" is a ubiquitous catabolic process involving cellular degradation via the lysosomal machinery. It is induced under cellular stress conditions such as amino acid and growth factor depletion, leading to formation of double membrane autophagic vacuoles or autophagosomes that deliver cytoplasmic components to lysosomes (158, 159). Autophagy has been reported to play an important role in regulating muscle cell growth and myogenesis and developmental remodeling (2, 160-163). Evolutionarily, this cellular process serves to conserve vital metabolic functions in the face of adverse conditions by making available amino acids and lipids via the process of cellular recycling. Thus, autophagy mobilizes intracellular nutrient resources and contributes to cell survival during unfavorable growth conditions, thereby representing a natural process that shows fiscal responsibility by reducing cellular energy deficits. In eukaryotic cells, induction of autophagy is tightly coupled to development and cell growth regulation and helps to maintain a homeostatic balance between the synthesis, degradation, and subsequent recycling of cellular products (164-166).

The most established mechanism of autophagy involves the formation of a double membrane vesicle around the targeted region, separating it from the rest of the cytoplasm. The vesicle then fuses with acidic lysosomes containing proteolytic enzymes, which subsequently degrade the internalized contents. While the role for autophagy in disease is not fully understood,

it is posited that autophagy may be beneficial by preventing or inhibiting the progression of some diseases such as neurodegeneration (removal of aggregates) and cancer (by sensitizing cancer cells to therapy by inducing apoptosis). Autophagy may play a protective role against bacterial infection by intracellular pathogens. Among the numerous components involved in the regulation of autophagy and growth, mTORC1 appears centrally placed to coordinately regulate the balance between growth and autophagy in response to cellular physiological conditions and environmental cues. For example, serum activation of mTORC1 leads to suppression of autophagy initiators (36, 158, 161, 167) and, conversely, mTOR inhibition induces autophagy in eukaryotic cells.

Although mTOR has been recognized as a key regulator of autophagy for more than a decade, the underlying regulatory mechanisms have not been fully elucidated (158, 168). In yeast, the first signaling component downstream of TOR in the autophagy pathway is Atg1. Atg1 plays a key role in the initial stages of autophagy induction and formation of the pre-autophagosome structures (169-171). In support of this, in *Saccharomyces cerevisiae*, Atg1 null or kinase-dead mutant strains cannot initiate autophagy under nutrient starvation or when TOR is inhibited (170, 172). Conversely, starvation or rapamycin treatment activates Atg1 (173). In higher eukaryotes, the counterpart of Atg1 is ULK (Uncoordinated-51-like kinase). ULK1 kinase was identified using siRNA screens to regulate autophagy (174). Over-expressing the kinase-dead mutants of ULK1 led to inhibition of autophagy in the NIH3T3 mouse embryonic fibroblasts (175). Autophagy was also suppressed in HeLa and HEK293 cells upon silencing of ULK1 and in ULK1-null mouse embryonic fibroblasts (176), thus confirming its role in regulating autophagy. It has been reported that mTORC1 phosphorylates ULK1 *in vitro* (176, 177). Inhibition of mTORC1 by rapamycin or serum starvation results in dephosphorylation of ULK1 in mammalian cells (176-178). This suggests that ULK1 functions as a direct effector of mTORC1 to regulate autophagy (Figure 1-6).

The conversion of soluble microtubule-associated protein light chain 3-I (LC3-I) to lipid bound LC3-II is associated with the formation of autophagosomes and presents an important marker of autophagy. Autophagosomes form via the elongation of small membrane structures known as autophagosome precursors. The formation of autophagosomes is initiated by class III phosphoinositide 3-kinase and Atg 6 (also known as Beclin-1) (Figure 1-6). In addition, the ubiquitin-like protein Atg8, the Atg4 protease, and the Atg12-Atg5-Atg16 proteins are involved in the autophagy process. Microtubule-associated proteins 1A/1B light chain 3A is a microtubule-associated protein that in humans is encoded by the MAP1LC3A gene. It mediates the physical interactions between microtubules and components of the cytoskeleton (179). LC3 is the mammalian homologue of yeast Atg8. The outer membrane of the autophagosome fuses with a lysosome to form an autolysosome or autophagolysosome where previously internalized contents are degraded via the acidic lysosome hydrolase enzymes (179, 180).

Both inhibition of mTOR and activation of AMPK can induce autophagy (181). In addition, AMPK can also directly phosphorylate ULK and induce autophagy (182). Glucose starvation reduces the ratio of ATP to AMP in eukaryotic cells. Increased AMP concentrations activate the 5′-AMP-activated protein kinase (AMPK), and this activation is regulated by the upstream Serine/threonine kinase (STK) 11 (also known as LKB1) that phosphorylates AMPKα on T172 (181, 183). Activated AMPK inhibits mTORC1 by phosphorylating and activating TSC2, a negative regulator of mTORC1 (184). It has been recently shown that AMPK can inhibit mTORC1 directly by phosphorylating raptor at S863, thus bypassing the TSC (185).

Apoptosis

Apoptosis and autophagy are closely inter-connected types of programmed cell death. Apoptosis is induced in C2C12 cells upon treatment with tumor necrosis factor (TNF)-α and

cycloheximide or staurosporine (165). Under these treatment conditions, C2C12 cells show features characteristic of apoptosis, including caspase-3 cleavage, chromatin condensation and DNA fragmentation. Caspase-3 cleavage and cleavage of Poly ADP ribonuclease (PARP) are also induced in cells upon long-term (several hours to days) serum depletion, suggesting that serum withdrawal rather than amino acid deprivation triggers apoptosis (24, 158, 179, 186). Starvation up regulates multiple pro-apoptotic proteins and caspase-8. These alterations in pro-apoptotic proteins render starved C2C12 cells more susceptible to TNF-α/cycloheximide-induced apoptosis than occurs in non-starved cells. Therefore, amino acid deprivation of C2C12 cells induces a complex form of cell death with hallmarks of both apoptosis and autophagy (165). Recently, Peterson *et al* showed that knockdown of DEPTOR, an mTOR binding protein, induced apoptosis linking mTOR as a regulator of apoptosis. Through serum deprivation, DEPTOR knockdown also made cells resistant to apoptosis as evidenced by reduced cleavage of caspase-3 and PARP (47). Similarly, PRAS40 regulates apoptosis in malignant melanoma (187). As the role of mTOR in regulating autophagy and apoptosis is being established in various cell types and since both PRAS40 and DEPTOR are considered negative regulators of mTOR, we hypothesized that knockdown of these protein partners of mTOR would affect both these events in the C2C12 myocytes. The roles of PRAS40 and DEPTOR in regulating autophagy and apoptosis events were studied in Chapters 4 and 5 respectively.

Myogenesis

The development of skeletal muscle from the embryonic somite is a regulated multistep process. The pluripotent mesodermal cells, in response to various signals from neighboring tissues, engage themselves to a more committed myogenic lineage fate and initiate expression of genes that eventually transform them into skeletal muscle cells. These paracrine signals initiate

the expression of transcription factors from the MyoD family in mesodermal cells turning them into myoblasts. Later, MyoD induction leads to the withdrawal of myoblasts from the cell cycle and initiates the expression of other transcription factors such as myogenin. Myogenin activates many muscle structural genes during differentiation and the formation of multinucleated myotubes. The journey and development of cells of the myogenic lineage into functional myotubes is termed myogenesis (188). The initial phase of muscle differentiation depends on the activities of the PI3K (189).

Williamson *et al* previously demonstrated that decreased expression of p21 (a member of the Kip/Cip family of negative cell cycle regulators) inhibited myotube formation in C2C12 cells treated with 5-aminoimidazole-4-carboxamide-1-β-D-ribonucleoside (AICAR) (190). The role of p21 in regulating cell cycle in general is summarized in details [see (191)for review] and more defined in myoblasts, with respect to its inhibition of proliferation, stimulation of differentiation, mediated by its interaction with MyoD (discussed below) (192-195). Myoblasts express multiple basic-helix-loop-helix (bHLH) transcription factors [see 62, 63 for review] that cooperate with pRb and pRb-related proteins to inhibit progression through G1 [49]. The myogenic factor MyoD provides an example of bHLH containing transcription factor. MyoD plays an important role in the process of myogenesis and the pro-myogenic properties of MyoD are exerted by its stimulatory effects on gene expression. This transcription factor binds to the promoter region of genes associated with growth arrest, including cyclin D3 (194, 196), p21 (192, 197-199) and pRb, and thereby increases their activity (145, 152, 194). MyoD can also bind directly to cdk4 and disrupt its kinase activity, in turn facilitating the maintenance of hypo-phosphorylated pRb during growth arrest (200). MyoD is expressed in proliferating myoblasts (131, 201, 202) and whole muscle of aged mice (203).

mTOR and catabolic disease

Sepsis

The Society for Critical Care Medicine defines sepsis as "a systemic inflammatory response to infection." Even with the ever growing repertoire of antibiotics, the incidence and mortality from bacterial sepsis is far from being within medically acceptable limits (204). Gram-negative bacteria are the most common cause of sepsis in patients (205, 206). The mortality associated with gram-negative infection is, in part, related to endotoxin – a component of the bacterial cell wall (207). Chemically, the bacterial endotoxin consists of lipids, polysaccharides and trace amounts of amino acids (208). The pathological effect of these gram-negative bacteria is mostly manifested due to the lipopolysaccarides (LPS), which have local and systemic effects (209). When sustained, tissue damage can also be caused by the indirect effect of the inflammatory mediators (e.g., TNFα, interleukin (IL)-1, IL-6) released in response to the microbial by-products.

Sepsis is the tenth leading cause of death in the US, despite the advances made in antibiotics and patient care. The rapid loss of lean muscle mass in septic patients results in a negative nitrogen balance. This loss of muscle mass is a two-pronged problem, one being the disproportionate and accelerated loss of muscle due to upregulation of proteolysis, and the second being the inhibition of new protein synthesis. The cellular mechanism underlying sepsis-induced inhibition of protein synthesis has not been fully elucidated. Our research will focus on the regulation of cellular signaling that leads to the reduction in protein synthesis and will emphasize on the potential roles of PRAS40 and DEPTOR, two regulators of mTOR kinase.

Although sepsis-induced atrophy is multifactoral and caused both by increased proteolysis and decreased synthesis (210), only the latter will be investigated herein. Sepsis

decreases the synthesis of muscle proteins, especially in fast-twitch fibers, which predominates in the gastrocnemius (211, 212). The reduction in protein synthesis during sepsis results from a decrease in translational efficiency since ribosome content is not altered (213, 214). The ability of sepsis to modulate protein synthesis in the muscle also involves 5' cap-dependent mechanisms which will be extensively studied in this proposed research. LPS is widely used to mimic the systemic and molecular effects of gram-negative bacteria (215). Emerging data show that TNFα is produced in response to LPS and sepsis via stimulation of toll-like receptor 4 (TLR4) and results in decreased phosphorylation of 4E-BP1, which in turn alters the distribution of 4E-BP1 with eIF4E (from active to inactive complex) (211, 216-221). It has also been reported that sepsis and LPS decrease S1108 phosphorylation of eIF4G (87, 217, 218, 222-224). Vary *et al* were the first to show that the assembly of the eIF4E•eIF4G complex was reduced in skeletal muscle from septic rats (225). Sepsis and LPS also decrease the phosphorylation of mTOR on S2481 and S2448 in skeletal muscle (226-229). A consensus has emerged pertaining to the ability of sepsis to impair eIF4F formation in skeletal muscle. In general, septic insults, such as those imposed by cecal ligation and puncture (CLP) and LPS decrease 4E-BP1 phosphorylation (51, 228). This change increases the amount of the inactive eIF4E·4EBP1 complex and reciprocally decreases the active eIF4E·eIF4G complex. Thus, the sepsis-induced reduction in eIF4E·eIF4G may inhibit the mRNA-ribosome binding and thereby limit muscle protein synthesis.

The metabolic consequences of various catabolic stresses and anabolic stimuli are integrated by mTOR (Figure 1-1) (230). Sepsis and LPS decrease mTOR kinase activity in muscle as evidenced by the coordinate decrease in mTOR autophosphorylation at S2481 as well as the decreased phosphorylation of 4E-BP1 and S6K1 (14, 32, 51, 228). However, despite its importance, there is a paucity of data pertaining to the mechanism mediating the sepsis-induced decrease in skeletal muscle mTOR activity. It has been shown that muscle-specific inactivation of raptor, but not rictor, in mice produces muscle atrophy (231). As described above, raptor is a

scaffold protein regulating mTOR kinase activity and the subsequent downstream phosphorylation of 4E-BP1 and S6K1 (232). However, whether sepsis modulates the mTOR·raptor interaction, as well as other newly recognized protein-protein interactions regulating cap-dependent translation in skeletal muscle, has not been investigated, and this gap is addressed by the data provided in Chapter 3. Other models of muscle wasting (e.g., immobilization, Chapter 5) will also be used to investigate selected aspects of mTOR kinase regulation.

Summary

The research proposed herein is unique in its integration of knowledge concerning protein synthesis (as regulated at mRNA translation initiation) mediated by PRAS40 and DEPTOR derived from experiments conducted in a variety of cell lines and its application to the impaired protein synthesis activity following different catabolic insults. Data obtained through the completion of these studies will further the understanding of the cellular and molecular mechanisms underlying the effects of these two important regulators of mTOR in skeletal muscle *per se*. Finally, using *in vivo* electroporation, this research also seeks to study the effect of DEPTOR in mouse gastrocnemius following hind-limb immobilization. Thus far, DEPTOR protein content has not been experimentally manipulated *in vivo* and this study will be the first to ascertain if DEPTOR knockdown is able to overcome the loss of skeletal mass following a model of disuse atrophy.

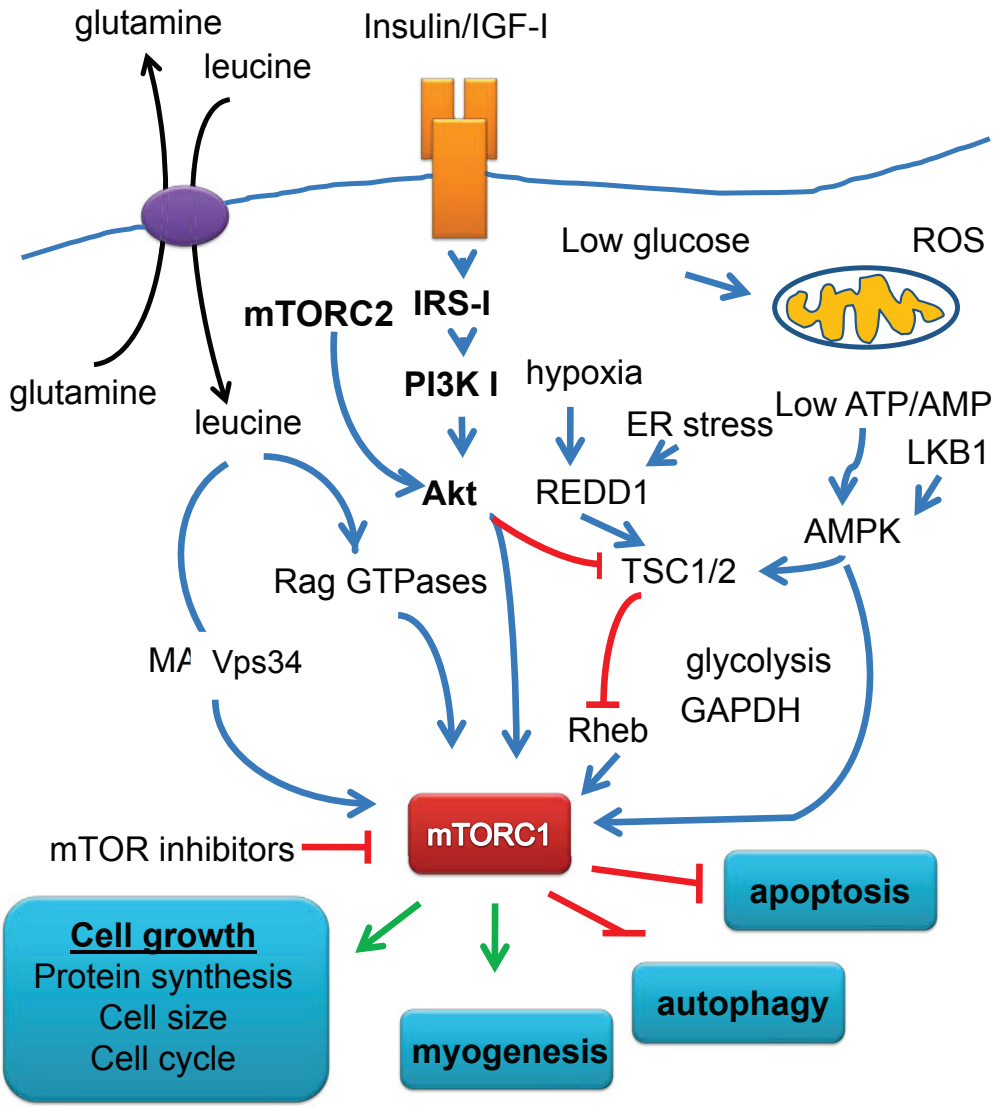

Figure 1—1. The mTOR kinase pathway regulates multiple cellular functions in response to a variety of upstream inputs. mTOR integrates signals from multiple stimuli such as nutrients (amino acids), growth factors [(IGF-I)/insulin], energy status (ATP/AMP levels), cellular stresses (hypoxia, ER stress) and in turn is able to regulate downstream substrates via phosphorylation of key cellular process modulators. mTOR serves as a central kinase sensor regulating protein synthesis by orchestrating protein-protein interactions and establishing the signaling cascade that ultimately controls translation initiation, apoptosis, autophagy, and myogenesis.

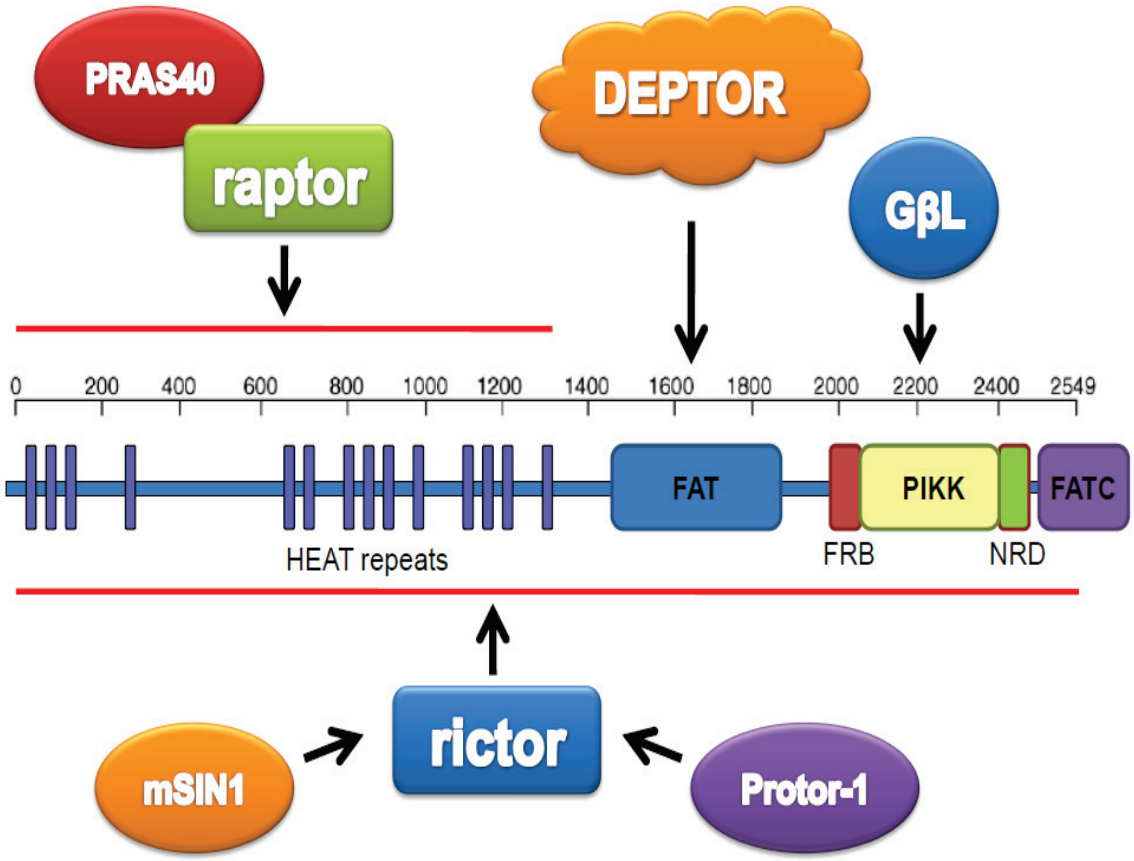

Figure 1—2. **mTOR and its protein binding partners**. Based on the associated proteins, mTOR is considered to reside in two complexes, as explained in the accompanying text. The common partners of mTOR are GβL and DEPTOR which are present in both TOR complexes. While raptor and PRAS40 along with the common partners form mTORC1; rictor along with mSIN1 and protor-1 forms mTORC2. Note not all HEAT repeats (~20) are shown. Arrows indicate amino acid positions where these proteins interact. Red lines indicate multiple possible interactions with the mTOR for raptor and rictor in the regions covered by the lines.

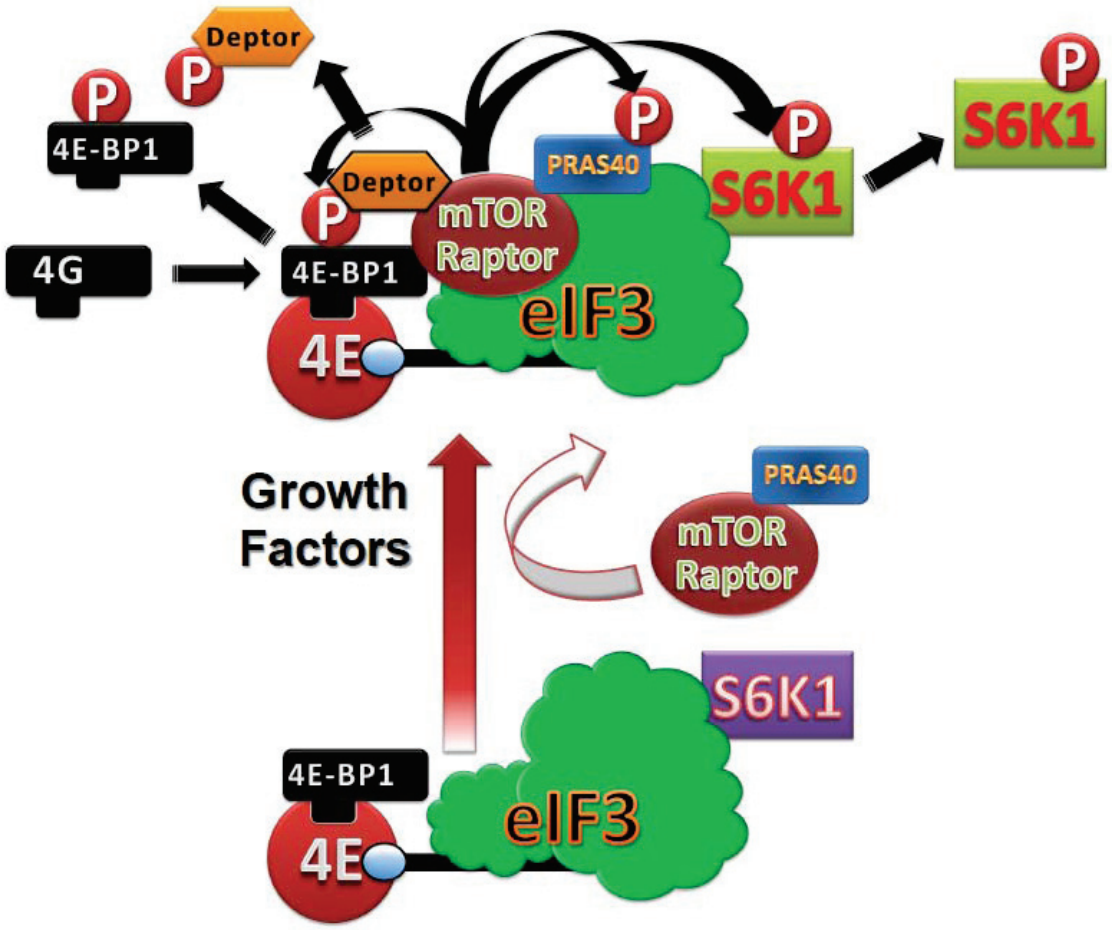

Figure 1—3. **mTORC1: regulation of protein synthesis and cell growth**. As detailed in the accompanying text, mTORC1 integrates signals from various upstream events to regulate phosphorylation of its substrates which in turn provides a favorable physical interaction between various protein factors to promote protein synthesis and cell growth. Please note the sizes of the proteins and factors depicted in the illustration are not to scale (≠ molecular weight). The illustration is only meant to recognize the key proteins involved in the regulation of protein synthesis. Arrows indicate phosphorylation events and/or the direction of movement either away or towards the complex. Unlabelled stick with knob at the end represents the mRNA (stick) with the cap (knob). Also note only two conditions; unstimulated (inactive) and stimulated (active) conditions are shown. For clarity GβL is not shown but is present in both active and inactive states. mTOR-raptor are shown as a complex for simplicity, another illustration showing mTOR-raptor interaction and modeled conformation change is shown in Figure 1-4.

Figure 1—4. **Regulation of mTORC1 by PRAS40 and DEPTOR binding**. Panel A: In unstimulated basal or under unfavorable conditions (starvation or cellular stress) mTOR-raptor are tightly bound to each other and DEPTOR is bound to mTOR. Panel B: In contrast, under stimulated or favorable condition (addition of nutrients/amino acids particularly leucine or addition of growth factors such as IGF-I) mTOR-raptor are in an open/loose conformation, PRAS40 and DEPTOR are no longer part of the mTORC1 complex and the PRAS40 substrate competitor 4E-BP1 is shown to replace PRAS40.

A

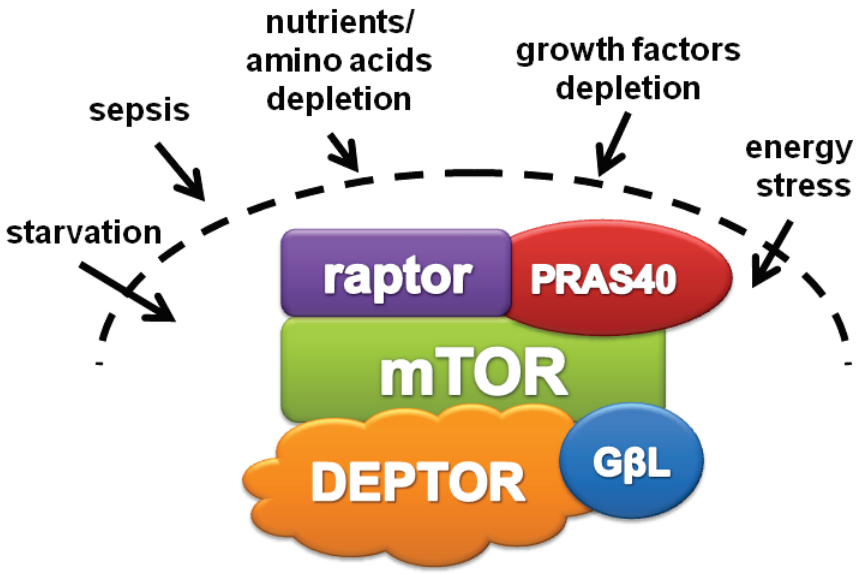

Inactive state: mTOR-raptor bind tightly
Deptor is part of the inactive complex

B

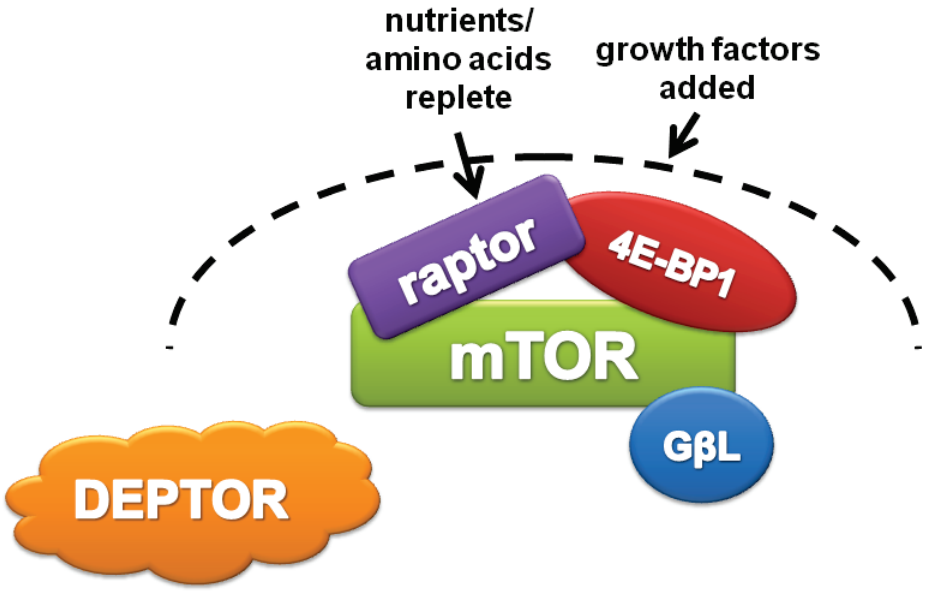

Active state: mTOR-raptor bind loosely
Deptor is degraded

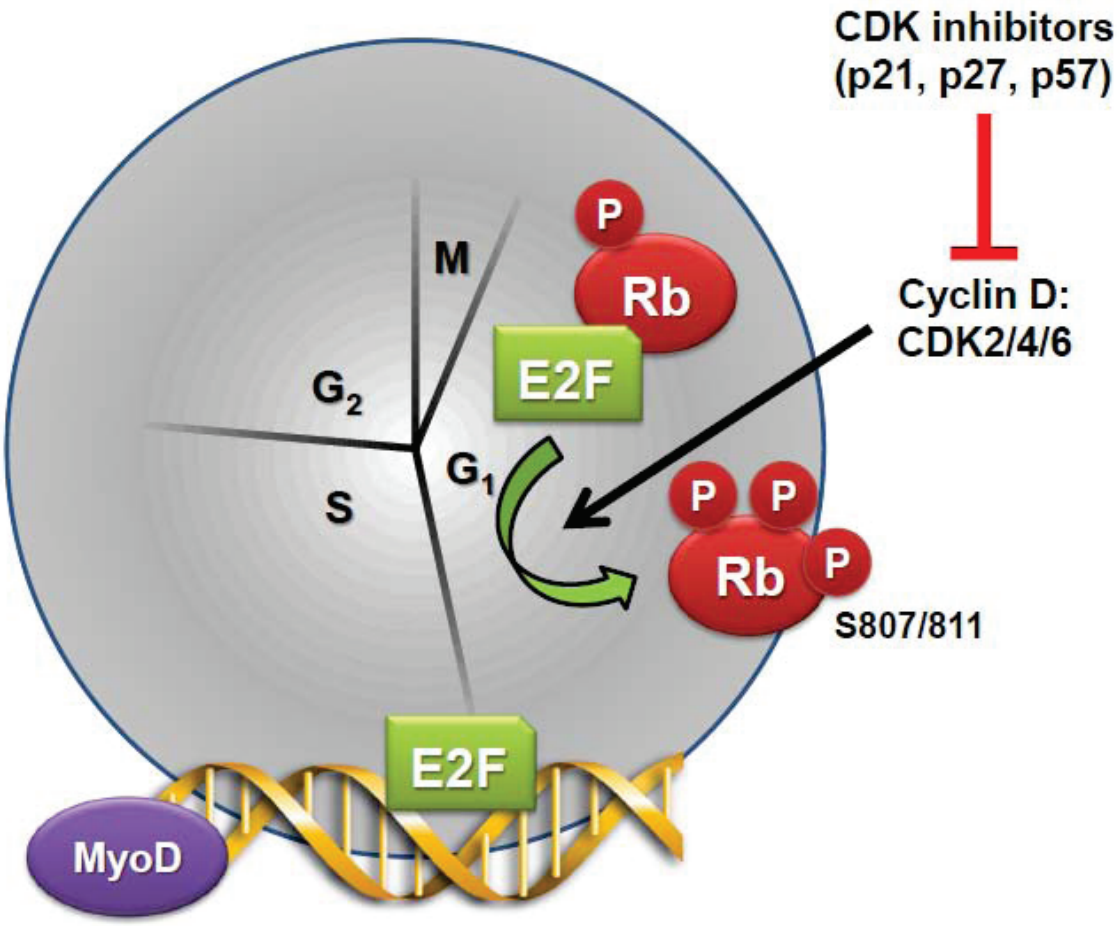

Figure 1—5. **pRb mediated regulation of cell cycle**. Cell cycle phases: the first gap phase (G1); the DNA synthesis phase (S); the second gap phase (G2); and finally mitosis (M). Cell cycle progress is regulated by the activities of complexes of cyclins and cyclin-dependent kinases (cdks), which phosphorylate retinoblastoma (pRb) protein, thereby facilitating cell-cycle progression. Advancement through G1 phase is facilitated by the D-type cyclins (D1, D2, D3), which form active complexes with cdk4 or cdk6, and E-type cyclins (E1, E2) in combination with cdk2. Cyclin-D–cdk4 and cyclin-D–cdk6 complexes are regulated by cdk inhibitors p21 or p27. Release of E2F regulates transcription of genes required for DNA synthesis and in myocytes, transcription factor MyoD.

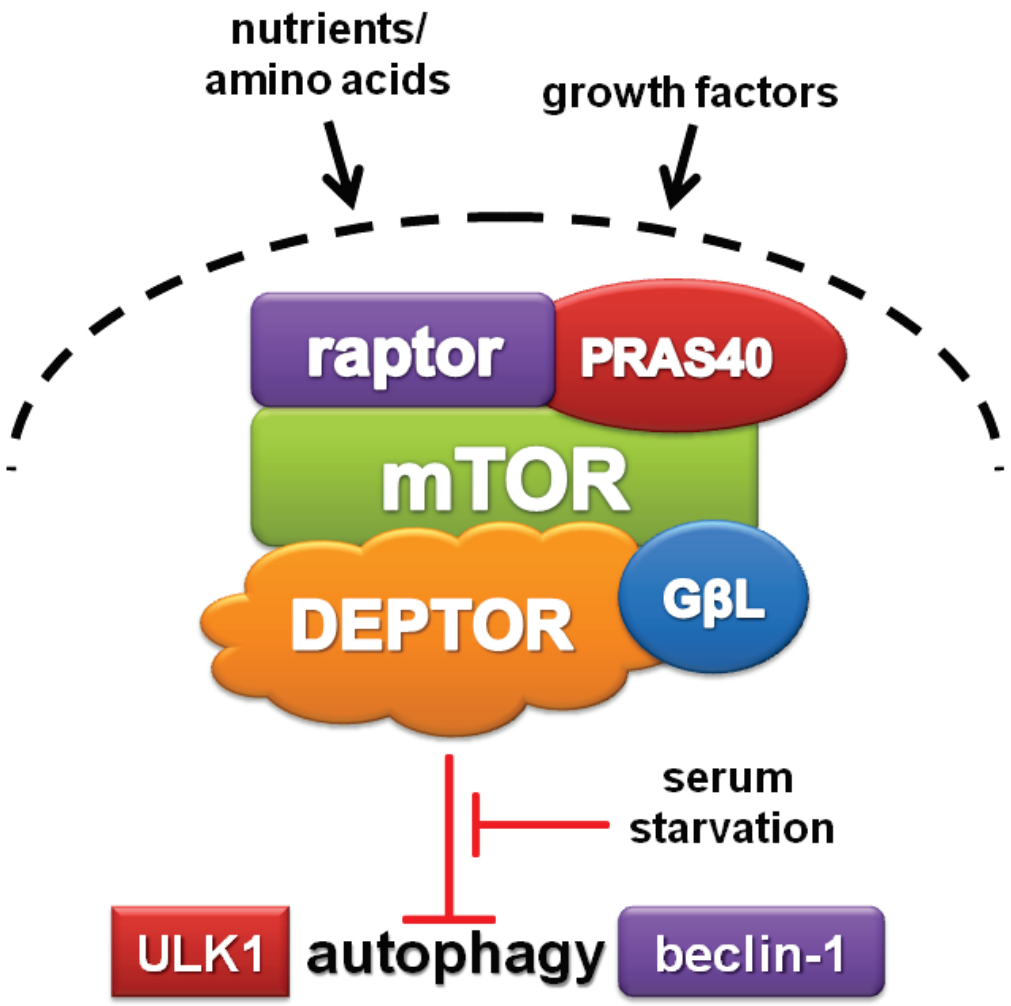

Figure 1—6. **mTORC1 regulates autophagy**. In response to growth factors activated mTOR inhibits beclin-1(atg6), other autophagy related proteins (4, 5, 8, 12 and 16) and ULK1 (initiators of autophagy), thereby inhibiting autophagy. Conversely, upon serum starvation, mTOR activity is inhibited and the removal of the inhibitor signal from mTOR promotes autophagy.

Chapter 2

Materials and Methods

General methods

Animals. Animal facilities and experimental protocols were reviewed and approved by the Institutional Animal Care and Use Committee of The Pennsylvania State University College of Medicine and adhere to the National Institutes of Health Guide for Care and Use of Laboratory Animals.

Rats used in Chapter 3: Specific pathogen-free male Sprague-Dawley rats (200-225 g; Charles River Breeding Laboratories, Cambridge, MA) were quarantined and acclimated for 1 week in a controlled environment. Water and standard rat chow (Rodent Chow 8604, Harlan-Teklad, Madison, WI) were provided *ad libitum*.

Mice used in Chapter 5: Specific pathogen-free adult male C57BL/6 mice (~23-28 g body wt; Charles River Breeding Laboratories) were maintained on a 12:12-h light-dark cycle, with water and food (Rodent Chow 8604; Harlan-Teklad) provided *ad libitum*.

Cell culture. C2C12 myoblasts were obtained from the American Type Culture Collection (ATCC, Manassas, VA). After receipt, they were immediately seeded in growth medium (GM) composed of 1x high Glucose Dulbecco's Modified Eagle's Medium (DMEM; Gibco/ Invitrogen; Carlsbad, CA) supplemented with 10% fetal bovine serum (FBS), penicillin (100 IU/ml), streptomycin (100 µg/ml) (all from Mediatech, Herndon, VA) under 5% CO_2 at 37 °C and were labeled as passage 2. Myoblasts were further sequentially subcultured into serial passages and unless required for specific experiments were not allowed to reach a confluent state (i.e., cells

were subcultured when about 80-85% confluent to prevent myotube formation). Cells were stored in freezing media (final concentration: 20% FBS, DMEM, antibiotics and 7% DMSO), when not required immediately, using Nunc freezing containers with isopropanol for controlled gradient freezing temperatures in -80 °C freezer at least overnight. Cells were then transferred to cardboard storage boxes and stored either at -80 °C for short-term (1-3 months) or liquid nitrogen for long-term storage. When required, myoblasts were allowed to reach 100% confluency and were switched to differentiation medium (DM) which consisted of DMEM with the above antibiotics-antimycotics and 2% horse serum (Hyclone, Logan, UT) to promote myoblast fusion and differentiation to myotubes (233, 234). Myotubes were differentiated for 6 days in DM before experimental manipulation with fresh DM provided every other day. Myotubes were provided with fresh differentiation medium on day 6 and experiments were performed on day seven. To simulate basal mTOR activity, in chapter 4, experiments measuring protein synthesis and the phosphorylation of mTOR substrates were performed with serum-free DMEM without antibiotics-antimycotics and in chapter 5 we used 2% FBS without antibiotics-antimycotics for 8 h. AICAR (Toronto Research Chemicals, Ontario, Canada) when present was added at a final concentration of 2 mM for 8 h. IGF-I (Genentech Inc., San Francisco,CA) when present was used at final concentration of 100 ng/ml for the last 20 min of the experiment in chapter 4 and 1 h in chapter 5. These changes in treatment protocols were based on suggestions made by external reviewers of the manuscript submitted as part of chapter 4. The doses of chemicals used were based on their ability to maximally suppress and activate protein synthesis in C2C12 cells, respectively (235, 236).

Tissue homogenization and CHAPS lysis buffer. The tissue preparation was the same as previously described by our laboratory (32, 51, 211, 228). Muscle was homogenized in ice-cold CHAPS lysis buffer composed of (in mmol/L): 20 HEPES [pH 7.4], 2 EGTA, 50 β-glycerophosphate, 0.3% 3[(3-Cholamidopropyl) dimethylammonio]- propanesulfonic acid (CHAPS), 100 KCl, 2 EDTA, 50 NaF, 0.5 PMSF, 1 benzamidine, 1 sodium orthovanadate, and 2 μg/mL leupeptin) and 1 protease inhibitor cocktail tablet from Roche (56, 237).

SDS-PAGE sample buffer and gels for electrophoresis. Sample buffer used for tissue and cell lysate proteins separated by sodium dodecyl sulfate (SDS)-PAGE was based in Laemeli's protocol and consisted of (final concentrations): 62.5 mM Tris-HCl (pH 6.8), 12.5% v/v glycerol, 1.25% SDS, 1.25% v/v β- mercaptoethanol, 0.1% bromophenol blue, and was prepared as either 2x or 5x stock. Following determination of protein concentration using bicinchoninic acid (BCA) (Pierce Biotechnology, Rockford, IL) assay method (bovine serum albumin was used for preparing the protein standards), samples were normalized to give a final concentration of 1 μg/μl after addition of the SDS-sample buffer. Small Bio-Rad gels were hand cast and used routinely. When needed, large gels were used to accommodate either large sample numbers (more than 15) or to help resolve small proteins (e.g., 4E-BP1). 5%, 10% or 15% gels were poured in house and used for electrophoresis).

Western blotting analysis. After treatment cells were rinsed 2x with cold Dulbecco's Phosphate Buffered Saline (DPBS) and collected on ice in CHAPS lysis buffer. Lysates were sonicated for 10 min and then kept on a rocker for 30 min in the cold prior to being clarified (14000 x *g* for 10 min at 4 °C). A portion of the resulting cell supernatant was used to determine protein concentration via a BCA assay. Sample buffer (5x) was added and samples were loaded according to total protein content (20 μg) on polyacrylamide gels for separation by SDS-PAGE.

Proteins were transferred to Polyvinylidene Fluoride (PVDF) membrane (Biotrace; PALL, Pensacola, FL), blocked in 5% nonfat dry milk, and incubated overnight at 4 °C with phosphospecific and total antibodies given in Table 2-1.

Table 2—1. List of antibodies used.

Antibody (Source)
4E-BP1(1)
4E-BP1 T37/46-p (1) and (2)
Akt (2)
Akt S473-p (2)
Akt T308-p (2)
AMPKα (2)
AMPK T172-p (2)
Acetyl-CoA Carboxylase (ACC) (2)
ACC S79-p (2)
β-actin (2)
eIF4E (2) (11)
eIF4E S209-p (2)
eIF4G (2)
eIF3f (3)
eIF3b (3)
eIF4G S1108-p (2)
mTOR (2)
mTOR S2481-p (2)
mTOR S2448-p (2)
PRAS40 (4) (2)
PRAS40 T246 (4) (2)
rpS6 (2)
rpS6 S240/244-p (2)

LKB1 (2)
LKB1 S428-p (2)
S6K1 (2) (5)
S6k1 T389-p (2)
P21 (5)
P27 (5)
P53 (5)
MyoD (5)
MHC (6)
pRb (5)
pRb-S807/811-p (2)
Raptor (2) (1)
Raptor S792
DEPTOR (7)
CDK2 (5)
CDK4 (5)
CDK6 (5)
Cylcin D3 (2)
Caspase-3 (2)
Cleaved Caspase-3 (2)
Cleaved PARP (2)
Beclin-1 (2)
LC3 (2)
TSC1 (2)

TSC2 (1)	GSKα/β S21/9-p (2)
TSC2 T1462-p (1)	eIF4A (2)
REDD1 (8)	PABP (2)
GSKα/β (2)	GβL (2)
Goat anti rabbit (9)	Donkey anti rabbit (10)
Mouse anti human (9)	eIF4B (2)
Donkey anti goat (9)	eIF4B S422-p (2)
Goat anti mouse (9)	β-tubulin (5)
Rabbit anti rat (9)	Atg-7 (2)

Source information (numerical key):

1. Bethyl Labs, Montomery, TX
2. Cell Signaling, Boston, MA
3. Abcam, Cambridge, MA
4. Biosource, Camarillo, IL
5. SantaCruz Biotechnology, Santa Cruz CA
6. MF-20, Developmental Studies Hybridoma Bank, Iowa City, IA
7. Millipore, Billerica, MA
8. Peprotech Inc., Chicago, IL
9. Sigma, St. Louis, MO
10. ECL – Amersham, Piscataway NJ
11. Drs Jefferson and Kimball, Hershey, PA

Excess primary antibody was removed by washing in 1x TBS + 0.1% Tween 20 for 10-20 minutes, and membranes were incubated with horseradish peroxidase-conjugated goat anti-rabbit or goat anti-mouse secondary antibody (Sigma). Blots were rinsed with 1x TBS + 0.1% Tween 20 to remove excess secondary antibody and were treated with enhanced chemiluminescence (ECL plus) Western blotting reagents (Amersham), and then developed using the Gene Gnome (Bioscience, UK). Uncompressed tiff images were analyzed using National

Institutes of Health (NIH) ImageJ 1.6 software. After development, blots were stripped by treatment with a solution containing 62.5 mM Tris, pH 6.8, 2% (weight/volume) SDS, and 100 mM β-mercaptoethanol in a 50 °C water bath for 15 minutes, reblocked with milk, rinsed, and incubated at 4 °C overnight with antibodies for total proteins on blots which were probed earlier with phosphospecific antibodies. Antibodies against β-actin or β-tubulin served as an additional control for equal protein loading of samples.

Co-immunoprecipitation. The eIF4E•4EBP1 and eIF4E•eIF4G complexes were quantified as described (32, 51, 211, 228). Briefly, eIF4E was immunoprecipitated from aliquots of supernatants using an anti-eIF4E monoclonal antibody (kindly provided by Drs. Jefferson and Kimball; Hershey, PA). Antibody-antigen complexes were collected using magnetic beads, subjected to SDS-PAGE, and finally transferred to a PVDF membrane. Blots were incubated with a mouse anti-human eIF4E antibody, rabbit anti-rat 4E-BP1 antibody, or rabbit anti-eIF4G antibody. The homogenate was clarified by centrifugation and an aliquot of the supernatant was combined with either anti-TSC2, anti-mTOR, anti-raptor, or anti-eIF3b antibody, and immune complexes were isolated with goat anti-rabbit BioMag IgG (PerSeptive Diagnostics, Boston, MA) beads. The beads were collected, washed with CHAPS buffer, precipitated by centrifugation and subjected to SDS-PAGE as described above. All blots were then developed with ECL and analyzed as described above for Western blotting. Co-immunoprecipitation of the PRAS40•raptor, PRAS40•eIF3f, and PRAS40•PRAS40 complexes were quantified as described (238). An aliquot (normalized to equal total protein) of the resulting supernatant was combined with anti-PRAS40 antibody and immune complexes isolated with a goat anti-rabbit BioMag IgG (PerSeptive Diagnostics) beads. Samples were treated as described above.

Plasmids. Plasmids used in the transfection and generation of lentivirus particles were purchased from Addgene (Addgene, Cambridge, MA) and the specific plasmid catalogue number is given in parenthesis. Original plasmid submitting author is acknowledged and papers are referenced as source of plasmid.

Plasmid DNA preparation. All plasmid DNA was amplified in either DH5α or XL-1 Blue Supercompetent Cells® (Stratagene, Cedar Creek, TX) and purified with an endotoxin-free GigaPrep kit (Qiagen, Valencia, CA) as described for *in vivo* studies or (Qiagen Plasmid Maxi kit) for cell culture transfections. The pLL3.7 GFP plasmid (Addgene plasmid # 11795) expressing GFP was utilized for fluorescence imaging of cells and muscles and served as a control plasmid in pilot studies to determine appropriate time course and dosage.

shRNA interference. The lentiviral plasmid pLKO.1-mPRAS40 used was that described by Vander Haar *et al* (114) (Addgene plasmid #15480) and targeted the mouse sequence 5'-GAG CCC ACT GAA ACA GAG ACA-3'; the scramble shRNA was used as a negative control as previously reported (37) with hairpin sequence: CCT AAG GTT AAG TCG CCC TCG CTC TAG CGA GGG CGA CTT AAC CTT AGG (Addgene plasmid #1864). The plasmids were transformed in DH5α cells and isolated using the Qiagen EndoFree Giga prep kit (Qiagen). The actual DNA sequence was confirmed at the Pennsylvania State University College of Medicine DNA sequence core facility. For DEPTOR KD in chapter 5, we used the lentiviral plasmid pLKO.1-mDEPTOR described by Peterson *et al* (47) which targeted the mouse sequence 5'- CCG GCG CAA GGA AGA CAT TCA CGA TCT CGA GAT CGT GAA TGT CTT CCT TGC GTT TTT G -3' (Addgene plasmid # 21337). Packaging plasmids psPAX2 and envelope protein plasmid pMD2.G were obtained from Torono Lab (Addgene plasmid #12260 and #12259, respectively). Transfection was carried out as described below.

Transfection and generation of stable knockdown cells. HEK393FT (Invitrogen) cells were transfected with Lipofectamine 2000 (Invitrogen) utilizing the following protocol. HEK293FT cells were grown in DMEM media; 80-85% confluent plates were rinsed once with Opti-MEM media (Invitrogen) and then incubated with Opti-MEM media for 4 h before transfection. psPAX2 and pMD2.G, along with either scramble (Appendix 1-1) or pLKO.1-mPRAS40 or pLKO.1-mDEPTOR, were added after mixing with Lipofectamine 2000 as per manufacturer's instructions (Invitrogen). Opti-MEM media was changed after overnight incubation with DMEM containing 10% FBS without antibiotics to allow cells to take up plasmids and recover. Culture media was collected at 36 h and 72 h, and viral particles present in the supernatant were harvested after a 15 min spin at 1500 x g to remove cellular debris. The supernatant was then further filtered using a 0.45 μm syringe filter. Supernatant containing virus was either stored at -80 ºC for long-term storage or at 4 ºC for immediate use. Low passage (usually passage 3 or 4) C2C12 cells at < 60% confluence were infected twice overnight with 3 ml of viral supernatant containing 8 μg/ml polybrene in serum free – antibiotic free DMEM. Fresh DMEM media containing 10% FBS, antibiotics, and 2 μg/ml puromycin (Sigma) was added the next day. Cells that survived under puromycin selection were either harvested (as stable cells) and stored or used immediately.

^{35}S-methionine labeling. C2C12 myocytes were grown in six-well plates and treated as described under cell culture section. Protein synthesis was measured on day 3 in myoblasts following seeding or on day 7 following addition of DM in myotubes. For metabolic labeling 10 μCi of radiolabeled ^{35}S-methionine (MP Biologicals, PA) was added to each well of a 6 well plate and radiolabel incorporation into trichloroacetic acid (TCA) precepitable proteins were measured via liquid scintillation as previously described (239).

Cell cycle. Myoblasts were transfected with either a scramble (Control) shRNA or a shRNA targeting PRAS40 or DEPTOR (see individual chapters for study details). Cells were seeded in 10 cm dishes and used at 60% confluence (~24 h post seeding). Cells were trypsinized, washed with DPBS and fixed in cold 70% ethanol overnight at -20 °C. Cells were then stained with 100 µg/ml solution of propidium iodide buffer containing 0.1% Triton-X100 and 0.001% DNAse free RNAse at 37 °C for 30 min immediately prior to FACS analysis. 10,000 (for PRAS40 study) and 20,000 (for DEPTOR study) cells per sample were counted and cell cycle phase was measured by propidium iodide staining intensity using a BD FACS-Calibur flow cytometer (Becton Dickinson, Bedford, MA) and ModFit software LT Version 3.2 (Verity Software,Topsham, ME).

Cell size and proliferation. To determine cell size, transfected myoblasts were seeded in 10 cm dishes and used at 60% confluence. For cell number, cells were seeded at similar densities and counted at different time points. Myoblasts were trypsinized and suspended in DMEM with 10% FBS. Cells were then diluted 1:10 or 1:20 (DMEM: Isoton) in Isoton II solution (Beckman Coulter, Fullerton, CA) and assayed using the Beckman Coulter Counter and particle size analyzer as per manufacturer's recommendation (Beckman Coulter). Cell size analysis was performed using the AccuComp® Z2 Coulter counter software (Beckman Coulter).

MTT assay. C2C12 myoblasts (~10,000/well) were grown in a 96-well plate for 24 h and then rinsed with PBS to remove the interfering phenol red from the DMEM media. This was followed by the addition of methylthiazoletetrazolium (MTT; 50 µg/100 µl) to cells in each well for 4 h at 37 °C (240). MTT containing PBS was aspirated, wells were rinsed 2x with PBS, and 100 µl of DMSO was added to each well to dissolve the resulting formazan and absorbance at 570 nm was read in a plate reader Spectramax (Molecular Devices, Sunnyvale, CA).

Cell differentiation. Approximately $0.5x10^6$ myoblasts transfected with scramble or shPRAS40 or shRNA targeting DEPTOR were seeded in 10 cm plates and photographed daily using a Nikon digital camera (Nikon Corp., Tokyo, Japan) mounted on a binocular microscope using 10x objective lens. Images were composed and edited in Photoshop 7.0 (Adobe Systems Incorporated, San Jose, CA). Background was reduced using contrast and brightness adjustments to enhance reprint, and all modifications were applied to the whole image. Similarly treated plates were collected at days 3, 5, 7, and 9 for Western blotting to measure myosin heavy chain (MHC) expression as a functional end-point to measure differentiation biochemically as myoblasts were allowed to fuse and form differentiated post-mitotic myotubes by switching the media to 2% horse serum once the plates were confluent (day 3-4).

Cell apoptosis and autophagy controls. Same passage C2C12 myoblasts as PRAS40 KD or DEPTOR KD and Scramble control cells were treated with 2 μM staurosporine in culture media for 4 hr to induced apoptosis and collected in the CHAPS media. To induce autophagy, C2C12 myoblasts were treated with Hanks Buffered Salt Solution (HBSS) for 6 hr and cells collected in CHAPS buffer.

Materials and Methods for Chapter 3

Cecal ligation and puncture (CLP) model of sepsis. Sepsis was induced by cecal ligation and puncture (CLP) (32, 51). Rats were anesthetized with pentobarbital (50-60 mg/kg) and a midline laparotomy was performed. The cecum was ligated at its base and punctured twice using a 20 g needle. The cecum was returned to the peritoneal cavity, the muscle and skin layers were closed separately, and rats were resuscitated with 10 ml of 0.9% sterile saline (37 °C) administered subcutaneously. The nonseptic control animals received a laparotomy with intestinal

manipulation and fluid resuscitation. After surgery, all rats were fasted, but permitted free access to water. Hence, any observed change between septic and nonseptic rats cannot be attributed to differences in nutritional status. In a second study, septic and nonseptic rats were administered 1.35 g/kg body weight (BW) of leucine (54 g/L) by oral gavage 24 h after CLP, and muscle was excised 30 min thereafter. This leucine dose maximally stimulates muscle protein synthesis and indices of translation initiation in nonseptic rats at the time point examined (241). Although we have previously reported there is no difference in the plasma leucine concentrations between control and septic rats gavaged with leucine (32, 51), we quantified leucine concentrations in the current study by high-pressure liquid chromatography (HPLC).

Muscle protein synthesis. *In vivo* protein synthesis in gastrocnemius was determined approximately 24 h after CLP or sham surgery using the flooding-dose technique (242). Briefly, rats were anesthetized with intraperitoneal pentobarbital (100 mg/kg) and a catheter was placed in the carotid artery. A bolus injection of L-[2,3,4,5,6-3H] phenylalanine (Phe; 150 mM, 30 μCi/ml; 1 ml/100 g BW) was injected via the jugular vein, and serial blood samples were drawn after 2, 6 and 10 min for measurement of Phe concentration and radioactivity. Immediately after the final blood sample, the gastrocnemius from one leg was frozen *in vivo* between aluminum blocks pre-cooled to the temperature of liquid nitrogen, and the other muscle was rapidly excised with a portion being homogenized directly and the remainder freeze-clamped. Blood was centrifuged and plasma was collected. All tissue and plasma samples were stored at -80 °C until analyzed. The frozen muscle was powdered under liquid nitrogen and a portion used to estimate the rate of incorporation of [^{3}H]-Phe into protein (15). Total RNA was determined and translational efficiency was calculated by dividing the rate of synthesis by the total RNA per tissue.

Statistical analysis. Experimental data for each condition are summarized as means ± SE, where the number of animals in each treatment group is indicated in the legend to the figure or table. Statistical evaluation of the data was performed using either Student *t*-test for two-group comparisons or ANOVA followed post hoc by Student-Neuman-Keuls test for multiple group comparisons (GraphPad InStat, version 3.05; GraphPad, La Jolla, Calif). Differences between the groups were considered significant when $P < 0.05$.

Materials and Methods for Chapter 4

Multiprobe template production for RNase protection assay. Primer selection for mouse genes of interest was determined using GeneFisher software (243). The lengths of amplified regions were chosen to allow distinct resolution during electrophoretic separation. Primers were synthesized (IDT, Coralville, IA) with restriction sites for EcoRI or KpnI at the 5' end and with three extra bases at the extreme 5' end as follows:

Table 2—2. List of primers used to make RPA multiprobes.

PRAS40	Forward	5'-GCA GAA TTC GCC CGA TCG TCA GAT GAG GAG A-3’
	Reverse	5’-CCT GGT ACC TCA GCT TCT GGA AGT CGC TGG TA-3’
mTOR	Forward	5'-GCA GAA TTC GGC CAG TGG ACC AGT TGA GAC A-3’
	Reverse	5’-CCT GGT ACC CAG CTC AGA CCA GCA GGA CAC A-3’
Raptor	Forward	5'-GCA GAA TTC CAT GCA TAG CTG TCG CCG ACA-3’
	Reverse	5’-CCT GGT ACC ACA ATG AGC GAA CGG TGC GAA-3’
S6K1	Forward	5'-GCA GAA TTC GAC CAT GGG GGA GTT GGA CCA T-3’
	Reverse	5’-CCT GGT ACC CTC CAG AAT GTT CCG CTC TGC TT-3’
4E-BP1	Forward	5'-GCA GAA TTC CGG GGA CTA CAG CAC CAC TC-3’

	Reverse	5'-CCT GGT ACC GGG CAG TTG GCT CTG GTT GG-3'
L32	Forward	5'-GCA GAA TTC CGG CCT CTG GTG AAG CCC AA-3'
	Reverse	5'-GCAGGT ACC CCT TCT CCG CAC CCT GTT GTC A-3'

PCR was conducted with HotStarTaq DNA polymerase (Qiagen) and mouse total RNA was reverse transcribed with Superscript first-strand synthesis system for RT-PCR (Invitrogen). PCR products were phenol-chloroform extracted, ethanol precipitated, and sequentially digested with KpnI and EcoRI (Promega, Madison, WI). Digested products were gel purified, re-extracted, and cloned into KpnI/EcoRI-digested pBluescript II SK+ (Stratagene). Plasmid DNA was isolated with both QIAprep spin miniprep and plasmid maxi kits (Qiagen). Final constructs were linearized with EcoRI, gel purified, and quantitated spectrophotometrically. The template was prepared so that a 2 μl aliquot contained 10 ng each of PRAS40, S6K1, mTOR, 4E-BP1, and raptor, and 20 ng of L32.

RNA extraction and RNase protection assay. Total RNA was extracted from cells using Tri reagent (Molecular Research Center, Cincinnati, OH), exactly as previously described (42). Concentration, purity, and integrity of the isolated RNA were assessed using a UV/VIS spectrophotometer (Beckman, Fullerton, CA). mRNA expression was determined by RNase protection assay. A 2 μl aliquot of template was prepared with T7 polymerase with buffer (Fermentas, Hanover, MD), NTPs, and tRNA (Sigma), RNasin and DNase (Promega), and [^{32}P]-UTP (Amersham Biosciences). Unless otherwise noted, the entire RNase protection assay procedure, including labeling conditions, component concentrations, sample preparation, and gel electrophoresis, was as published (42). Gels were exposed to a PhosphorImager screen (Molecular Dynamics) and data were visualized and analyzed by ImageQuant software (version 5.2; Molecular Dynamics). Signal densities within the linear range for mRNAs were normalized to densities for mouse ribosomal protein L32 mRNA.

Cellular DNA isolation and analysis. To analyze nucleosomal DNA fragmentation, $2.5x10^6$ C2C12 cells were processed as described by Zhivotovsky *et. al.* (244) with minor modifications. Cells, 80% confluent were trypsinized and centrifuged for 5 min at 4000 rpm to removed media. The cell pellet was resuspended in total DNA extraction buffer (400 mM NaCl; 10 mM Tris-HCl, pH 7.5; 10 mM EDTA with 50 µg/ml RNAse A and 0.2% SDS) and incubated at 37 °C overnight. Proteinase K was added the following day to a final concentration of 50 µg/ml for 4 h at 37 °C. NaCl was then added to the DNA extraction mix to obtain a final concentration of 1.23 M and the extraction mix was left on ice overnight. The following day the mixture was centrifuged at 17,000 rpm for 1 h at 4 °C. The supernatant containing the low molecular weight DNA was removed and extracted 2x with phenol- chloroform followed by a final rinse in chloroform. The extract was then subjected to ethanol precipitation in 0.1 volume of 3 M sodium acetate and 2 volumes of 100% ethanol at -20 °C for 1 hour. The samples were centrifuged at 4000 rpm to pellet the DNA and the pellet was washed with 70% ethanol and air dried. The pellet was resuspended in Tris-EDTA buffer (pH 8.0) and the amount of DNA measured spectrophotometrically. Positive control apoptotic DNA from U937 cells was from Roche DNA-ladder kit (Roche Diagnostics Corporation, Indianapolis, IN). DNA (8 µg per sample/lane, and 3 or 5 µg/lane for positive control apoptotic DNA) was loaded onto a 1.5% agarose gel, subjected to electrophoresis (55 V for 2.5 h) in 1x Tris-Borate-EDTA buffer and scanned using the Typhoon fluorescent imager (Molecular Dynamics).

Plasmid isolation for *in vivo* electroporation. For plasmid transfection into skeletal muscle *in vivo*, plasmid DNA was purified with the endotoxin-free GigaPrep kit (Qiagen) according to the manufacturer's protocol with minor modifications. DH5α cells (Stratagene) transformed with the plasmid were plated onto LB agar plates with ampicillin (selective antibiotic) and grown overnight at 37 °C. The next day, a single colony was selected and a 5 ml starter culture (LB

medium containing 100 µg/ml of ampicillin) was inoculated and incubated at 37 °C on an orbital shaker for 8 hours at ~ 250-300 rpm. This starter culture was diluted 1:100 into five 1L Erlenmeyer flasks each containing 500 ml of selective medium. Bacterial cultures were grown overnight (typically 18-20 h) at ~250-300 rpm. Plasmid isolation followed the Qiagen Endotoxin GigaPrep manufacturer's protocol with recommended options to increase yield and the DNA was eluted directly in ~2 ml preservative-free "normal saline for injection" (sterile 0.9% NaCl solution). The plasmid solution in saline was heated at 55 °C for 30 min and DNA concentration and quality was assessed via the NanoDrop ND-1000 spectrophotometer (Thermo Scientific, Wilmington, DE) using saline as a blank. A final concentration of 1.5 mg/ml was achieved by dilution the DNA with saline. Plasmid DNA was aliquoted into 110 µl volumes to give a concentration of 150 µg/100µl and stored at -80 °C until used for *in vivo* injection.

Materials and Methods for Chapter 5

RNA extraction and quantitation. Total RNA was isolated from C2C12 myocytes transfected with either scramble or DEPTOR shRNA using RNeasy mini kit (Qiagen). For animal tissue, total RNA was isolated from 35-50 mg of skeletal muscle using 1 ml of Tri-reagent (Molecular Research Center, Inc., Cincinnati, OH). The RNA pellet was reconstituted in 100 µl of RNase free water and subjected to RNA cleanup using RNeasy mini kit (Qiagen). On column DNase I treatment was performed to remove any residual DNA contamination. RNA was eluted from the column with 30-50 µl RNase-free water, and the total RNA (1-2 µl) concentration was determined (NanoDrop 2000; Thermo Scientific).

Reverse transcription. Total RNA (1-5 µg) was primed with 200 ng of oligo dT, 100 ng of random primer and 0.5 mM dNTP mix at 65 °C for 5 min and then kept on ice for 1-2 min.

cDNA was synthesized from the primed reaction using 200 units of superscript III reverse transcriptase, 40 units of RNaseOut, 1x first strand buffer and 5 mM dithiothreitol in a 20 µl reaction volume (Invitrogen). The reaction was incubated at 25 °C for 5 min, then at 50 °C for 1 h followed by 70 °C for 15 min to inactivate the reverse transcriptase. To control for residual DNA contamination, each RNA sample was subjected to cDNA synthesis as described above without the superscript-III transcriptase. The cDNA was stored at -20 °C.

Real-time quantitative PCR. Real-time quantitative PCR using primers shown in Table 2-3 was performed using 25-65 ng of cDNA in a StepOnePlus system using TaqMan gene expression assays and the gene expression master mix (Applied Biosystems, Foster City, CA). The cycling parameters were an initial 50 °C for 2 min and 95 °C for 10 min and 40 cycles of 95 °C for 15 sec and 60 °C for 1 min. Real-time PCR quantitation was based on the Ct values, where Ct is defined as the PCR cycle number that crosses an arbitrary signal threshold on the amplification plot. The comparative quantitation method $2^{-\Delta\Delta Ct}$ was used in presenting gene expression of target genes in reference to an endogenous control and $2^{-\Delta Ct}$ was used in presenting expression of each house keeping gene in validating the use of endogenous control gene. ΔCt is expressed as the difference between the target and control samples $^{(Ct\ target\ -\ Ct\ control)}$.

Table 2—3. Real-time PCR primers used in the study

Gene symbol	Gene Name	Assay ID *	Pubmed RefSeq
Actb	Actin, beta	Mm01205647_gl	NM_007393.3
Gapdh	Glyceraldehydes-3-phosphate dehydrogenase	Mm999999915_gl	NM_008084.2
Rpl32	Ribosome protein L32	Mm02528467_gl	NM_172086.2
B2m	Beta-2 microglobulin	Mm00437762_ml	NM_009735.3
Depdc6 (DEPTOR)	DEP domain containing 6	Mm01195339_ml	NM_145470.2 and NM_001037937.2
Hprt	hypoxanthine guanine phosphoribosyl transferase1	Mm00446968_ml	NM_013556.2

***In vivo* electroporation**. Mice were briefly anesthetized with isoflurane (2–3% in O_2) for plasmid injection, *in vivo* electroporation and subsequent hindlimb immobilization. Once mice were anesthetized, the lower hindlimbs were shaved to expose the skin, swabbed with 70% alcohol, and air-dried to clean the injection site. Plasmid DNA (100 μg total in 150 μl of 0.9% sterile saline) was slowly injected at multiple sites (~3) directly into the gastrocnemius through the skin via a 1-ml insulin syringe fitted with a 28-gauge needle (Becton-Dickinson). A plasmid targeting DEPTOR was injected into both the right and left gastrocnemius of one cohort of mice, while a second group of mice received bilateral injection of the scrambled control plasmid. Square-wave electric impulses generated by an electroporator (model ECM 830, BTX, San Diego, CA) were delivered to muscle in both legs via caliper electrodes (Harvard apparatus, model 384, BTX) coated with electrode conductive gel. The electrodes were applied to the lower hindlimb with only slight pressure to ensure proper contact. Pulse trains were delivered with a 200 V/cm field strength (8 pulses, 40 ms/pulse, 100 ms interval) on the basis of previously described parameters (245-247). Careful excision of the transfected muscle was performed 72 h following the electroporation procedure (see below). Parameters for *in vivo* electroporation were optimized in preliminary studies (data not shown) and are comparable to those reported by others (245-248).

Hindlimb immobilization. Following *in vivo* electroporation, one hindlimb was wrapped with a single layer of surgical tape. Superglue was then applied to the tape and a 1.5 ml plastic microfuge tube without the lid was placed over the leg, maintaining the foot in a plantar-flexed position. The contralateral leg was not immobilized and functioned as the internal control. The contralateral leg does not undergo hypertrophy and the validity of this unilateral hindlimb immobilization has been previously reported (13, 249). Food and water consumption of mice with the DEPTOR KD plasmid did not differ from mice that received control plasmid (data not

shown). Thus, *in vivo* studies generated muscles in four experimental groups: (a) muscle injected with control plasmid which remained mobile, (b) muscle injected with control plasmid but was then immobilized, (c) muscle injected with DEPTOR KD plasmid which remained mobile, and (d) muscle injected with DEPTOR KD plasmid and was immobilized.

***In vivo* protein synthesis**. The *in vivo* rate of protein synthesis in the gastrocnemius (hereafter referred to as muscle) was determined in Control and DEPTOR KD treated mice 3 d after plasmid electroporation and immobilization. Protein synthesis was determined using the flooding-dose technique, exactly as described (242, 250). Mice were injected intraperitoneally with [^{3}H]-L-phenylalanine (150 mM, 30 μCi/ml; 1 ml/100 g body wt), and blood was collected 15 min later for determining the plasma phenylalanine concentration and radioactivity. Thereafter, muscles were rapidly excised, freeze-clamped, and then stored at -70 °C. Muscle was processed exactly as previously described (212, 251). The rate of protein synthesis was calculated by dividing the amount of radioactivity incorporated into protein by the plasma phenylalanine-specific radioactivity, and the advantages and disadvantages of this method have been reviewed (252). The specific radioactivity of the plasma phenylalanine was measured by HPLC analysis of supernatant from TCA extracts of plasma.

Statistical analysis for chapters 4 and 5. Results for individual cell experiments ($n \geq 6$) were replicated in at least three independent experiments and when applicable are presented as means ± SE calculated from the pooled data. Data were analyzed by unpaired Student's *t*-test in two-group comparisons or with ANOVA and Tukey's posttest in multigroup comparisons to determine treatment effect when ANOVA indicated a difference among the means. GraphPad Prism version 5.0 (GraphPad) was used for analysis. Differences between groups were considered significant at $P < 0.05$.

Chapter 3

Sepsis-induced alterations in protein-protein interactions within mTOR Complex1 and the modulatory effect of leucine on muscle protein synthesis

Abstract

Sepsis-induced muscle atrophy is produced in part by decreased protein synthesis mediated by inhibition of mTOR. The present study tests the hypothesis that alteration of specific protein-protein interactions within the mTORC1 (mTOR complex 1) contribute to the decreased mTOR activity observed after cecal ligation and puncture in rats. Sepsis decreased *in vivo* translational efficiency (protein synthesis normalized to mRNA content) in gastrocnemius and reduced the phosphorylation of eukaryotic initiation factor (eIF) 4E-binding protein (BP)-1, S6 kinase (S6K)-1 and mTOR, compared to time-matched pair-fed controls. Sepsis decreased T246-phosphorylated PRAS40, and reciprocally increased S792-phosphorylated raptor. Despite these phosphorylation changes, sepsis did not alter PRAS40 binding to raptor. The amount of the mTOR-raptor complex did not differ between groups. In contrast, the binding and retention of both 4E-BP1 and S6K1 to raptor was increased and, conversely, the binding of raptor with eIF3 was decreased in sepsis. These changes in mTORC1 in the basal state were associated with enhanced 5'-AMP activated kinase activity. Acute *in vivo* leucine stimulation increased muscle protein synthesis in control, but not septic rats. This muscle leucine resistance was associated with coordinated changes in raptor-eIF3 binding and 4E-BP1 phosphorylation. Overall, our data suggest the sepsis-induced decrease in muscle protein synthesis may be mediated by the inability of 4E-BP1 and S6K1 to be phosphorylated and released from mTORC1 as well as the decreased

recruitment of eIF3 necessary for a functional 48S complex. These data provide additional mechanistic insight into the molecular mechanisms by which sepsis impairs both basal protein synthesis and the anabolic response to the nutrient signal leucine in skeletal muscle.

Introduction

Negative nitrogen balance and the erosion of lean body mass are defining characteristics of bacterial infection and can adversely affect morbidity and mortality in sepsis (19). The observed atrophy is undoubtedly multifactorial, but it is in part mediated by decreased synthesis of both myofibrillar and sarcoplasmic proteins in skeletal muscle that are preferentially composed of fast-twitch (e.g., gastrocnemius) fibers (211). This sepsis-induced decrease in muscle protein synthesis results from reduced translational efficiency and is predominantly controlled at the level of peptide-chain initiation (14). In turn, translation initiation is regulated by a number of specialized proteins termed eukaryotic initiation factors (eIFs), many of which are sensitive to hormonal and nutritional signals functioning in a cooperative manner to adjust translation to match cellular requirements. A rate-controlling step in translation initiation is mediated by eIF4F and involves the binding of mRNA to the 43S preinitiation complex. This multimeric eIF4F complex is composed of several proteins including: eIF4E, which directly binds the m7GTP-cap structure; eIF4A, which together with eIF4B unwinds secondary structure via its ATP-dependent RNA helicase activity; and eIF4G, which serves as an adaptor protein. eIF4G is the nucleus for the formation of the initiation complex, as evidenced by its binding sites not only for eIF4E but also for eIF4A and eIF3 (104). As a result, eIF4G recruits the 40S subunit to the 5' end of mRNA and coordinates the circularization of mRNA via its interactions with eIF4E, poly (A)-binding protein (PABP), and eIF3.

Formation of the eIF4F complex controls cap-dependent initiation by regulating the availability of "free" eIF4E. Although sepsis does not alter the total amount of cellular eIF4E, it shifts the distribution of eIF4E from the active to the inactive complex (51, 211). The binding of eIF4E to eIF4E-binding protein-1 (4E-BP1) allows association with mRNA, but it prevents binding to eIF4G and consequently the formation of the active eIF4F complex (56) (Figure 3-1). Nutrients and growth factors positively modulate the ordered phosphorylation of 4E-BP1, releasing 4E-BP1 from eIF4E, and thereby stimulating cap-dependent mRNA translation by enhancing formation of the active eIF4E•eIF4G complex. The phosphorylation of 4E-BP1 is mediated by the conserved serine (S)/threonine (T) protein kinase mammalian target of rapamycin (mTOR) (253). A consensus has emerged pertaining to the ability of sepsis to impair eIF4F formation in skeletal muscle. In general, septic insults − such as those imposed by cecal ligation and puncture (CLP) and endotoxin (lipopolysaccharide; LPS)− decrease 4E -BP1 phosphorylation (51, 228). This change increases the amount of the inactive eIF4E•4EBP1 complex and reciprocally decreases the active eIF4E•eIF4G complex. The sepsis-induced reduction in eIF4E•eIF4G diminishes mRNA binding with the ribosome and thereby limits muscle protein synthesis.

The metabolic consequences of various catabolic stresses and anabolic stimuli are integrated by mTOR (14) (Figure 3-1). Sepsis and endotoxin decrease mTOR kinase activity as evidenced by the coordinate decrease in mTOR autophosphorylation at Ser2481 as well as the decreased phosphorylation of the mTOR substrates 4E-BP1 and S6K1 (32, 51, 211, 228). However, despite its importance, there is a paucity of data pertaining to the mechanism mediating the sepsis-induced decrease in skeletal muscle mTOR activity. In general, mTOR is partitioned between two large multi-protein complexes having distinct functions. One of the mTOR complexes, mTORC2, is considered rapamycin-insensitive and while an important regulator of the cytoskeleton organization appears to have little influence on mRNA translation (254).

Conversely, the other mTOR complex (mTORC1), consisting of mTOR, GβL (G-protein β-subunit like protein/mLST8), PRAS (proline-rich Akt substrate)-40, raptor (regulatory associated protein of mTOR), and DEPTOR (aka DEP domain containing 6; DEPDC) (56, 253), regulates mTOR activity in a rapamycin-sensitive manner (253) and is altered by sepsis (211). Consistent with this observation, muscle-specific inactivation of raptor, but not rictor, in mice produces muscle atrophy (231). In this regard, raptor is a scaffold protein, which regulates mTOR kinase activity and the subsequent downstream phosphorylation of 4E-BP1 and S6K1. The importance of 4E-BP1 has been discussed above and the ordered phosphorylation of S6K1 activates the protein resulting in the phosphorylation of more than a dozen substrates, many of which affect cap-dependent translation (255). However, whether sepsis modulates the mTOR•raptor interaction as well as other newly recognized protein-protein interactions regulating cap-dependent translation in skeletal muscle has not been investigated, and this gap is addressed by the data provided herein.

Results

Sepsis impairs muscle protein synthesis, mTOR kinase activity and formation of the eIF4F complex. Approximately 24 h after induction of sepsis, translational efficiency of gastrocnemius was assessed *in vivo* and found to be reduced 37% in septic rats compared to time-matched control rats (control = 114 ± 9 vs septic = 72 ± 10 nmol Phe incorporated/mg RNA/h; n = 8 per group; $P < 0.05$). Note that values are normalized to total RNA content, which provides an estimate of ribosomal number in muscle. Therefore, the data indicate the sepsis-induced reduction in muscle protein synthesis was due to impaired translation *per se* and not a decrease in the relative abundance of ribosomes.

Representative Western blots of muscle homogenates for total and phosphorylated proteins playing a central role in regulating protein translation are presented in Figure 3-2A. Sepsis decreased 4E-BP1 phosphorylation as well as the phosphorylation of mTOR at S2448 and S2481, collectively indicating a decrement in mTOR kinase activity. The phosphorylation of S6K1 (on T389) tended to be reduced in muscle from septic rats (data not shown as previously published), but definitive changes were difficult to document because of the relatively low constitutive phosphorylation of S6K1 in the basal fasted state *in vivo*. However, both S1108-phosphorylated eIF4G and S240/244-phosphorylated ribosomal protein S6 (an S6K1 substrate) and rapamycin-sensitive (e.g., mTOR-dependent), were decreased in muscle from septic rats. These sepsis-induced decreases in phosphorylation were independent of a change in the total amount of 4E-BP1, S6, mTOR or eIF4G. Finally, when the same amount of eIF4E was immunoprecipitated from both groups, the amount of 4E-BP1 bound to eIF4E (e.g., inactive complex) was increased and, conversely, the amount of eIF4G bound to eIF4E (e.g., active complex) was decreased in muscle from septic rats, compared to control values (Figure 3-2B). These data indicate sepsis decreases functional eIF4F complex formation. Quantitation for the immunoblots in Figure 3-2 are not presented because comparable changes in these endpoints have been previously reported by our laboratory (32, 51, 211). These data are presented herein to confirm the fidelity of the septic model and provide the necessary background for the remainder of the investigation.

Sepsis alters upstream regulators of mTOR. The overall energy status of muscle is sensed by AMPK, which is activated by phosphorylation in various catabolic conditions (256). AMPK T172-phosphorylation in gastrocnemius from CLP-treated rats was increased by 65%, compared to time-matched control values (Figure 3-3A and 3-3C). The phosphorylation of ACC, a downstream substrate for AMPK, was increased 60%, and this change was independent of a change in total ACC protein (Figure 3-3A and 3-3E). AMPK is an LKB1 substrate and

increased LKB1 S428-phosphorylation is important in activating AMPK (257). Sepsis increased S428-phosphorylated LBK1 greater than 50% (Figure 3-3B and 3-3D). REDD1 is a novel stress-response gene, which is up-regulated by a diverse array of catabolic insults in an AMPK-dependent manner (48) and decreases mTOR activity (49). Muscle from septic rats had a greater than 8-fold increase in REDD1 protein, compared to control values (Figure 3-3B and 3-3F).

As Akt is upstream of mTOR and modulates its S/T kinase activity, we assessed Akt phosphorylation on two sites thought to be necessary for its full activation (253). Sepsis coordinately decreased both T308-phosphorylated (e.g., PI3K-dependent) and S473-phosphorylated (e.g., mTORC2-dependent) Akt in muscle by approximately 40% (Figure 3-4A, 3-4C, and 3-4E). However, there was a discordant sepsis-induced change in the phosphorylation of two downstream Akt substrates. That is, while sepsis decreased PRAS40 phosphorylation (T246) by 40% (Figure 3-4B and 3-4D), no change in S21/9-phosphorylated GSK3α/β was detected in gastrocnemius (Figure 3-4B and 3-4F).

Activated Akt directly phosphorylates TSC2 on T1462 and ultimately relieves the inhibitory action of the TSC1•TSC2 complex on mTOR activity (258). AMPK and REDD1 also alter mTOR kinase activity at least in part by modulation of TSC2 phosphorylation and TSC1•TSC2 complex formation. However, the total amount of TSC1, TSC2, T1462-phosphorylated TSC2 and the amount of the TSC1•TSC2 heterodimer in muscle did not differ between control and septic rats (Figure 3-5).

Sepsis-induced change in mTORC1. mTORC1 is a multi-protein complex regulating protein synthesis and consisting of mTOR, raptor, GβL, PRAS40 and DEPTOR (38, 56, 253). Of these proteins, the total amount of mTOR (Figure 3-1A), PRAS40 (Figure 3-3B), GβL (Figure 3-6A) and raptor (Figure 3-6A) did not differ between control and septic rats. However, sepsis increased raptor phosphorylation (S792) by almost 90% (Figure 3-6B). Finally, sepsis increased

the total DEPTOR, an mTOR-interacting protein believed to be a negative regulator of mTOR (47), in septic muscle by 70%, compared to control values (Figure 3-6C).

Raptor functions as a scaffold protein recruiting substrates to mTORC1 via short TOS (mTOR signaling) motifs in its substrates (38, 56). Therefore, raptor was immunoprecipitated and then immunobloted for PRAS40, 4E-BP1, S6K1 and GβL. While sepsis did not alter the association of raptor with PRAS40 or GβL (Figure 3-7A), it did increase both 4E-BP1 (Figure 3-7A and 3-7B) and S6K1 (Figure 3-7A and 3-7C) binding to raptor by 70%.

In addition, when raptor was immunoprecipitated, the amount of mTOR bound to raptor did not differ between control and septic rats (Figure 3-7A). While this finding was unexpected, it was confirmed by performing the reverse immunoprecipitation procedure (data not shown). However, we did detect a greater than 90% reduction in mTOR•raptor interaction in rats treated with rapamycin (data not shown), indicating our ability to detect a change in this protein-protein complex. With regard to mTORC2, there was no sepsis-induced change in the total amount of rictor in muscle homogenates or the amount of rictor bound to an mTOR immunoprecipitate (data not shown).

Sepsis-induced change in eIF3. The largest translation initiation factor, eIF3, is composed of 13 nonidentical subunits (87). While the physiological function of each subunit is not known, it is clear that eIF3 must bind to mTORC1 for optimal mTOR kinase activity (72). We assessed the total amount of two different subunits, eIF3-b (e.g., one of the 5 conserved core polypeptides essential for translation) and eIF3-f (e.g., the subunit shown to be rapidly degraded by the ubiquitin-proteasome). Our results indicate the total content of eIF3b and eIF3f in muscle homogenates did not differ between control and septic rats (Figure 3-8A). Moreover, there was no sepsis-induced change in the amount of total or phosphorylated eIF4B, total eIF4A1, or total PABP - all proteins implicated in regulating mRNA protein translation (Figure 3-8A). Finally, we immunoprecipitated eIF3b from muscle and determined the amount of bound raptor. Data in

Figure 3-8B and 3-8C indicate that sepsis decreased the amount of the eIF3•raptor complex by 40%.

Leucine-induced changes in mTORC1. In the second study, leucine was orally gavaged approximately 24 h after induction of sepsis or sham surgery. Leucine administration to control rats increased muscle protein synthesis by 37% and this anabolic response was completely absent in septic rats (Figure 3-9A). This leucine resistance was not due to sepsis- or leucine-induced changes in mTOR•raptor binding (Figure 3-9B), but it was associated with concordant changes in raptor binding to eIF3 (Figure 3-9C). The phosphorylation of both 4E-BP1 (Figure 3-9D) and S6K1 (data not shown) was also increased by leucine in control but not septic rats (Figure 3-9D), and such a response is consistent with the change in mTOR kinase activity anticipated by above-mentioned changes in raptor•eIF3b binding. The differential ability of leucine to alter raptor•eIF3 binding could not be attributed to altered raptor S792-phosphorylation (Figure 3-9E) or PRAS40 T246-phosphorylation (Figure 3-9F). Acute leucine stimulation did not alter basal AMPKα or Akt phosphorylation in control rats or the sepsis-induce change in phosphorylation for these two proteins (data not shown). Finally, none of the observed differences between control and septic rats could be attributed to differences in the plasma leucine either under basal conditions (control = 112 ± 28 μmol/L and septic 133 ± 19 μmol/L; P = NS) or in response to the leucine gavage (control = 967 ± 34 μmol/L and septic = 1002 ± 55 μmol/L; P = NS).

Discussion

mTOR signaling occupies a central role in integrating nutrient, energy and growth stimuli to regulate muscle protein synthesis (7) (Figure 3-1). Sepsis and endotoxin impair mTOR kinase activity in muscle as evidenced by the reduction in mTOR autophosphorylation as well as

decreased phosphorylation of downstream substrates 4E-BP1 and S6K1 (32, 228). The data in the present study confirm these observations. While we acknowledge that this study is largely descriptive in nature, our data do suggest potential mechanisms by which sepsis impairs mTOR kinase. Of the two mTOR-containing protein complexes, mTORC1 appears primarily involved in regulating protein synthesis (38, 56). However, our data indicate that under basal post-absorptive conditions sepsis does not alter the assembly of the mTOR•raptor complex in skeletal muscle where protein synthesis and translational efficiency was simultaneously ascertained to be reduced. These findings in septic rats differ from those reported in alcohol-treated rats where impaired muscle protein synthesis and mTOR kinase activity was associated with an increased mTOR•raptor binding (259). The reason for the difference in mTOR•raptor binding between these two catabolic conditions is not evident, and little insight is gained from *in vitro* studies in non-muscle cells where the mTOR•raptor interaction to the withdrawal of serum (e.g., growth factors) and/or amino acids has also often been shown to be divergent (38, 56, 115, 260). We speculate that such divergent results suggest that other protein binding partners are more critically involved in regulating mTORC1 activity under catabolic conditions than the simple association of mTOR and raptor.

Cellular stresses inhibit mTORC1 through a diverse array of potential mechanisms. For example, AMPK activation in response to energy stress inhibits protein synthesis in cultured myocytes and *in vivo* muscle (1). Our data demonstrate an LKB1-dependent sepsis-induced increase in AMPK activation, as evidenced by the enhanced phosphorylation of AMPK and ACC. In turn, AMPK phosphorylates multiple targets. One mechanism whereby AMPK decreases protein synthesis is via the TSC complex, as increased TSC2 phosphorylation as well as enhanced formation of the TSC1•TSC2 heterodimer can negatively regulate mTOR activity (185). However, although AMPK in muscle was activated by sepsis, this mechanism does not appear operational because TSC1•TSC2 association and the AMPK-sensitive T1462-phosphorylation of

TSC2 did not differ between control and septic rats. AMPK may also inhibit mTOR kinase activity in a TSC-independent manner as raptor S792-phosphorylation facilitates recruitment of the 14-3-3 protein (185). Such a sepsis-induced increase in raptor phosphorylation was detected and is consistent with the increased raptor phosphorylation observed in rats administered the AMPK activator AICAR (1) and in cultured myocytes incubated with endotoxin (261). Collectively, these data suggest that AMPK "senses" an energy deficit (e.g., increased AMP/ATP ratio) in muscle, presumably as a result of mitochondrial dysfunction, which may mediate part of the sepsis-induced decrease in protein synthesis in this tissue. Such a sepsis-induced defect in mitochondrial oxidative phosphorylation has been reported in cardiac muscle (262). Our data indicate sepsis also up-regulates the REDD1 protein in muscle, a response comparable to that observed after AMPK activation by AICAR (32). The ability of REDD1 to negatively regulate mTOR appears to proceed via the binding of REDD1 to 14-3-3, the latter of which normally binds to and inhibits TSC2 activity (48). Since such a redistribution of 14-3-3 from TSC2 to REDD1 would not be expected to disrupt the TSC1•TSC2 complex, our data cannot exclude this as a possible mechanism for the sepsis-induced inhibition of mTOR activity.

PRAS40 also binds to raptor and is believed to be a translational repressor, so its over-expression decreases mTOR activity (37). Upon phosphorylation induced by insulin and other growth factors, PRAS40 is released from raptor and thereby enhances protein synthesis by facilitating the engagement of 4E-BP1 and S6K1 with the limiting amount of raptor. Multiple lines of evidence indicate PRAS40 T246-phosphorylation is Akt-dependent (263), and our current data showing a sepsis-induced decrease in both Akt activation and PRAS40 phosphorylation support such a mechanism. Moreover, Akt may directly phosphorylate mTOR (264). Collectively, these results are also consistent with the endotoxin-induced reduction in Akt, mTOR and PRAS40 phosphorylation seen in cultured myotubes (261). Therefore, the lack of a significant difference in the amount of the PRAS40•raptor complex in muscle from septic rats

was unexpected. Although PRAS40 preferentially binds to raptor, it can also interact with the kinase domain of mTOR (37); however, no difference in the amount of the PRAS40•mTOR complex was detected in muscle of control and septic rats (unpublished observation).

In contrast, we did detect a sepsis-induced increase in the amount of 4E-BP1•raptor (Figure 3-7A and 3-7B) and S6K1•raptor complex in skeletal muscle (Figure 3-7A and 3-7C). Recruitment of these mTOR substrates to mTORC1 is necessary for their canonical phosphorylation by mTOR kinase, and raptor is known to preferentially bind the non-phosphorylated substrates (56). We interpret the increased complex formation in raptor immunoprecipitates, in conjunction with the reduced phosphorylation of 4E-BP1 and S6K1 in total tissue homogenates, to indicate there is no sepsis-induced defect in the 4E-BP1 or S6K1 binding to raptor *per se*, but that their subsequent phosphorylation and release from mTORC1 is impaired. This *in vivo* scenario differs from that seen *in vitro* where cells cultured under the catabolic conditions produced by the absence of amino acids and/or growth factors demonstrate a reduced formation of 4E-BP1•raptor (115, 265). It is noteworthy that the sepsis-induced change in mTOR kinase activity was associated with a marked increase in DEPTOR, a negative regulator of mTORC1 activity (47) and the importance of this increase warrants investigation.

eIF3 is a multi-subunit protein complex which serves as a docking site for the binding of several components of the translational machinery (87). Incubation of myotubes with various catabolic agents has been reported to decrease eIF3f content, and eIF3f knockdown decreases protein synthesis (266) and produces muscle atrophy (267). However, our data demonstrate the total eIF3f content did not differ in muscle of control and septic rats. Moreover, the interaction of eIF3 with the eIF4F•mRNA complex facilitates the binding of mRNA to the 43S ribosomal complex and formation of the 48S complex. S6K1 dissociates from eIF3 upon activation (72) and, therefore, catabolic states would be expected to increase the association of hypo-phosphorylated (e.g., inactive) S6K1 with eIF3. Conversely, the binding of mTORC1 to eIF3

would be expected to decrease under conditions where protein synthesis is inhibited. Consistent with this expectation, our current data indicate sepsis decreased the binding of raptor in mTORC1 to eIF3b. Finally, eIF4B is an ancillary factor for optimal ATPase/RNA helicase activity of eIF4A in the functional eIF4F complex. Phosphorylation of eIF4B enhances its association with eIF3 and promotes translation. Although eIF4B associates with eIF3 under insulin-stimulated conditions, but not serum-starved conditions (72), this association was not investigated in the current study because a significant sepsis-induced change in S422-phosphorylated eIF4B in whole muscle homogenate was not detected. The absence of a decrease in eIF4B phosphorylation was unexpected as eIF4B is a known substrate for S6K1 and Akt, and the kinase activity of both proteins was concomitantly down-regulated by sepsis (14, 32, 51).

In our second study, we used acute *in vivo* leucine stimulation to perturb protein balance as a physiological approach to identify potential intracellular signaling intermediates contributing to the sepsis-induced decrease in muscle protein synthesis. In this regard, we confirmed that muscle from septic rats is essentially unresponsive to the ability of leucine to enhance protein synthesis and stimulate mTOR kinase activity (51). As discussed above in the basal state, the sepsis-induced leucine resistance could not be attributed to altered mTOR•raptor binding, but it was consistent with the inability of leucine to increase raptor•eIF3 binding as observed in control muscle. Furthermore, this defect in raptor•eIF3 binding and mTOR kinase activity could not be explained by differential raptor phosphorylation, at least at residue S792, as seen in other conditions (185). As AMPKα directly phosphorylates the S792 residue of raptor (185), these data suggest the sepsis-induced increase in AMPKα activity is an unlikely mediator of leucine resistance. Finally, PRAS40 phosphorylation is necessary for leucine- stimulated mTOR kinase activity (e.g., S6K1 phosphorylation) in cardiac muscle (122). Our data support this conclusion in skeletal muscle of control rats. However, in contrast, the leucine-induced increment in PRAS40 phosphorylation was comparable in both control and septic rats, suggesting PRAS40

phosphorylation may not be causative in the sepsis-induced leucine resistance. The systematic study of other mechanisms by which sepsis impairs the anabolic effect of leucine is beyond the scope of the current manuscript, but it might involve the G protein Rag (268) or Vps34 (269). In conclusion, the multitude of signaling events described herein provide a conceptual framework regarding the ability of sepsis to impair muscle protein synthesis via altering protein-protein interactions within mTOR1, specifically the binding of 4E-BP1 and eIF3 with raptor, which may impair both basal and nutrient stimulated increases in muscle protein synthesis (Figure 3-10).

Acknowledgements

The authors thank Drs. Jefferson and Kimball from the Penn State College of Medicine for the generous gift of eIF4E antibody.

Citation of publication

Abid A. Kazi, Anne M. Pruznak, Robert A. Frost, and Charles H. Lang. Sepsis-Induced Alterations in Protein-Protein Interactions within mTOR Complex 1 and the Modulating Effect of Leucine on Muscle Protein Synthesis. SHOCK, Vol. 35, No. 2, pp. 117—125, 2011.

DOI: 10.1097/SHK.0b013e3181ecb57c

Figure 3—1. **Regulation of muscle protein synthesis**. Simplified schematic of the integrating role of mTOR (mammalian target of rapamycin) in controlling diverse cellular signals, such as hormones, nutrients and stress, regulating protein synthesis. The mTORC1 (mTOR complex 1) consisting of mTOR, raptor (regulatory associated protein of mTOR), GβL (G-protein β-subunit like protein; aka mLST8), PRAS40 (proline-rich Akt substrate) and DEPTOR (aka DEP domain containing 6; DEPDC-6) stimulates translation initiation and protein synthesis by increasing phosphorylation of both 4E-BP1 (eukaryotic initiation factor [eIF]-4E binding protein-1) and S6K1 (ribosomal protein S6 kinase-1). In contrast, mTORC2, consisting of mTOR, rictor (rapamycin-insensitive companion of mTOR), GβL, DEPTOR, mSIN1 (mammalian stress-activated protein kinase-interacting protein), and PRR5 (proline-rich protein-5) appears to have minimal impact on muscle protein synthesis. The phosphorylation of 4E-BP1 decreases the inactive 4E-BP1•eIF4E complex and increases the eIF4E•eIF4G complex thereby enhancing cap-dependent translation. Activation of S6K1 phosphorylates a host of proteins which can differentially regulation protein synthesis. Growth factors, such as insulin and IGF-I (insulin-like growth factor-1), signal through binding to their cognate receptors and regulate mTORC1 via a PI3K (phosphatidylinositol-3' kinase) -Akt-dependent pathway. Akt destablizes the TSC (tuberous sclerosis complex)-1/2 protein-protein complex thereby activating mTOR via the small GTPase Rheb (Ras homolog enriched in brain). In addition, nutrients such as the branched-chain amino acid leucine, increase translation via a mechanism affecting mTOR probably distal to or at the level of Rheb and possibly mediated by the family of Rag G-proteins or Vps34 (vacuolar protein sorting 34). The cellular energy status (i.e., AMP/ATP ratio) transduced by LKB1 modulation of AMPK (5'-AMP activated protein kinase) activity.

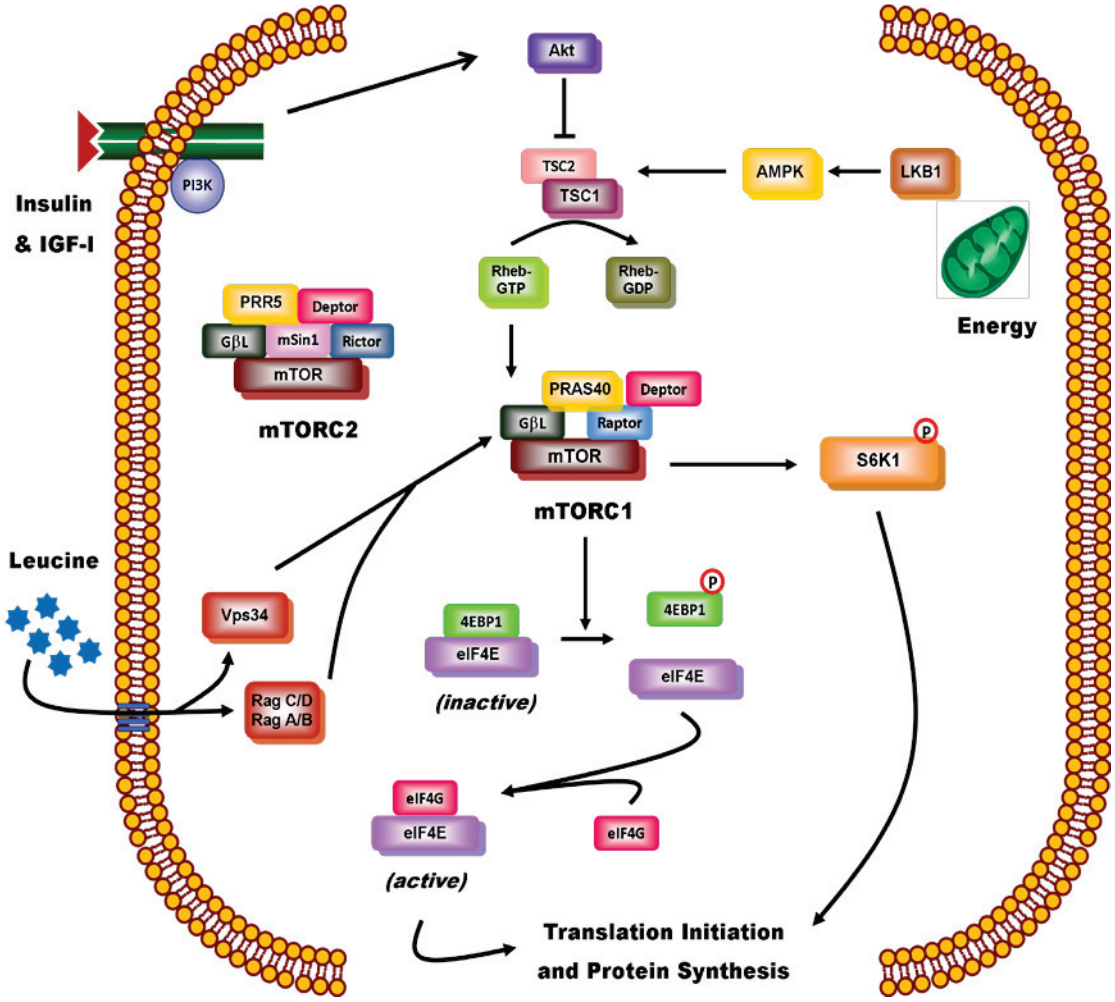
Akt
PI3K
Insulin
& IGF-I
TSC2
TSC1
AMPK
LKB1
Energy
Rheb-
GTP
Rheb-
GDP
PRR5
Deptor
GβL
mSin1
Rictor
mTOR
mTORC2
PRAS40
Deptor
GβL
Raptor
mTOR
mTORC1
S6K1
P
Leucine
Vps34
Rag C/D
Rag A/B
4EBP1
eIF4E
(inactive)
4EBP1
P
eIF4E
eIF4G
eIF4E
(active)
eIF4G
Translation Initiation
and Protein Synthesis

Figure 3—2. **Effect of sepsis on the relative content of total and phosphorylated proteins regulating translation initiation in skeletal muscle**. Gastrocnemius was sampled 24 h after cecal ligation and puncture or from time-matched pair-fed sham control rats. Panel A, muscle homogenates were processed and representative Western blots for phosphorylated mTOR, 4E-BP1, S6 and eIF4G are presented. Panel B, eIF4E was immunoprecipitated (IP) from muscle homogenates and immunoblotted for either 4E-BP1, eIF4G or eIF4E, and representative blots shown. Arrow refers to the most heavily phosphorylated form of 4E-BP1 and hence most active form of the protein. Sample size was 7-10 rats per group for each protein and representative immunoblots are presented.

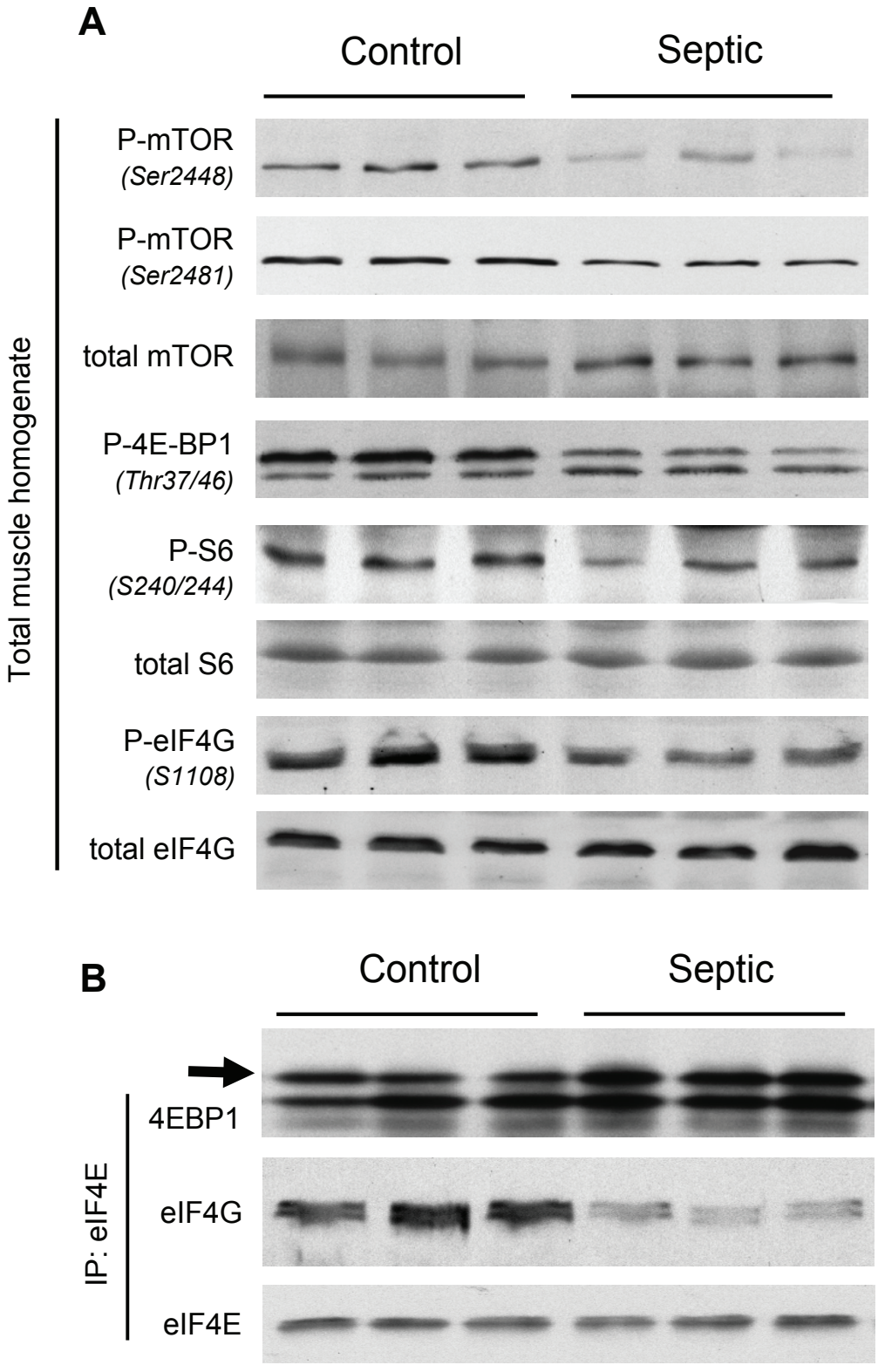
A
Control
Septic
Total muscle homogenate
P-mTOR
(Ser2448)
P-mTOR
(Ser2481)
total mTOR
P-4E-BP1
(Thr37/46)
P-S6
(S240/244)
total S6
P-eIF4G
(S1108)
total eIF4G
B
Control
Septic
IP: eIF4E
4EBP1
eIF4G
eIF4E

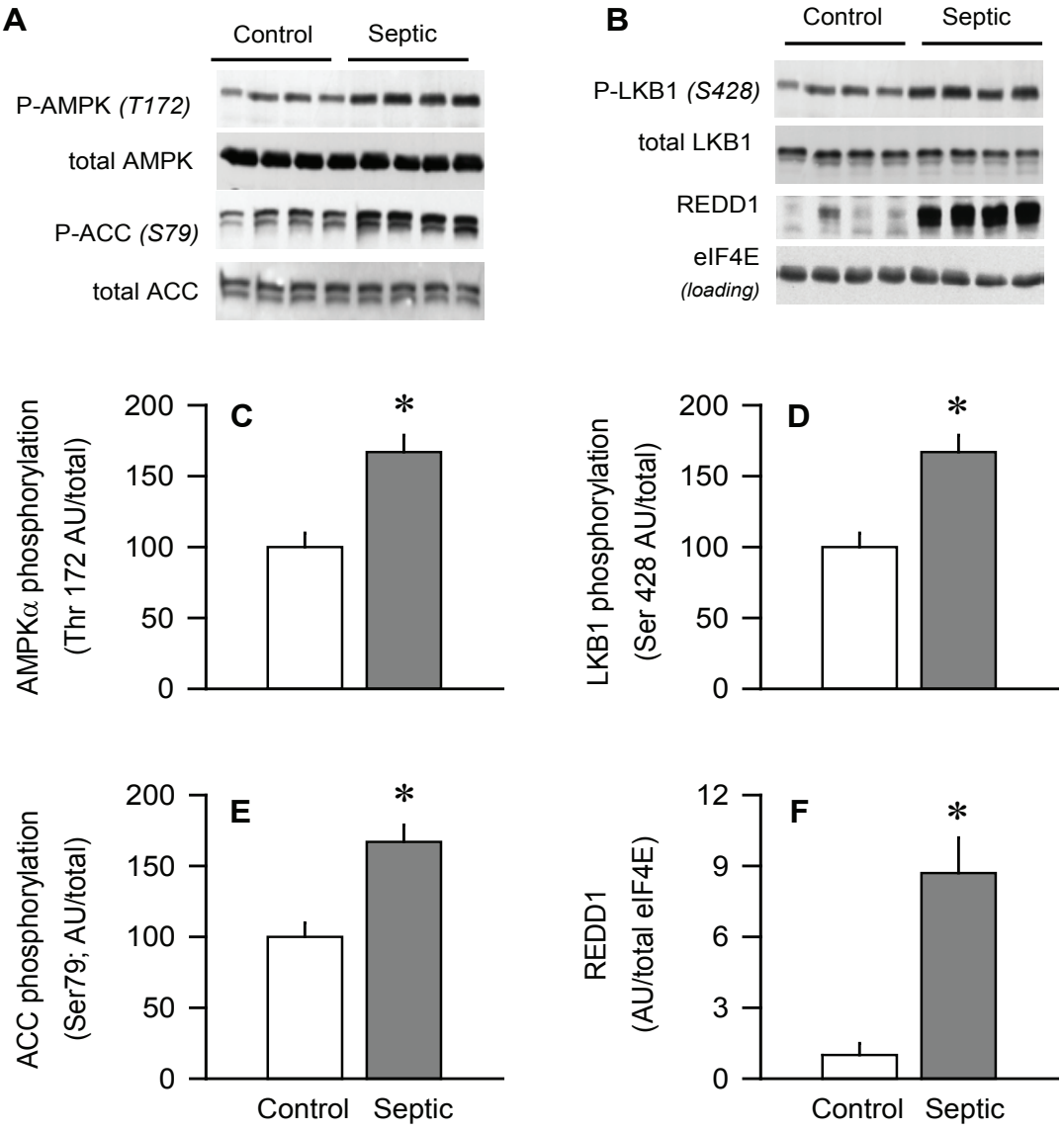

Figure 3—3. **Effect of sepsis on the total amount and phosphorylation of AMPK, ACC, and LKB1 as well as total REDD1 protein in gastrocnemius**. Panels A and B, representative Western blots for total and phosphorylated proteins. Bar graphs, quantitation of all Western blot data for T172-phosphorylated AMPK (panel C), S428-phosphorylated LKB1 (panel D), S79-phosphorylated ACC (panel E), and total REDD1 (panel F) normalized to the total amount of the respective protein or loading control, and the control value set at 100 arbitrary units (AUs). Values are means ± SEM; n = 7-10 rats each. *$P < 0.05$, compared to time-matched pair-fed control values.

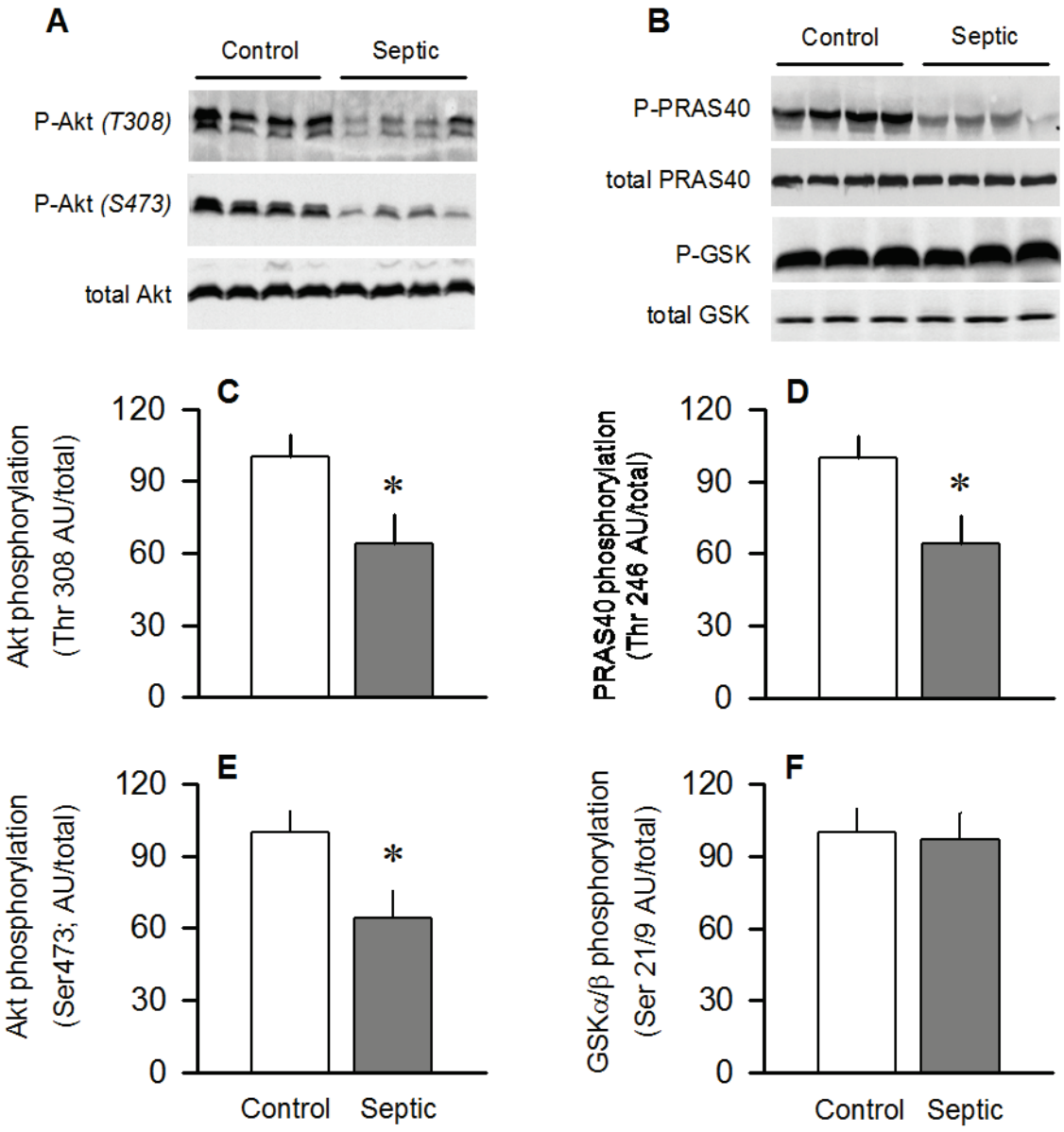

Figure 3—4. Effect of sepsis on phosphorylation of Akt and downstream target proteins PRAS40 and GSK in gastrocnemius. Panels A and B, are representative Western blots of phosphorylated and total Akt, PRAS40 and GSK. Panels C and E, quantitation of all Western blot data for T308- and S473-phosphorylated Akt, respectively, normalized to total Akt. Panels D and F, quantitation of all Western blot data for T246-phosphorylated PRAS40 and S21/9-phosphorylated GSKα/β, respectively, normalized to total protein. Values for control animals were set at 100 AU. Values are means ± SEM; n = 7-10 rats each. *$P < 0.05$, compared to time-matched pair-fed control values.

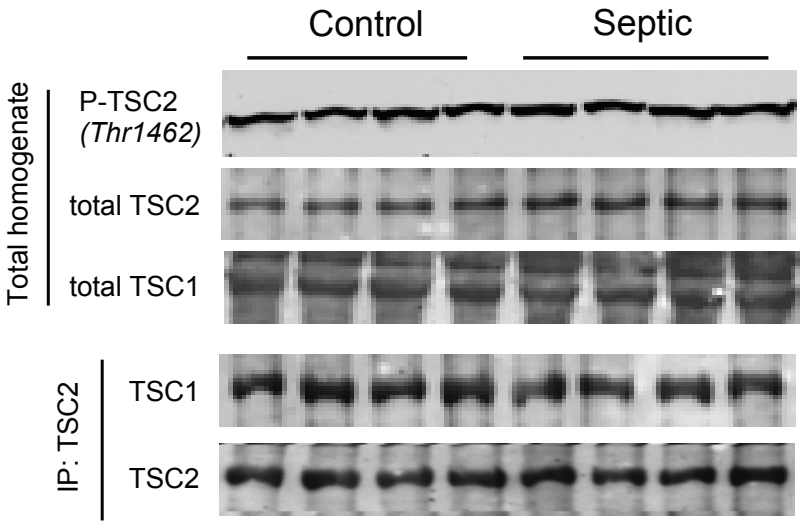

Figure 3—5. **Effect of sepsis on tuberous sclerosis complex (TSC) in gastrocnemius**. Top three panels, representative Western blots from T1462-phosphorylated TSC2 and total TSC2, and total TSC1, respectively. Bottom two panels, representative immunoblots of TSC1 and TSC2 performed after immunoprecipitation (IP) of TSC2 from muscle homogenates. Statistical analysis of data from 7-10 rats per group indicate no statistical significance for any endpoint between control and septic rats (data not shown).

Figure 3—6. **Effect of sepsis on raptor phosphorylation and total DEPTOR**. Panel A, representative Western blots for S792-phosphorylated raptor as well as total raptor, GβL and DEPTOR , respectively. Statistical analysis of all data indicated there was no significant difference in the amount of total raptor or GβL between muscle from control and septic rats (data not shown). Panels B and C, quantitation of Western blot data for phosphorylated raptor and total DEPTOR, respectively, normalized to loading protein and control value set at 100 AU. Values are means ± SEM; n = 5-10 rats each. *$P < 0.05$, compared to time-matched pair-fed control values.

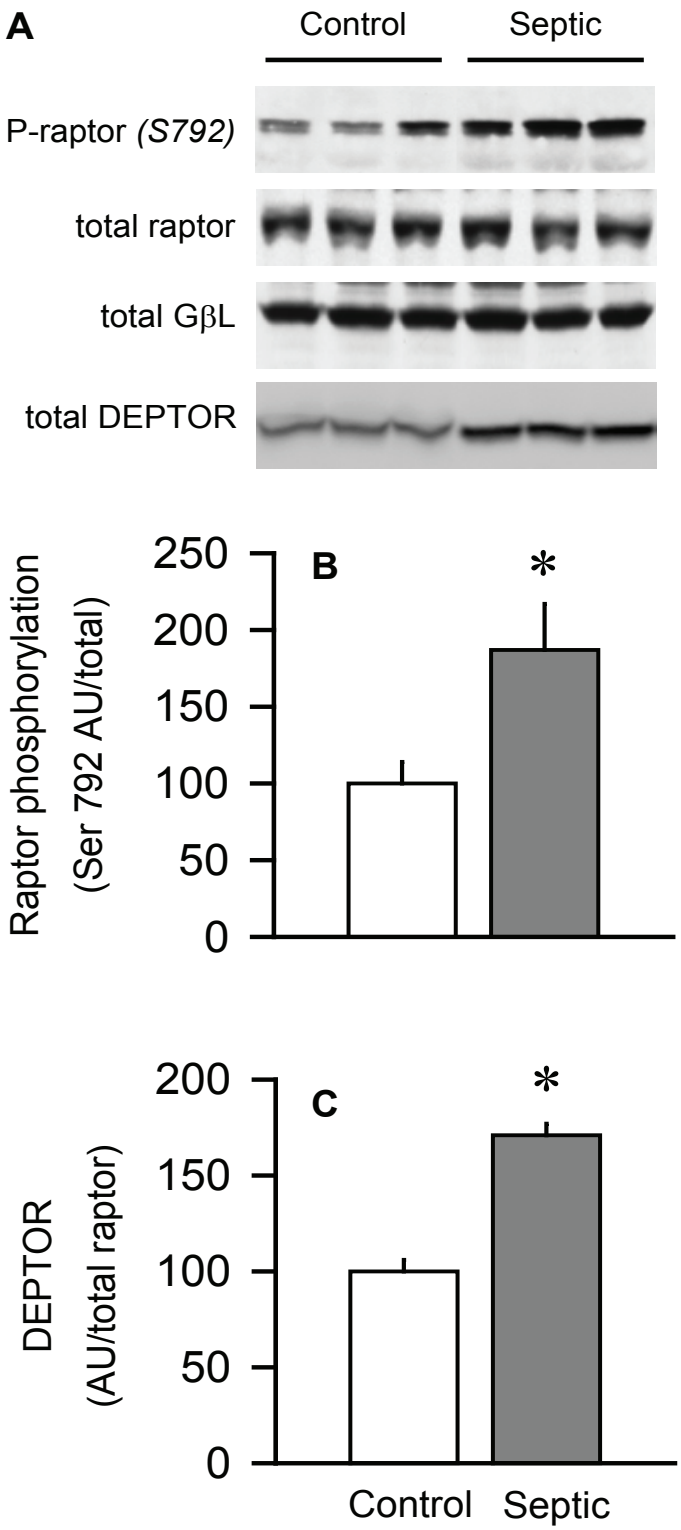
A
Control
Septic
P-raptor (S792)
total raptor
total GβL
total DEPTOR
B
Raptor phosphorylation
(Ser 792 AU/total)
250
200
150
100
50
0
*
C
DEPTOR
(AU/total raptor)
200
150
100
50
0
*
Control
Septic

Figure 3—7. **Effect of sepsis on binding of raptor to various partner proteins in gastrocnemius**. Panel A, raptor was immunoprecipitated (IP) and then immunoblotted for PRAS40, 4E-BP1, S6K1, GβL, mTOR or raptor. Panels B and C, quantitation of Western blot data normalized to amount of raptor in the IP, with control value set at 100 AU. Values are means ± SEM; n = 6 rats each. *$P < 0.05$, compared to time-matched pair-fed control values.

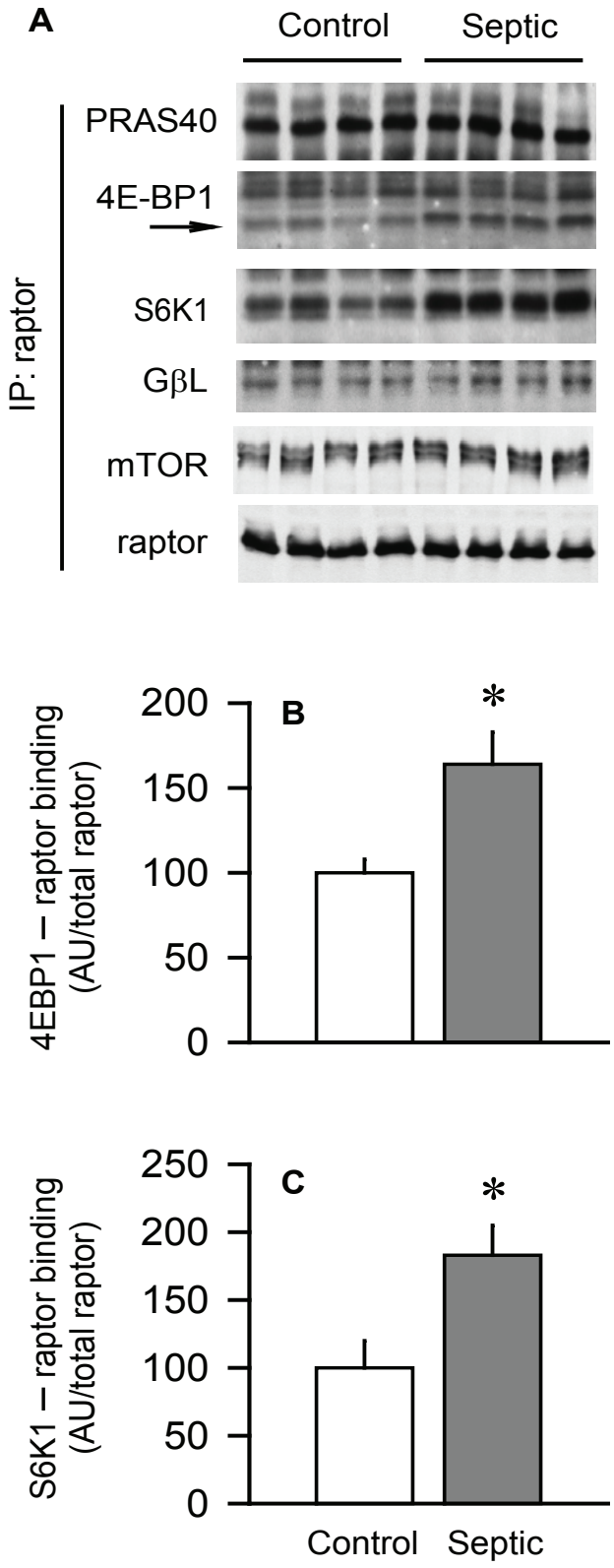
A
Control
Septic
PRAS40
4E-BP1
S6K1
GβL
mTOR
raptor
IP: raptor
B
4EBP1 – raptor binding
(AU/total raptor)
200
150
100
50
0
*
C
S6K1 – raptor binding
(AU/total raptor)
250
200
150
100
50
0
*
Control
Septic

Figure 3—8. **Effect of sepsis on total eIF3 and eIF3•raptor in muscle**. Panel A, representative Western blots of total and S422-phosphorylated eIF4B, eIF4A1, PABP, eIF3-b and eIF3-f. For each of these proteins, there was no statistical difference in the relative amount of the protein in muscle between control and septic rats (quantitative data not shown). Panel B, eIF3b was immunoprecipitated (IP) from muscle and immunoblotting performed for both raptor and eIF3b. Panel C, bar graph, quantitation of Western blot data of eIF3•raptor binding normalized to the amount of eIF3b in the IP, where control value was set at 100 AU. Values are means ± SEM; n = 5 rats each. **P* < 0.05, compared to time-matched pair-fed control values.

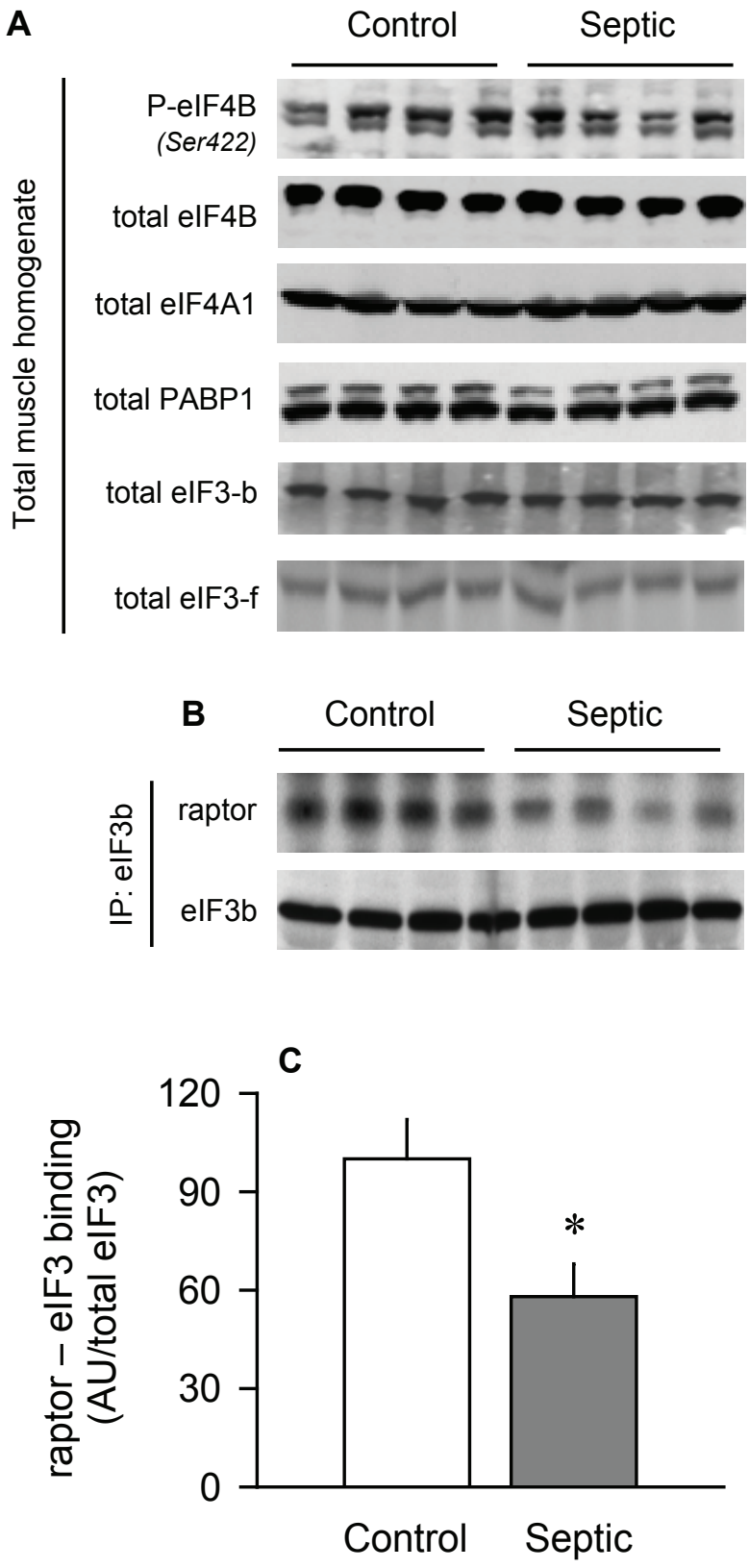
A
Control
Septic
Total muscle homogenate
P-eIF4B
(Ser422)
total eIF4B
total eIF4A1
total PABP1
total eIF3-b
total eIF3-f
B
Control
Septic
IP: eIF3b
raptor
eIF3b
C
raptor – eIF3 binding
(AU/total eIF3)
120
90
60
30
0
*
Control
Septic

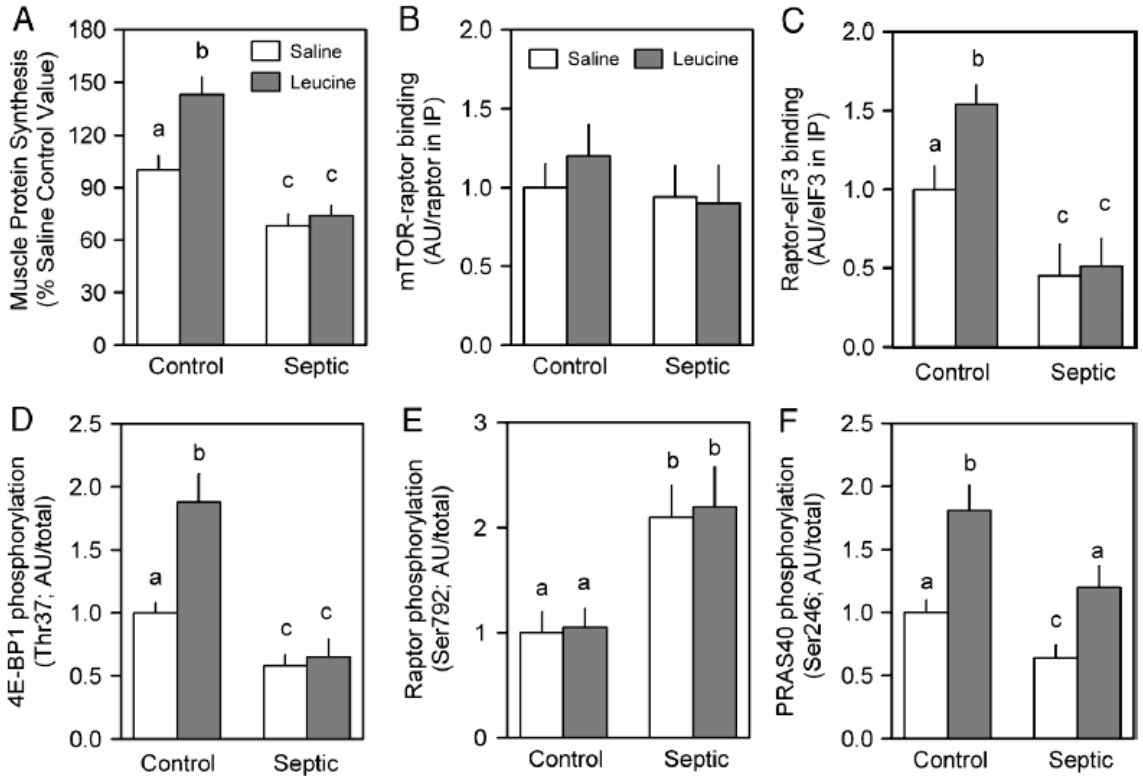

Figure 3—9. **Leucine-induced changes in protein synthesis and mTORC1 in skeletal muscle from control and septic rats**. Gastrocnemius was sampled 30 min after oral administration of a maximally-stimulating dose of the branched-chain amino acid leucine. *In vivo* muscle protein synthesis was determined as described in Methods (panel A). Bar graphs are quantitation of immunoblots after immunoprecipitation (IP) of either raptor (panel B) or eIF3b (panel C). Western blot data from whole muscle tissue homogenates have also been quantitated (panels D, E, and F). There was no sepsis- or leucine-effect on the total amount of raptor, mTOR, eIF3b, 4E-BP1, or PRAS40 (data not shown). Saline-treated control values were arbitrarily set to either 1.0 AU. Values are means ± SEM; n = 7-9 rats per group. Values with different letters are statistically different ($P < 0.05$).

Figure 3—10. **Schematic for sepsis-induced changes in mTORC1**. Under basal conditions S6K1 is associated with the eIF3 at the PIC (pre-initiation complex). In addition, 4E-BP1 is bound to the eIF4E which in turn is bound to the m^7-GTP cap of the mRNA at the 5' end. Under inhibitory conditions (as in rapamycin-treated) mTOR/raptor complex are not part of this mRNA-preinitiation complex. Upon stimulation (as in following anabolic stimulation), mTOR/raptor complex is recruited to the eIF3 complex. Activated mTOR then phosphorylates both S6K1 (at T389) and 4E-BP1 (at several sites in a hierarchy manner). Upon phosphorylation, these mTOR substrates (S6K1 and 4E-BP1) dissociate from the eIF3. The unbound dissociated (phosphorylated) S6K1 can be further phosphorylated by PDK1 at T229, this latter secondary phosphorylation is believed to be required for the full activation of the S6 kinase which is capable of phosphorylating more than 10 known substrates. All abbreviations are defined in Figure 3-1.

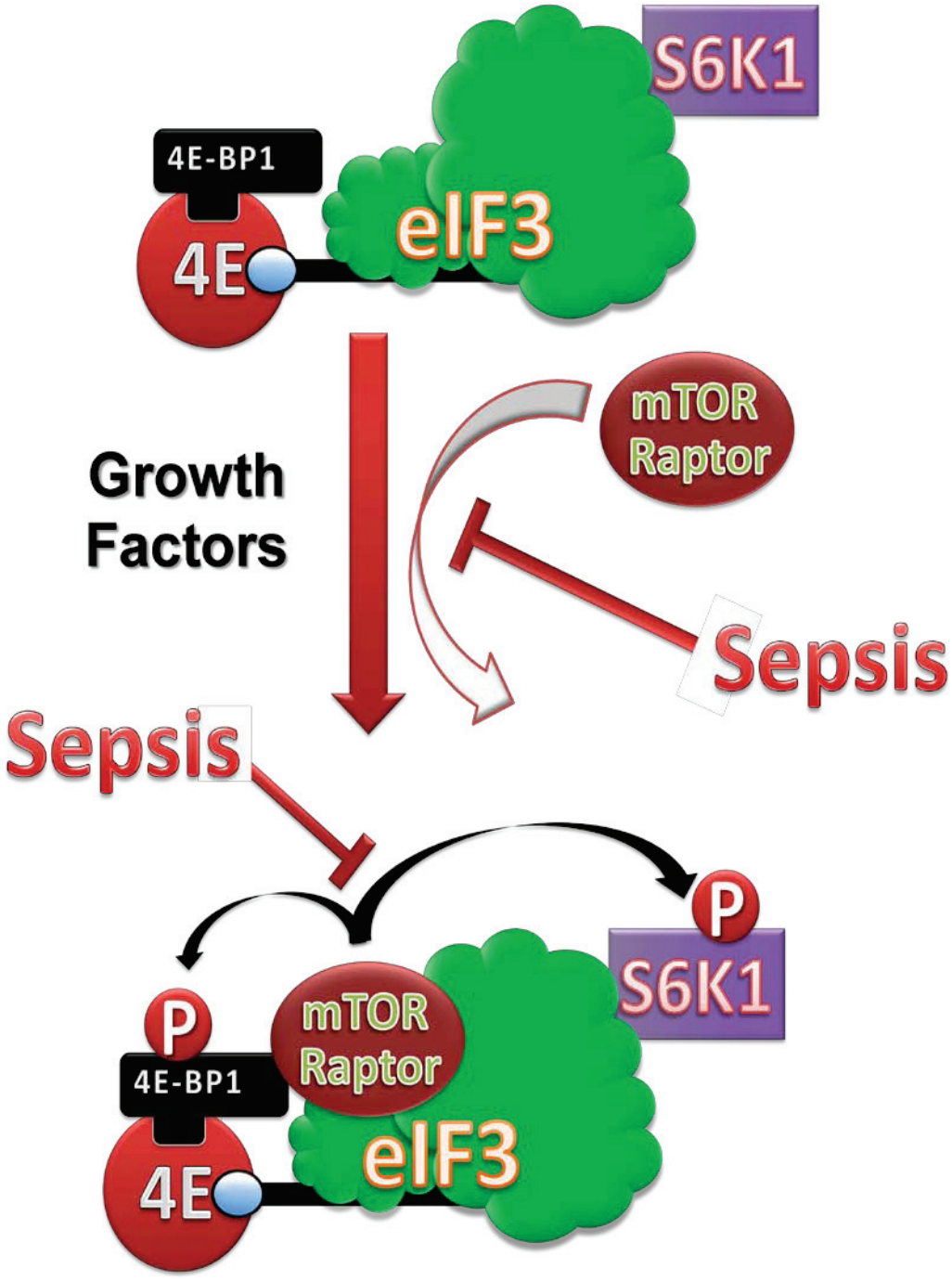
S6K1
4E-BP1
4E
eIF3
Growth
Factors
mTOR
Raptor
Sepsis
Sepsis
P
S6K1
P
mTOR
Raptor
4E-BP1
4E
eIF3

Chapter 4

PRAS40 regulates protein synthesis and cell cycle in C2C12 myoblasts

Abstract

PRAS40 is an mTOR binding protein which has complex effects on cell metabolism. Our study tests the hypothesis that PRAS40 knockdown (KD) in C2C12 myocytes will increase protein synthesis via up-regulation of mTOR-S6K1 pathway. PRAS40 KD was achieved using lentiviruses to deliver shRNA targeting PRAS40 or a scrambled control. C2C12 cells were used as either myoblasts or differentiated to myotubes. Knockdown reduced PRAS40 mRNA and protein content by 80% of time-matched control values but did not alter the phosphorylation of mTOR substrates, 4E-BP1 or S6K1, in either myoblasts or myotubes. No change in protein synthesis in myotubes was detected as measured by the incorporation of ^{35}S-methionine. In contrast, protein synthesis was reduced 25% in myoblasts. PRAS40 KD in myoblasts also decreased proliferation rate with an increased percent of cells retained in G1 phase. PRAS40 KD myoblasts were larger in diameter and had a decreased rate of myotube formation as assessed by myosin heavy chain content. Immunoblotting revealed a 25-30% decrease in total p21 and S807/811 phosphorylated Rb protein considered critical for G1 – S phase progression. Reduction in protein synthesis was not due to increased apoptosis as cleaved caspase-3 and DNA laddering were not different between groups. Our results suggest that a reduction in PRAS40 specifically impairs myoblast protein synthesis, cell cycle, proliferation, and differentiation to myotubes.

Introduction

Skeletal muscle is a dynamic and plastic tissue that undergoes both acute and chronic changes in response to various external stimuli. Muscle serves as the largest protein reservoir in the body and can be called upon as a source of energy as the physiological need arises. Protein stores in muscle are maintained by the ingestion of protein/amino acid - containing meals which stimulate protein synthesis and suppress protein breakdown (9, 10). Conversely, during periods of starvation or disuse, muscle protein breakdown exceeds protein synthesis (13), providing amino acids to support hepatic gluconeogenesis and acute phase protein synthesis. Protein synthesis in general is largely regulated at the level of translation initiation which in turn is primarily regulated by mTOR (mammalian target of rapamycin) (270, 271).

Normal cellular function is dependent on the integration and regulation of cell signaling pathways governing cell cycle, protein synthesis and degradation, cell proliferation, and apoptosis. The S/T protein kinase mTOR plays an important role in these pathways (25, 27, 272), and dysregulation of mTOR signaling networks leads to numerous diseases (273). mTOR is contained within two distinct complexes, mTORC1 and mTORC2 (38, 72, 271). The former complex is composed of mTOR, raptor, LST8/G-protein β-subunit like protein (GβL), Proline Rich Akt Substrate 40kD (PRAS40), and DEPTOR (274).

Exposure of muscle to growth factors and nutrients increases protein translation initiation via the mTOR pathway thereby stimulating protein synthesis (103). In response to growth factor signaling, the PI3K pathway enhances Akt via PDK1. Activated Akt then phosphorylates PRAS40 on T246 releasing PRAS40 from the mTOR/raptor complex and enhances the binding of PRAS40 to the cellular anchor protein 14-3-3 (37, 275). Conversely, in the absence of growth factors, PRAS40 is hypo-phosphorylated and remains bound to mTOR-raptor and thereby inhibits binding of other mTOR substrates, such as the ribosomal protein S6

kinase (S6K1) and the translational repressor eukaryotic initiation factor 4E binding protein (4E-BP1), thereby suppressing CAP-dependent protein translation initiation (37).

The necessity of mTOR activation for the subsequent phosphorylation of S6K1 and 4E-BP1 has been demonstrated previously, however, the role of PRAS40 in mTORC1 is poorly defined. Present data place PRAS40 either at the level of mTOR (as an Akt substrate) or as a direct downstream substrate of mTOR where it is phosphorylated on S183 (118, 276). Several reports have implicated PRAS40 as a negative regulator of mTOR via its inhibition of mTOR substrates (37, 114, 115), while in contrast others have shown PRAS40 is required for mTOR signaling (119). These opposing data have given rise to controversies regarding the role of PRAS40 in regulating protein translation initiation via mTORC1. Despite several reports implicating PRAS40 as a regulator of protein translation initiation in a variety of cells, there is a paucity of information related to its role in skeletal muscle. In the previous chapter, we identified that sepsis reduced phosphorylation of PRAS40 and this was associated with reduced protein translation initiation, given the pivotal role mTOR plays in response to environmental cues in regulating protein translation initiation, cell cycle and proliferation, it is reasonable to suspect that one or more of these mTOR functions might be altered by PRAS40 in myocytes. Therefore, the purpose of our current investigation was to examine changes in C2C12 myocyte protein synthesis, cell proliferation and cell cycle in response to PRAS40 knockdown using shRNA-based *in vitro* experimental approaches.

Results

Effect of PRAS40 knockdown in C2C12 myotubes. C2C12 stable cell lines deficient in PRAS40 or scramble controls were created using short hairpin RNA (shRNA). shRNA were retrovirally delivered to myoblasts and some of these myoblasts were allowed to differentiate and

form myotubes following puromycin selection. shRNA directed towards PRAS40 in myotubes reduced PRAS40 protein levels by greater than 80%, compared to scramble control values (Figure 4-1A and 4-1B). As anticipated PRAS40 knockdown also reduced the PRAS40 mRNA content by ~65% in infected myotubes (Figure 4-1C). In contrast, PRAS40 knockdown did not alter the mRNA content for 4E-BP1, mTOR, S6K1 or raptor, proteins central to the functioning of the mTOR signaling pathway.

Knockdown of PRAS40 in differentiated myotubes did not alter global protein synthesis compared with scramble controls as measured by ^{35}S-methionine incorporation into protein (Figure 4-2A). To determine whether the responsiveness of the PRAS40 knockdown cells to external stimuli was compromised, cells were incubated with either an anabolic (IGF-I) or catabolic (AICAR) agent. Addition of IGF-I to the myotubes increased protein synthesis, whereas, AICAR inhibited protein synthesis (Figure 4-2A). Contrary to expectations, the magnitude of the changes produced by these agents was the same in both control and PRAS40 knockdown cells. To confirm protein synthesis data, we performed Western blotting for mTOR and its substrates and binding partners. PRAS40 knockdown cells remained responsive to both types of stimuli and their response was similar and comparable to the scramble controls (Figure 4-2B). For example, IGF-I increased phosphorylation of S6K1 (T389) and PRAS40 (T246), while AICAR increased phosphorylation of raptor (S792) and AMPK (T172).

PRAS40 knockdown decreases protein synthesis in C2C12 myoblasts. While the preceding data were obtained from post-mitotic differentiated myotubes (>95%), we also determined whether myoblasts would yield comparable results. In myoblasts, the knockdown of PRAS40 decreased global protein synthesis by ~25% under basal conditions (Figure 4-3A). Despite the decrease in basal protein synthesis in the PRAS40 knockdown cells, the ability of these cells to respond positively or negatively to IGF-I or AICAR, respectively, was unaltered. Contrary to expectations, the decreased protein synthesis observed in PRAS40 knockdown cells

under basal conditions was not associated with any difference in phosphorylation state of the mTOR substrates S6K1 and 4E-BP1, compared to the scramble control values (Figure 4-3B) or changes in protein-protein interaction of PRAS40-raptor-eIF3 between the two groups (Figure 4-3C). In myoblasts, the ability of IGF-I to stimulate T389 phosphorylation of S6K1 and AICAR to increase S792 phosphorylation of raptor did not differ between scrambled and PRAS40 knockdown cells (Figure 4-3D).

PRAS40 knockdown alters myoblast cell size and proliferation. Vander Haar *et al* (114) reported that overexpression of wildtype PRAS40 decreased cell size in HEK 293 cells, whereas, knockdown of Lobe (a PRAS40 ortholog in *Drosophila*) increased cell size (37). Hence, we hypothesized that knocking down PRAS40 would also increase cell size in myocytes. PRAS40 knockdown increased the diameter (16.8 ± 0.1 μm) of low passage proliferating (~60% confluent) myoblasts compared to scramble control cells (14.0 ± 0.1 μm) as measured using either the Coulter counter particle size analyzer (Figure 4-4A) or FACS flow cytometry analysis (data not shown). The PRAS40 knockdown cells also had an increased mean cell volume (Figure 4-4B). However, unexpectedly we found that PRAS40 knockdown cells grew slower compared to time-matched scramble controls (Figure 4-5A), although both cell types were seeded at the same initial density. To exclude anchorage-dependence/altered capacity to attach, cells were seeded and counted 4-8 h after seeding to allow for attachment. An equal number of cells were harvested following trypsinization in both the control and PRAS40 knockdown cells, suggesting no significant difference in the ability of PRAS40 knockdown cells to attach to the culture plates (data not shown). To confirm that the proliferation rate of PRAS40 knockdown cells was slower, we used an independent colorimetric assay based on the conversion of the MTT tetrazolium salt to its formazan product. Consistent with the above presented data, the MTT assay revealed that PRAS40 knockdown cells had a 25% lower rate of proliferation (Figure 4-5B).

PRAS40 and apoptosis. To determine whether an increased rate of apoptosis in PRAS40 knockdown cells was responsible for the slower rate of proliferation we collected low molecular weight DNA and performed an apoptosis DNA laddering assay. Figure 4-6A illustrates there is no difference between the scramble control and the PRAS40 knockdown cells and that neither group of cells were undergoing active apoptosis within the detectable limits of the assay. These findings were confirmed by Western blotting for caspase-3/ PARP cleavage which failed to detect a significant difference between the groups. Myoblasts incubated with staurosporine were used as a positive control and demonstrated increased caspase-3 and PARP cleavage (Figure 4-6B). Collectively, these data suggest that the decreased protein synthesis and reduced proliferation in the PRAS40 knockdown myoblasts cannot be attributed to increased apoptosis.

PRAS40 knockdown inhibits cell cycle progression. To determine the mechanism for the lower proliferation rate in PRAS40 knockdown cells, we stained myoblasts with propidium iodide to study cell cycle events. Compared to control values, PRAS40 knockdown myoblasts had a greater proportion of cells in G1/G0 of the cell cycle and fewer cells in active S – phase (Figure 4-7A and 4-7B, respectively; and Table 4-1). Because PRAS40 knockdown cells were arrested in G1/G0 of the cell cycle, we assessed whether proteins regulating cell cycle, especially the G1 – S transition, were concomitantly altered. Figure 4-7C illustrates there was a 25-30% reduction in S807/811 phosphorylation of Rb, consistent with reduced progression from G1 to S phase. In myoblasts with PRAS40 knockdown a 20-30% reduced expression of p21 was also detected in these cells. There was no difference in the other proteins analyzed which regulate cell cycle - p53, cdk 4/6, p27 and cyclin D1 (Figure 4-7D).

PRAS40 alters myogenesis. Our data demonstrate the presence of a concomitant delay in proliferation and altered cell cycle in PRAS40 knockdown myoblasts. Since mTOR also regulates autophagy which in turn plays an important role in cell differentiation (277, 278), we

determined the expression of proteins important in regulating autophagy. While there were no changes in the early markers for autophagy including, Atg 7 and Beclin 1 (Figure 4-8A), our data indicate that PRAS40KD decreased the ratio of LC3B-II/LC3B-I (Figure 4-8A and 4-8B).

Next we determined whether such changes might be of physiological relevance to skeletal muscle development. In this regard, we seeded the same number of myoblasts and tracked their progression to form myotubes (Figure 4-9). We observed that control cells reached confluent status earlier than the PRAS40 knockdown and began fusion to form substantial number of myotubes by day 5, whereas PRAS40 knockdown cells only sparsely formed myotubes by day 5. These data suggest that myotube formation and myogenesis is delayed in PRAS40 knockdown cells.

To quantitate these findings, cell lysates were collected at various stages of development of myoblasts and myotubes to measure the expression of myosin heavy chain (MHC) – a protein expressed only in differentiated matured myotubes. While MHC expression was absent in myoblasts (day 3) and there was an initial delay in MHC expression in PRAS40 knockdown cells (days 5 and 7), by day 9 the expression of MHC in both scramble control and PRAS40 knockdown cells were comparable (Figure 4-10A and 4-10B). The protein content of the muscle transcription factor MyoD did not differ between scramble control and PRAS40KD cells (Figure 4-10A).

Discussion

In vitro studies performed in HEK293 and other rapidly dividing cell lines have identified PRAS40 as an mTORC1 binding protein and a regulator for mTOR activity (37, 114, 118, 119). As the reduction of PRAS40 using RNAi leads to increased phosphorylation of mTOR substrates S6K1 and 4E-BP1, it has been posited that PRAS40 functions as a negative regulator of mTOR

and translation initiation. To the contrary, our results show PRAS40 is required for protein synthesis in rapidly dividing myoblasts and the reduction of PRAS40 in these cells decreases protein synthesis. In contradistinction, reduction of PRAS40 did not significantly affect protein synthesis in differentiated myotubes indicating a developmental-specific effect of PRAS40 in this cell type. The reason for this difference between our findings and earlier reports is unclear but may be related to differences in cell type, experimental conditions, end-point measured, and /or the extent of PRAS40 knockdown. Furthermore, knockdown of PRAS40 in both myoblasts and myotubes did not alter the ability of these cells to respond to either an anabolic (IGF-I) or catabolic (AICAR) stimuli. Our data show that addition of IGF-I increased phosphorylation on S6K1 (T389) and PRAS40 (T246) in these myocytes, while treatment with AICAR increased the phosphorylation on raptor (S792). Correspondingly, protein synthesis was altered as anticipated in both myoblasts and myotubes in response to IGF-I and AICAR. Collectively, these data demonstrate the normal responsiveness of PRAS40 knockdown cells – both myoblasts and myotubes.

Cell cycle progression is linked to cell size and typically cells must attain a certain size before they replicate and divide. However, exceptions to this norm may be observed under artificial (e.g., pharmaceutical drugs or transformed immortalized cancer cells) or disease (e.g., cardiac hypertrophy) conditions. mTOR also plays an important role in regulating cell growth (59, 133, 272, 279). In this regard, the over expression of PRAS40 decreases cell size in HEK293 cells. Conversely, knockdown of PRAS40 in the same cells and of Lobe – an ortholog of PRAS40 in *Drosophila* S2 cells - increased cell size (37, 114). Consistent with these earlier observations, knockdown of PRAS40 in myoblasts also increased cell size. However, unexpectedly, PRAS40 knockdown cells were fewer in number, compared with the scramble controls. Furthermore, we observed that PRAS40 knockdown myoblasts had a slower rate of proliferation. This change could not be attributed to differential cell binding or attachment to the

culture plates. Another potential explanation for the decreased cell number is increased apoptosis in myoblasts with PRAS40 knockdown. However, the role of PRAS40 in regulating apoptosis is controversial. Whereas knockdown of PRAS40 inhibited tumor growth and proliferation via induction of apoptosis in melanoma cells (187), PRAS40 knockdown reduced the ability of TNFα and cycloheximide to induce apoptosis in HeLa cells (280). Using two different approaches – caspase 3 cleavage and DNA laddering - our data suggest that the lower proliferation rate in myoblasts could not be attributed to increased apoptosis. In general, it is believed that mTOR integrates signals to regulate cell size and cell cycle. However, increased cell size due to inhibition of myostatin was shown to be insensitive to rapamycin suggesting an mTOR-independent regulation of muscle size. Also, maintenance of the hypertrophy during chronic myostatin deficiency does not require altered Akt/mTOR activity (281, 282). Previously, Hentges *et al* implicated mTOR in regulating cell size and proliferation via different and independent mechanisms (22). Therefore, although PRAS40 knockdown cells are larger than controls, cells deficient in PRAS40 have lower proliferation suggesting that PRAS40 may be an important modulatory binding partner of mTOR which potentially uncouples cell size and cell cycle, thus, proliferation.

mTOR regulates cell cycle as evidenced by the ability of rapamycin to arrest cells in the G1 phase (22, 133, 270, 283-285). Propidium iodide staining revealed that myoblasts with PRAS40 knockdown had a greater proportion of cells in the G1/G0 phase, compared to scramble controls, and fewer cells in the active S phase. Collectively, these data suggest PRAS40 is required for mTOR activity in regulating cell cycle and that knockdown of PRAS40 in myoblasts retarded cell cycle progression. Alternatively, we cannot exclude the possibility that the reduction in PRAS40 alters cell cycle kinetics by an undetermined mechanism which is mTOR-independent. Since PRAS40 knockdown cells were arrested in G1/G0 of the cell cycle we focused on elucidating the underlying mechanism causing cell cycle arrest. Regulation of cell

cycle progression by the cyclin-dependent kinase (cdk) inhibitor p21 blocks cells from entering into the DNA synthesis (or S) phase in many cell types. The opposite role of p21 in skeletal muscle growth and differentiation compared to its role in HEK293 cells has received recent attention. In HEK293 cells, AICAR increased phosphorylation of p53 with an increased expression of p21 (190, 286). While p21 null mice develop normally during embryogenesis (287) due to the presence and activation of another redundant cdk inhibitor – p57 (288), myocytes from these mice have difficulty differentiating to myotubes (198). C2C12 myoblasts treated with AICAR were arrested in G1 and H9c2 cardiomyocytes had reduced expression of p21 protein (190). Since PRAS40 knockdown myoblasts were arrested in G1, we screened for proteins which regulate cell cycle especially in G1 – S transition. Retinoblastoma protein (pRb) regulates G1 exit in the cell cycle. pRb is phosphorylated upon mitogenic activation which disrupts pRb binding to E2F transcription factor thus allowing transcription of proteins which are essential for G1 – S transition. We found that after PRAS40 knockdown there was a reduction of pRb S807/811 phosphorylation consistent with reduced progression from G1 to S phase. In contrast, no change in the total amount of p53, cdk 4/6, cyclin D1 or p27 was detected. It has been reported that protein expression of p21 can be independent of these other regulatory proteins (289, 290). However, we observed that similar to AICAR treatment, PRAS40 knockdown myoblasts had reduced expression of p21. Because decreased p21 expression adversely affects myotube formation and differentiation, we determined whether PRAS40 knockdown myoblasts exhibited delayed differentiation.

These results are consistent with those of Williamson *et al* showing that prolonged G1/G0 and reduced p21 expression in C2C12 myocytes produced by AICAR decreased cell cycling and delayed myotube formation (190). To determine whether PRAS40 knockdown would delay myoblast fusion and thereby myotube formation, we monitored the progression and ability of these cells to form myotubes in culture. Time lapse imaging and Western blotting

analysis for myosin heavy chain (a marker for matured myotubes) indicated that knockdown of PRAS40 in C2C12 myoblasts delayed myotube formation. Autophagy is another mTOR regulated cellular event that plays an important role in differentiation of myoblasts to mature myocytes (158, 167, 168, 186). Our results indicate that PRAS40KD decreases autophagy in myoblasts as inferred from the reduction in LC3BII/LC3B-I ratio. These changes suggest PRAS40 regulates muscle proliferation and differentiation via regulation of cell cycle and autophagy regulatory proteins.

In summary, PRAS40 knockdown in differentiated myotubes did not alter protein synthesis. In contrast, PRAS40 knockdown in C2C12 myoblasts decreased protein synthesis independent of a change in the phosphorylation of S6K1 and 4E-BP1, suggesting that PRAS40 is not a negative regulator of mTOR –mediated translation initiation in this cell type. Moreover, both myoblasts and myotubes remained responsive to anabolic and catabolic stimuli when PRAS40 was reduced. Knockdown of PRAS40 inhibited G1-S phase transition of cell cycle and lowered proliferation rate in myoblasts supporting the contention that PRAS40 is required for this aspect of mTOR signaling. Our data suggest that PRAS40 knockdown in C2C12 myoblasts impairs the ability of mTOR to regulate cell size and proliferation and that PRAS40 is required for these mTOR-associated functions. We confirm that PRAS40 plays an important role in regulation of cell size and show that it also affects cell proliferation and differentiation. Understanding the role of PRAS40 in proliferation and differentiation of myocytes as outlined here may prove important in designing new strategies to manage the muscle wasting associated with catabolic insults such as sepsis, alcohol abuse, and aging.

Acknowledgements

We thank Drs. Ly Hong-Brown and Robert Frost for discussions and critical readings of

the manuscript. We thank Danuta Huber and Anne Pruznak for technical support, Dr. David Spector for technical help with viral purification and transfection, Dr. Arun Das with MTT assay and reagents, and Dr. Samina Alam for help with the DNA laddering assay and reagents. We also thank David Stanford of the Penn State Flow Cytometry Core facility for help with cell cycle analysis imaging. This work was supported in part by grants from the NIH (GM38032 and AA11290) to CHL and Pennsylvania Department of Health using Tobacco Settlement Funds (AAK). The Department specifically disclaims responsibility for any analyses, interpretations or conclusions.

Citation of publication:

Kazi, A. **A**. **and C**. **H**. **Lang**. PRAS40 regulates protein synthesis and cell cycle in C2C12 myoblasts. *Mol Med* **16**(9-10): 359-371, 2010.

DOI: 10.2119/molmed.2009.00168

Figure 4—1. **Effect of PRAS40 knockdown in C2C12 myotubes**. Panel A: representative Western blot of PRAS40 protein in Control (shScramble) and PRAS40 knockdown (shPRAS40) myotubes. Panel B: quantification of Western blot data. Values are means ± SE; n = 10 per group. $P < 0.05$ compared to time-matched scramble control values. Panel C: representative autoradiographs from RPAs for PRAS40 and other proteins important in controlling protein synthesis. Except for PRAS40, there are no changes in the mRNA expression. L32 serves as loading control.

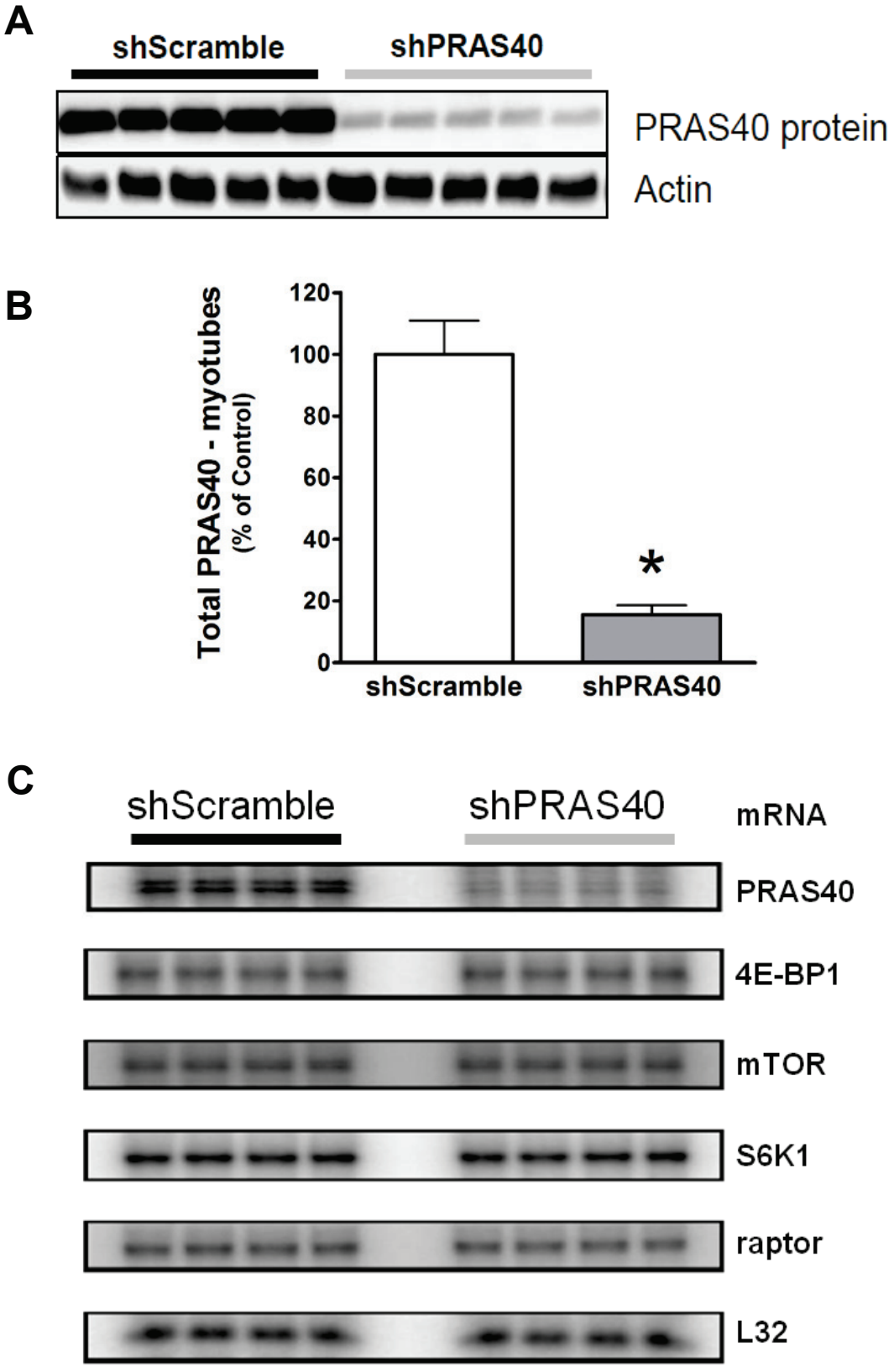
A
shScramble
shPRAS40
PRAS40 protein
Actin
B
Total PRAS40 - myotubes
(% of Control)
120
100
80
60
40
20
0
*
shScramble
shPRAS40
C
shScramble
shPRAS40
mRNA
PRAS40
4E-BP1
mTOR
S6K1
raptor
L32

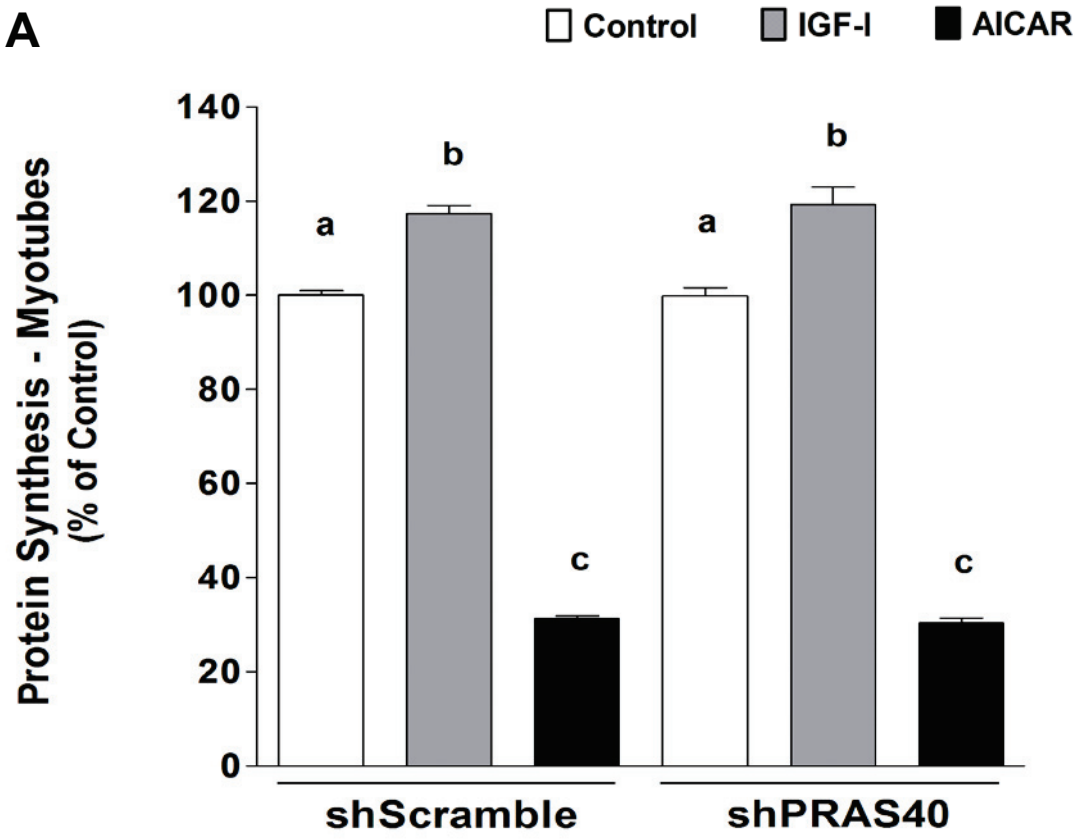

Figure 4—2. **Effect of IGF-I and AICAR on shScramble and shPRAS40 knockdown myotubes**. Myotubes transfected with shScramble and shPRAS40 and incubated with vehicle (Control), AICAR (2 mM; 8 h) or IGF-I (100 ng/ml; 20 min), and labeled with 35S-methionine. Panel A (above): Protein synthesis in myotubes. Values are means ± SE for n = 8-10 for each condition. Means not sharing the same superscript (a, b, and c) are significantly different ($P<0.05$). For quantification, data were normalized to scramble control values. Panel B (right): Representative Western blots of various total and phosphorylated proteins where cells were treated as described above except that the isotope was omitted. Representative blot of 3 independent experiments with 4 replicates per experiment.

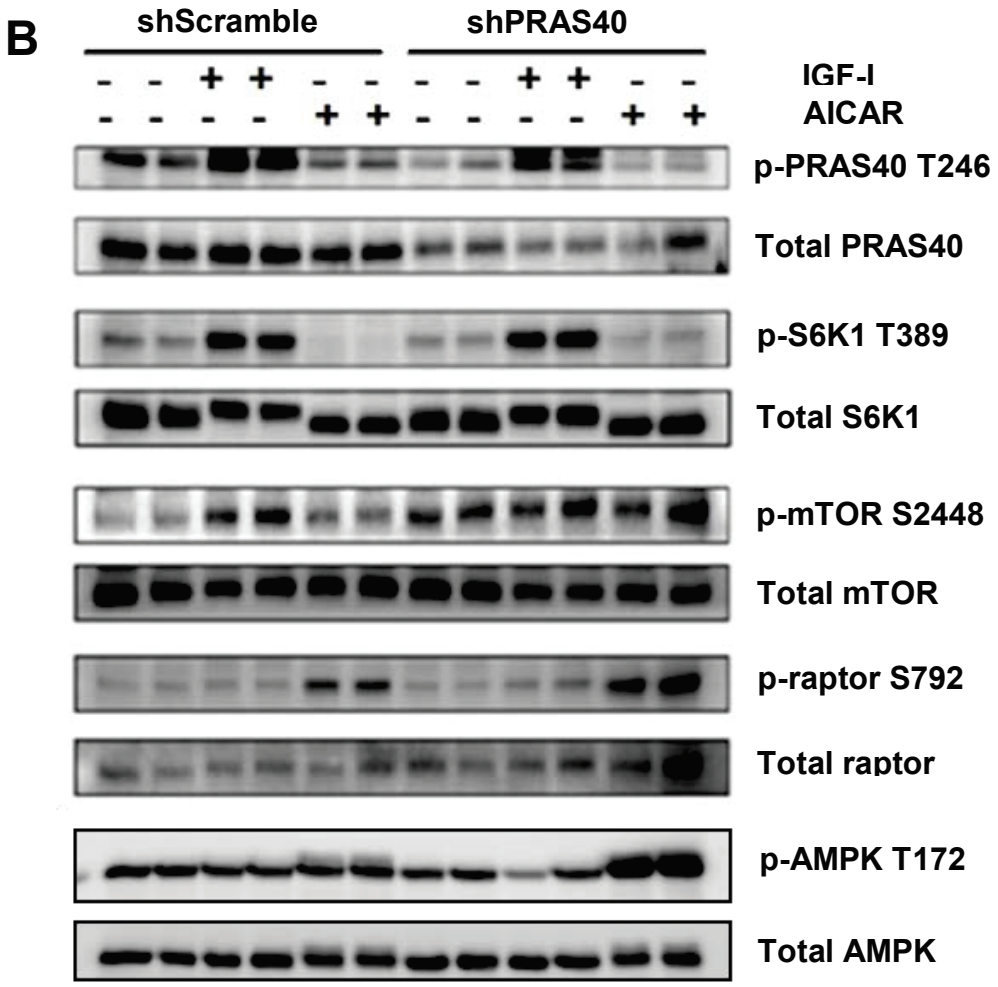
B
shScramble
shPRAS40
IGF-I
AICAR
p-PRAS40 T246
Total PRAS40
p-S6K1 T389
Total S6K1
p-mTOR S2448
Total mTOR
p-raptor S792
Total raptor
p-AMPK T172
Total AMPK

Figure 4—3. **Effect of IGF-I and AICAR on protein synthesis in control and PRAS40 knockdown C2C12 myoblasts**. Myoblasts were incubated with vehicle (Control), AICAR or IGF-I as described in Figure 4- 2. Panel A: Protein synthesis in myoblasts was measured on day 3, and values are means ± SE for n = 8 for each condition. Means not sharing the same superscript are significantly different ($P<0.05$). Panel B: Effect of PRAS40 knockdown on total and phosphorylated 4E-BP1, S6K1 and PRAS40 in C2C12 myoblasts. Representative Western blots for proteins involved in the mTORC1 complex mediated translation initiation. Except for the reduction in total and phosphorylated PRAS40, there were no significant differences between the two groups. Panel C: Effect of PRAS40KD on protein-protein interaction. Equal amount of total protein from shScramble (4 left lanes) and shPRAS40 KD (4 right lanes) myoblasts were immunoprecipitated using in excess amount of anti-PRAS40 antibody to pull down proteins interacting with PRAS40. The antigen-antibody immune-complex was then probed with antibodies against PRAS40, raptor and eIF3f. The lower 3 blots represent the whole cell lysate (WCL) which was probed with total antibody against raptor and phosphospecific and total antibody against PRAS40. The amount of raptor and eIF3f bound to PRAS40 did not differ between control and PRAS40 KD cells. Panel D: Representative Western blots of various total and phosphorylated proteins treated as described in Figure 4-2. Representative blot of 3 independent experiments with 4 replicates per experiment.

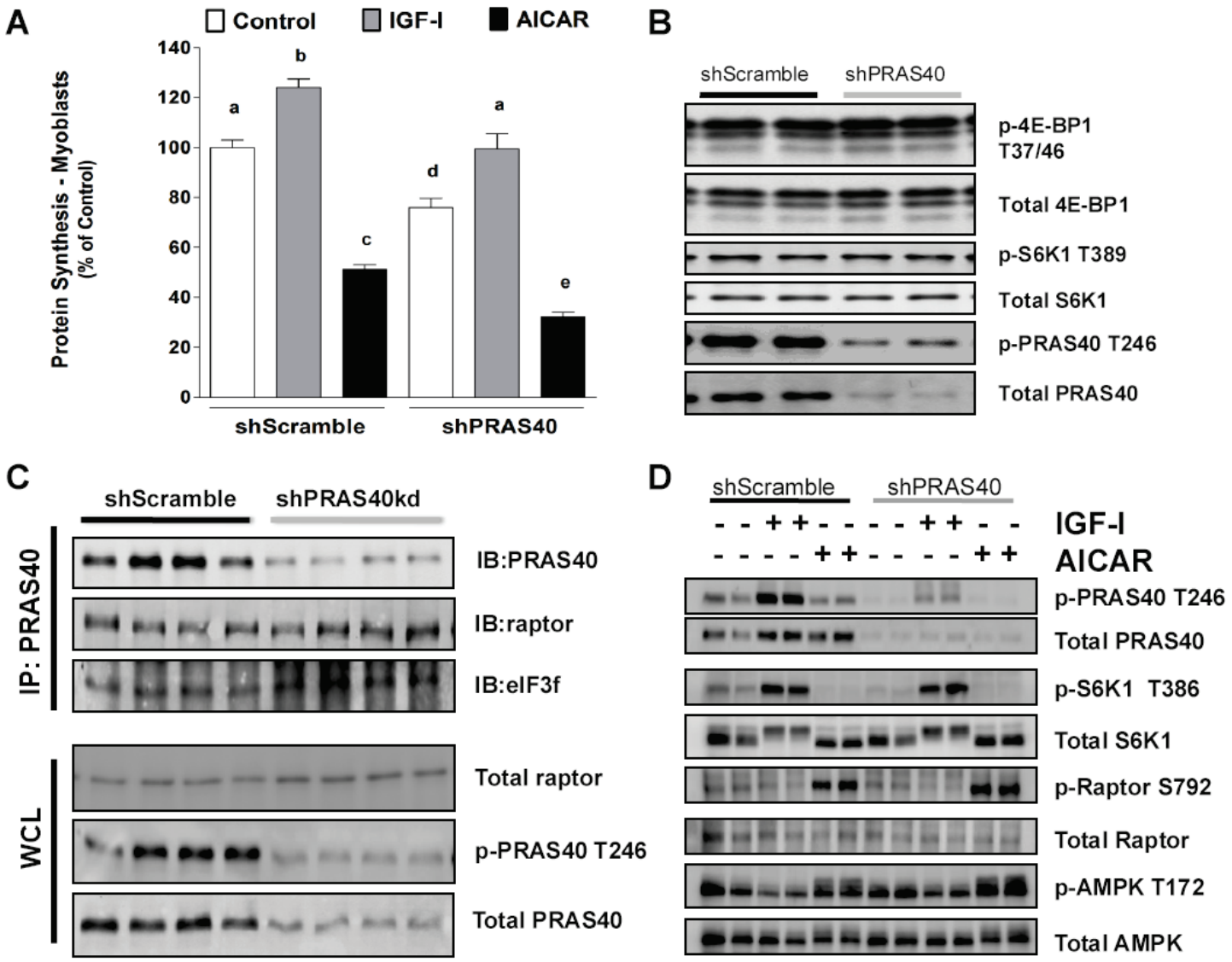
A
Control
IGF-I
AICAR
Protein Synthesis - Myoblasts
(% of Control)
140
120
100
80
60
40
20
0
a
b
c
d
a
e
shScramble
shPRAS40
B
shScramble
shPRAS40
p-4E-BP1
T37/46
Total 4E-BP1
p-S6K1 T389
Total S6K1
p-PRAS40 T246
Total PRAS40
C
shScramble
shPRAS40kd
IP: PRAS40
IB:PRAS40
IB:raptor
IB:eIF3f
WCL
Total raptor
p-PRAS40 T246
Total PRAS40
D
shScramble
shPRAS40
IGF-I
AICAR
p-PRAS40 T246
Total PRAS40
p-S6K1 T386
Total S6K1
p-Raptor S792
Total Raptor
p-AMPK T172
Total AMPK

Figure 4—4. **Effect of PRAS40 knockdown on cell size in C2C12 myoblasts**. Panel A: Cell size was measured using the Coulter Counter particle size analyzer and shown in parenthesis. n = 8 for each condition. Panel B: Mean cell volume of myoblasts as described in Panel A; Mean cell volume in cells with PRAS40 knockdown is increased. Bar graph is mean ± SE; n= 7-9 for each condition, **P*<0.0001. Where absent, standard error bars are too small to be visualized.

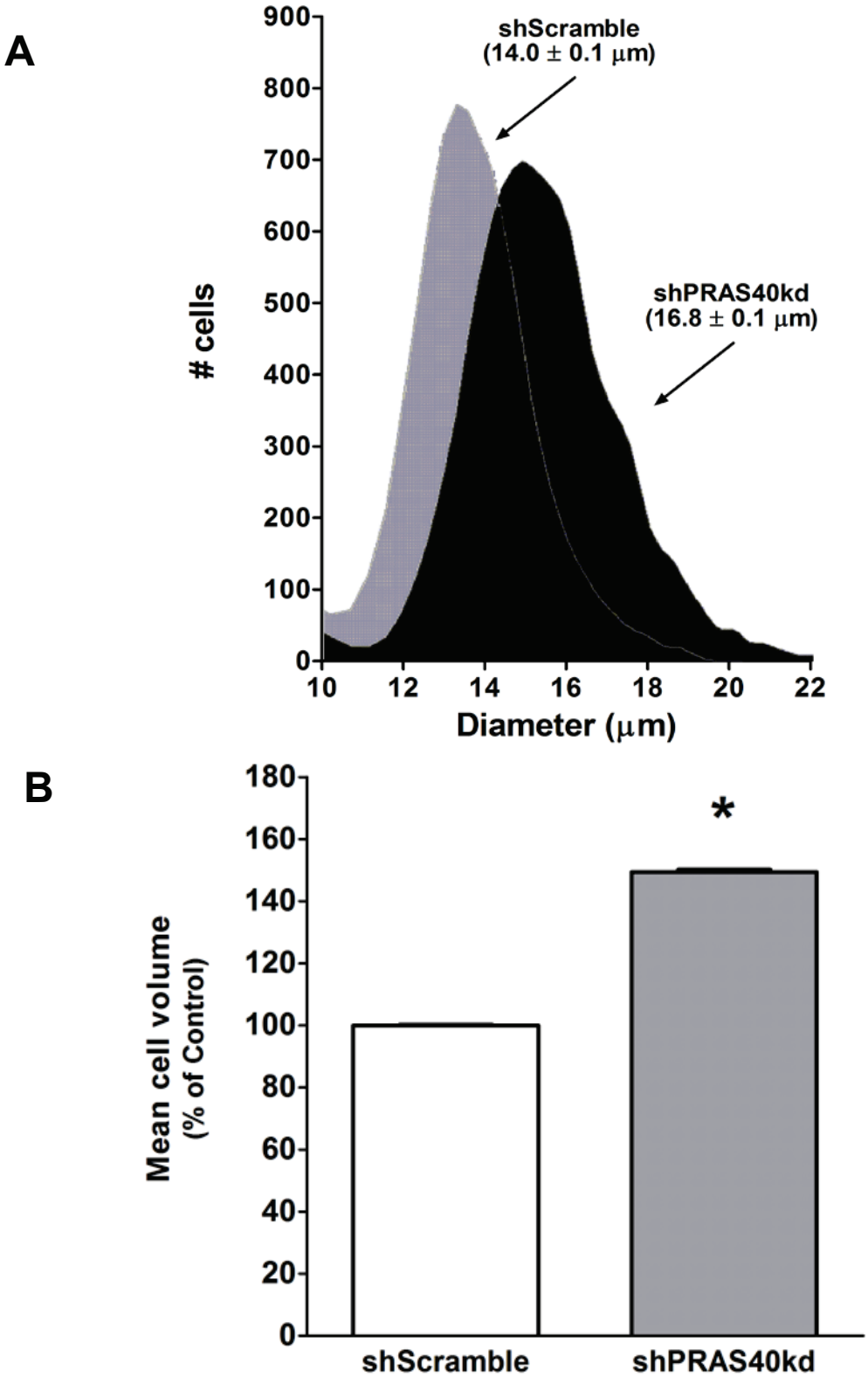
A
shScramble
(14.0 ± 0.1 μm)
shPRAS40kd
(16.8 ± 0.1 μm)
cells
Diameter (μm)
B
Mean cell volume
(% of Control)
*
shScramble
shPRAS40kd

Figure 4—5. **Effect of PRAS40 knockdown on C2C12 myoblasts proliferation**. Panel A: Proliferation rate was determined in stably transfected myoblasts with shScramble and shPRAS40. Myoblasts were seeded at the same density and counted using the Coulter counter as described in the Methods section. Time intervals are indicated in the figure; n = 5 for each treatment time point; experiments were repeated at least 3 times. Panel B: To measure proliferative rate acutely (24 h), an independent alternative approach using MTT was used. Values are means ± SE for n = 32 for each condition; (*P <0.0001).

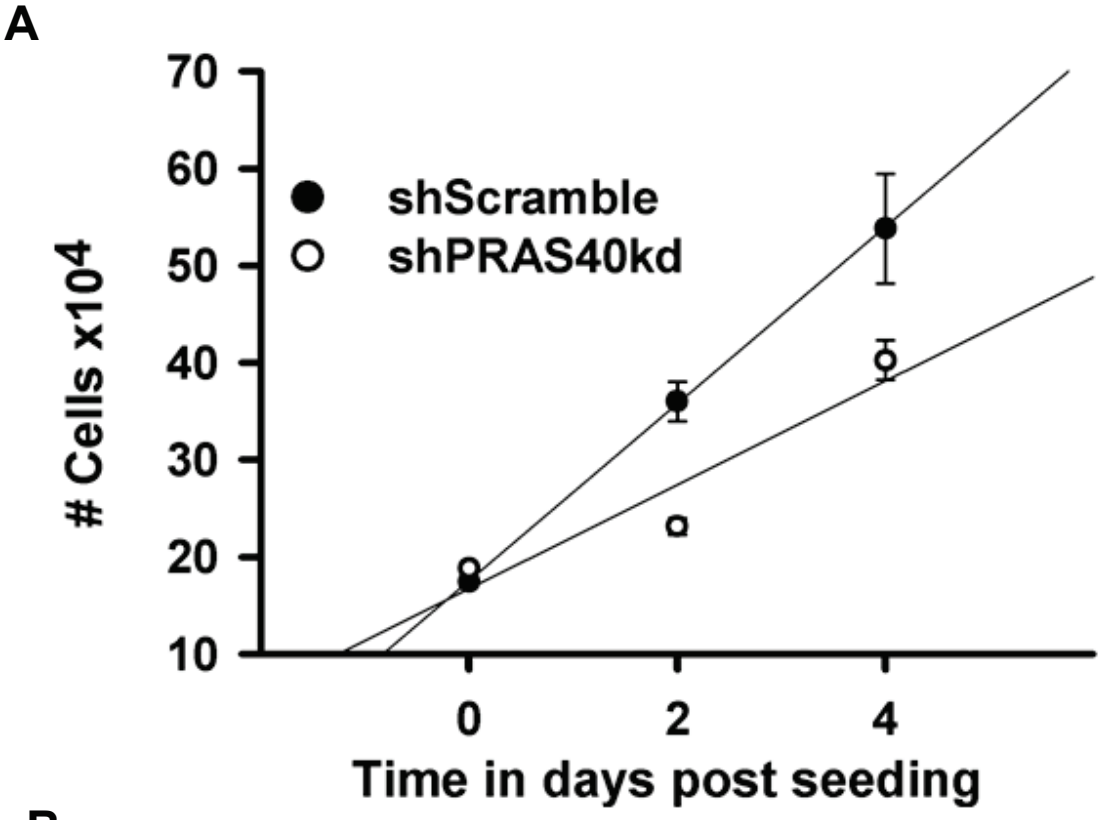
A
70
60
50
40
30
20
10
Cells x10^4
shScramble
shPRAS40kd
0
2
4
Time in days post seeding

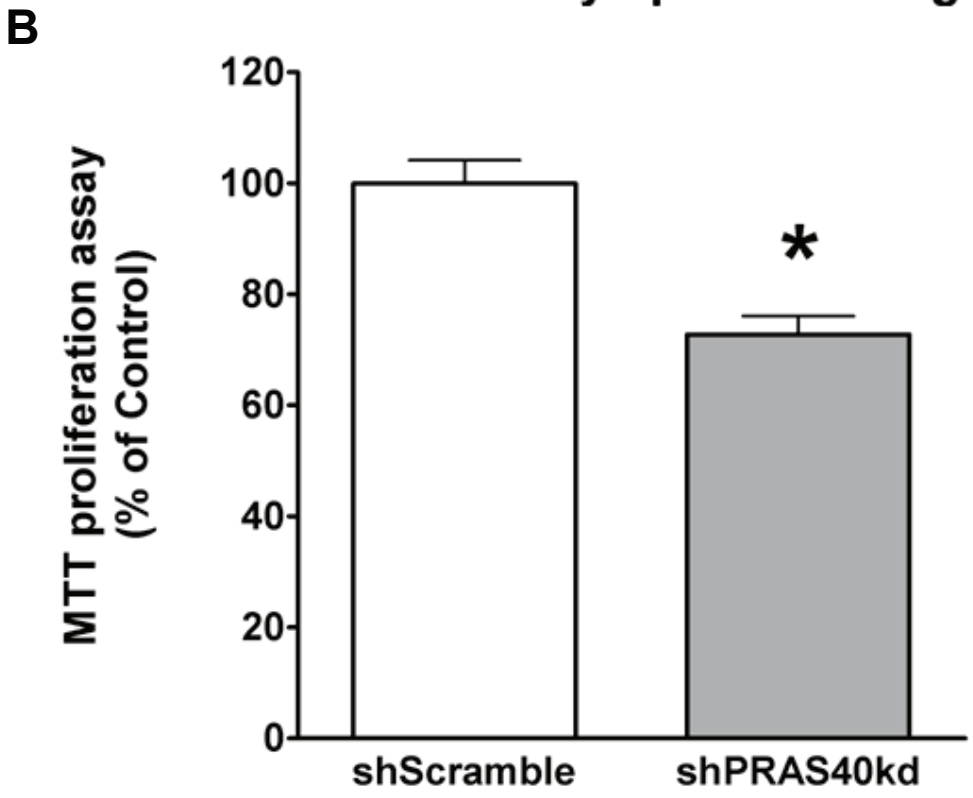
B
120
100
80
60
40
20
0
MTT proliferation assay
(% of Control)
*
shScramble
shPRAS40kd

Figure 4—6. **Effect of PRAS40 knockdown on apoptosis in C2C12 myoblasts**. Panel A: DNA laddering assay. Low molecular weight DNA was extracted from stably transfected myoblasts with shScramble and shPRAS40. No regular laddering pattern was observed in either the shScramble or shPRAS40 transfected myoblasts. For sample, DNA 8 μg/lane and for positive apoptotic control DNA, 3 or 5 μg/lane was loaded. Panel B: Myoblasts were transfected with either control (shScramble) shRNA or shRNA targeting PRAS40 and cell lysates were collected for Western blotting. Representative Western blots of whole cell lysates probed using antibodies against cleaved caspase-3, PARP, and phosphorylated and total PRAS40 are shown. Staurosporine treated myoblasts served as positive control.

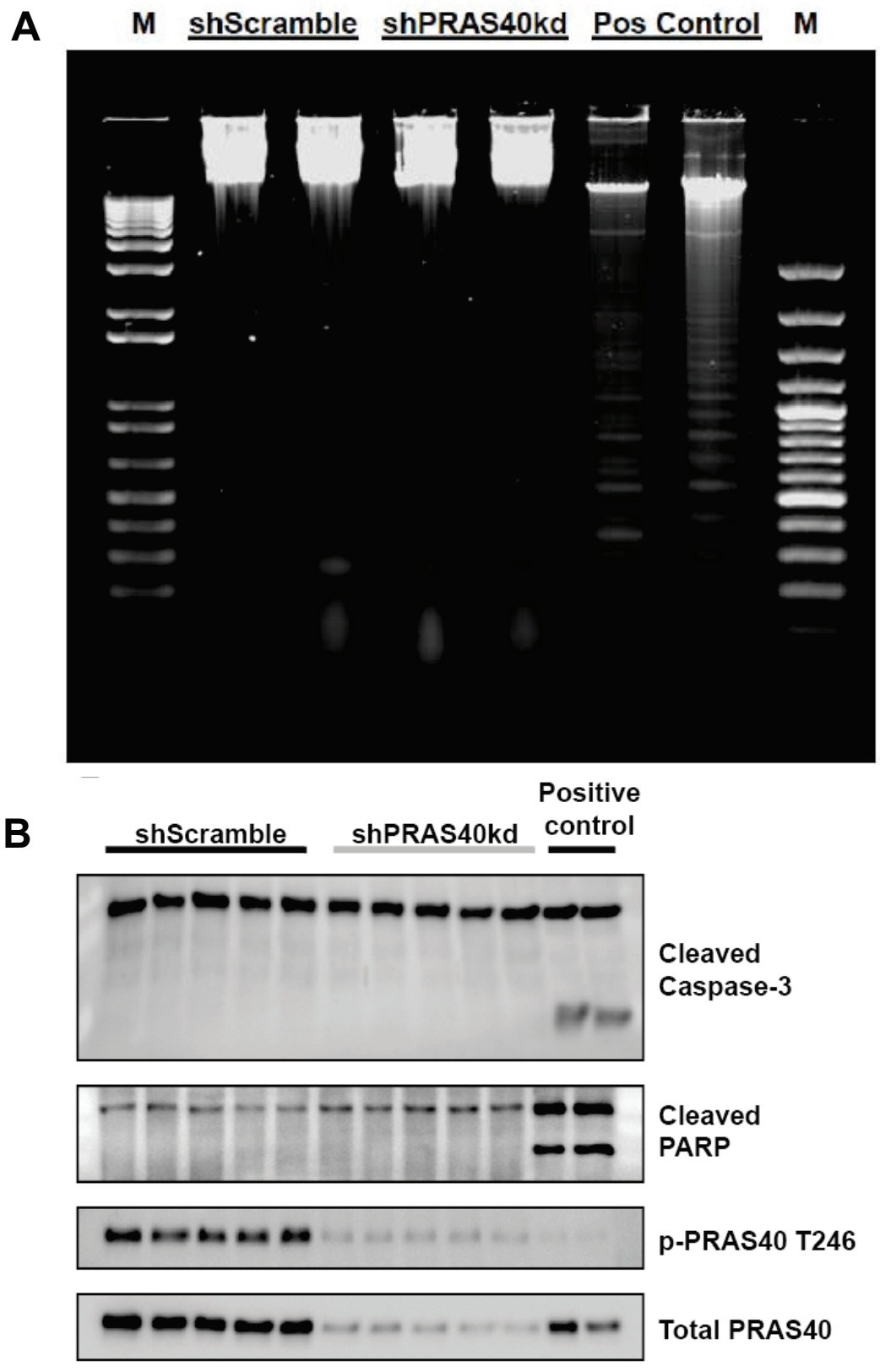
A
M
shScramble
shPRAS40kd
Pos Control
M
B
shScramble
shPRAS40kd
Positive control
Cleaved Caspase-3
Cleaved PARP
p-PRAS40 T246
Total PRAS40

Figure 4—7. **Effect of PRAS40 knockdown on C2C12 myoblasts cell cycle**. Myoblasts were transfected with either control (shScramble) shRNA or shRNA targeting PRAS40. Myoblasts were grown in DMEM media supplemented with 10% FBS for 24 hours and stained with propidium iodide stain to study cell cycle using FACS. Representative forward scatter histogram highlighting G1 and G2 phases of cell cycle for Control (shScramble; Panel A) and PRAS40 knockdown (shPRAS40kd; Panel B) are shown. Panel C: Cell lysates from myoblasts as described in (A and B) were collected for Western blotting analysis. Representative Western blots of whole cell lysates probed using antibodies against total and p-PRAS40 (T246), total p21, and pRb (S807/811) and actin. Panel D: Cell lysates from myoblasts as described in (A and B) were collected for Western blotting analysis. Representative Western blots of whole cell lysates probed using antibodies against Rb, p53, Cyclin D1, cdk4, cdk6, and p27 are shown.

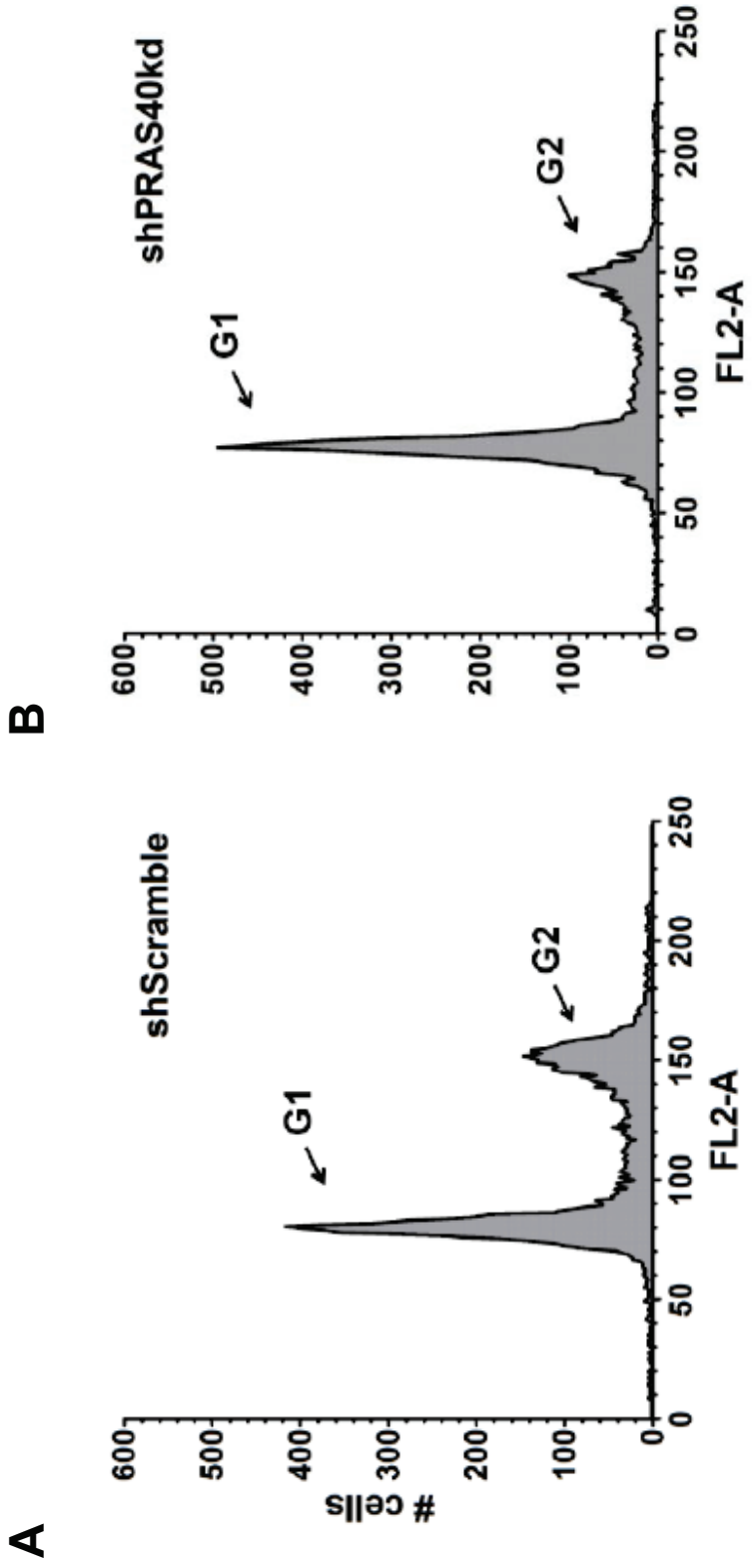
A
shScramble
cells
FL2-A
G1
G2
0
100
200
300
400
500
600
0
50
100
150
200
250
B
shPRAS40kd
G1
G2
FL2-A

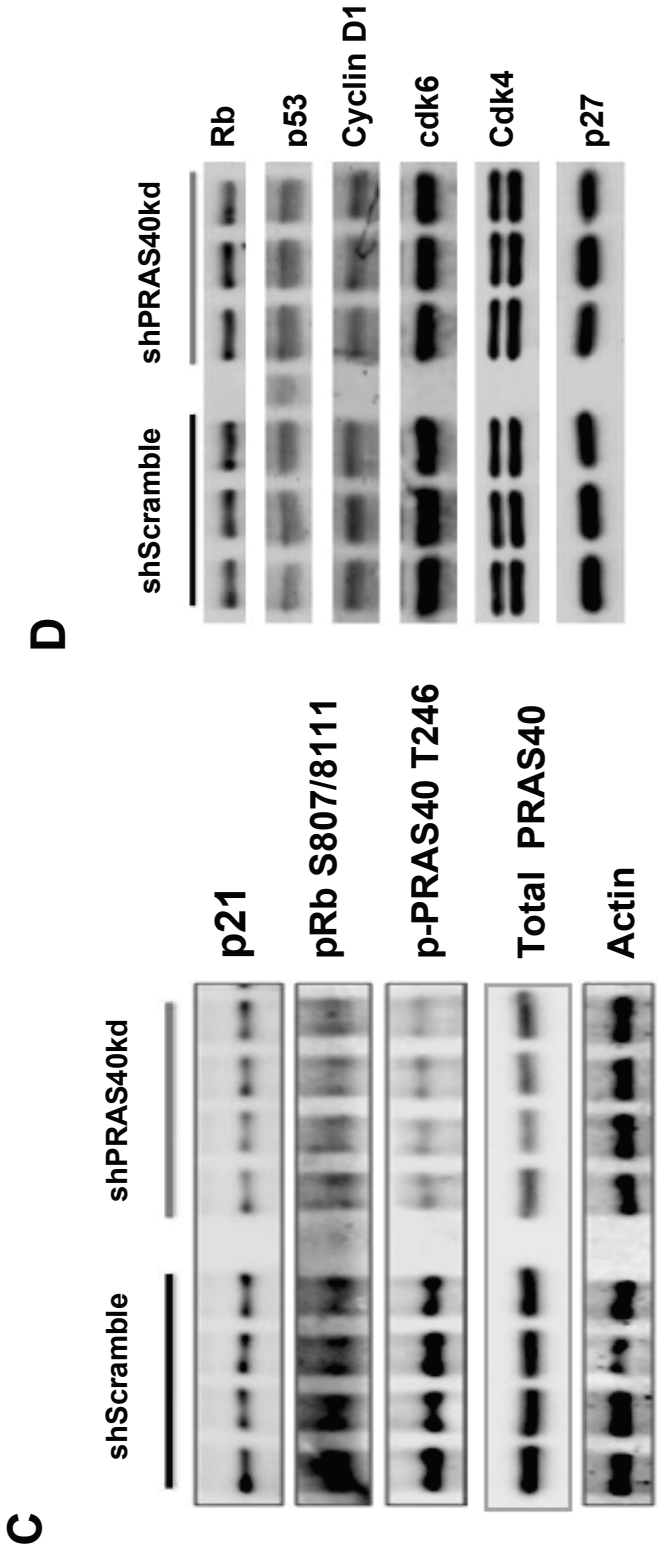
C
shScramble
shPRAS40kd
p21
pRb S807/8111
p-PRAS40 T246
Total PRAS40
Actin
D
shScramble
shPRAS40kd
Rb
p53
Cyclin D1
cdk6
Cdk4
p27

Figure 4—8. **Effect of PRAS40 knockdown on autophagy**. Myoblasts were transfected with either control (shScramble) shRNA or shRNA targeting PRAS40 and cell lysates were collected for Western blotting. Panel A: Representative Western blots of whole cell lysates probed using antibodies against total Atg 7, Beclin 1, LC3B and PRAS40 are shown. Nutrient starved myoblasts treated with Hanks balanced salt solution serve as positive control. Panel B: quantification of Western blot data. Values are means ± SE; n = 10 per group. $*P < 0.05$ compared to time-matched scramble control values.

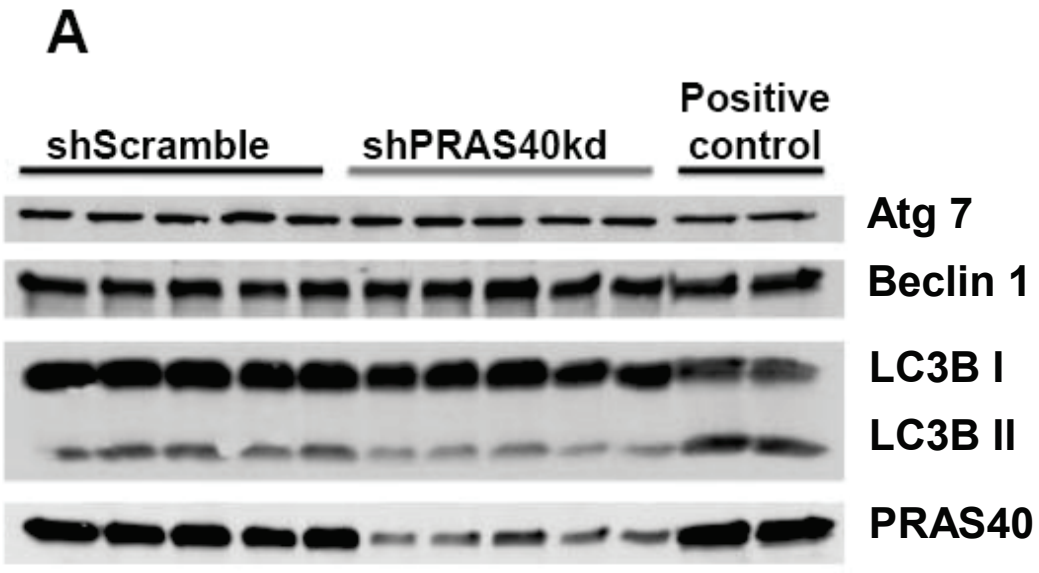
A
shScramble
shPRAS40kd
Positive control
Atg 7
Beclin 1
LC3B I
LC3B II
PRAS40

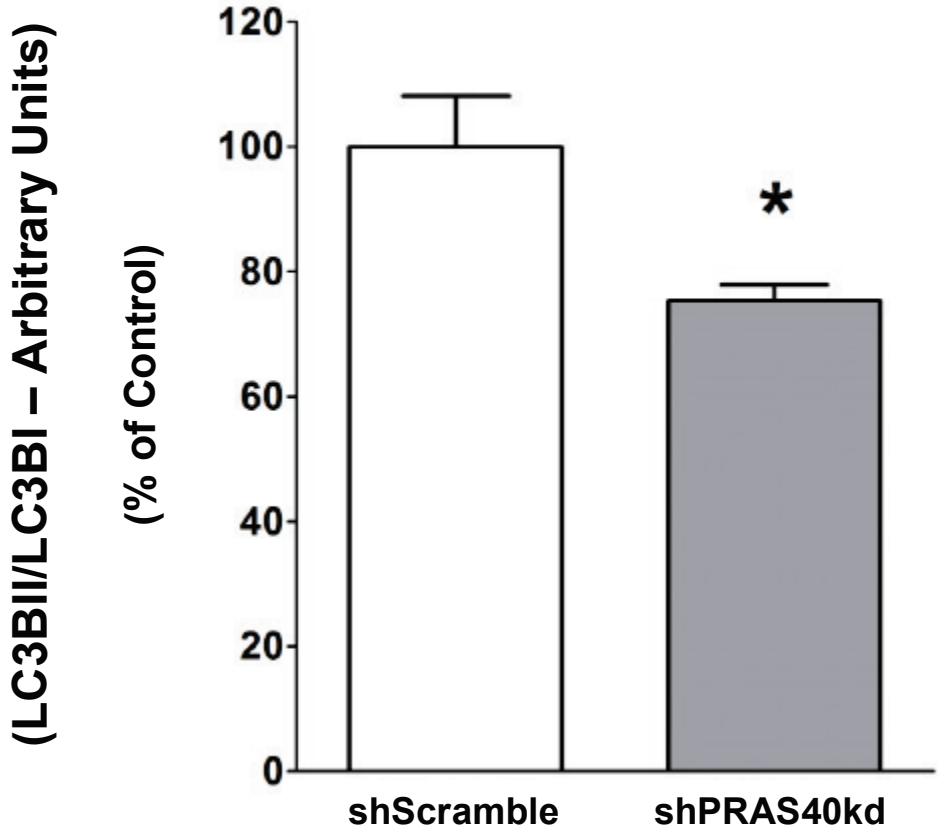
(LC3BII/LC3BI – Arbitrary Units)
(% of Control)
120
100
80
60
40
20
0
*
shScramble
shPRAS40kd

Figure 4—9. **Effect of PRAS40 knockdown on C2C12 differentiation**. Myoblasts were transfected with either control (shScramble) shRNA or shRNA targeting PRAS40. Cells were plated at the same density and photographed daily (10x objective magnification; Nikon digital camera mounted on binocular microscope) to visually record changes in cell proliferation (time to reach confluence) and formation of myotubes. On Day 3 when the plates were fully confluent, the media was switched to 2% horse serum (DM = differentiation media) to induce myotube formation.

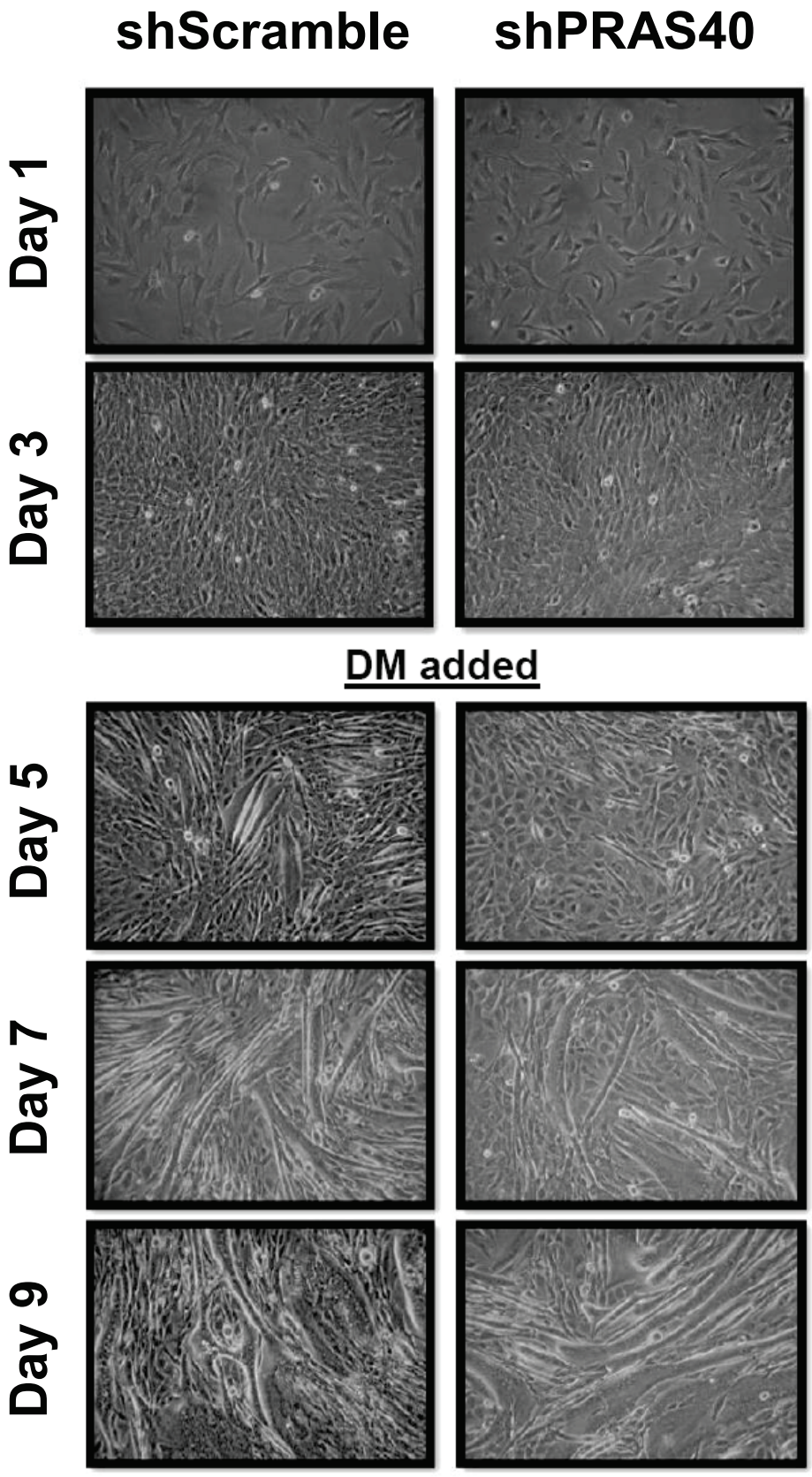
shScramble
shPRAS40
Day 1
Day 3
DM added
Day 5
Day 7
Day 9

Figure 4—10. **PRAS40 knockdown in C2C12 myocytes delays myosin heavy chain protein expression**. Panel A: representative Western blots for myosin heavy chain (MHC) and the muscle specific transcription factor MyoD in samples treated as in Figure 4—9. Panel B: Quantification of MHC Western blots in Panel A, Values are means ± SE for n = 6 for each condition. *$P<0.05$; compared to time-matched control values. ND=not detected.

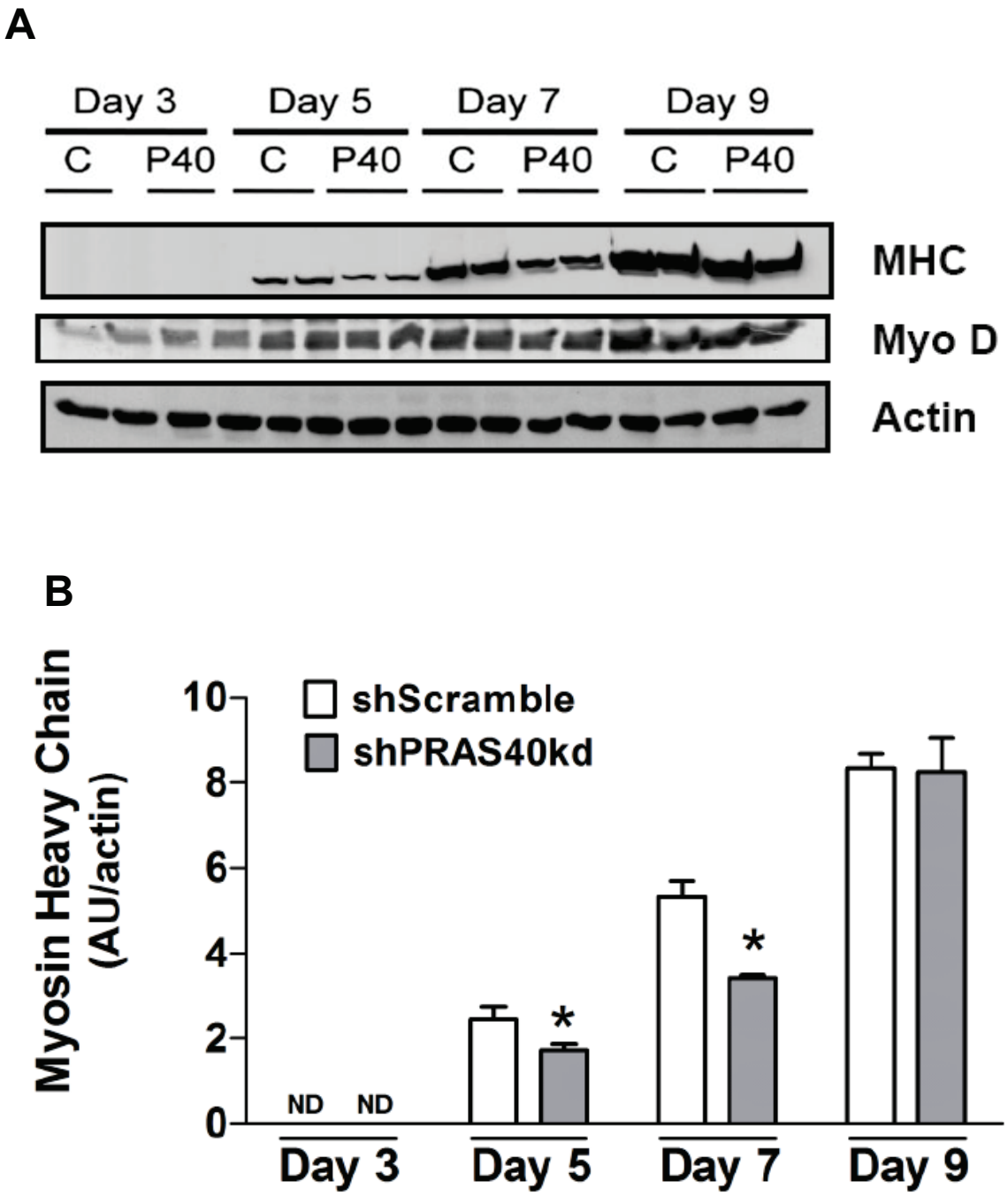
A
Day 3
Day 5
Day 7
Day 9
C
P40
C
P40
C
P40
C
P40
MHC
Myo D
Actin
B
Myosin Heavy Chain
(AU/actin)
10
8
6
4
2
0
shScramble
shPRAS40kd
ND
ND
*
*
Day 3
Day 5
Day 7
Day 9

Table 4—1. Effect of PRAS40 knockdown on cell cycle in C2C12 myoblasts.

Cell cycle	% G1	% S	% G2
shScramble	52.9 ± 1.1	34.6 ± 1.3	12. 5 ± 0.3
shPRAS40kd	65.0 ± 0.8*	25.1 ± 0.6*	9.9 ± 0.5*

Myoblasts were transfected with either control (scramble) shRNA or shRNA targeting PRAS40. Values are shown as means ± SE for n = 12 for each condition. *$P<0.05$ compared to time-matched control values.

Chapter 5

DEPTOR knockdown enhances mTOR activity and protein synthesis in skeletal muscle

Abstract

DEPTOR is an mTOR binding protein that affects cell metabolism. We hypothesized that knock down (KD) of DEPTOR in C2C12 myocytes will increase protein synthesis via stimulating mTOR-S6K1 signaling. DEPTOR KD was achieved using lentiviral particles containing shRNA targeting the mouse DEPTOR mRNA sequence and control cells were transfected with a scrambled control shRNA. KD reduced DEPTOR mRNA and protein content by 90%, which increased phosphorylation of mTOR kinase substrates, 4E-BP1 and S6K1, and concomitantly increased protein synthesis. However, the responsiveness of KD myocytes to anabolic (IGF-I) and catabolic (AICAR) stimuli was unaltered. DEPTOR KD myoblasts were both larger in diameter and exhibited an increased mean cell volume. DEPTOR KD increased the percentage of cells in the S phase, coincident with an increased phosphorylation (S807/S811) of pRb protein which is critical for the G1-S phase transition. DEPTOR KD did not appear to alter basal apoptosis or autophagy as evidenced by the lack of change for cleaved caspase-3 and LC3B, respectively. DEPTOR KD increased proliferation rate and enhanced myotube formation. Finally, *in vivo* DEPTOR KD (~50% reduction) by electroporation into gastrocnemius of C57/BL6 mice did not alter weight or protein synthesis in control muscle. However, DEPTOR KD prevented atrophy produced by 3 days of hindlimb immobilization, at least in part by increasing protein synthesis. Thus, our data support the hypothesis that DEPTOR is an important

regulator of protein metabolism in myocytes and demonstrate that decreasing DEPTOR expression *in vivo* is sufficient to ameliorate muscle atrophy.

Introduction

Skeletal muscle serves as the largest protein reservoir in the body, and its content represents a balance between rates of protein synthesis and degradation in the tissue. The process of protein synthesis is tightly regulated because of its high demand for cellular energy. Of the 3 regulatory steps involved in protein synthesis – translation initiation, elongation and termination – initiation plays the most significant role in regulating mRNA translation (291-293). At a molecular level, mTOR (mammalian target of rapamycin) kinase is a key regulator of translation initiation being activated upon feeding and conversely inhibited in response to catabolic insults such as sepsis, excess glucocorticoids, alcohol or disuse atrophy (1, 15, 33, 294). Exposure of muscle to growth factors and nutrients increases initiation via the mTOR pathway, thereby stimulating protein synthesis (10, 293, 295, 296).

mTOR is sequestered within two distinct complexes: mTOR complex (mTORC)-1 and mTORC2. mTORC1 is composed of mTOR, raptor (regulatory associated protein of TOR), LST8/G-protein β-subunit like protein (GβL), proline-rich Akt substrate 40 kDa (PRAS40) and DEPTOR (DEP-domain containing partner of TOR) (25, 38, 54, 297). In contrast, mTORC2 consists of mTOR, rictor (rapamycin insensitive companion of mTOR), LST8/GβL, PRR5L (proline rich protein 5-like), protor (protein observed with Rictor-1), and DEPTOR (47, 294). As noted above, DEPTOR is a constituent of both mTOR complexes and is considered a negative regulator of mTOR function, as DEPTOR knock down increases phosphorylation of signaling substrates downstream of both mTORC1 and mTORC2 (47). Conversely, overexpression of DEPTOR in cell culture models inhibits signaling pathways downstream of both mTOR-

containing complexes. Additionally, in the absence of growth factors or in the presence of mTOR inhibitors the mTOR-DEPTOR binding is strengthened which thereby decreases mTOR activity and suppresses cap-dependent protein translation initiation (298). DEPTOR is also a phospho-protein and as such can undergo post-translational modification which affects its binding to mTOR. For example, in response to growth factor signaling, DEPTOR is phosphorylated and quickly degraded via the ubiquitin proteasome system (UPS) pathway (47).

Despite the few reports implicating DEPTOR as a regulator of translation initiation in, cancer and transformed cells, there is a paucity of information related to its role in regulating other cellular functions especially in skeletal muscle. Given the essential role mTOR plays in regulating protein translation initiation, cell cycle and proliferation, we posited that one or more of these mTOR functions are regulated by DEPTOR in myocytes. Therefore, the purpose of our current investigation was to examine changes in C2C12 myocyte protein synthesis, cell proliferation and cell cycle in response to DEPTOR KD using short hairpin (sh)-RNA–based *in vitro* experimental approaches. In addition, we have previously reported that the inhibition of mTORC1 activity observed in response to sepsis or glucocorticoid excess was associated with an increase in DEPTOR protein level (33). Therefore, we also assessed whether *in vivo* DEPTOR KD by electroporation could ameliorate the decrease in muscle mass and protein synthesis seen in a catabolic condition associated with an elevation in DEPTOR.

Results

Effect of DEPTOR knockdown in C2C12 myoblasts. shRNA directed towards DEPTOR in C2C12 myoblasts reduced DEPTOR protein levels by >90%, compared to scramble control values (Figure 5-1A, 5-1B). As expected, DEPTOR knockdown also reduced the DEPTOR mRNA content by ~95% in infected C2C12 cells (Figure 5-1C). The knockdown of

DEPTOR increased global protein synthesis by ~ 50% under basal conditions (Figure 5-1D). To determine if the change in global protein synthesis was associated with mTOR-mediated signal transduction events, we performed Western blotting for mTOR substrates and binding partners. DEPTOR KD significantly (P<0.05) increased phosphorylation of mTORC1 substrates S6K1 (T389) (Control= 100 ± 5 AU; DEPTOR KD= 151 ± 7 AU) and 4E-BP1 (T37/46) (Control= 100 ± 10 AU; DEPTOR KD= 129 ± 4 AU). However, the increased phosphorylation of 4E-BP1 resulted from a concomitant and comparable increase in total 4E-BP1 protein expression in these myocytes. In addition, DEPTOR KD also increased (P<0.05) the phosphorylation (T246) of PRAS40 (Control=100 ± 17 AU; DEPTOR KD= 193 ± 7 AU), an mTORC2 substrate (Figure 5-1E). To assess off-target effects of the shRNA mediated DEPTOR KD, we performed Western blot analysis for proteins critical to the mTOR signaling pathway, including mTOR, raptor, S6K1, and found that there were no changes in the total protein content for these proteins (Figure 5-1E and Figure 5-2B).

To determine whether DEPTOR KD altered myocyte responsiveness to external stimuli, cells were incubated with either an anabolic (IGF-I) or catabolic (AICAR) agent. As expected, incubation of control myocytes with IGF-I increased protein synthesis, whereas AICAR inhibited protein synthesis (Figure 5-2A). A comparable bidirectional response for protein synthesis towards IGF-I and AICAR was also seen in DEPTOR KD cells. To confirm the protein synthesis data, we performed Western blotting for mTOR and its substrates and binding partners. Cells with DEPTOR KD remained responsive to both types of stimuli and their response was comparable to the scramble controls (Figure 5-2B). For example, IGF-I increased phosphorylation of mTOR (S2448), S6K1 (T389), eIF4B (S422), Akt (S473) and PRAS40 (T246), while AICAR increased phosphorylation of raptor (S792) and AMPK (T172) in both control and DEPTOR KD cells.

DEPTOR knockdown increases myoblast size and proliferation. Based on the previous data, we hypothesized that DEPTOR KD would also increase myoblast size. DEPTOR KD increased the diameter (17.0 ± 0.1 μm) of low passage proliferating (~60% confluent) myoblasts, compared to scramble control cells (15.3 ± 0.1 μm), as measured using either the Coulter counter particle size analyzer (Figure 5-3A) or FACS flow cytometry analysis (data not shown). Mean cell volume was also increased in myocytes with DEPTOR KD (Figure 5-3B). When both cell types were seeded at the same low initial density, the initial rate of proliferation between day 0 and day 4 did not differ between control and DEPTOR KD cells. However, at days 6 and 8, the cell number was greater in cells with DEPTOR KD, compared to time-matched control cells (Figure 5-4A). To exclude variations in the ability of the cell types to attach to the plates, cells were seeded and counted 4-8 h after seeding to allow for attachment. An equal number of cells were harvested after trypsinization in both the control and DEPTOR KD condition, suggesting no significant difference in the ability of these cells to attach to the culture plates (data not shown). To confirm that the proliferation rate of DEPTOR KD cells was faster, we used an independent colorimetric assay based on the conversion of the MTT tetrazolium salt to its formazan product. Consistent with the above data, the MTT assay revealed that DEPTOR KD increased the rate of proliferation by ~20% (Figure 5-4B). Apoptosis poses another potential mechanism which may affect cell number and thus proliferation. However, Western analysis for the apoptotic markers cleaved caspase-3 and PARP did not differ between groups under our experimental conditions (Figure 5-5).

DEPTOR knockdown enhances cell cycle progression. To address the underlying mechanism by which DEPTOR KD increased proliferation, we stained myoblasts with propidium iodide to study cell cycle. A smaller proportion of cells in G1/G0 of the cell cycle were detected in myocytes with DEPTOR KD, compared with the control values (Figure 5-6A and 5-6B, and Table 5-1). We assessed whether proteins regulating the cell cycle, especially the G1 to S

transition, were concomitantly altered. Figure 5-6C and 5-6D illustrate an increased S807/S811 phosphorylation of pRb consistent with increased progression from the G1 to S phase in myoblasts with DEPTOR KD. To further accentuate differences in the cell cycle we also synchronized cells by serum starvation. Following G1/G0 arrest, cells were released by the addition of serum and cells analyzed once again at 16 h using flow cytometry. Figure 5-7A shows DEPTOR KD dramatically increased the percent of cells in the S-phase of the cell cycle following serum stimulation, compared with time-matched scramble control myoblasts. This change in cell cycle following arrest and release was verified by Western analysis for pRb expression (Figure 5-7B). We also performed Western blot analysis for proteins crucial for cell cycle regulation, namely, p21, p27, p53, cdk -2, -4, and -6, and cyclin D1and found no change between control and DEPTOR KD myoblasts (Figure 5-7C and 5-7D).

DEPTOR KD alters myogenesis. Our data demonstrate the presence of a concomitant increase in proliferation and altered cell cycle in DEPTOR KD myoblasts. Since mTOR also regulates autophagy which in turn plays an important role in cell differentiation (299, 300), we determined the expression of proteins important in regulating autophagy and found that there was no statistical difference in LC3B-II/LC3B-I ratio between control and DEPTOR KD myoblasts (Control= 100 ± 8 AU; DEPTOR KD= 116 ± 10 AU) under normal physiological conditions (Figure 5-7E).

Next we determined whether such changes in altered cell cycle and proliferation might be of physiological relevance to skeletal muscle development. In this regard, we seeded the same number of myoblasts and tracked their progression to form myotubes (Figure 5-8A and 5-8B). We observed that DEPTOR KD cells reached confluent status earlier than control cells. To quantitate these findings, cell lysates were collected at various stages of myocytes development to measure the expression of myosin heavy chain (MHC) – a protein expressed only in differentiated matured myotubes. In control cells, MHC expression was absent in myoblasts (day 3) and MHC

expression in control cells was first detected on day 7 (Figure 5-8B). In contrast, in cells with DEPTOR KD, MHC could be detected on the blots by day 5. By day 9, both scramble control and DEPTOR knockdown cells exhibited MHC expression, with the content of MHC being increased in the DEPTOR KD cells (Figure 5-8A and 5-8B). The protein content of the muscle transcription factor MyoD (used as an additional internal control) did not differ between scramble control and DEPTOR KD cells (Figure 5-8B).

DEPTOR KD *in vivo* prevents muscle loss due to immobilization. To determine the effect of DEPTOR KD on muscle growth *in vivo*, we electroporated the shRNA plasmid targeting DEPTOR message into the gastrocnemius of C57/BL6 mice. Using this technique, DEPTOR mRNA content was decreased ~50% (Figure 5-9A). The hallmark of disuse atrophy is loss of muscle mass in the immobilized leg compared to the contralateral control leg. Figure 5-9B illustrates the decreased muscle mass following 3 days of hindlimb immobilization in the control animals and prevention of this atrophic response in the muscle where DEPTOR was decreased. *In vivo* –determined rates of protein synthesis were also quantitated in these same muscles (Figure 5-9C). In control muscle, there was no difference in protein synthesis in the gastrocnemius injected with scrambled control and DEPTOR KD plasmid. In contrast, in the immobilized leg, DEPTOR KD prevented the decreased rate of protein synthesis. The delta for the decrement in protein synthesis between control vs immobilized muscle was significantly ($P<0.05$) greater in Control (1.27 ± 0.14 nmols Phe/h/mg protein), compared to DEPTOR KD (0.34 ± 0.16 nmols Phe/h/mg protein).

Discussion

DEPTOR has recently been identified as an mTOR binding protein. Using RNAi this mTOR-interacting protein was reported to negatively regulate both mTORC1 and mTORC2, as

evidenced by increasing phosphorylation of known substrates. While the role of DEPTOR has been studied in cancer and other transformed cell lines using short-term transient RNAi transfections (47, 124), its role in regulating long-term mTOR-mediated events in skeletal muscle is not known. Moreover, as mTOR regulates multiple metabolic processes such as protein synthesis, cell size (growth), cell cycle, proliferation, and development, we posited that decreasing DEPTOR would affect one or more of these mTOR – mediated events. Therefore, the purpose of our investigation was to ascertain the role of DEPTOR in mTOR-mediated events in skeletal muscle, and to this end, we generated C2C12 myoblasts which had a stable KD of DEPTOR mRNA and protein expression. DEPTOR KD by ~90% *in vitro* increased protein synthesis by ~50% in myoblasts. Our data are consistent with the fact that DEPTOR is not the only regulator of protein synthesis. Protein translation initiation, being an energy consuming process, has multiple regulatory mechanisms and it is anticipated that KD of DEPTOR would activate such mechanism(s) which would restrain changes in protein synthesis. Such compensatory changes could in part explain the discordance between the percentage of DEPTOR KD and the percent increase in protein synthesis. Consistent with our data, Rapamycin and Torin-1 (e.g., both mTOR inhibitors) also suppress protein synthesis ~ 50% (301). Alternatively, while protein synthesis is regulated primarily at the translation initiation step, other steps such as elongation and termination also influence protein synthesis. Therefore, the observed difference in percent of DEPTOR KD and the percent increase in protein synthesis *in vitro* is within the expected range. While previous reports have used the phosphorylation of T389-S6K1 and T37/46-4E-BP1 (surrogate markers of mTORC1) and S473-Akt (mTORC2 substrate) to implicate DEPTOR as a putative negative regulator of mTOR, and such results are confirmed in the present study, this appears to be the first report of DEPTOR KD on protein synthesis *per se*.

We postulated that DEPTOR KD would increase the anabolic and decrease the catabolic response of myocytes. Unfortunately, the data generated in this regard are equivocal and open to

divergent interpretation. For example, while IGF-I increased protein synthesis in both control and DEPTOR KD cells, both the percent and absolute increase in protein synthesis appears reduced in KD cells. However, this conclusion has two caveats: 1) protein synthesis in the basal and IGF-I stimulated condition was determined in different cells and it is therefore not possible to calculate a standard error and hence perform a statistical analysis on the incremental change, and 2) data interpretation may be further complicated by a "ceiling effect" present in the DEPTOR KD cells stimulated with IGF-I. Our supporting Western blot data, which shows comparable phosphorylation of AKT, PRAS40 and S6K1 in control and DEPTOR KD cells, suggests that IGF-I responsiveness is largely unchanged between the two groups. In contradistinction, our data could also be interpreted to indicate that DEPTOR KD actually increases the maximal responsiveness of cells to IGF-I, as the absolute rate of protein synthesis is higher in DEPTOR KD cells than in control cells. Such an interpretation is possible because the IGF-I concentration used in the current study was purposefully selected to be maximally stimulating. Resolution of this issue will require complete dose- and time-response studies in both control and DEPTOR KD cells. Similar difficulties in data interpretation are encountered in evaluating the response of two groups to the catabolic agent AICAR.

Cell growth is a reliable indicator of increased mTOR activity in a variety of cell types (272, 302) and, therefore, we studied the impact of decreasing the cellular content of DEPTOR. Typically under normal physiological conditions, cells must attain a genetically determined set size before they can replicate and divide, thus ensuring that the daughter cells are of an appropriate size following mitosis (59, 133). This regulation of growth and cell division is lost under some disease states (e.g., cardiac hypertrophy, cancer) or artificial (e.g., use of certain pharmaceutical agents) conditions. mTOR plays an important role in regulating cell growth (133). In this context, knockdown of DEPTOR in MEF and HeLa cells increases cell size (47). Consistent with this report, DEPTOR KD in myoblasts also increased cell size, and was

associated with a coordinate increase in the rate of proliferation, compared to control cells. Thus, our data provide support to the previous report suggesting that DEPTOR functions as a negative modulator of mTOR function in regulating cell size (47).

One potential explanation for the increased cell number in myoblasts with DEPTOR KD could be their resistance to undergo apoptosis, as previously demonstrated using a different cell line (47). In a subset of myeloma in which DEPTOR is over expressed, this protein decreases apoptosis, and this response is in contrast to its activity as a negative regulator of mTOR (47, 123-125). Akt regulates and promotes cell survival via the serum/glucocorticoid regulated kinase1 (SGK1) (mTORC2 substrate), and since DEPTOR KD activates Akt, we queried whether myocytes with DEPTOR KD were resistant to apoptosis. Activated mTOR phosphorylates and inhibits signals to the pro-apoptotic proteins, such as caspase-3, which play a critical role in induction of cellular apoptosis. Using the cleavage of caspase-3 and PARP, which are reliable markers of apoptosis, our data suggest there is no difference in the ability of control and DEPTOR KD myoblasts to undergo apoptosis under normal growth conditions. Therefore, our observed difference in proliferation rate could not be attributed to a change in apoptosis.

mTOR is also central in regulating cell cycle, as evidenced by the ability of the mTOR inhibitor rapamycin to arrest cells in the G1 phase (22, 26, 59, 272, 285, 303, 304). Furthermore, arresting cells in G1/G0 by serum starvation suggests that the mTOR signaling pathway regulates cell growth and cell cycle progression in response to nutrient availability (23, 24, 305, 306). Propidium iodide staining of asynchronous myoblasts revealed that DEPTOR KD decreased the proportion of cells in the G1/G0 phase, compared to scramble control. Further, the proportion of DEPTOR KD myocytes in the active S phase was increased when determined under conditions in which the cell cycle was synchronized and then cells released from cycle arrest. Collectively, these data suggest DEPTOR is required for mTOR activity in regulating cell cycle and that DEPTOR KD enhances myoblast cycle progression, consistent with its role as a negative

regulator of mTOR activity. However, we cannot exclude the possibility that the reduction of DEPTOR alters cell cycle kinetics by an undetermined mTOR-independent mechanism.

Because DEPTOR KD decreased the percentage of cells in G1/G0 phase and concomitantly increased the number of cells in the active S phase, we focused on elucidating the potential mechanisms. mTOR can regulate cell cycle progression by a rapamycin-sensitive pathway by promoting RNA polymerase I and III activity via phosphorylation and inactivation of pRb (307, 308). In addition, rapamycin also prevents the mitogen-induced downregulation of the cyclin-dependent kinase inhibitor p27 (309). The pRb regulates G1 exit in the cell cycle. Upon mitogenic activation, pRb is phosphorylated, resulting in disruption of pRb binding to the E2F transcription factor, thus allowing transcription of proteins that are essential to cell cycle regulation and transition from G1 to S phase. We detected an increase in phosphorylation of pRb S807/S811 concurrent with increased progression from the G1 to S phase (147, 310). Because DEPTOR KD increases Akt activity (47), we also studied this pathway as it might affect cell cycle by modulating glycogen synthase kinase (GSK) activity. As GSK3 has been implicated in regulating cell cycle via cyclin D1, and cyclin D1 mediates pRb phosphorylation (311-314), we examined the effect of DEPTOR KD on these proteins. The role of cyclin D1, p53, p27, cdk -2, -4, and -6 in mTOR-mediated cell cycle regulation is controversial. While Muise-Helmericks implicated cyclin D1-mediated pRb phosphorylation (311), Faber *et al* have reported changes in cell cycle regulation independent of these regulatory proteins (315). In contrast to previous observations by Muise-Helmericks, we did not detect a change in the total amount of p21, p27, p53, cdk 2, 4, and 6, or cyclin D1 (Figure 5-7C and 5-7D), suggesting that under our specific experimental conditions and cell type, the regulation of G1 to S phase does not involve a major role for these regulatory proteins. Our data support changes in cell cycle kinetics without changes in these regulatory proteins, as reported by Faber *et al* (315). We cannot exclude the possibility that there may yet be other pathways involving pRb which are independent of cyclin D1. One

such mechanism involves the stress-regulated mitogen-activated protein kinase p38 which phosphorylates pRb, in a cell cycle-independent manner (143).

To determine the effect of DEPTOR KD on myotube formation and myogenesis and whether DEPTOR KD would enhance myoblast fusion, we monitored myotube formation. Time lapse imaging and Western analysis for MHC (a marker for matured myotubes) indicated that knockdown of DEPTOR in C2C12 myoblasts enhanced myotube formation. Additionally, the lack of change in the MyoD content between the two groups suggests that differentiation stimulated by DEPTOR KD does not affect the expression of the MyoD transcription factor, thereby suggesting a different mechanism. Autophagy is another mTOR regulated cellular event that plays an important role in differentiation of myoblasts to mature myocytes (158, 167, 168, 186). Our results indicate that DEPTOR KD does not alter autophagy in C2C12 myoblasts under normal physiological conditions. Collectively, these changes suggest DEPTOR regulates muscle proliferation and differentiation via regulation of cell cycle regulatory proteins.

Finally, we also determined whether the reduction in DEPTOR *in vivo* was capable of altering muscle protein synthesis and mass. To this end, the gastrocnemius was electroporated with the same plasmid construct used in our cell culture model. Using this technique for gene transfer, DEPTOR mRNA was decreased ~50%. The exact mechanism for the smaller decrease in DEPTOR KD *in vivo* versus *in vitro* is not known but may included: a) the *in vitro* KD of DEPTOR was determined in myocytes following stable integration using puromycin selection, while the *in vivo* KD was relatively transient (3 days). b) probably most important, not all fibers take up the shRNA targeting DEPTOR when transfected *in vivo*. c) the *in vitro* response does not have the same hormonal, mechanical or neural influences, as would be present *in vivo*. Finally, the *in vitro* protein synthetic response was measured in myoblasts while the *in vivo* response was determined primarily in myotubes which are differentiated post-mitotic cells. In contrast, reducing DEPTOR largely prevented the atrophic response produced by immobilization and, in

part, this response was mediated by an increased muscle protein synthesis. In summary, our data suggest that reducing DEPTOR is sufficient to prevent an atrophy-mediated decrease in muscle protein synthesis and muscle mass.

Understanding the role of DEPTOR in myocyte cell cycle and proliferation and the ability of this protein to regulate protein synthesis *in vivo* as described may prove important for designing new strategies to manage the muscle wasting associated with catabolic insults such as sepsis, alcohol abuse and aging.

Figure 5—1. **Effect of DEPTOR knockdown in C2C12 myoblasts**. Panel A: representative Western blot of DEPTOR protein in Control (Scramble) and DEPTOR knockdown (KD) myoblasts. Panel B: quantification of Western blot data. Values are means ± SE; n = 12 per group. $P < 0.05$ compared to time-matched scramble control values. Panel C: Real time-PCR showing decreased DEPTOR mRNA in myoblasts transfected with lentiviruses targeting DEPTOR. rpL32 served as the internal reference control gene and its expression did not differ between Control and DEPTOR KD cell (data not shown). Values are means ± SE; n = 12 per group. $P < 0.05$ compared to time-matched scramble control values. Panel D: Effect of DEPTOR KD on myocyte protein synthesis. Values are means ± SE for n = 12 for each condition. For bar graphs, $*P<0.05$, compared to control values. Panel E: Effect of DEPTOR KD on mTORC1 and mTORC2 signaling in C2C12 myoblasts. Representative Western blots for protein substrates involved in the mTORC1 and mTORC2 complex mediated signal transduction. Where absent, standard error bars are too small to be visualized.

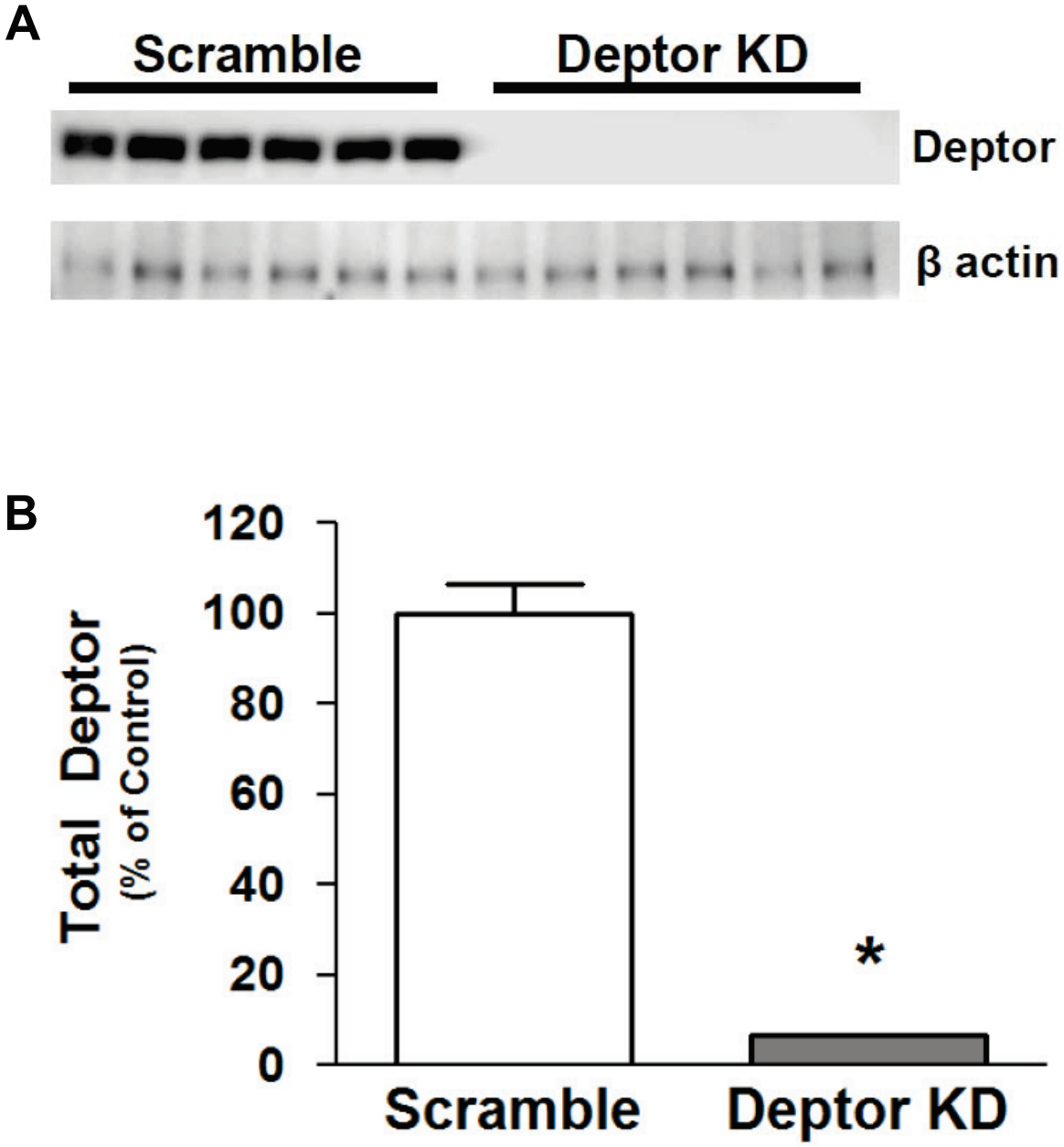
A
Scramble
Deptor KD
Deptor
β actin
B
Total Deptor
(% of Control)
120
100
80
60
40
20
0
*
Scramble
Deptor KD

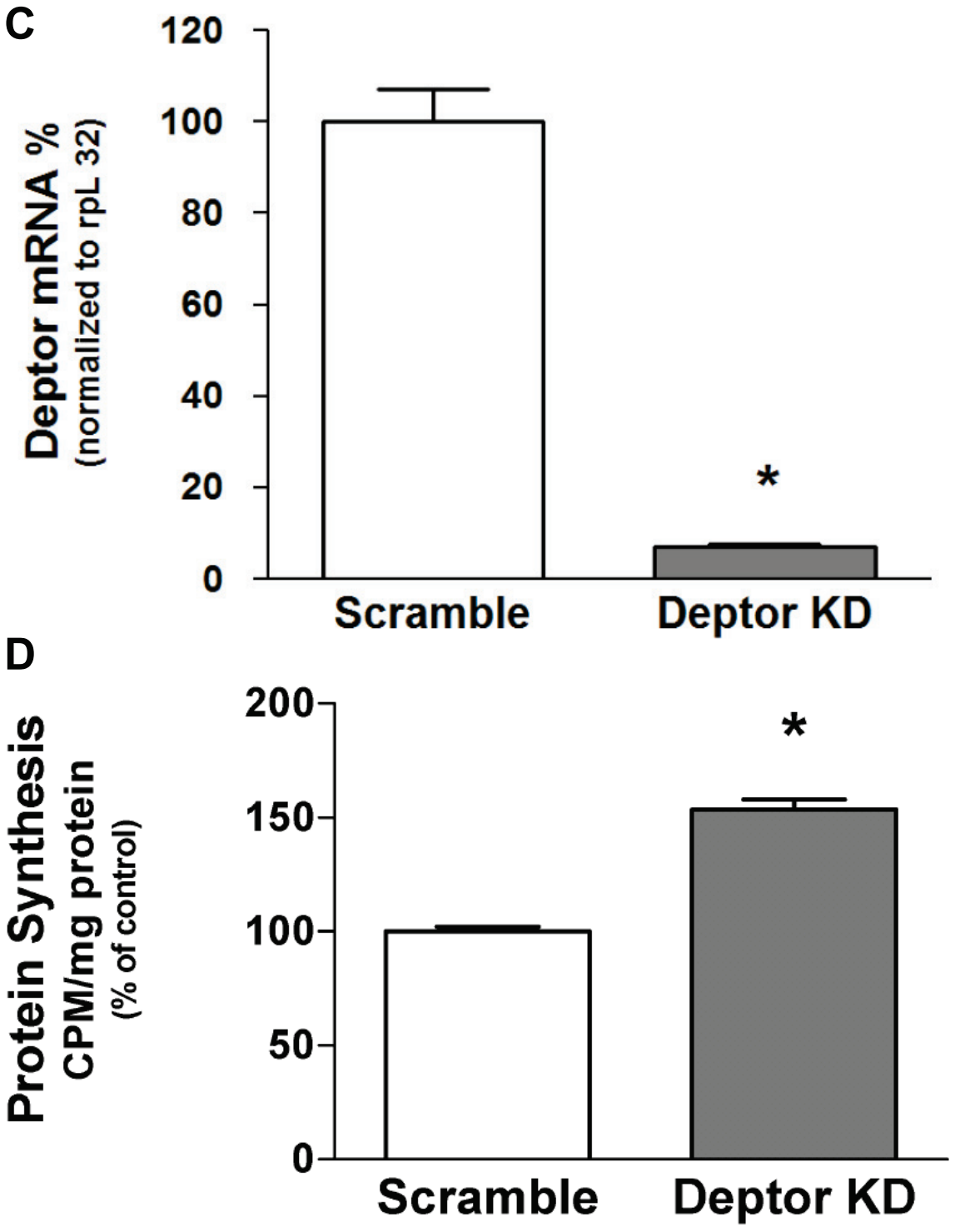
C
Deptor mRNA %
(normalized to rpL 32)
120
100
80
60
40
20
0
*
Scramble
Deptor KD
D
Protein Synthesis
CPM/mg protein
(% of control)
200
150
100
50
0
*
Scramble
Deptor KD

E

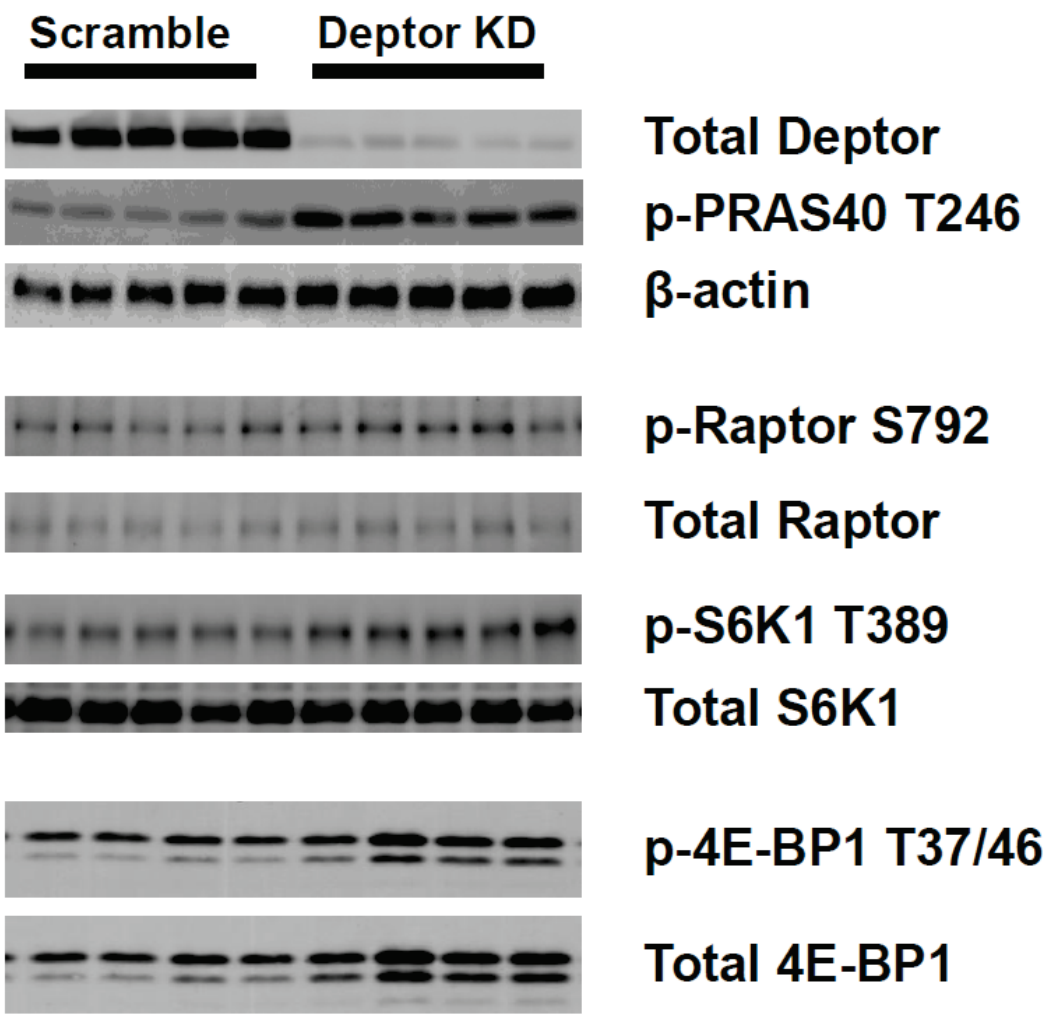
Scramble
Deptor KD
Total Deptor
p-PRAS40 T246
β-actin
p-Raptor S792
Total Raptor
p-S6K1 T389
Total S6K1
p-4E-BP1 T37/46
Total 4E-BP1

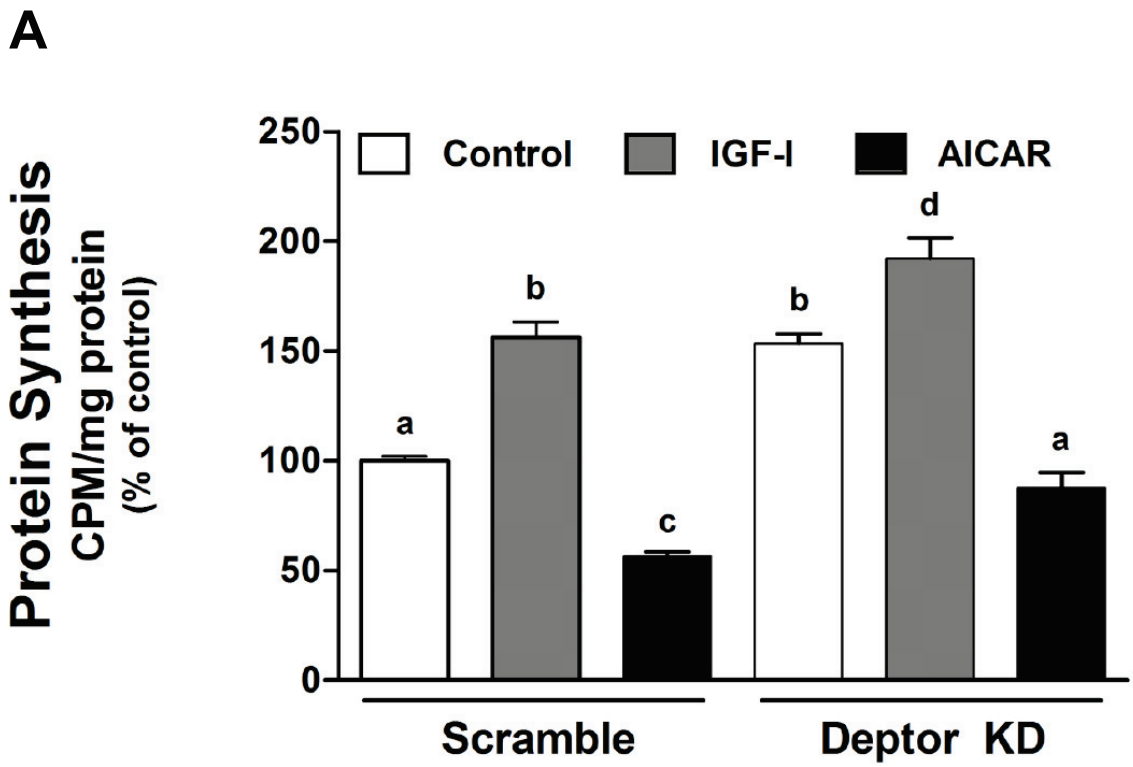

Figure 5—2. Effect of IGF-I and AICAR on Scramble (control) and DEPTOR knockdown (KD) C2C12 myoblasts. Cells were transfected with scramble and DEPTOR KD containing lentiviral particles and incubated with vehicle (control), IGF-I (100 ng/mL; 1 h) or AICAR (2 μM; 8 h) and labeled with ^{35}S-methionine. Panel A (above): Protein synthesis in myoblasts. Values are mean ± SE for n = 8-10 for each condition. Means not sharing the same superscript (a, b, c, and d) are significantly different ($P<0.05$). For quantification, data were normalized to scramble control values. Panel B (right): Representative Western blots for various total and phosphorylated proteins, where cells were treated as described above, except that isotope was omitted. Blot is representative of at least three independent experiments with 2-4 replicates per experiments.

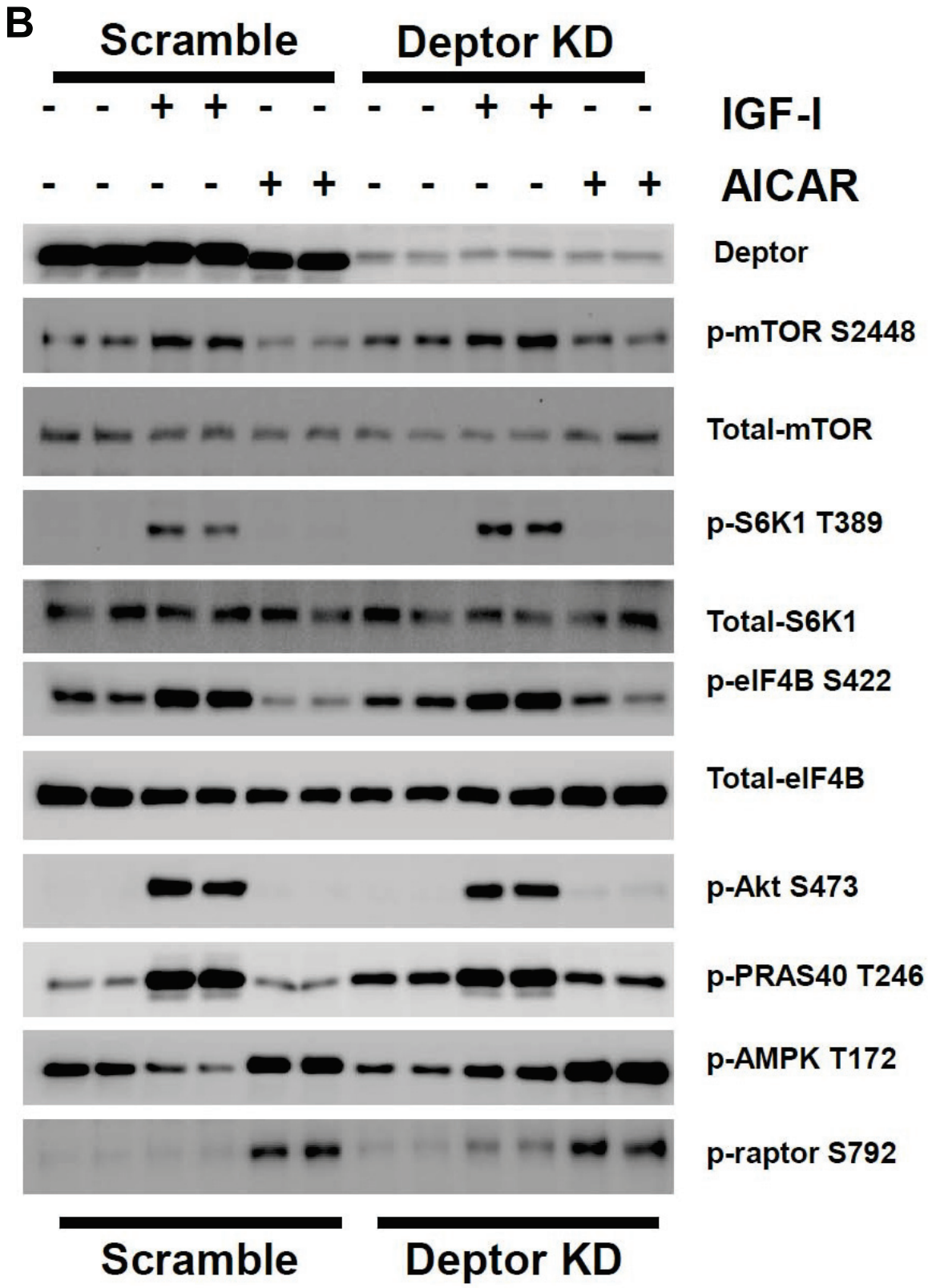
B
Scramble
Deptor KD
- - + + - - - - + + - -
IGF-I
- - - - + + - - - - + +
AICAR
Deptor
p-mTOR S2448
Total-mTOR
p-S6K1 T389
Total-S6K1
p-eIF4B S422
Total-eIF4B
p-Akt S473
p-PRAS40 T246
p-AMPK T172
p-raptor S792
Scramble
Deptor KD

Figure 5—3. **Effect of DEPTOR knockdown (KD) on cell size in C2C12 myoblasts**. Panel A: Cell size, shown in parenthesis, was measured using the Coulter Counter particle size analyzer; n = 8 for each condition. Panel B: Mean cell volume of myoblasts. Bar graph is mean ± SE; n= 7-9 for each condition, **P*<0.0001. Where absent, standard error bars are too small to be visualized.

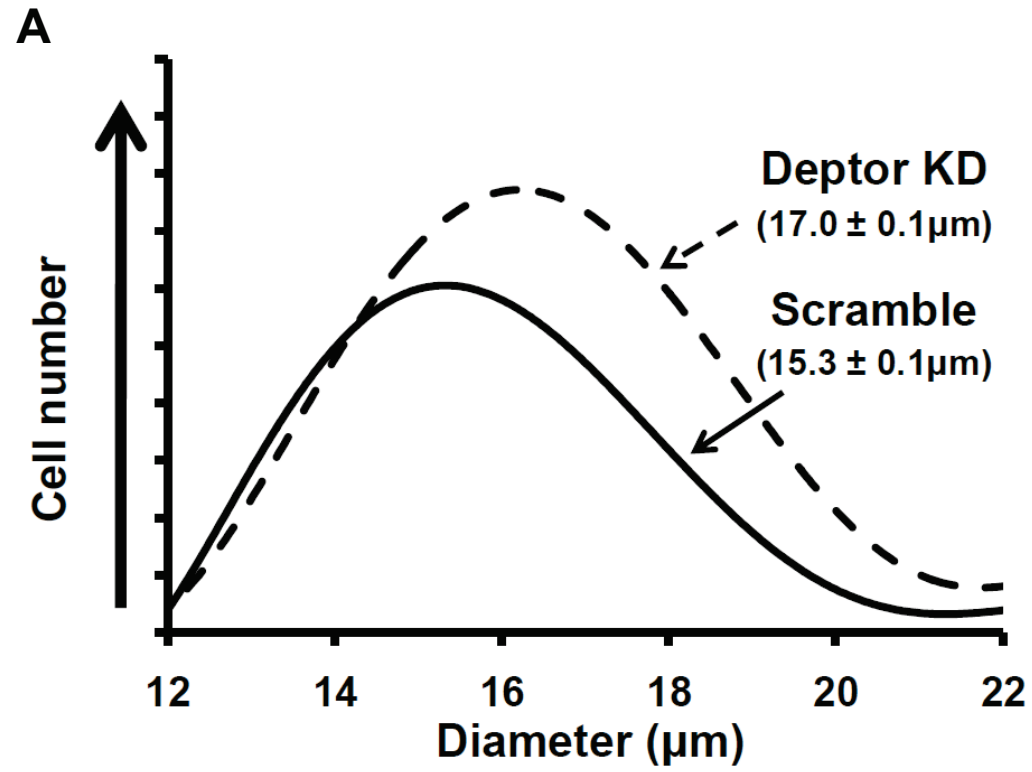
A
Cell number
Deptor KD
(17.0 ± 0.1μm)
Scramble
(15.3 ± 0.1μm)
12
14
16
18
20
22
Diameter (μm)

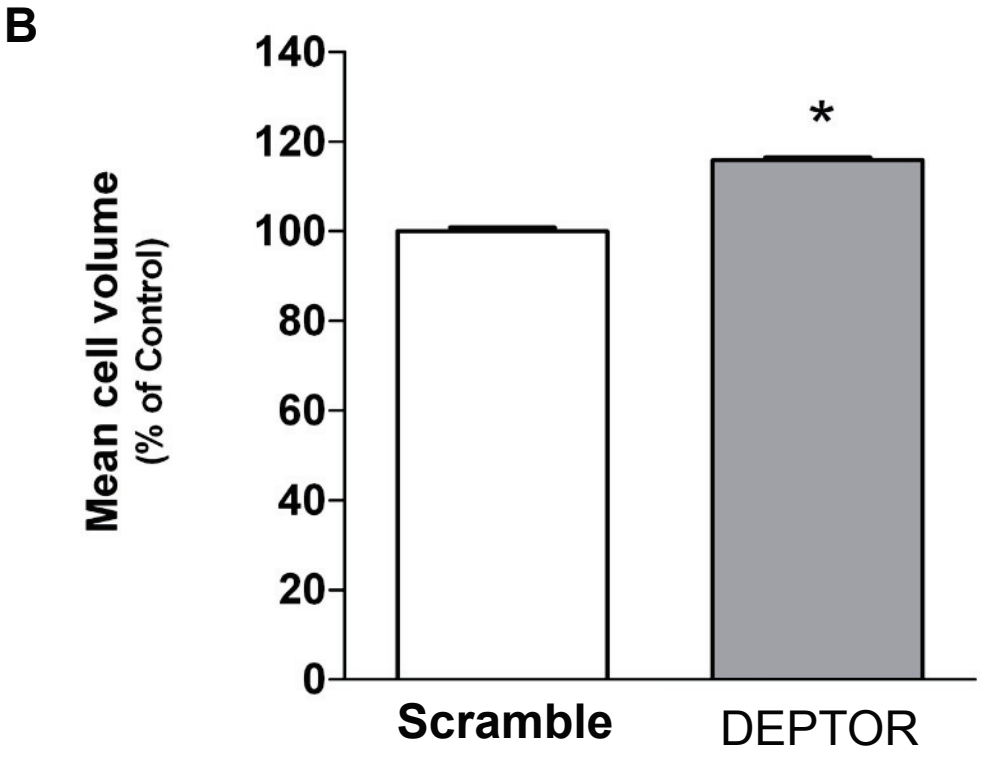
B
Mean cell volume
(% of Control)
140
120
100
80
60
40
20
0
*
Scramble
DEPTOR

Figure 5—4. **Effect of DEPTOR knockdown (KD) on C2C12 myoblast proliferation**. Panel A: Proliferation rate was determined in stably transfected myoblasts with Scramble and DEPTOR KD. Myoblasts were seeded at the same density and counted using the Coulter counter as described in Experimental procedures section. Time intervals are indicated in the figure; n = 6 for each treatment time point; experiments were repeated at least 3 times. Panel B: Proliferation rate was measured using an independent MTT assay. Cells were treated with MTT for 4 hours and formazan produced was measured colorimetrically. Bar graph is mean ± SE; n= 16-18 for each condition, **P*<0.0001; experiments were repeated at least 3 times.

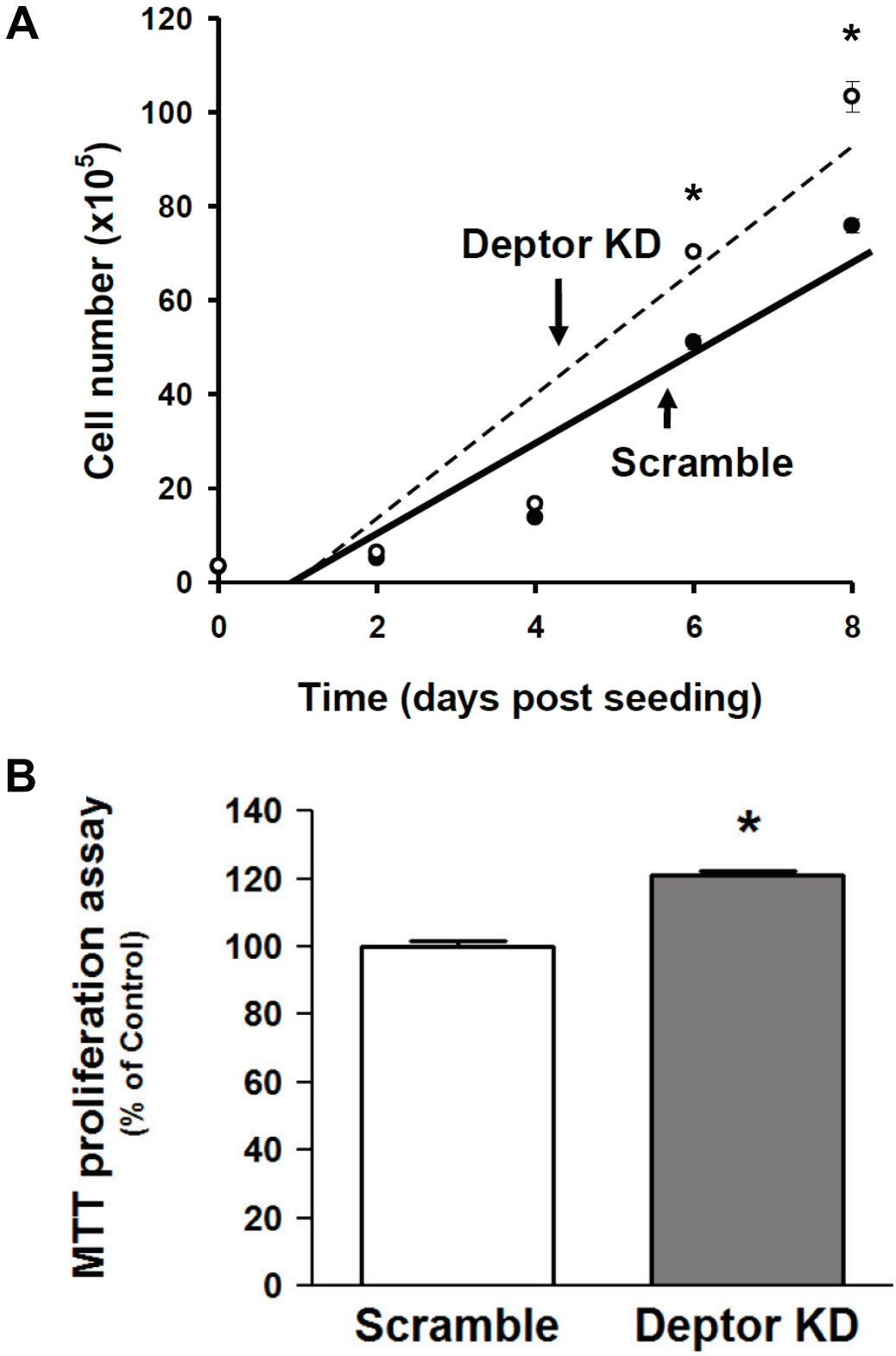
A
120
100
80
60
40
20
0
Cell number (x10^5)
*
*
Deptor KD
Scramble
0
2
4
6
8
Time (days post seeding)
B
140
120
100
80
60
40
20
0
MTT proliferation assay
(% of Control)
*
Scramble
Deptor KD

Figure 5—5. Effect of DEPTOR knockdown (KD) on apoptosis. Changes in basal apoptosis were measured in scramble control and DEPTOR KD myoblasts. To determine changes in apoptosis, cells were probed with antibody that recognizes caspase-3 and its cleaved product following apoptosis (top blot). Middle Western blot shows no changes in the cleavage of PARP another marker for apoptosis. Blot showing β-actin serves as loading control (bottom blot). Last column marked by "+" represents a positive control, as described under Methods.

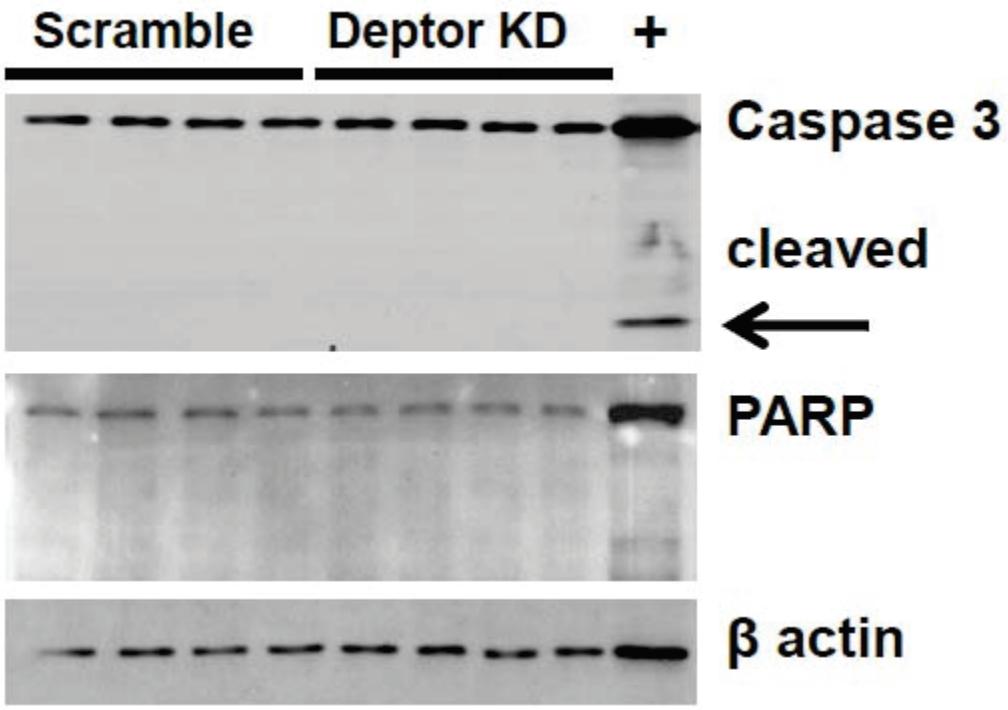
Scramble
Deptor KD
+
Caspase 3
cleaved
PARP
β actin

Figure 5—6. **Effect of DEPTOR knockdown (KD) on cell cycle in C2C12 myoblasts**. Myoblasts were transfected with either control (Scramble) shRNA or shRNA targeting DEPTOR. Myoblasts were grown in DMEM media supplemented with 10% FBS for 18-24 hours and stained with propidium iodide to assess cell cycle using FACS. Representative forward scatter histogram highlighting G1 and G2 phases of cell cycle for scramble Control (Panel A) and KD; (Panel B) are shown. The percentage of cells in each stage of the cell cycle for each treatment group is shown in the accompanying pie graphs. FL2-A (Propidium Iodide fluorescence). Panel C: Western blotting of samples (normalized to total protein content for loading) as described above. Blots were probed with total DEPTOR antibody to show the different groups (top band) and with phospho-specific antibody to detect phosphorylation on S807/S811 of pRb protein (middle band). Lower band shows β-tubulin to confirm equal loading. Panel D: Quantification of Western blot from panel C for phosphorylation on S807/S811 of pRb protein.

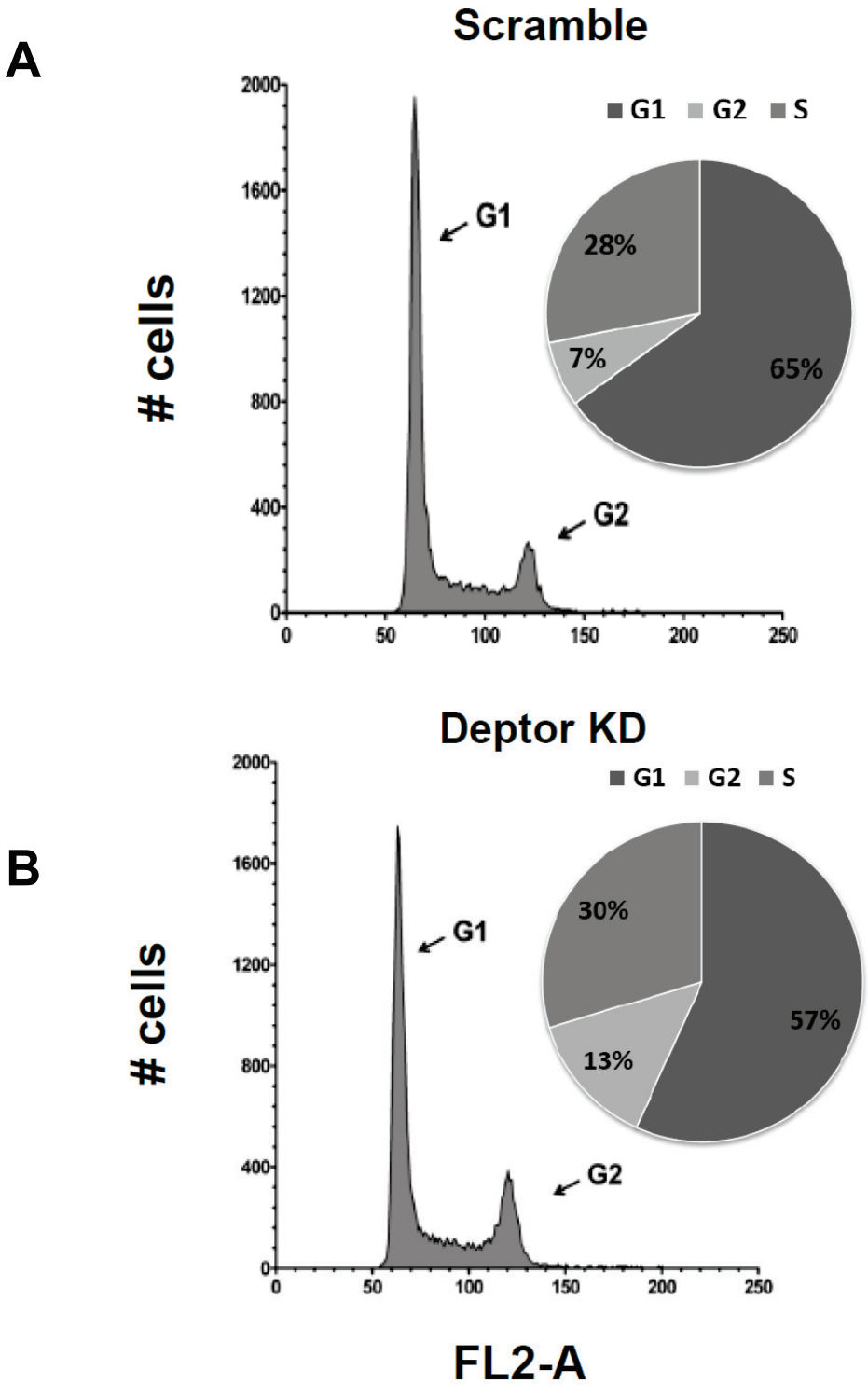
A
Scramble
G1 G2 S
28%
7%
65%
G1
G2
cells
2000
1600
1200
800
400
0
0 50 100 150 200 250
B
Deptor KD
G1 G2 S
30%
13%
57%
G1
G2
cells
FL2-A

C

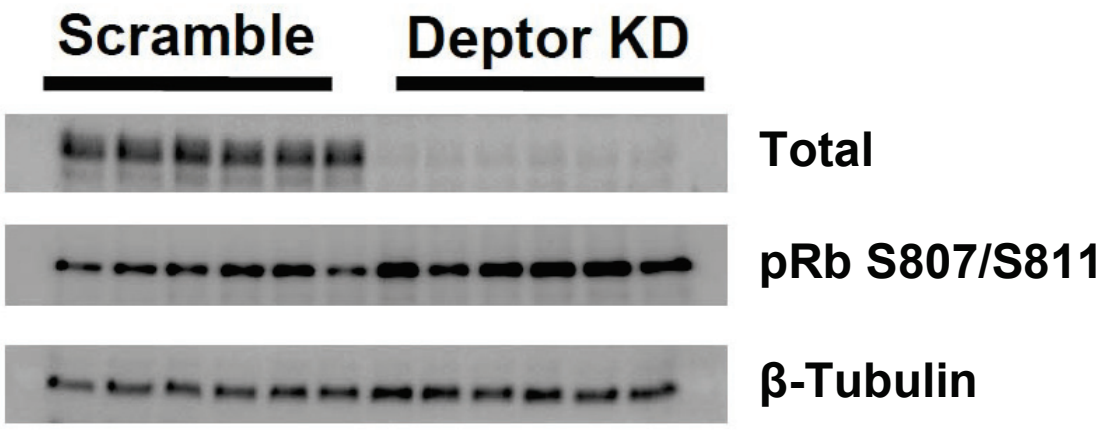
Scramble
Deptor KD
Total
pRb S807/S811
β-Tubulin

D

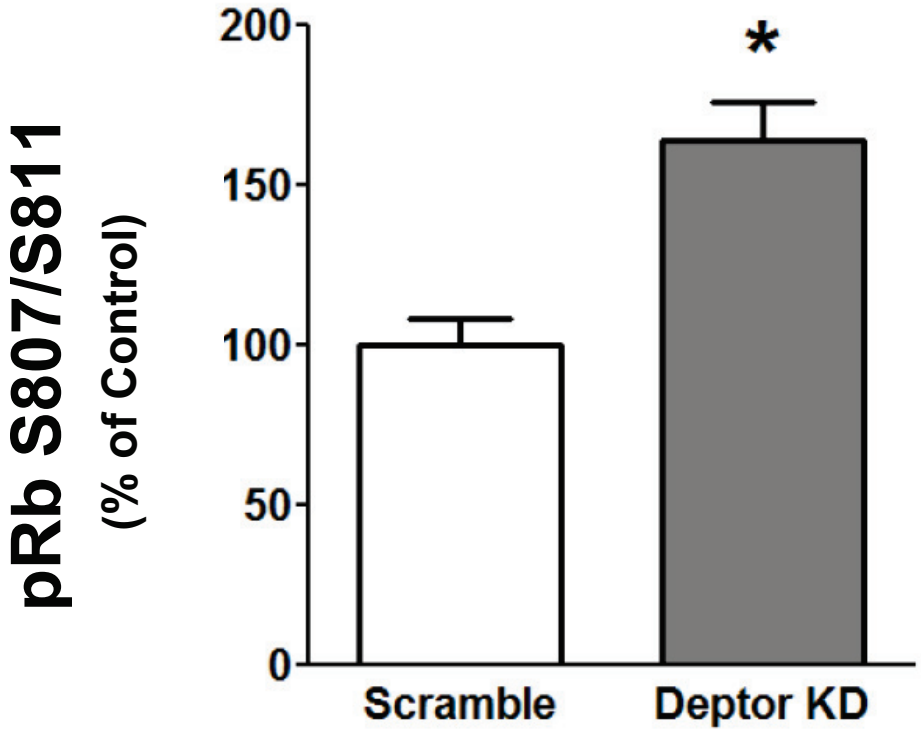
pRb S807/S811
(% of Control)
200
150
100
50
0
*
Scramble
Deptor KD

Figure 5—7A-B. **Effect of DEPTOR knockdown (KD) on cell cycle regulation**. Control and DEPTOR KD myoblasts were grown in DMEM media supplemented with 10% FBS overnight to 50-60% confluency. Myoblasts were then serum starved for 18-24 h in serum free DMEM to arrest them in G1-G0 phase. Serum starved myocytes were then released from the cell cycle arrest by the addition of fresh media containing 10% FBS. At 16 h these proliferating cells were fixed. Panel A: Bar graph shows the percent of cells in S-phase of the cell cycle in serum starved cells (0 h) and after addition of serum (16 h); mean ± SE; n= 5-6 for each condition. **P*<0.05, compared to time-matched control values. Panel B: Western blot of samples (normalized to total protein content for loading) as described above. Blots were probed with total DEPTOR antibody (top band) and with phospho-specific antibody to detect phosphorylation on S807/S811 of pRb protein (middle band). Lower band was probed with β-tubulin to confirm equal loading.

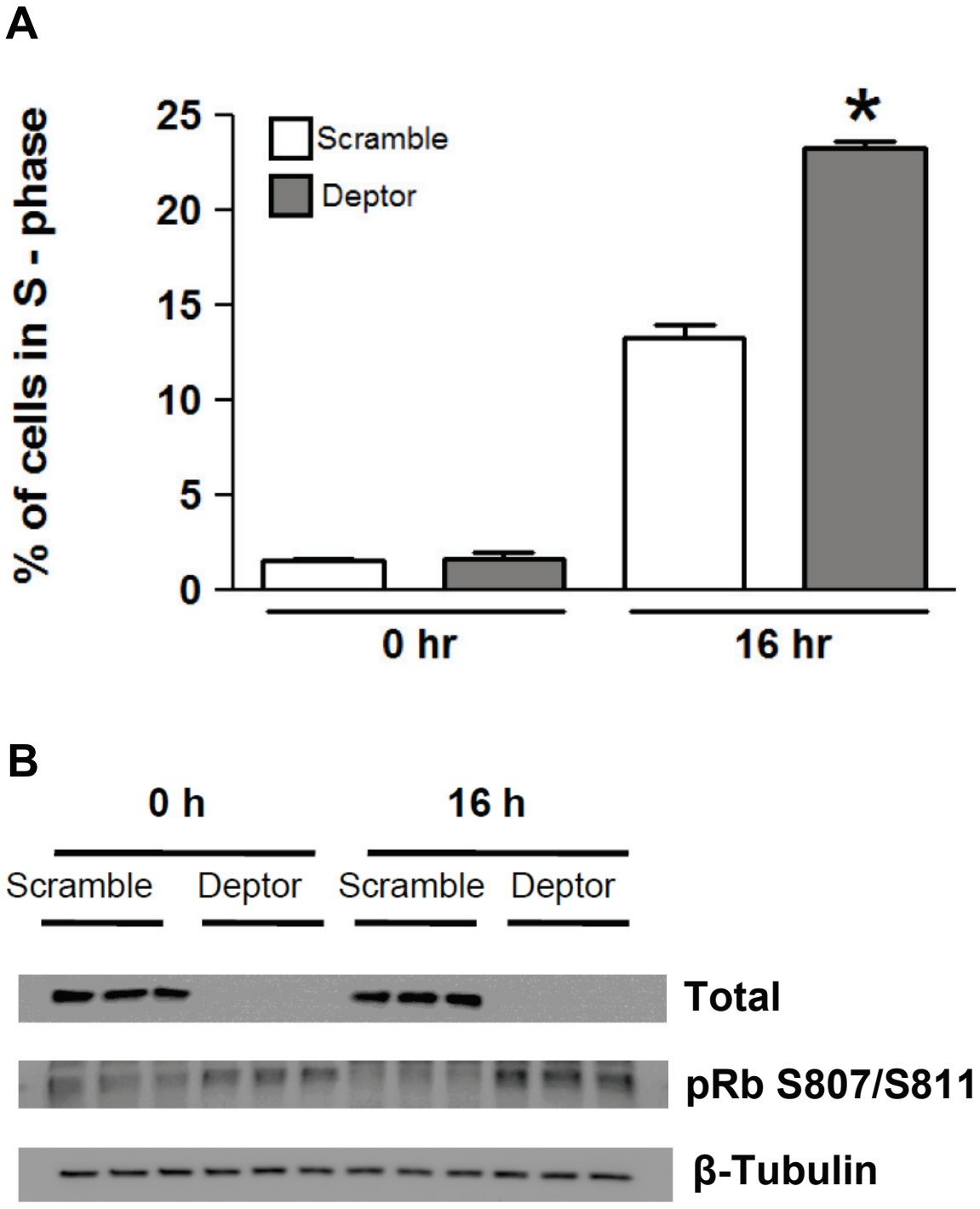
A
% of cells in S - phase
25
20
15
10
5
0
Scramble
Deptor
*
0 hr
16 hr
B
0 h
16 h
Scramble
Deptor
Scramble
Deptor
Total
pRb S807/S811
β-Tubulin

Figure 5—7C-D. Effect of DEPTOR knockdown (KD) on cell cycle regulatory protein. Changes in the content of cell cycle regulatory proteins were determined in stably transfected myoblasts with Scramble and DEPTOR KD using Western analysis. Panel C: Representative Western blots showing total DEPTOR expression and protein content of cell cycle inhibitors p21 and p27, cell cycle regulators cyclin D1 and p53 (with actin loading control) are shown. Panel D: Cyclin dependent kinases (cdk) -2, 4, and -6 content was determined using appropriate antibodies. No changes in total proteins were seen between scramble control and DEPTOR KD myoblasts.

C

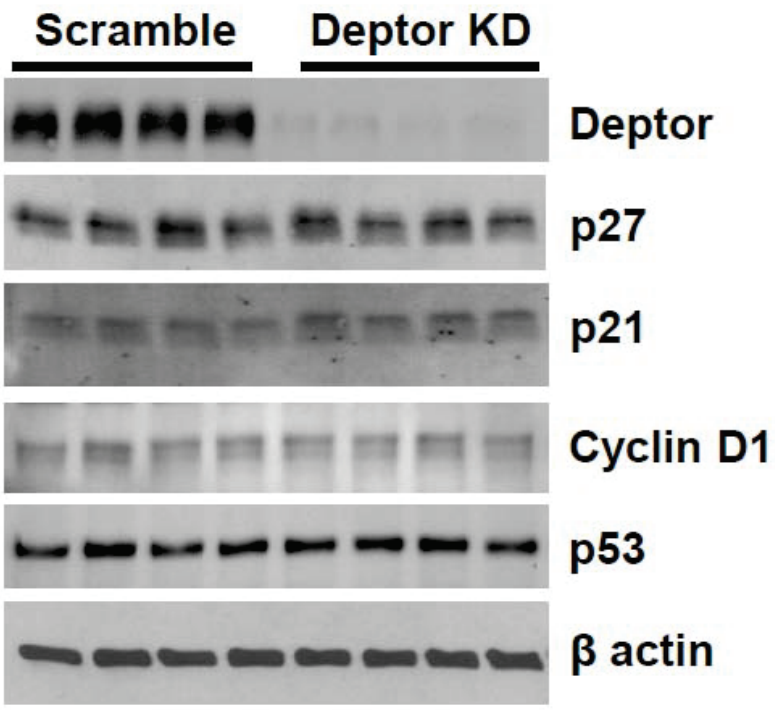
Scramble
Deptor KD
Deptor
p27
p21
Cyclin D1
p53
β actin

D

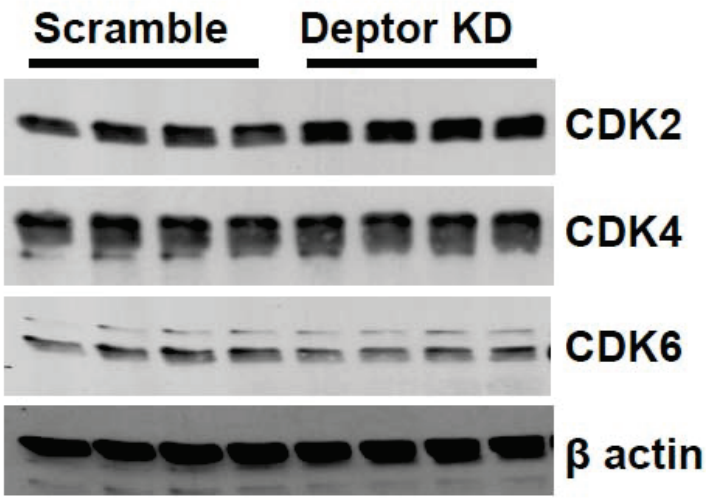
Scramble
Deptor KD
CDK2
CDK4
CDK6
β actin

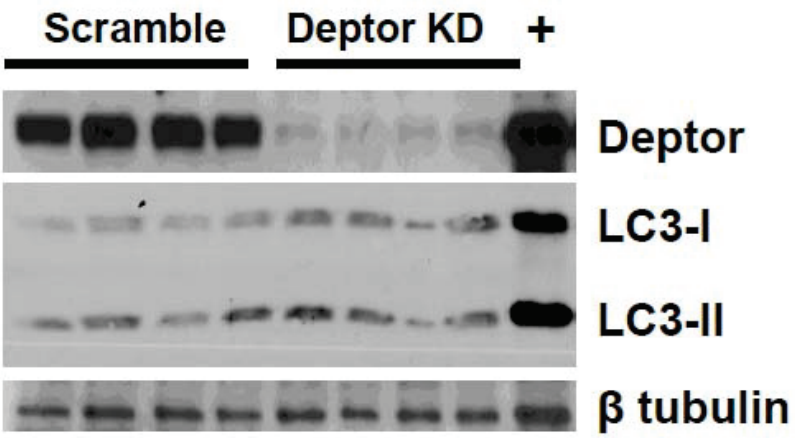

Figure 5—7E. Effect of DEPTOR knockdown (KD) on autophagy markers. Top Western blot showing expression of DEPTOR in the two groups and the positive control (+). Induction of basal autophagy was measured in scramble control and DEPTOR KD myoblasts using the well established autophagy marker LC3B (middle blot). No changes in LC3B-II/LC3B-I ratio were seen between scramble control and DEPTOR KD myoblasts. Blot showing β-actin serves as loading control (bottom blot).

Figure 5—8. **Effect of DEPTOR knockdown (KD) on C2C12 differentiation**. Panel A: Myoblasts were transfected with either control (scramble) shRNA or shRNA targeting DEPTOR. Cells were plated at the same density and photographed daily (10x objective magnification) to visually record changes in cell proliferation (time to reach confluence) and formation of myotubes. On Day 3-4 when the plates were confluent, the media was switched to 2% horse serum (DM = differentiation media) to induce myotube formation. DEPTOR KD in C2C12 myocytes enhances MHC protein expression. Panel B: Representative Western blots for DEPTOR protein, MHC and the muscle-specific transcription factor MyoD in samples treated as in Figure 5-8A. β-tubulin serves as a loading control.

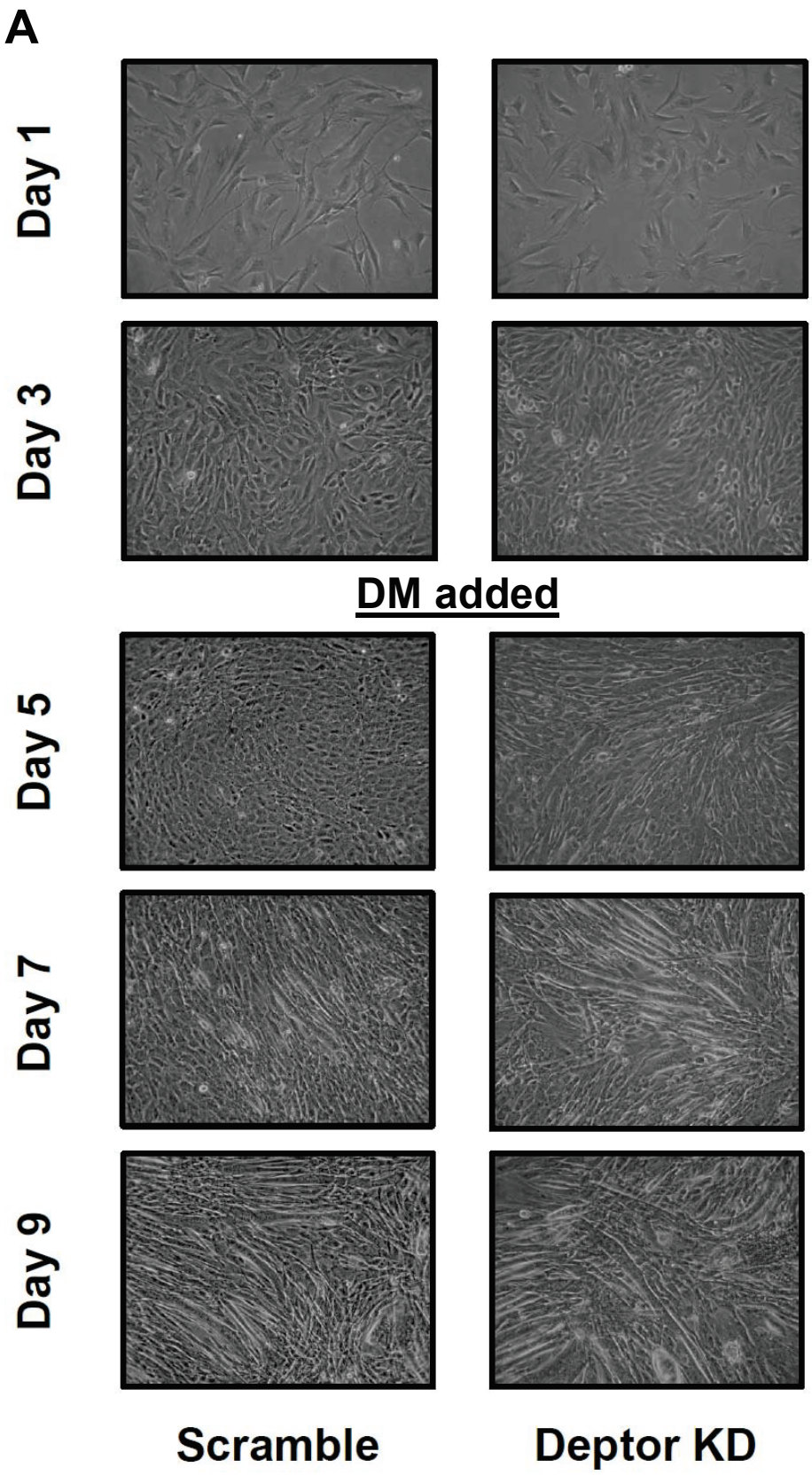
A
Day 1
Day 3
DM added
Day 5
Day 7
Day 9
Scramble
Deptor KD

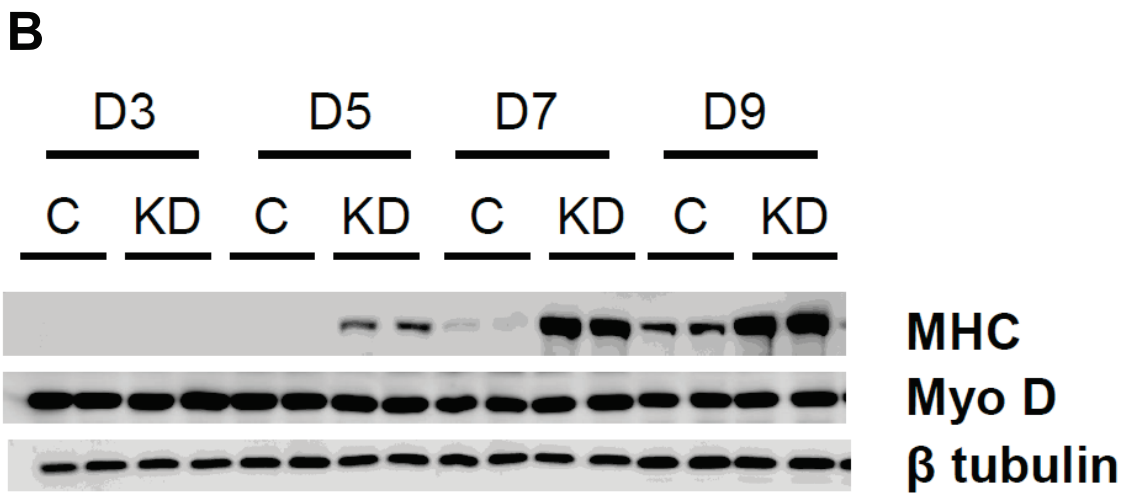
B
D3
D5
D7
D9
C
KD
C
KD
C
KD
C
KD
MHC
Myo D
β tubulin

Figure 5—9. **Effect of *in vivo* DEPTOR knockdown (KD) on skeletal muscle weight and protein synthesis**. Gastrocnemius of C57/BL6 mice were electroporated with plasmids containing either Scramble (Control) shRNA or shRNA targeting DEPTOR mRNA. Panel A: 3 d following electroporation the animals were anesthetized and the muscle was excised, homogenized, and mRNA in the homogenate was quantified using real time PCR. Bar graph shows DEPTOR mRNA content normalized to rpL32 which serves as an endogenous control. Values are mean ± SE; n= 5-6 for each condition. *$P<0.05$, compared to control values. Panel B: Animals were treated as described above then immediately following electroporation one hindlimb was immobilized to induce disuse atrophy as described in the Materials and Methods. At day 3, muscles were excised. Figure 5-9B shows muscle weight and Figure5- 9C shows the *in vivo*-determined rate of protein synthesis. For Figures 5-9B and 5-9C, values are means ± SE; n= 9-10 for each condition. Means with different superscripts (a, b and c) are significantly different (*$P<0.05$).

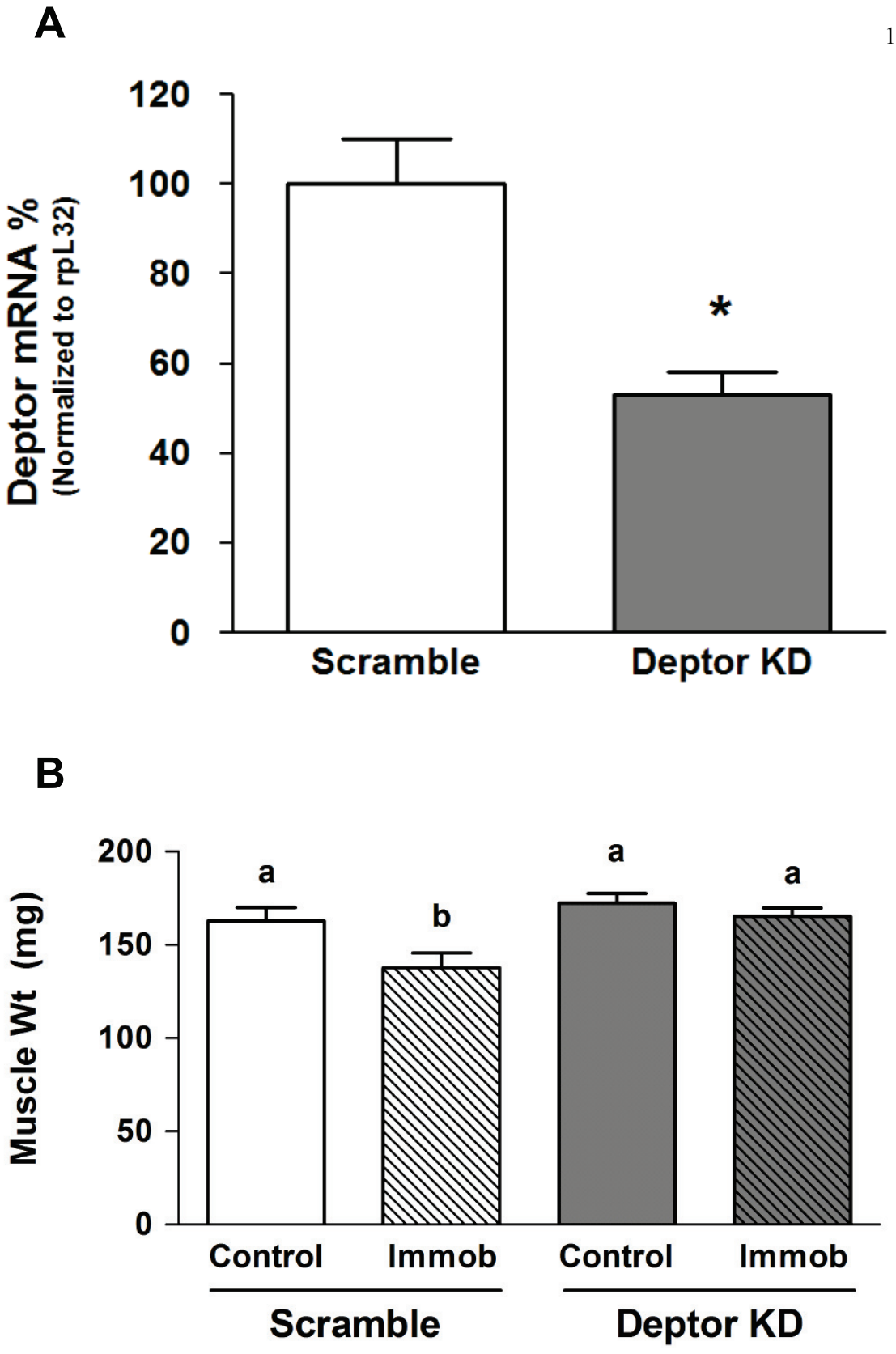
A
Deptor mRNA %
(Normalized to rpL32)
120
100
80
60
40
20
0
*
Scramble
Deptor KD
B
Muscle Wt (mg)
200
150
100
50
0
a
b
a
a
Control
Immob
Control
Immob
Scramble
Deptor KD

c

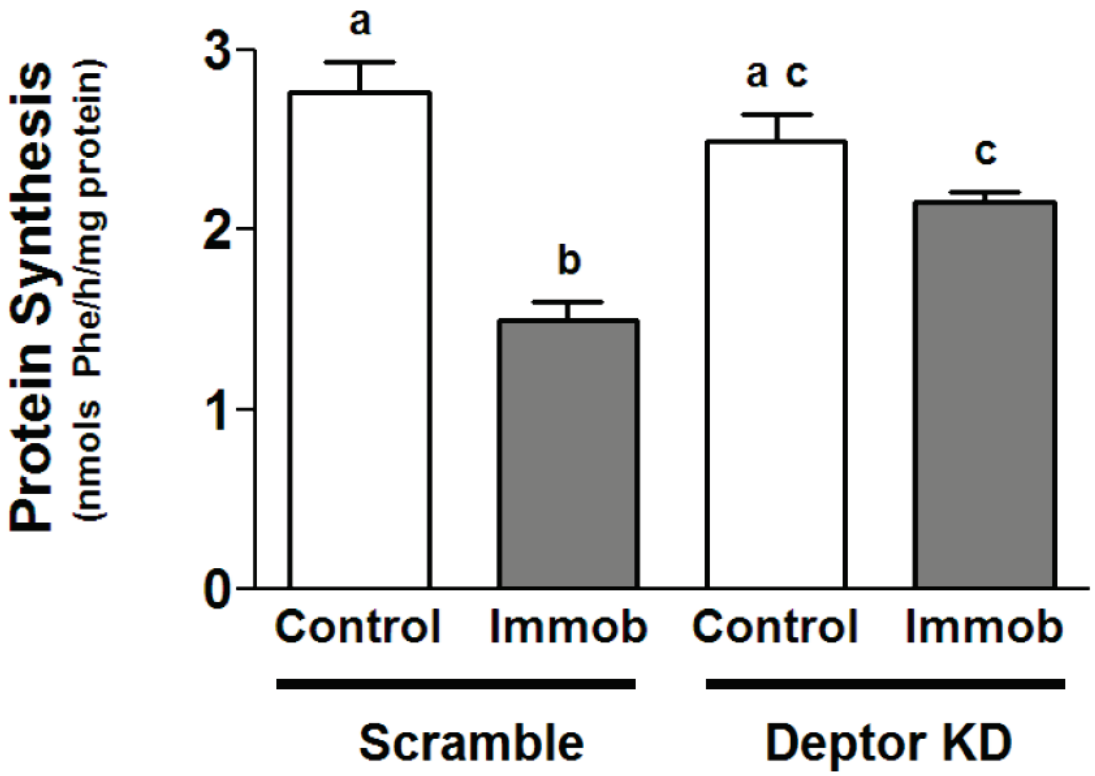
Protein Synthesis
(nmols Phe/h/mg protein)
3
2
1
0
a
b
a c
c
Control
Immob
Control
Immob
Scramble
Deptor KD

Table 5—1. **Effect of** DEPTOR **knockdown on cell cycle in C2C12 myoblasts.**

Cell cycle	**% G1**	**% S**	**% G2**
Scramble	65.1 ± 1.6	28.0 ± 0.8	6.9 ± 0.9
DEPTOR **KD**	56.7 ± 1.5*****	29.7 ± 0.7	13.6 ± 0.9*****

Myoblasts were transfected with either control (scramble) shRNA or shRNA targeting DEPTOR. Values are shown as means ± SE for $n = 12$ for each condition. *$P<0.05$ compared to time-matched control values.

Chapter 6

Summary, future directions and concluding remarks

The primary goal of the studies described in this dissertation was to determine how translation initiation is regulated under catabolic conditions, and if the suppression of translation initiation involved two recently identified binding partners of mTOR, PRAS40 and DEPTOR. Another goal was to determine if knockdown (KD) of PRAS40 and DEPTOR would affect mTOR-mediated processes, such as translation initiation, and thereby alter protein synthesis in myocytes. Based on the results of these preliminary goals, we included cell size, cell cycle, proliferation, and myogenesis as the end-points, to study the effect of PRAS40 and DEPTOR KD in later studies. To date, several reports have implicated both PRAS40 and DEPTOR as negative regulators of mTOR-mediated translation initiation, but as of yet, the effect of knocking down these protein partners of mTOR in regulation of cell proliferation, cell cycle, autophagy and myogenesis have not been characterized. Using cecal ligation and puncture to induce sepsis in Chapter 3, we first studied the effect of sepsis on protein translation initiation and reported that decreased phosphorylation of PRAS40 and increased content of DEPTOR may be involved in the sepsis-induced inhibition of mTOR-mediated translation initiation in rat gastrocnemius (as determined using established surrogate markers). These exciting findings encouraged us to look at the role of PRAS40 and DEPTOR in muscle cells and were included in this dissertation as two independent studies.

Using first an *in vitro* (PRAS40 and DEPTOR) and later an *in vivo* (DEPTOR) approach, we demonstrate that these proteins do function as regulators of mTOR-mediated processes in myocytes. While others have used S6K1 and 4E-BP1, two well established surrogate markers of mTOR kinase as end-points to imply increased protein synthesis, this is the first report measuring global protein synthesis *per se* following the knockdown of either PRAS40 or DEPTOR. Although the molecular mechanism(s) were not pursued in-depth in these studies, important observations showing the effect of PRAS40 and DEPTOR KD on cell cycle, proliferation, autophagy, and myogenesis were made in the context of skeletal muscle.

In sickness and in health: Control of protein balance

The importance of the mTOR signaling pathway in homeostatic balance is well established, and emerging data show an expanding role of mTOR in diseased conditions. Many diseases were outlined in the Introduction that had an underlying dysregulation of the mTOR signaling pathway. The working hypothesis in Chapter 3 posited, based on our previous data, that catabolic insults (e.g., sepsis), inhibit protein translation initiation by altering protein-protein interactions of the components of this process, especially those regulated by mTORC1 signaling.

Studies outlined in Chapter 4 identified PRAS40 as a component of mTORC1 that was required for translation under basal condition, as knockdown of PRAS40 in myoblasts inhibited protein synthesis, cell proliferation, cell cycle, and progression of myogenesis. Prior to the publication of this study, PRAS40 was solely considered as a

negative regulator of mTOR. Only one report by Fonseca *et al.,* (119) suggested that PRAS40 is required for mTORC1-mediated signaling. Our study confirmed and provided additional support to Fonseca *et al.,* by identifying other functions of PRAS40 in muscle cells and showed that KD of PRAS40 directly affected cell cycle and myogenesis. The reason for the observed difference between our findings and reports by other investigators is unclear but could be related to differences in cell type, developmental stage of the cell, the extent of PRAS40 KD or the experimental conditions. PRAS40 KD in differentiated myotubes did not alter protein synthesis. However, in contrast, PRAS40 KD in rapidly dividing C2C12 myoblasts decreased protein synthesis independent of a change in the phosphorylation of S6K1 and 4E-BP1, thus suggesting PRAS40 is not a negative regulator of mTOR–mediated translation in this cell type. The observation that KD of PRAS40 inhibited G1-S phase transition of cell cycle and decreased proliferation rate further adds support to our conclusion that PRAS40 is required for mTOR-mediated regulation of the aforementioned events. In general, understanding the changes in protein balance that occur during wasting conditions remains limited. Such knowledge regarding the molecular mechanisms involved in regulating translation holds the promise to improve the prognosis and treatment of individuals afflicted with diseases characterized by loss of lean body mass and negative nitrogen balance.

Studies detailed in Chapter 5 directly address the central hypothesis and identify that DEPTOR, a new protein partner of mTOR, plays an important role in maintaining the homeostatic balance between protein synthesis and muscle loss induced by disuse

atrophy. As anticipated, in culture, DEPTOR KD increased mTOR activity and global mRNA translation/protein synthesis. C2C12 myoblasts with reduced DEPTOR expression showed enlarged cell size, accelerated cell cycle progression (reduced G1 and hyper-phosphorylation of pRb) and proliferation (cell division) among other functions largely attributed to mTOR kinase.

Recurring questions: Evolving answers

Historically, cell proliferation has been inversely correlated with cell differentiation, i.e., signals that promote proliferation inhibit differentiation. In this regard, IGF-I and its cognate receptor have been widely studied and shown to have mitogen activity and to induce proliferation in muscle cells by reprogramming/recruiting satellite cells to undergo proliferation. We observed that DEPTOR KD accelerates both C2C12 myocyte proliferation and differentiation. While increased proliferation is consistent with the role of DEPTOR as a negative regulator of mTORC1, the enhanced differentiation which is thought to imply decreased mTORC1 activity (as manifest with serum withdrawal) is intriguing. Thus, the positive effect of DEPTOR KD on both C2C12 proliferation and differentiation is unexpected as myocyte differentiation has been traditionally coupled with cell cycle arrest. Almost 3 decades ago, Schmid *et al.,* reported a preferential enhancement of myoblast differentiation by IGF-I and IGF-II in primary cultures of chicken embryonic cells (316). Cellular signaling and myogenesis studies in C2C12 cells have identified Akt as a major regulator of cell differentiation, as

evidenced by the role of PI3K and Akt inhibitors in inhibiting myotube formation (317). Conversely, Akt activation has been shown to induce cell differentiation and myotube formation. DEPTOR KD may increase mTOR activation by sensitizing the pathway to positive regulators of mTOR signaling, similar to treating control cells with growth factors (e.g., IGF-I and IGF-II). This activation could then enhance myoblast differentiation, as reported by Schmid *et al*. Another possible explanation for the induction of both proliferation and differentiation is based on previous reports showing that IGF-I functions in a time-dependent biphasic manner, where IGF-I stimulates cell proliferation early on and then enhances differentiation later in the cell cycle (153, 318). Thus, by reducing DEPTOR content, we may be sensitizing mTOR signaling to the stimulation by growth factors.

As alluded to earlier, sparse data are available on the role of DEPTOR in general and its role in skeletal muscle in particular. Peterson *et al.,* proposed that DEPTOR KD stimulates mTOR-mediated S6K1 phosphorylation. S6K1 has a known positive effect on cell size and proliferation and activated S6K1 further enhances mTOR signaling (47, 72, 123). Conversely, overexpression of DEPTOR or use of the mTOR inhibitor resveratrol negatively regulates mTOR signaling mediated by increased mTOR-DEPTOR interaction. Assuming that DEPTOR is a negative regulator of mTOR, and based on current literature and the established role of growth factors in activating mTOR-mediated cell growth and proliferation, we propose the following model (Figure 6-1) in skeletal muscle. Decreasing DEPTOR initially enhances proliferation via mTOR-S6K1 stimulation, and then later via increased autocrine activity increases IGF-II production.

This increased IGF-II enhances Akt-mediated signaling which in turn enhances myoblast differentiation. Thus, similar to the previously described biphasic role of IGF-I, initially DEPTOR KD may regulate mTORC1-mTORC2 via a positive feedback loop, whereas later removal of the inhibitory signal (DEPTOR) may reach a certain maximal cellular threshold that uncouples the two mTOR complexes, making one complex more sensitive than the other to cellular stressors, such as contact inhibition, energy depletion or ER stress from increased global protein synthesis.

Cdk inhibitors regulate myotube formation (190). Of particular note is the role of the cdk inhibitor p27, whose expression is induced by contact inhibition. The increased proliferation rate of DEPTOR KD cells results in an increased number of cells in the culture dish. Thus, these DEPTOR KD cells become crowded and cover the limited surface area becoming contact inhibited. We hypothesize that increase contact inhibition results in increased expression of p27 which results in enhanced myotube differentiation. A simple future approach to determine if indeed, enhanced differentiation observed is due to contact inhibition of DEPTOR KD cells (as a result of increase proliferation rate), would be to seed plates at artificially high densities such that both scramble control and DEPTOR KD cells reach confluence as soon as they settle and attach to the culture dish (few hours to overnight). One could then lyse the cells and determine the expression of the cdk inhibitor p27 and compare its expression when plates reach confluent status at different times. Similarly, to determine if mTOR is inhibited due to a decrease in energy levels following increased demand (increased proliferation=greater number of cells), we could also probe for the activation of the energy sensor – AMPK.

The importance of IGF-I as a mitogen throughout development has been clearly demonstrated in IGF-I and IGF-IR knockout mouse studies, and also in transgenic mice over-expressing IGF-I, as presented in the Introduction. IGF-I functions as a mitogen in many cultured cell lines (e.g., T lymphocytes, osteoblasts and mouse fibroblasts) and enhances cell progression. Multiple independent investigators have confirmed that IGF-I is also involved in muscle differentiation of mesenchymal cells. Benito *et al.,* reported that IGF-I induces proliferation and differentiation in fetal brown adipocytes, further suggesting that these cellular processes are not mutually exclusive at least in fetal cells (319). At this time, we lack definitive evidence for which mechanism is operational and experiments designed to answer these questions would help elucidate how DEPTOR is regulated or regulates IGF-I-mediated mutagen signaling in C2C12 cells. Alternatively, we cannot exclude the possibility that the reduction in DEPTOR alters cell cycle kinetics and differentiation by an undetermined mechanism that is mTOR-independent.

To further dissect the role of DEPTOR in myogenesis, we examined the effect of DEPTOR KD on the expression of MHC, an important marker of muscle differentiation. Consistent with our morphometric findings, we observed that expression of MHC is also enhanced in DEPTOR KD C2C12 cells. Collectively, our data demonstrate that DEPTOR modulates C2C12 cell proliferation and differentiation. Additional proof of principal is provided using *in vivo* data to support the notion that DEPTOR is a negative regulator of protein synthesis since knockdown of DEPTOR in murine gastrocnemius prevented loss of muscle mass following hindlimb immobilization. At least part of the efficacy of DEPTOR KD to prevent muscle loss in this condition was due to an increase

in protein synthesis. Additional studies are needed to determine whether DEPTOR might also impact the protein degradation side of the protein balance equation. Our data identify DEPTOR as an important regulator of mTOR-mediated protein translation *in vivo* and provide a rationale to further pursue DEPTOR as a target for regulating translational control in catabolic states using traditional pharmaceutical approaches.

The purpose of this study was to examine the mechanisms responsible for changes in protein metabolism following KD of DEPTOR in the context of catabolic insults in skeletal muscle using hindlimb immobilization as a catabolic model. The muscle-sparing effect of DEPTOR KD in the hindlimb immobilization model, as demonstrated in Chapter 5, is novel and exciting. However, in the control animals, contrary to our hypothesis, there was no increase in protein synthesis in the control muscles electroporated with DEPTOR KD plasmid. The differences seen between control and DEPTOR KD muscles in comparison to the groups where the muscles were immobilized suggest that perhaps DEPTOR has a more important regulatory role in fine tuning the translational control. Thus, under unfavorable "immobilized" conditions, rather than normal basal "control" conditions, DEPTOR may regulate translation initiation mediated by other protein-protein interactions as discussed in Chapter 3. Such a muscle-sparing effect of DEPTOR KD under catabolic conditions would be advantageous in a clinical setting for the following reasons: (1) There is no adverse effect (increased hypertrophy) of DEPTOR KD in control and normal muscle, and (2) under catabolic conditions; DEPTOR KD suppresses muscle atrophy in part by enhancing muscle protein synthesis.

Despite the rapid loss of muscle mass in the hindlimb immobilization model, we were not able to demonstrate a significantly sustained KD of DEPTOR beyond 3 days, using the current *in vivo* electroporation approach. Since protein synthesis is an energy consuming process, it is likely that the process is regulated by multi-tier redundant pathways as it is not physiologically favorable to have a constitutively uncontrolled increase in protein synthesis. Our ability (or inability) to sustain DEPTOR KD precluded us from examining the role of DEPTOR in models of disuse atrophy over a longer duration, thus limiting the study of protein-protein interactions only to an early time. It is possible that primary cells could be isolated from the transfected animals and treated with puromycin for selection and used to ascertain the role of DEPTOR KD *in vitro*. However such analysis would seem to be comparable to the cell culture work already performed. Alternatively, a pharmacological approach might be adapted. Small molecule inhibitors of the PDZ interacting proteins could be used, thus disrupting mTOR-DEPTOR interaction. This interaction has been proposed to be important for mTOR-DEPTOR regulation, and disrupting this interaction might reasonably be expected to increase muscle protein synthesis under catabolic conditions (320, 321).

As presented in Chapter 3, the protein-protein interaction of the mTORC1 complex is important in regulating translation initiation. Future studies are required to better understand the role of DEPTOR in regulating mTOR-mediated events under various physiological conditions. Holz *et al* provided a thorough investigation of the interactions of mTOR complex 1 proteins with the pre-initiation complex proteins, however, since then 2 additional proteins that were examined herein (PRAS40 and DEPTOR) were reported to interact with mTOR. Therefore, in the near future, it is

scientifically justified to pursue the interaction of these proteins at the eIF3-preinitiation complex under basal, stimulated, and suppressed conditions in order to understand where these proteins are in time and space in relation to each other under the various physiological conditions. Is phosphorylation of DEPTOR and its subsequent dissociation from the mTOR complex a pre-requisite for mTOR-raptor complex to be recruited to the pre-initiation complex? In mTORC2, how does mTOR get activated while DEPTOR is still attached, i.e., what events have to occur for mTOR activation? Are there other kinases that can phosphorylate DEPTOR *in vivo* and *in vitro*? Does DEPTOR play any function in cellular compartmentalization of mTOR, as has been reported for other proteins (i.e., Rag GTPase proteins), in regulating mTOR function? What role does phosphorylation play in regulating DEPTOR half-life? How would phospho-mimic DEPTOR or non-phosphorylatable DEPTOR regulate mTOR-mediated cellular processes? Does DEPTOR have tissue specific roles, i.e., does it play a different role in the muscle, brain or liver?

Some findings raise more questions than answers!

In conclusion, despite the many recent advances expanding our knowledge about the growth factor-PI3K-Akt-mTOR-S6K1 pathway, understanding of this signaling network is far from complete, and many important questions remain. For example, we know little about how mTORC2 is regulated and, in turn, the biological processes that it controls. Though mTORC2 activates mTORC1 via Akt, how are the two (mTORC1 and

mTORC2) signaling pathways integrated with each other? What functions do these complexes play in skeletal muscle, and what are the implications of their dysfunction or dysregulation in health and disease? Under what conditions does the signaling between the two mTOR complexes become uncoupled? The recent identification of new protein partners suggests that there may be more proteins yet to be identified. If so, what other biological processes do they regulate? How are the next generation drugs designed to preserve the normal function regulated by mTOR signaling, yet correct any dysfunction/dysregulation? Finding answers to these important questions are critical in understanding cellular biology and indispensible as we search for developing new therapeutic strategies to treat the many diseases that involve impaired mTOR signaling.

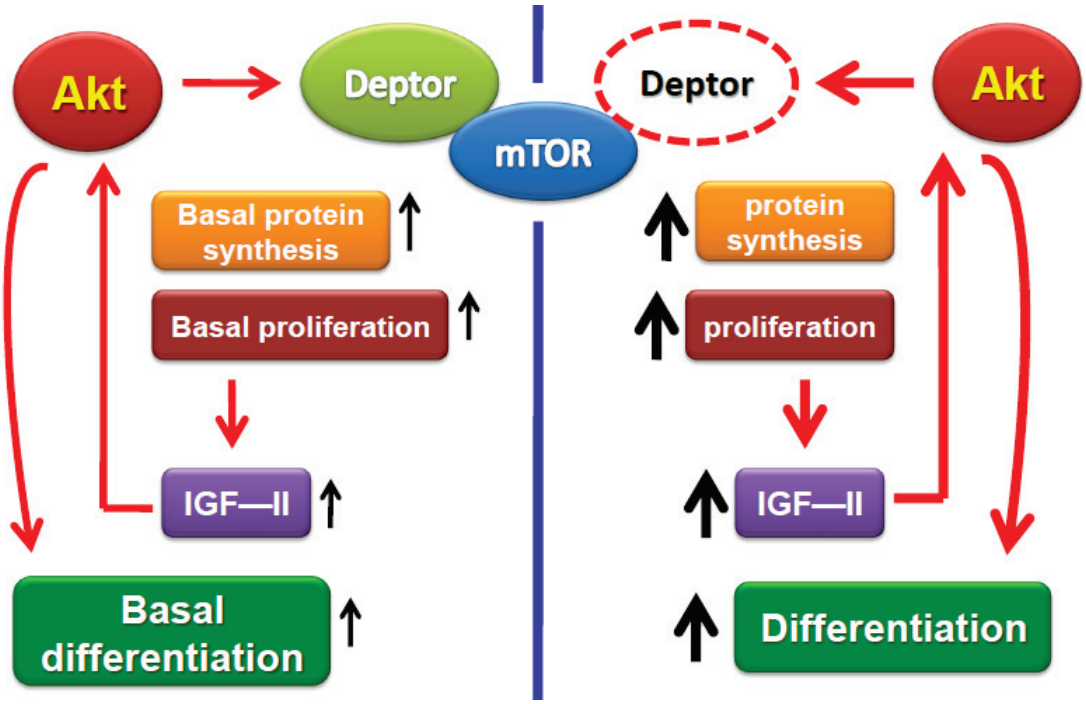

Figure 6—1. Model describing effect of DEPTOR KD on myocytes proliferation and differentiation. Under normal basal conditions, mTOR-DEPTOR interaction is regulated by insulin and growth factors to mediate protein synthesis, cell proliferation and differentiation, as depicted in the illustration by a thin upward arrow besides the events on the left half of the figure. However, upon DEPTOR KD (shown as incomplete oval), mTOR activity is enhanced, resulting in increased (thick upward arrow) protein synthesis and cell proliferation resulting in rapid increase in cell number in the culture dish. This increased number of proliferative cells produces more autocrine secretion of IGF—II, which further activates the PI3K-Akt pathway, leading to enhanced myocyte differentiation. At this stage, perhaps the two mTOR complexes are differently sensitive to cell stressors, such as contact inhibition (which increases cdk-inhibitor expression that favor cell cycle arrest and differentiation), energy stress and/or ER stress from increased global protein synthesis following DEPTOR KD.

Chapter 7

References

1. Pruznak AM, Kazi AA, Frost RA, Vary TC, Lang CH. (2008) Activation of AMP-activated protein kinase by 5-aminoimidazole-4-carboxamide-1-beta-D-ribonucleoside prevents leucine-stimulated protein synthesis in rat skeletal muscle. *J Nutr* **138:** 1887-1894.
2. Neufeld TP. (2003) Body building: regulation of shape and size by PI3K/TOR signaling during development. *Mech Dev* **120:** 1283-1296.
3. Baar K, Nader G, Bodine S. (2006) Resistance exercise, muscle loading/unloading and the control of muscle mass. *Essays Biochem* **42:** 61-74.
4. Rommel C, et al. (2001) Mediation of IGF-1-induced skeletal myotube hypertrophy by PI(3)K/Akt/mTOR and PI(3)K/Akt/GSK3 pathways. *Nat Cell Biol* **3:** 1009-1013.
5. Bodine SC, et al. (2001) Akt/mTOR pathway is a crucial regulator of skeletal muscle hypertrophy and can prevent muscle atrophy in vivo. *Nat Cell Biol* **3:** 1014-1019.
6. Glass DJ. (2005) Skeletal muscle hypertrophy and atrophy signaling pathways. *Int J Biochem Cell Biol* **37:** 1974-1984.
7. Glass DJ. (2010) PI3 kinase regulation of skeletal muscle hypertrophy and atrophy. *Curr Top Microbiol Immunol* **346:** 267-278.
8. Jaffe DM, Terry RD, Spiro AJ. (1978) Disuse atrophy of skeletal muscle. A morphometric study using image analysis. *J Neurol Sci* **35:** 189-200.
9. Kimball SR, Jefferson LS. (2006) Signaling pathways and molecular mechanisms through which branched-chain amino acids mediate translational control of protein synthesis. *J Nutr* **136:** 227S-231S.
10. Anthony JC, et al. (2002) Contribution of insulin to the translational control of protein synthesis in skeletal muscle by leucine. *Am J Physiol Endocrinol Metab* **282:** E1092-1101.
11. Booth FW, Seider MJ. (1979) Early change in skeletal muscle protein synthesis after limb immobilization of rats. *J Appl Physiol* **47:** 974-977.
12. Degens H, Alway SE. (2006) Control of muscle size during disuse, disease, and aging. *Int J Sports Med* **27:** 94-99.
13. Krawiec BJ, Frost RA, Vary TC, Jefferson LS, Lang CH. (2005) Hindlimb casting decreases muscle mass in part by proteasome-dependent proteolysis but independent of protein synthesis. *Am J Physiol Endocrinol Metab* **289:** E969-980.
14. Lang CH, Frost RA, Vary TC. (2007) Regulation of muscle protein synthesis during sepsis and inflammation. *Am J Physiol Endocrinol Metab* **293:** E453-459.
15. Hong-Brown LQ, et al. (2010) Alcohol and PRAS40 knockdown decrease mTOR activity and protein synthesis via AMPK signaling and changes in mTORC1 interaction. *J Cell Biochem* **109:** 1172-1184.
16. Hong-Brown LQ, Frost RA, Lang CH. (2001) Alcohol impairs protein synthesis and degradation in cultured skeletal muscle cells. *Alcohol Clin Exp Res* **25:** 1373-1382.

17. Argiles JM, Busquets S, Felipe A, Lopez-Soriano FJ. (2005) Molecular mechanisms involved in muscle wasting in cancer and ageing: cachexia versus sarcopenia. *Int J Biochem Cell Biol* **37:** 1084-1104.
18. Cooney RN, et al. (1999) Mechanism of IL-1 induced inhibition of protein synthesis in skeletal muscle. *Shock* **11:** 235-241.
19. Long CL, Jeevanandam M, Kim BM, Kinney JM. (1977) Whole body protein synthesis and catabolism in septic man. *Am J Clin Nutr* **30:** 1340-1344.
20. Jewett MC, Miller ML, Chen Y, Swartz JR. (2009) Continued protein synthesis at low [ATP] and [GTP] enables cell adaptation during energy limitation. *J Bacteriol* **191:** 1083-1091.
21. Zoncu R, Efeyan A, Sabatini DM. (2010) mTOR: from growth signal integration to cancer, diabetes and ageing. *Nat Rev Mol Cell Biol* **12:** 21-35.
22. Hentges KE, et al. (2001) FRAP/mTOR is required for proliferation and patterning during embryonic development in the mouse. *Proc Natl Acad Sci U S A* **98:** 13796-13801.
23. Jacinto E, Hall MN. (2003) Tor signalling in bugs, brain and brawn. *Nat Rev Mol Cell Biol* **4:** 117-126.
24. Asnaghi L, Bruno P, Priulla M, Nicolin A. (2004) mTOR: a protein kinase switching between life and death. *Pharmacol Res* **50:** 545-549.
25. Hay N, Sonenberg N. (2004) Upstream and downstream of mTOR. *Genes Dev* **18:** 1926-1945.
26. Sehgal SN. (1998) Rapamune (RAPA, rapamycin, sirolimus): mechanism of action immunosuppressive effect results from blockade of signal transduction and inhibition of cell cycle progression. *Clin Biochem* **31:** 335-340.
27. Hall MN. (2008) mTOR-what does it do? *Transplant Proc* **40:** S5-8.
28. Romano S, et al. (2010) FK506 binding proteins as targets in anticancer therapy. *Anticancer Agents Med Chem* **10:** 651-656.
29. MacMillan D, Currie S, Bradley KN, Muir TC, McCarron JG. (2005) In smooth muscle, FK506-binding protein modulates IP3 receptor-evoked Ca2+ release by mTOR and calcineurin. *J Cell Sci* **118:** 5443-5451.
30. Jacinto E, Lorberg A. (2008) TOR regulation of AGC kinases in yeast and mammals. *Biochem J* **410:** 19-37.
31. Gangloff YG, et al. (2004) Disruption of the mouse mTOR gene leads to early postimplantation lethality and prohibits embryonic stem cell development. *Mol Cell Biol* **24:** 9508-9516.
32. Lang CH, Frost RA. (2004) Differential effect of sepsis on ability of leucine and IGF-I to stimulate muscle translation initiation. *Am J Physiol Endocrinol Metab* **287:** E721-730.
33. Kazi AA, Pruznak AM, Frost RA, Lang CH. (2010) Sepsis-Induced Alterations in Protein-Protein Interactions within Mtor Complex 1 and the Modulating Effect of Leucine on Muscle Protein Synthesis. *Shock* **35**: 117-125.
34. Pende M, et al. (2004) S6K1(-/-)/S6K2(-/-) mice exhibit perinatal lethality and rapamycin-sensitive 5'-terminal oligopyrimidine mRNA translation and reveal a mitogen-activated protein kinase-dependent S6 kinase pathway. *Mol Cell Biol* **24:** 3112-3124.
35. Wei M, et al. (2008) Life span extension by calorie restriction depends on Rim15 and transcription factors downstream of Ras/PKA, Tor, and Sch9. *PLoS genetics* **4:** e13.
36. Sarbassov DD, Ali SM, Sabatini DM. (2005) Growing roles for the mTOR pathway. *Curr Opin Cell Biol* **17:** 596-603.
37. Sancak Y, et al. (2007) PRAS40 is an insulin-regulated inhibitor of the mTORC1 protein kinase. *Mol Cell* **25:** 903-915.

38. Kim DH, et al. (2002) mTOR interacts with raptor to form a nutrient-sensitive complex that signals to the cell growth machinery. *Cell* **110:** 163-175.
39. Sarbassov DD, Sabatini DM. (2005) Redox regulation of the nutrient-sensitive raptor-mTOR pathway and complex. *J Biol Chem* **280:** 39505-39509.
40. Vary TC. (2007) Acute oral leucine administration stimulates protein synthesis during chronic sepsis through enhanced association of eukaryotic initiation factor 4G with eukaryotic initiation factor 4E in rats. *J Nutr* **137:** 2074-2079.
41. Kimball SR, Shantz LM, Horetsky RL, Jefferson LS. (1999) Leucine regulates translation of specific mRNAs in L6 myoblasts through mTOR-mediated changes in availability of eIF4E and phosphorylation of ribosomal protein S6. *J Biol Chem* **274:** 11647-11652.
42. Krawiec BJ, Nystrom GJ, Frost RA, Jefferson LS, Lang CH. (2007) AMP-activated protein kinase agonists increase mRNA content of the muscle-specific ubiquitin ligases MAFbx and MuRF1 in C2C12 cells. *Am J Physiol Endocrinol Metab* **292:** E1555-1567.
43. Anthony JC, et al. (2002) Orally administered leucine enhances protein synthesis in skeletal muscle of diabetic rats in the absence of increases in 4E-BP1 or S6K1 phosphorylation. *Diabetes* **51:** 928-936.
44. Frost RA, Huber D, Pruznak A, Lang CH. (2009) Regulation of REDD1 by insulin-like growth factor-I in skeletal muscle and myotubes. *J Cell Biochem* **108:** 1192-1202.
45. Fingar DC, Blenis J. (2004) Target of rapamycin (TOR): an integrator of nutrient and growth factor signals and coordinator of cell growth and cell cycle progression. *Oncogene* **23:** 3151-3171.
46. Hornberger TA, et al. (2006) The role of phospholipase D and phosphatidic acid in the mechanical activation of mTOR signaling in skeletal muscle. *Proc Natl Acad Sci U S A* **103:** 4741-4746.
47. Peterson TR, et al. (2009) DEPTOR is an mTOR inhibitor frequently overexpressed in multiple myeloma cells and required for their survival. *Cell* **137:** 873-886.
48. DeYoung MP, Horak P, Sofer A, Sgroi D, Ellisen LW. (2008) Hypoxia regulates TSC1/2-mTOR signaling and tumor suppression through REDD1-mediated 14-3-3 shuttling. *Genes Dev* **22:** 239-251.
49. Kimball SR, Do AN, Kutzler L, Cavener DR, Jefferson LS. (2008) Rapid turnover of the mTOR complex 1 (mTORC1) repressor REDD1 and activation of mTORC1 signaling following inhibition of protein synthesis. *J Biol Chem* **283:** 3465-3475.
50. Shah OJ, Kimball SR, Jefferson LS. (2000) Glucocorticoids abate p70(S6k) and eIF4E function in L6 skeletal myoblasts. *Am J Physiol Endocrinol Metab* **279:** E74-82.
51. Lang CH, Frost RA. (2006) Glucocorticoids and TNFalpha interact cooperatively to mediate sepsis-induced leucine resistance in skeletal muscle. *Mol Med* **12:** 291-299.
52. Shah OJ, Anthony JC, Kimball SR, Jefferson LS. (2000) Glucocorticoids oppose translational control by leucine in skeletal muscle. *Am J Physiol Endocrinol Metab* **279:** 1185-1190.
53. Lang CH, Frost RA, Bronson SK, Lynch CJ, Vary TC. (2010) Skeletal muscle protein balance in mTOR heterozygous mice in response to inflammation and leucine. *Am J Physiol Endocrinol Metab* **298:** E1283-1294.
54. Kim DH, Sabatini DM. (2004) Raptor and mTOR: subunits of a nutrient-sensitive complex. *Curr Top Microbiol Immunol* **279:** 259-270.
55. Yonezawa K, Tokunaga C, Oshiro N, Yoshino K. (2004) Raptor, a binding partner of target of rapamycin. *Biochem Biophys Res Commun* **313:** 437-441.
56. Hara K, et al. (2002) Raptor, a binding partner of target of rapamycin (TOR), mediates TOR action. *Cell* **110:** 177-189.

57. Ali SM, Sabatini DM. (2005) Structure of S6 kinase 1 determines whether raptor-mTOR or rictor-mTOR phosphorylates its hydrophobic motif site. *J Biol Chem* **280:** 19445-19448.
58. Kawasome H, et al. (1998) Targeted disruption of p70(s6k) defines its role in protein synthesis and rapamycin sensitivity. *Proc Natl Acad Sci U S A* **95:** 5033-5038.
59. Fingar DC, et al. (2004) mTOR controls cell cycle progression through its cell growth effectors S6K1 and 4E-BP1/eukaryotic translation initiation factor 4E. *Mol Cell Biol* **24:** 200-216.
60. Pearce LR, Komander D, Alessi DR. (2009) The nuts and bolts of AGC protein kinases. *Nat Rev Mol Cell Biol* **11:** 9-22.
61. Aguilar V, et al. (2007) S6 kinase deletion suppresses muscle growth adaptations to nutrient availability by activating AMP kinase. *Cell Metab* **5:** 476-487.
62. Mieulet V, et al. (2007) S6 kinase inactivation impairs growth and translational target phosphorylation in muscle cells maintaining proper regulation of protein turnover. *Am J Physiol Cell Physiol* **293:** C712-722.
63. Shima H, et al. (1998) Disruption of the p70(s6k)/p85(s6k) gene reveals a small mouse phenotype and a new functional S6 kinase. *EMBO J* **17:** 6649-6659.
64. Thomas G. (2002) The S6 kinase signaling pathway in the control of development and growth. *Biol Res* **35:** 305-313.
65. Volarevic S, Thomas G. (2001) Role of S6 phosphorylation and S6 kinase in cell growth. *Prog Nucleic Acid Res Mol Biol* **65:** 101-127.
66. Montagne J, et al. (1999) Drosophila S6 kinase: a regulator of cell size. *Science* **285:** 2126-2129.
67. Filonenko VV, et al. (2004) Immunohistochemical analysis of S6K1 and S6K2 localization in human breast tumors. *Exp Oncol* **26:** 294-299.
68. Lyzogubov VV, et al. (2004) Immunohistochemical analysis of S6K1 and S6K2 expression in endometrial adenocarcinomas. *Exp Oncol* **26:** 287-293.
69. Savinska LO, et al. (2004) Immunohistochemical analysis of S6K1 and S6K2 expression in human breast tumors. *Eksp Onkol* **26:** 24-30.
70. Hornberger TA, Sukhija KB, Wang XR, Chien S. (2007) mTOR is the rapamycin-sensitive kinase that confers mechanically-induced phosphorylation of the hydrophobic motif site Thr(389) in p70(S6k). *FEBS Lett* **581:** 4562-4566.
71. Dennis PB, Pullen N, Pearson RB, Kozma SC, Thomas G. (1998) Phosphorylation sites in the autoinhibitory domain participate in p70(s6k) activation loop phosphorylation. *J Biol Chem* **273:** 14845-14852.
72. Holz MK, Ballif BA, Gygi SP, Blenis J. (2005) mTOR and S6K1 mediate assembly of the translation preinitiation complex through dynamic protein interchange and ordered phosphorylation events. *Cell* **123:** 569-580.
73. Perez-Tenorio G, et al. (2010) Clinical potential of the mTOR targets S6K1 and S6K2 in breast cancer. *Breast Cancer Res Treat* Oct 16.
74. Lee-Fruman KK, Kuo CJ, Lippincott J, Terada N, Blenis J. (1999) Characterization of S6K2, a novel kinase homologous to S6K1. *Oncogene* **18:** 5108-5114.
75. Kroczynska B, et al. (2009) Interferon-dependent engagement of eukaryotic initiation factor 4B via S6 kinase (S6K)- and ribosomal protein S6K-mediated signals. *Mol Cell Biol* **29:** 2865-2875.
76. Lopez de Quinto S, Martinez-Salas E. (2000) Interaction of the eIF4G initiation factor with the aphthovirus IRES is essential for internal translation initiation in vivo. *RNA* **6:** 1380-1392.

77. Shahbazian D, Parsyan A, Petroulakis E, Hershey J, Sonenberg N. (2010) eIF4B controls survival and proliferation and is regulated by proto-oncogenic signaling pathways. *Cell Cycle* **9:** 4106-4109.
78. Chen WW, Chan DC, Donald C, Lilly MB, Kraft AS. (2005) Pim family kinases enhance tumor growth of prostate cancer cells. *Molecular cancer research : MCR* **3:** 443-451.
79. Gingras AC, et al. (1999) Regulation of 4E-BP1 phosphorylation: a novel two-step mechanism. *Genes & development* **13:** 1422-1437.
80. Poulin F, Gingras AC, Olsen H, Chevalier S, Sonenberg N. (1998) 4E-BP3, a new member of the eukaryotic initiation factor 4E-binding protein family. *J Biol Chem* **273:** 14002-14007.
81. Banko JL, et al. (2005) The translation repressor 4E-BP2 is critical for eIF4F complex formation, synaptic plasticity, and memory in the hippocampus. *The Journal of neuroscience : the official journal of the Society for Neuroscience* **25:** 9581-9590.
82. Ayuso MI, Hernandez-Jimenez M, Martin ME, Salinas M, Alcazar A. (2010) New hierarchical phosphorylation pathway of the translational repressor eIF4E-binding protein 1 (4E-BP1) in ischemia-reperfusion stress. *J Biol Chem* **285:** 34355-34363.
83. Gingras AC, et al. (2001) Hierarchical phosphorylation of the translation inhibitor 4E-BP1. *Genes & development* **15:** 2852-2864.
84. Sonenberg N. (1988) Cap-binding proteins of eukaryotic messenger RNA: functions in initiation and control of translation. *Prog Nucleic Acid Res Mol Biol* **35:** 173-207.
85. Sonenberg N, Hinnebusch AG. (2009) Regulation of translation initiation in eukaryotes: mechanisms and biological targets. *Cell* **136:** 731-745.
86. Haghighat A, Sonenberg N. (1997) eIF4G dramatically enhances the binding of eIF4E to the mRNA 5'-cap structure. *J Biol Chem* **272:** 21677-21680.
87. Hinnebusch AG. (2006) eIF3: a versatile scaffold for translation initiation complexes. *Trends Biochem Sci* **31:** 553-562.
88. Sunami T, et al. (2009) Structural basis of human p70 ribosomal S6 kinase-1 regulation by activation loop phosphorylation *J Biol Chem* **285:** 4587-4594.
89. Gingras AC, Raught B, Sonenberg N. (1999) eIF4 initiation factors: effectors of mRNA recruitment to ribosomes and regulators of translation. *Annu Rev Biochem* **68:** 913-963.
90. Frankel LB, et al. (2008) Programmed cell death 4 (PDCD4) is an important functional target of the microRNA miR-21 in breast cancer cells. *J Biol Chem* **283:** 1026-1033.
91. Dorrello NV, et al. (2006) S6K1- and betaTRCP-mediated degradation of PDCD4 promotes protein translation and cell growth. *Science* **314:** 467-471.
92. LaRonde-LeBlanc N, Santhanam AN, Baker AR, Wlodawer A, Colburn NH. (2007) Structural basis for inhibition of translation by the tumor suppressor Pdcd4. *Mol Cell Biol* **27:** 147-156.
93. Yang HS, et al. (2003) The transformation suppressor Pdcd4 is a novel eukaryotic translation initiation factor 4A binding protein that inhibits translation. *Mol Cell Biol* **23:** 26-37.
94. Mahoney SJ, Dempsey JM, Blenis J. (2009) Chapter 2 cell signaling in protein synthesis ribosome biogenesis and translation initiation and elongation. *Progress in molecular biology and translational science* **90:** 53-107.
95. Ma XM, Blenis J. (2009) Molecular mechanisms of mTOR-mediated translational control. *Nature reviews. Molecular cell biology* **10:** 307-318.
96. Flashner MS, Vournakis JN. (1977) Specific hydrolysis of rabbit globin messenger RNA by S1 nuclease. *Nucleic acids research* **4:** 2307-2319.
97. Raught B, et al. (2004) Phosphorylation of eucaryotic translation initiation factor 4B Ser422 is modulated by S6 kinases. *EMBO J* **23:** 1761-1769.

98. Sachs AB, Varani G. (2000) Eukaryotic translation initiation: there are (at least) two sides to every story. *Nat Struct Biol* **7:** 356-361.
99. Rousseau D, Gingras AC, Pause A, Sonenberg N. (1996) The eIF4E-binding proteins 1 and 2 are negative regulators of cell growth. *Oncogene* **13:** 2415-2420.
100. DeFatta RJ, Nathan CA, De Benedetti A. (2000) Antisense RNA to eIF4E suppresses oncogenic properties of a head and neck squamous cell carcinoma cell line. *Laryngoscope* **110:** 928-933.
101. Averous J, Proud CG. (2006) When translation meets transformation: the mTOR story. *Oncogene* **25:** 6423-6435.
102. Larsson O, et al. (2007) Eukaryotic translation initiation factor 4E induced progression of primary human mammary epithelial cells along the cancer pathway is associated with targeted translational deregulation of oncogenic drivers and inhibitors. *Cancer Res* **67:** 6814-6824.
103. Lang CH, et al. (2003) Alcohol impairs leucine-mediated phosphorylation of 4E-BP1, S6K1, eIF4G, and mTOR in skeletal muscle. *Am J Physiol Endocrinol Metab* **285:** E1205-1215.
104. Hinton TM, Coldwell MJ, Carpenter GA, Morley SJ, Pain VM. (2007) Functional analysis of individual binding activities of the scaffold protein eIF4G. *J Biol Chem* **282:** 1695-1708.
105. Constantinou C, Clemens MJ. (2007) Regulation of translation factors eIF4GI and 4E-BP1 during recovery of protein synthesis from inhibition by p53. *Cell Death Differ* **14:** 576-585.
106. Haghighat A, Mader S, Pause A, Sonenberg N. (1995) Repression of cap-dependent translation by 4E-binding protein 1: competition with p220 for binding to eukaryotic initiation factor-4E. *EMBO J* **14:** 5701-5709.
107. Costa-Mattioli M, Sossin WS, Klann E, Sonenberg N. (2009) Translational control of long-lasting synaptic plasticity and memory. *Neuron* **61:** 10-26.
108. Ramirez-Valle F, Braunstein S, Zavadil J, Formenti SC, Schneider RJ. (2008) eIF4GI links nutrient sensing by mTOR to cell proliferation and inhibition of autophagy. *J Cell Biol* **181:** 293-307.
109. Hoeffer CA, Klann E. (2010) mTOR signaling: at the crossroads of plasticity, memory and disease. *Trends in neurosciences* **33:** 67-75.
110. Suzuki C, et al. (2008) PDCD4 inhibits translation initiation by binding to eIF4A using both its MA3 domains. *Proc Natl Acad Sci U S A* **105:** 3274-3279.
111. Rajkowitsch L, Vilela C, Berthelot K, Ramirez CV, McCarthy JE. (2004) Reinitiation and recycling are distinct processes occurring downstream of translation termination in yeast. *J Mol Biol* **335:** 71-85.
112. Kurata S, et al. (2010) Ribosome recycling step in yeast cytoplasmic protein synthesis is catalyzed by eEF3 and ATP. *Proc Natl Acad Sci U S A* **107:** 10854-10859.
113. Kovacina KS, et al. (2003) Identification of a proline-rich Akt substrate as a 14-3-3 binding partner. *J Biol Chem* **278:** 10189-10194.
114. Vander Haar E, Lee SI, Bandhakavi S, Griffin TJ, Kim DH. (2007) Insulin signalling to mTOR mediated by the Akt/PKB substrate PRAS40. *Nat Cell Biol* **9:** 316-323.
115. Wang L, Harris TE, Roth RA, Lawrence JC, Jr. (2007) PRAS40 regulates mTORC1 kinase activity by functioning as a direct inhibitor of substrate binding. *J Biol Chem* **282:** 20036-20044.
116. Schalm SS, Blenis J. (2002) Identification of a conserved motif required for mTOR signaling. *Curr Biol* **12:** 632-639.

117. von Manteuffel SR, et al. (1997) The insulin-induced signalling pathway leading to S6 and initiation factor 4E binding protein 1 phosphorylation bifurcates at a rapamycin-sensitive point immediately upstream of p70s6k. *Mol Cell Biol* **17:** 5426-5436.
118. Wang L, Harris TE, Lawrence JC, Jr. (2008) Regulation of proline-rich Akt substrate of 40 kDa (PRAS40) function by mammalian target of rapamycin complex 1 (mTORC1)-mediated phosphorylation. *J Biol Chem* **283:** 15619-15627.
119. Fonseca BD, Smith EM, Lee VH, MacKintosh C, Proud CG. (2007) PRAS40 is a target for mammalian target of rapamycin complex 1 and is required for signaling downstream of this complex. *J Biol Chem* **282:** 24514-24524.
120. Wang YH, Huang ML. (2009) Reduction of Lobe leads to TORC1 hypoactivation that induces ectopic Jak/STAT signaling to impair Drosophila eye development. *Mechanisms of development* **126:** 781-790.
121. Lang CH, Frost RA, Bronson SK, Lynch CJ, Vary TC. (2010) Skeletal muscle protein balance in mTOR heterozygous mice in response to inflammation and leucine. *Am J Physiol Endocrinol Metab* **298:** E1283-1294.
122. Sanchez Canedo C, et al. (2010) Activation of the cardiac mTOR/p70(S6K) pathway by leucine requires PDK1 and correlates with PRAS40 phosphorylation. *Am J Physiol Endocrinol Metab* **298:** E761-769.
123. Proud CG. (2009) Dynamic balancing: DEPTOR tips the scales. *J Mol Cell Biol* **1:** 61-63.
124. Boyd KD, et al. (2010) High expression levels of the mammalian target of rapamycin inhibitor DEPTOR are predictive of response to thalidomide in myeloma. *Leuk Lymphoma* **51:** 2126-2129.
125. de la Rubia J, Such E. (2010) DEPTOR expression and response to thalidomide: toward a new therapeutic target in multiple myeloma? *Leuk Lymphoma* **51:** 1960-1961.
126. Florini JR, Ewton DZ, Coolican SA. (1996) Growth hormone and the insulin-like growth factor system in myogenesis. *Endocr Rev* **17:** 481-517.
127. Barton-Davis ER, Shoturma DI, Sweeney HL. (1999) Contribution of satellite cells to IGF-I induced hypertrophy of skeletal muscle. *Acta Physiol Scand* **167:** 301-305.
128. Chakravarthy MV, Abraha TW, Schwartz RJ, Fiorotto ML, Booth FW. (2000) Insulin-like growth factor-I extends in vitro replicative life span of skeletal muscle satellite cells by enhancing G1/S cell cycle progression via the activation of phosphatidylinositol 3'-kinase/Akt signaling pathway. *J Biol Chem* **275:** 35942-35952.
129. Barton-Davis ER, Shoturma DI, Musaro A, Rosenthal N, Sweeney HL. (1998) Viral mediated expression of insulin-like growth factor I blocks the aging-related loss of skeletal muscle function. *Proc Natl Acad Sci U S A* **95:** 15603-15607.
130. Chakravarthy MV, Davis BS, Booth FW. (2000) IGF-I restores satellite cell proliferative potential in immobilized old skeletal muscle. *J Appl Physiol* **89:** 1365-1379.
131. Musaro A, et al. (2001) Localized Igf-1 transgene expression sustains hypertrophy and regeneration in senescent skeletal muscle. *Nat Genet* **27:** 195-200.
132. Owino V, Yang SY, Goldspink G. (2001) Age-related loss of skeletal muscle function and the inability to express the autocrine form of insulin-like growth factor-1 (MGF) in response to mechanical overload. *FEBS Lett* **505:** 259-263.
133. Fingar DC, Salama S, Tsou C, Harlow E, Blenis J. (2002) Mammalian cell size is controlled by mTOR and its downstream targets S6K1 and 4EBP1/eIF4E. *Genes & development* **16:** 1472-1487.
134. Nader GA, McLoughlin TJ, Esser KA. (2005) mTOR function in skeletal muscle hypertrophy: increased ribosomal RNA via cell cycle regulators. *Am J Physiol Cell Physiol* **289:** 1457-1465.

135. Hlaing M, Shen X, Dazin P, Bernstein HS. (2002) The hypertrophic response in C2C12 myoblasts recruits the G1 cell cycle machinery. *J Biol Chem* **277:** 23794-23799.
136. Coolican SA, Samuel DS, Ewton DZ, McWade FJ, Florini JR. (1997) The mitogenic and myogenic actions of insulin-like growth factors utilize distinct signaling pathways. *J Biol Chem* **272:** 6653-6662.
137. Hinds PW, et al. (1992) Regulation of retinoblastoma protein functions by ectopic expression of human cyclins. *Cell* **70:** 993-991006.
138. Buchkovich K, Duffy LA, Harlow E. (1989) The retinoblastoma protein is phosphorylated during specific phases of the cell cycle. *Cell* **58:** 1097-1105.
139. Goodrich DW, Wang NP, Qian YW, Lee EY, Lee WH. (1991) The retinoblastoma gene product regulates progression through the G1 phase of the cell cycle. *Cell* **67:** 293-302.
140. Frolov MV, Dyson NJ. (2004) Molecular mechanisms of E2F-dependent activation and pRB-mediated repression. *Journal of cell science* **117:** 2173-2181.
141. Burke JR, Deshong AJ, Pelton JG, Rubin SM. (2010) Phosphorylation-induced conformational changes in the retinoblastoma protein inhibit E2F transactivation domain binding. *J Biol Chem* **285:** 16286-16293.
142. Gorges LL, Lents NH, Baldassare JJ. (2008) The extreme COOH terminus of the retinoblastoma tumor suppressor protein pRb is required for phosphorylation on Thr-373 and activation of E2F. *Am J Physiol Cell Physiol* **295:** C1151-1160.
143. Delston RB, Matatall KA, Sun Y, Onken MD, Harbour JW. (2010) p38 phosphorylates Rb on Ser567 by a novel, cell cycle-independent mechanism that triggers Rb-Hdm2 interaction and apoptosis. *Oncogene* **30:** 588-599.
144. Izycka-Swieszewska E, et al. (2010) Analysis of PI3K/AKT/mTOR signalling pathway in high risk neuroblastic tumours. *Polish journal of pathology : official journal of the Polish Society of Pathologists* **61:** 192-198.
145. Dowdy SF, et al. (1993) Physical interaction of the retinoblastoma protein with human D cyclins. *Cell* **73:** 499-511.
146. Xiao ZX, Ginsberg D, Ewen M, Livingston DM. (1996) Regulation of the retinoblastoma protein-related protein p107 by G1 cyclin-associated kinases. *Proc Natl Acad Sci U S A* **93:** 4633-4637.
147. Ren S, Rollins BJ. (2004) Cyclin C/cdk3 promotes Rb-dependent G0 exit. *Cell* **117:** 239-251.
148. Hashemolhosseini S, et al. (1998) Rapamycin inhibition of the G1 to S transition is mediated by effects on cyclin D1 mRNA and protein stability. *J Biol Chem* **273:** 14424-14429.
149. Kawamata S, Sakaida H, Hori T, Maeda M, Uchiyama T. (1998) The upregulation of p27Kip1 by rapamycin results in G1 arrest in exponentially growing T-cell lines. *Blood* **91:** 561-569.
150. Gu W, et al. (1993) Interaction of myogenic factors and the retinoblastoma protein mediates muscle cell commitment and differentiation. *Cell* **72:** 309-324.
151. Delston RB, Matatall KA, Sun Y, Onken MD, Harbour JW. (2011) p38 phosphorylates Rb on Ser567 by a novel, cell cycle-independent mechanism that triggers Rb-Hdm2 interaction and apoptosis. *Oncogene* **30:** 588-599.
152. Kiess M, Gill RM, Hamel PA. (1995) Expression and activity of the retinoblastoma protein (pRB)-family proteins, p107 and p130, during L6 myoblast differentiation. *Cell Growth Differ* **6:** 1287-1298.
153. Rosenthal SM, Cheng ZQ. (1995) Opposing early and late effects of insulin-like growth factor I on differentiation and the cell cycle regulatory retinoblastoma protein in skeletal myoblasts. *Proc Natl Acad Sci U S A* **92:** 10307-10311.

154. Chakravarthy MV, Fiorotto ML, Schwartz RJ, Booth FW. (2001) Long-term insulin-like growth factor-I expression in skeletal muscles attenuates the enhanced in vitro proliferation ability of the resident satellite cells in transgenic mice. *Mech Ageing Dev* **122:** 1303-1320.
155. Kiyono T, et al. (1998) Both Rb/p16INK4a inactivation and telomerase activity are required to immortalize human epithelial cells. *Nature* **396:** 84-88.
156. Palmero I, et al. (1997) Accumulation of p16INK4a in mouse fibroblasts as a function of replicative senescence and not of retinoblastoma gene status. *Oncogene* **15:** 495-503.
157. Rosenthal SM, Cheng ZQ. (1995) Opposing early and late effects of insulin-like growth factor I on differentiation and the cell cycle regulatory retinoblastoma protein in skeletal myoblasts. *Proc Natl Acad Sci U S A* **92:** 10307-10311.
158. Jung CH, Ro SH, Cao J, Otto NM, Kim DH. (2010) mTOR regulation of autophagy. *FEBS Lett* **584:** 1287-1295.
159. Tassa A, Roux MP, Attaix D, Bechet DM. (2003) Class III phosphoinositide 3-kinase--Beclin1 complex mediates the amino acid-dependent regulation of autophagy in C2C12 myotubes. *Biochem J* **376:** 577-586.
160. Kanazawa T, et al. (2004) Amino acids and insulin control autophagic proteolysis through different signaling pathways in relation to mTOR in isolated rat hepatocytes. *J Biol Chem* **279:** 8452-8459.
161. Meijer AJ, Codogno P. (2004) Regulation and role of autophagy in mammalian cells. *Int J Biochem Cell Biol* **36:** 2445-2462.
162. Bechet D, Tassa A, Taillandier D, Combaret L, Attaix D. (2005) Lysosomal proteolysis in skeletal muscle. *Int J Biochem Cell Biol* **37:** 2098-2114.
163. Mammucari C, et al. (2007) FoxO3 controls autophagy in skeletal muscle in vivo. *Cell Metab* **6:** 458-471.
164. Mordier S, Deval C, Bechet D, Tassa A, Ferrara M. (2000) Leucine limitation induces autophagy and activation of lysosome-dependent proteolysis in C2C12 myotubes through a mammalian target of rapamycin-independent signaling pathway. *J Biol Chem* **275:** 29900-29906.
165. Martinet W, De Meyer GR, Herman AG, Kockx MM. (2005) Amino acid deprivation induces both apoptosis and autophagy in murine C2C12 muscle cells. *Biotechnol Lett* **27:** 1157-1163.
166. Schiaffino S, Mammucari C, Sandri M. (2008) The role of autophagy in neonatal tissues: just a response to amino acid starvation? *Autophagy* **4:** 727-730.
167. Mammucari C, Schiaffino S, Sandri M. (2008) Downstream of Akt: FoxO3 and mTOR in the regulation of autophagy in skeletal muscle. *Autophagy* **4:** 524-526.
168. Ravikumar B, et al. (2004) Inhibition of mTOR induces autophagy and reduces toxicity of polyglutamine expansions in fly and mouse models of Huntington disease. *Nat Genet* **36:** 585-595.
169. Noda T, Ohsumi Y. (1998) Tor, a phosphatidylinositol kinase homologue, controls autophagy in yeast. *J Biol Chem* **273:** 3963-3966.
170. Straub M, Bredschneider M, Thumm M. (1997) AUT3, a serine/threonine kinase gene, is essential for autophagocytosis in Saccharomyces cerevisiae. *J Bacteriol* **179:** 3875-3883.
171. Schlumpberger M, et al. (1997) AUT1, a gene essential for autophagocytosis in the yeast Saccharomyces cerevisiae. *J Bacteriol* **179:** 1068-1076.
172. Matsuura A, Tsukada M, Wada Y, Ohsumi Y. (1997) Apg1p, a novel protein kinase required for the autophagic process in Saccharomyces cerevisiae. *Gene* **192:** 245-250.
173. Kamada Y, et al. (2000) Tor-mediated induction of autophagy via an Apg1 protein kinase complex. *J Cell Biol* **150:** 1507-1513.

174. Chan EY, Kir S, Tooze SA. (2007) siRNA screening of the kinome identifies ULK1 as a multidomain modulator of autophagy. *J Biol Chem* **282:** 25464-25474.
175. Hara T, et al. (2008) FIP200, a ULK-interacting protein, is required for autophagosome formation in mammalian cells. *J Cell Biol* **181:** 497-510.
176. Jung CH, et al. (2009) ULK-Atg13-FIP200 complexes mediate mTOR signaling to the autophagy machinery. *Molecular biology of the cell* **20:** 1992-2003.
177. Ganley IG, et al. (2009) ULK1.ATG13.FIP200 complex mediates mTOR signaling and is essential for autophagy. *J Biol Chem* **284:** 12297-12305.
178. Hosokawa N, et al. (2009) Nutrient-dependent mTORC1 association with the ULK1-Atg13-FIP200 complex required for autophagy. *Molecular biology of the cell* **20:** 1981-1991.
179. Tanida I. (2011) Autophagy basics. *Microbiology and immunology* **55:** 1-11.
180. Wohlgemuth SE, Seo AY, Marzetti E, Lees HA, Leeuwenburgh C. (2010) Skeletal muscle autophagy and apoptosis during aging: effects of calorie restriction and life-long exercise. *Experimental gerontology* **45:** 138-148.
181. Meley D, et al. (2006) AMP-activated protein kinase and the regulation of autophagic proteolysis. *J Biol Chem* **281:** 34870-34879.
182. Lee JW, Park S, Takahashi Y, Wang HG. (2010) The association of AMPK with ULK1 regulates autophagy. *PLoS One* **5:** e15394.
183. Boudeau J, et al. (2004) Analysis of the LKB1-STRAD-MO25 complex. *J Cell Sci* **117:** 6365-6375.
184. Inoki K, Zhu T, Guan KL. (2003) TSC2 mediates cellular energy response to control cell growth and survival. *Cell* **115:** 577-590.
185. Gwinn DM, et al. (2008) AMPK phosphorylation of raptor mediates a metabolic checkpoint. *Mol cell* **30:** 214-226.
186. Annovazzi L, et al. (2009) mTOR, S6 and AKT expression in relation to proliferation and apoptosis/autophagy in glioma. *Anticancer Res* **29:** 3087-3094.
187. Madhunapantula SV, Sharma A, Robertson GP. (2007) PRAS40 deregulates apoptosis in malignant melanoma. *Cancer Res* **67:** 3626-3636.
188. Keren A, Tamir Y, Bengal E. (2006) The p38 MAPK signaling pathway: a major regulator of skeletal muscle development. *Mol Cell Endocrinol* **252:** 224-230.
189. Kwiecinska P, Roszkiewicz B, Lokociejewska M, Orzechowski A. (2005) Elevated expression of NF-kappaB and Bcl-2 proteins in C2C12 myocytes during myogenesis is affected by PD98059, LY294002 and SB203580. *Cell Biol Int* **29:** 319-331.
190. Williamson DL, Butler DC, Alway SE. (2009) AMPK inhibits myoblast differentiation through a PGC-1alpha-dependent mechanism. *Am J Physiol Endocrinol Metab* **297:** E304-314.
191. Sherr CJ, Roberts JM. (1999) CDK inhibitors: positive and negative regulators of G1-phase progression. *Genes & development* **13:** 1501-1512.
192. Halevy O, et al. (1995) Correlation of terminal cell cycle arrest of skeletal muscle with induction of p21 by MyoD. *Science* **267:** 1018-1021.
193. Skapek SX, Rhee J, Spicer DB, Lassar AB. (1995) Inhibition of myogenic differentiation in proliferating myoblasts by cyclin D1-dependent kinase. *Science* **267:** 1022-1024.
194. Cenciarelli C, et al. (1999) Critical role played by cyclin D3 in the MyoD-mediated arrest of cell cycle during myoblast differentiation. *Mol Cell Biol* **19:** 5203-5217.
195. Singh BN, Rao KS, Rao Ch M. (2010) Ubiquitin-proteasome-mediated degradation and synthesis of MyoD is modulated by alphaB-crystallin, a small heat shock protein, during muscle differentiation. *Biochimica et biophysica acta* **1803:** 288-299.

196. Magenta A, et al. (2003) MyoD stimulates RB promoter activity via the CREB/p300 nuclear transduction pathway. *Mol Cell Biol* **23:** 2893-2906.
197. Guo K, Wang J, Andres V, Smith RC, Walsh K. (1995) MyoD-induced expression of p21 inhibits cyclin-dependent kinase activity upon myocyte terminal differentiation. *Mol Cell Biol* **15:** 3823-3829.
198. Hawke TJ, et al. (2003) p21 is essential for normal myogenic progenitor cell function in regenerating skeletal muscle. *Am J Physiol Cell Physiol* **285:** C1019-1027.
199. Kaliman P, Vinals F, Testar X, Palacin M, Zorzano A. (1996) Phosphatidylinositol 3-kinase inhibitors block differentiation of skeletal muscle cells. *J Biol Chem* **271:** 19146-19151.
200. Cheng WL, et al. (2011) Inhibitory effect of human breast cancer cell proliferation via p21-mediated G1 cell cycle arrest by araliadiol isolated from Aralia cordata Thunb. *Planta medica* **77:** 164-168.
201. Cooper RN, et al. (1999) In vivo satellite cell activation via Myf5 and MyoD in regenerating mouse skeletal muscle. *J Cell Sci* **112 (Pt 17):** 2895-2901.
202. Cornelison DD, Wold BJ. (1997) Single-cell analysis of regulatory gene expression in quiescent and activated mouse skeletal muscle satellite cells. *Dev Biol* **191:** 270-283.
203. Musaro A, et al. (1995) Enhanced expression of myogenic regulatory genes in aging skeletal muscle. *Exp Cell Res* **221:** 241-248.
204. Wenzel RP. (2002) Treating sepsis. *N Engl J Med* **347:** 966-967.
205. Couto RC, et al. (2007) A 10-year prospective surveillance of nosocomial infections in neonatal intensive care units. *Am J Infect Control* **35:** 183-189.
206. Shah SS, et al. (2007) Bloodstream infections after median sternotomy at a children's hospital. *J Thorac Cardiovasc Surg* **133:** 435-440.
207. Russell JA. (2006) Management of sepsis. *N Engl J Med* **355:** 1699-1713.
208. Cavaillon JM, Adib-Conquy M. (2006) Bench-to-bedside review: endotoxin tolerance as a model of leukocyte reprogramming in sepsis. *Crit Care* **10:** 233.
209. Koshiba T, Hashii T, Kawabata S. (2007) A structural perspective on the interaction between lipopolysaccharide and factor C, a receptor involved in recognition of Gram-negative bacteria. *J Biol Chem* **282:** 3962-3967.
210. Balk RA. (2000) Pathogenesis and management of multiple organ dysfunction or failure in severe sepsis and septic shock. *Crit Care Clin* **16:** 337-352.
211. Lang CH, Frost RA. (2007) Sepsis-induced suppression of skeletal muscle translation initiation mediated by tumor necrosis factor alpha. *Metabolism* **56:** 49-57.
212. Vary TC, Kimball SR. (1992) Sepsis-induced changes in protein synthesis: differential effects on fast- and slow-twitch muscles. *Am J Physiol* **262:** C1513-1519.
213. Lang CH, Frost RA, Vary TC. (2007) Regulation of Muscle Protein Synthesis During Sepsis and Inflammation. *Am J Physiol Endocrinol Metab* **293:** E453-459.
214. Vary TC, Kimball SR. (1992) Regulation of hepatic protein synthesis in chronic inflammation and sepsis. *Am J Physiol* **262:** C445-452.
215. Schoneveld AH, et al. (2005) Toll-like receptor 2 stimulation induces intimal hyperplasia and atherosclerotic lesion development. *Cardiovasc Res* **66:** 162-169.
216. Sonenberg N, Gingras AC. (1998) The mRNA 5' cap-binding protein eIF4E and control of cell growth. *Curr Opin Cell Biol* **10:** 268-275.
217. Vary TC. (2006) IGF-I stimulates protein synthesis in skeletal muscle through multiple signaling pathways during sepsis. *Am J Physiol Regul Integr Comp Physiol* **290:** R313-321.

218. Vary TC, Deiter G, Lang CH. (2006) Cytokine-triggered decreases in levels of phosphorylated eukaryotic initiation factor 4G in skeletal muscle during sepsis. *Shock* **26:** 631-636.
219. Vary TC, Lang CH. (2005) IGF-I activates the eIF4F system in cardiac muscle in vivo. *Mol Cell Biochem* **272:** 209-220.
220. Lang CH, Frost RA, Nairn AC, MacLean DA, Vary TC. (2002) TNF-alpha impairs heart and skeletal muscle protein synthesis by altering translation initiation. *Am J Physiol Endocrinol Metab* **282:** E336-347.
221. Lang CH, Frost RA, Svanberg E, Vary TC. (2004) IGF-I/IGFBP-3 ameliorates alterations in protein synthesis, eIF4E availability, and myostatin in alcohol-fed rats. *Am J Physiol Endocrinol Metab* **286:** E916-926.
222. Gingras AC, et al. (1999) Regulation of 4E-BP1 phosphorylation: a novel two-step mechanism. *Genes & development* **13:** 1422-1437.
223. LeFebvre AK, et al. (2006) Translation initiation factor eIF4G-1 binds to eIF3 through the eIF3e subunit. *J Biol Chem* **281:** 22917-22932.
224. Moerke NJ, et al. (2007) Small-molecule inhibition of the interaction between the translation initiation factors eIF4E and eIF4G. *Cell* **128:** 257-267.
225. Vary TC, Jefferson LS, Kimball SR. (2001) Insulin fails to stimulate muscle protein synthesis in sepsis despite unimpaired signaling to 4E-BP1 and S6K1. *Am J Physiol Endocrinol Metab* **281:** E1045-1053.
226. Kimball SR, et al. (2003) Endotoxin induces differential regulation of mTOR-dependent signaling in skeletal muscle and liver of neonatal pigs. *Am J Physiol Endocrinol Metab* **285:** E637-644.
227. Kristof AS, Marks-Konczalik J, Billings E, Moss J. (2003) Stimulation of signal transducer and activator of transcription-1 (STAT1)-dependent gene transcription by lipopolysaccharide and interferon-gamma is regulated by mammalian target of rapamycin. *J Biol Chem* **278:** 33637-33644.
228. Lang CH, Frost RA. (2005) Endotoxin disrupts the leucine-signaling pathway involving phosphorylation of mTOR, 4E-BP1, and S6K1 in skeletal muscle. *J Cell Physiol* **203:** 144-155.
229. Lang CH, Pruznak AM, Frost RA. (2005) TNFalpha mediates sepsis-induced impairment of basal and leucine-stimulated signaling via S6K1 and eIF4E in cardiac muscle. *J Cell Biochem* **94:** 419-431.
230. Zhou H, Huang S. (2010) The complexes of mammalian target of rapamycin. *Current protein & peptide science* **11:** 409-424.
231. Bentzinger CF, et al. (2008) Skeletal muscle-specific ablation of raptor, but not of rictor, causes metabolic changes and results in muscle dystrophy. *Cell Metab* **8:** 411-424.
232. Sarbassov DD, et al. (2004) Rictor, a novel binding partner of mTOR, defines a rapamycin-insensitive and raptor-independent pathway that regulates the cytoskeleton. *Curr Biol* **14:** 1296-1302.
233. Lawson MA, Purslow PP. (2000) Differentiation of myoblasts in serum-free media: effects of modified media are cell line-specific. *Cells Tissues Organs* **167:** 130-137.
234. Portier GL, Benders AG, Oosterhof A, Veerkamp JH, van Kuppevelt TH. (1999) Differentiation markers of mouse C2C12 and rat L6 myogenic cell lines and the effect of the differentiation medium. *In vitro cellular & developmental biology. Animal* **35:** 219-227.
235. Williamson DL, Bolster DR, Kimball SR, Jefferson LS. (2006) Time course changes in signaling pathways and protein synthesis in C2C12 myotubes following AMPK activation by AICAR. *Am J Physiol Endocrinol Metab* **291:** E80-89.

236. Frost RA, Lang CH, Gelato MC. (1997) Transient exposure of human myoblasts to tumor necrosis factor-alpha inhibits serum and insulin-like growth factor-I stimulated protein synthesis. *Endocrinology* **138:** 4153-4159.
237. Lang CH, Pruznak AM, Nystrom GJ, Vary TC. (2009) Alcohol-induced decrease in muscle protein synthesis associated with increased binding of mTOR and raptor: Comparable effects in young and mature rats. *Nutrition & metabolism* **6:** 4.
238. Lang CH, Frost RA, Vary TC. (2008) Acute alcohol intoxication increases REDD1 in skeletal muscle. *Alcohol Clin Exp Res* **32:** 796-805.
239. Hong-Brown LQ, Brown CR, Huber DS, Lang CH. (2007) Alcohol regulates eukaryotic elongation factor 2 phosphorylation via an AMP-activated protein kinase-dependent mechanism in C2C12 skeletal myocytes. *J Biol Chem* **282:** 3702-3712.
240. Das A, Desai D, Pittman B, Amin S, El-Bayoumy K. (2003) Comparison of the chemopreventive efficacies of 1,4-phenylenebis(methylene)selenocyanate and selenium-enriched yeast on 4-(methylnitrosamino)-1-(3-pyridyl)-1-butanone induced lung tumorigenesis in A/J mouse. *Nutr Cancer* **46:** 179-185.
241. Crozier SJ, Kimball SR, Emmert SW, Anthony JC, Jefferson LS. (2005) Oral leucine administration stimulates protein synthesis in rat skeletal muscle. *J Nutr* **135:** 376-382.
242. Vary TC, Lang CH. (2008) Assessing effects of alcohol consumption on protein synthesis in striated muscles. *Methods Mol Biol* **447:** 343-355.
243. Giegerich R, Meyer F, Schleiermacher C. (1996) GeneFisher--software support for the detection of postulated genes. *Proc Int Conf Intell Syst Mol Biol* **4:** 68-77.
244. Zhivotovsky B, Nicotera P, Bellomo G, Hanson K, Orrenius S. (1993) Ca2+ and endonuclease activation in radiation-induced lymphoid cell death. *Exp Cell Res* **207:** 163-170.
245. Le Doux JM. (2008) Gene therapy protocols. Humana Press, Totowa, N.J. Methods Mol Biol. 2008; 434: v.
246. Corovic S, et al. (2010) The influence of skeletal muscle anisotropy on electroporation: in vivo study and numerical modeling. *Med Biol Eng Comput* **48:** 637-648.
247. Gissel H. (2010) Effects of varying pulse parameters on ion homeostasis, cellular integrity, and force following electroporation of rat muscle in vivo. *Am J Physiol Regul Integr Comp Physiol* **298:** R918-929.
248. Tuckow AP, Vary TC, Kimball SR, Jefferson LS. (2010) Ectopic expression of eIF2Bepsilon in rat skeletal muscle rescues the sepsis-induced reduction in guanine nucleotide exchange activity and protein synthesis. *Am J Physiol Endocrinol Metab* **299:** E241-248.
249. Tucker KR, Seider MJ, Booth FW. (1981) Protein synthesis rates in atrophied gastrocnemius muscles after limb immobilization. *J Appl Physiol* **51:** 73-77.
250. Lang CH, Lynch CJ, Vary TC. (2010) BCATm deficiency ameliorates endotoxin-induced decrease in muscle protein synthesis and improves survival in septic mice. *Am J Physiol Regul Integr Comp Physiol* **299:** R935-944.
251. Lang CH, Frost RA, Jefferson LS, Kimball SR, Vary TC. (2000) Endotoxin-induced decrease in muscle protein synthesis is associated with changes in eIF2B, eIF4E, and IGF-I. *Am J Physiol Endocrinol Metab* **278:** E1133-1143.
252. Garlick PJ, McNurlan MA, Essen P, Wernerman J. (1994) Measurement of tissue protein synthesis rates in vivo: a critical analysis of contrasting methods. *Am J Physiol* **266:** E287-297.
253. Laplante M, Sabatini DM. (2009) mTOR signaling at a glance. *J Cell Sci* **122:** 3589-3594.

254. Jacinto E, et al. (2004) Mammalian TOR complex 2 controls the actin cytoskeleton and is rapamycin insensitive. *Nat Cell Biol* **6:** 1122-1128.
255. Ruvinsky I, Meyuhas O. (2006) Ribosomal protein S6 phosphorylation: from protein synthesis to cell size. *Trends Biochem Sci* **31:** 342-348.
256. Hardie DG. (2007) AMP-activated/SNF1 protein kinases: conserved guardians of cellular energy. *Nat Rev Mol Cell Biol* **8:** 774-785.
257. Xie Z, Dong Y, Scholz R, Neumann D, Zou MH. (2008) Phosphorylation of LKB1 at serine 428 by protein kinase C-zeta is required for metformin-enhanced activation of the AMP-activated protein kinase in endothelial cells. *Circulation* **117:** 952-962.
258. Tee AR, Blenis J, Proud CG. (2005) Analysis of mTOR signaling by the small G-proteins, Rheb and RhebL1. *FEBS Lett* **579:** 4763-4768.
259. Lang CH, Pruznak AM, Nystrom GJ, Vary TC. (2009) Alcohol-induced decrease in muscle protein synthesis associated with increased binding of mTOR and raptor: Comparable effects in young and mature rats. *Nutr Metab (Lond)* **6:** 4.
260. Oshiro N, et al. (2004) Dissociation of raptor from mTOR is a mechanism of rapamycin-induced inhibition of mTOR function. *Genes Cells* **9:** 359-366.
261. Frost RA, Nystrom GJ, Lang CH. (2009) Endotoxin and interferon-gamma inhibit translation in skeletal muscle cells by stimulating nitric oxide synthase activity. *Shock* **32:** 416-426.
262. Levy RJ, Vijayasarathy C, Raj NR, Avadhani NG, Deutschman CS. (2004) Competitive and noncompetitive inhibition of myocardial cytochrome C oxidase in sepsis. *Shock* **21:** 110-114.
263. Nascimento EBM, Ouwens DM. (2009) PRAS40: target or modulator of mTORC1 signalling and insulin action? *Arch Physiol Biochem* **115:** 163-175.
264. Nave BT, Ouwens M, Withers DJ, Alessi DR, Shepherd PR. (1999) Mammalian target of rapamycin is a direct target for protein kinase B: identification of a convergence point for opposing effects of insulin and amino-acid deficiency on protein translation. *Biochem J* **344:** 427-431.
265. Zhang L, Kimball SR, Jefferson LS, Shenberger JS. (2009) Hydrogen peroxide impairs insulin-stimulated assembly of mTORC1. *Free Radic Biol Med* **46:** 1500-1509.
266. Zhou C, et al. (2005) PCI proteins eIF3e and eIF3m define distinct translation initiation factor 3 complexes. *BMC Biol* **3:** 14.
267. Lagirand-Cantaloube J, et al. (2008) The initiation factor eIF3-f is a major target for atrogin1/MAFbx function in skeletal muscle atrophy. *EMBO J* **27:** 1266-1276.
268. Sancak Y, et al. (2008) The Rag GTPases bind raptor and mediate amino acid signaling to mTORC1. *Science* **320:** 1496-1501.
269. Backer JM. (2008) The regulation and function of Class III PI3Ks: novel roles for Vps34. *Biochem J* **410:** 1-17.
270. Dunlop EA, Tee AR. (2009) Mammalian target of rapamycin complex 1: signalling inputs, substrates and feedback mechanisms. *Cell Signal* **21:** 827-835.
271. Gingras AC, Raught B, Sonenberg N. (2004) mTOR signaling to translation. *Curr Top Microbiol Immunol* **279:** 169-197.
272. Schmelzle T, Hall MN. (2000) TOR, a central controller of cell growth. *Cell* **103:** 253-262.
273. Balasubramanian S, et al. (2009) mTOR in growth and protection of hypertrophying myocardium. *Cardiovasc Hematol Agents Med Chem* **7:** 52-63.
274. Peterson TR, et al. (2009) DEPTOR Is an mTOR Inhibitor Frequently Overexpressed in Multiple Myeloma Cells and Required for Their Survival. *Cell* **137:** 873-886.

275. Kovacina KS, et al. (2003) Identification of a proline-rich Akt substrate as a 14-3-3 binding partner. *J Biol Chem* **278:** 10189-10194.
276. Oshiro N, et al. (2007) The proline-rich Akt substrate of 40 kDa (PRAS40) is a physiological substrate of mammalian target of rapamycin complex 1. *J Biol Chem* **282:** 20329-20339.
277. Srinivas V, Bohensky J, Shapiro IM. (2009) Autophagy: a new phase in the maturation of growth plate chondrocytes is regulated by HIF, mTOR and AMP kinase. *Cells Tissues Organs* **189:** 88-92.
278. Zeng M, Zhou JN. (2008) Roles of autophagy and mTOR signaling in neuronal differentiation of mouse neuroblastoma cells. *Cell Signal* **20:** 659-665.
279. Shaw RJ, Cantley LC. (2006) Ras, PI(3)K and mTOR signalling controls tumour cell growth. *Nature* **441:** 424-430.
280. Thedieck K, et al. (2007) PRAS40 and PRR5-like protein are new mTOR interactors that regulate apoptosis. *PLoS One* **2:** e1217.
281. Sartori R, et al. (2009) Smad2 and 3 transcription factors control muscle mass in adulthood. *Am J Physiol Cell Physiol* **296:** C1248-1257.
282. Welle S, Burgess K, Thornton CA, Tawil R. (2009) Relation between extent of myostatin depletion and muscle growth in mature mice. *Am J Physiol Endocrinol Metab* **297:** E935-40.
283. Zhang LH, Lin FR. (2009) [Effect of rapamycin on leukemia cell lines.]. *Zhongguo Shi Yan Xue Ye Xue Za Zhi* **17:** 870-873.
284. Shafer A, Zhou C, Gehrig PA, Boggess JF, Bae-Jump VL. (2009) Rapamycin potentiates the effects of paclitaxel in endometrial cancer cells through inhibition of cell proliferation and induction of apoptosis. *Int J Cancer*. Mar 1;126(**5**):1144-54.
285. Rosner M, Fuchs C, Siegel N, Valli A, Hengstschlager M. (2009) Functional interaction of mammalian target of rapamycin complexes in regulating mammalian cell size and cell cycle. *Hum Mol Genet* **18:** 3298-3310.
286. Imamura K, Ogura T, Kishimoto A, Kaminishi M, Esumi H. (2001) Cell cycle regulation via p53 phosphorylation by a 5'-AMP activated protein kinase activator, 5-aminoimidazole- 4-carboxamide-1-beta-D-ribofuranoside, in a human hepatocellular carcinoma cell line. *Biochem Biophys Res Commun* **287:** 562-567.
287. Deng C, Zhang P, Harper JW, Elledge SJ, Leder P. (1995) Mice lacking p21CIP1/WAF1 undergo normal development, but are defective in G1 checkpoint control. *Cell* **82:** 675-684.
288. Zhang P, et al. (1999) p21(CIP1) and p57(KIP2) control muscle differentiation at the myogenin step. *Genes Dev* **13:** 213-224.
289. Lee YJ, et al. (2009) Involvement of a p53-independent and post-transcriptional up-regulation for p21WAF/CIP1 following destabilization of the actin cytoskeleton. *Int J Oncol* **34:** 581-589.
290. Parker SB, et al. (1995) p53-independent expression of p21Cip1 in muscle and other terminally differentiating cells. *Science* **267:** 1024-1027.
291. Lin TA, et al. (1994) PHAS-I as a link between mitogen-activated protein kinase and translation initiation. *Science* **266:** 653-656.
292. Smith MR, et al. (1991) Modulation of the mitogenic activity of eukaryotic translation initiation factor-4E by protein kinase C. *New Biol* **3:** 601-607.
293. Kimball SR. (2006) Interaction between the AMP-activated protein kinase and mTOR signaling pathways. *Med Sci Sports Exerc* **38:** 1958-1964.
294. Kazi AA, Lang CH. (2010) PRAS40 regulates protein synthesis and cell cycle in C2C12 myoblasts. *Mol Med* **16:** 359-371.

295. Anthony JC, et al. (2000) Leucine stimulates translation initiation in skeletal muscle of postabsorptive rats via a rapamycin-sensitive pathway. *J Nutr* **130:** 2413-2419.
296. Pham PT, et al. (2000) Assessment of cell-signaling pathways in the regulation of mammalian target of rapamycin (mTOR) by amino acids in rat adipocytes. *J Cell Biochem* **79:** 427-441.
297. Kim DH, et al. (2003) GbetaL, a positive regulator of the rapamycin-sensitive pathway required for the nutrient-sensitive interaction between raptor and mTOR. *Mol Cell* **11:** 895-904.
298. Liu M, et al. (2010) Resveratrol Inhibits mTOR Signaling by Promoting the Interaction between mTOR and DEPTOR. *J Biol Chem* **285:** 36387-36394.
299. Srinivas V, Bohensky J, Shapiro IM. (2009) Autophagy: a new phase in the maturation of growth plate chondrocytes is regulated by HIF, mTOR and AMP kinase. *Cells Tissues Organs* **189:** 88-92.
300. Zeng M, Zhou JN. (2008) Roles of autophagy and mTOR signaling in neuronal differentiation of mouse neuroblastoma cells. *Cell Signal* **20:** 659-665.
301. Thoreen CC, et al. (2009) An ATP-competitive mammalian target of rapamycin inhibitor reveals rapamycin-resistant functions of mTORC1. *J Biol Chem* **284:** 8023-8032.
302. Thomas G, Hall MN. (1997) TOR signalling and control of cell growth. *Curr Opin Cell Biol* **9:** 782-787.
303. Peponi E, et al. (2006) Activation of mammalian target of rapamycin signaling promotes cell cycle progression and protects cells from apoptosis in mantle cell lymphoma. *Am J Pathol* **169:** 2171-2180.
304. Wang X, Proud CG. (2009) Nutrient control of TORC1, a cell-cycle regulator. *Trends Cell Biol* **19:** 260-267.
305. Crespo JL, Hall MN. (2002) Elucidating TOR signaling and rapamycin action: lessons from Saccharomyces cerevisiae. *Microbiol Mol Biol Rev* **66:** 579-591.
306. Oldham S, Hafen E. (2003) Insulin/IGF and target of rapamycin signaling: a TOR de force in growth control. *Trends Cell Biol* **13:** 79-85.
307. White RJ. (1997) Regulation of RNA polymerases I and III by the retinoblastoma protein: a mechanism for growth control? *Trends Biochem Sci* **22:** 77-80.
308. Hashemolhosseini S, et al. (1998) Rapamycin inhibition of the G1 to S transition is mediated by effects on cyclin D1 mRNA and protein stability. *J Biol Chem* **273:** 14424-14429.
309. Luo Y, et al. (1996) Rapamycin resistance tied to defective regulation of p27Kip1. *Mol Cell Biol* **16:** 6744-6751.
310. Munger K, Howley PM. (2002) Human papillomavirus immortalization and transformation functions. *Virus Res* **89:** 213-228.
311. Muise-Helmericks RC, et al. (1998) Cyclin D expression is controlled post-transcriptionally via a phosphatidylinositol 3-kinase/Akt-dependent pathway. *J Biol Chem* **273:** 29864-29872.
312. Ong CS, Zhou J, Ong CN, Shen HM. (2010) Luteolin induces G1 arrest in human nasopharyngeal carcinoma cells via the Akt-GSK-3beta-Cyclin D1 pathway. *Cancer Lett* **298:** 167-175.
313. Yeste-Velasco M, et al. (2007) Glycogen synthase kinase-3 is involved in the regulation of the cell cycle in cerebellar granule cells. *Neuropharmacology* **53:** 295-307.
314. Diehl JA, Cheng M, Roussel MF, Sherr CJ. (1998) Glycogen synthase kinase-3beta regulates cyclin D1 proteolysis and subcellular localization. *Genes Dev* **12:** 3499-3511.
315. Faber AC, Chiles TC. (2007) Inhibition of cyclin-dependent kinase-2 induces apoptosis in human diffuse large B-cell lymphomas. *Cell Cycle* **6:** 2982-2989.

316. Schmid C, Steiner T, Froesch ER. (1983) Preferential enhancement of myoblast differentiation by insulin-like growth factors (IGF I and IGF II) in primary cultures of chicken embryonic cells. *FEBS letters* **161:** 117-121.
317. Kato S, Du K. (2007) TRB3 modulates C2C12 differentiation by interfering with Akt activation. *Biochem Biophys Res Commun* **353:** 933-938.
318. Adi S, Bin-Abbas B, Wu NY, Rosenthal SM. (2002) Early stimulation and late inhibition of extracellular signal-regulated kinase 1/2 phosphorylation by IGF-I: a potential mechanism mediating the switch in IGF-I action on skeletal muscle cell differentiation. *Endocrinology* **143:** 511-516.
319. Benito M, Valverde AM, Lorenzo M. (1996) IGF-I: a mitogen also involved in differentiation processes in mammalian cells. *Int J Biochem Cell Biol* **28:** 499-510.
320. Fujii N, et al. (2007) An antagonist of dishevelled protein-protein interaction suppresses beta-catenin-dependent tumor cell growth. *Cancer Res* **67:** 573-579.
321. Thorsen TS, et al. (2010) Identification of a small-molecule inhibitor of the PICK1 PDZ domain that inhibits hippocampal LTP and LTD. *Proc Natl Acad Sci U S A* **107:** 413-418.

Appendix A

Scramble control and knockdown plasmid backbone

Figure showing the control and knockdown plasmids backbone highlighting the various features as illustrated. The abbreviations are explained in the table below. (Note this image and the accompanying information is provided at the supplier's website: www.addgene.org)

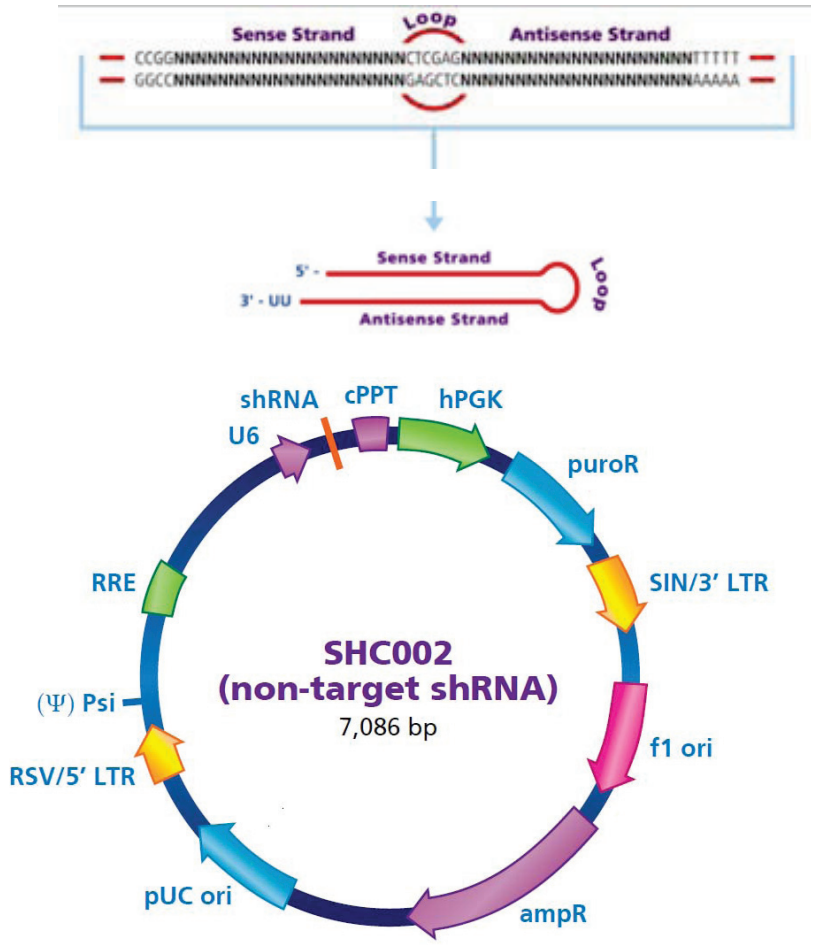

Table Appendix-1 TRC1 Vector Description and Features

Name	Description
cPPT	Central polypurine tract
hPGK	Human phosphoglycerate kinase eukaryotic promoter
puroR	Puromycin resistance gene for mammalian selection
SIN/3'LTR	3' self inactivating long terminal repeat
f1 ori	f1 origin of replication
ampR	Ampicillin resistance gene for bacterial selection
pUC ori	pUC origin of replication
RSV/5' LTR	5' long terminal repeat
(Ψ) Psi	RNA packaging signal
RRE	Rev response element
U6	promoter

Appendix B

Reprint Permission from Publishers or Authorized Copyright Holder

Portions of this dissertation have been published in peer - reviewed journals [(reference # 33 pertains to Chapter 3 in this dissertation and is published in the Journal SHOCK; DOI: 10.1097/SHK.0b013e3181ecb57c) and (reference # 294 pertains to Chapter 4 and is published in the Journal Molecular Medicine; DOI: 10.2119/molmed.2009.00168)] and material is used with permission of the copy right holder. Copyright license follows.

Wolters Kluwer Health

Lippincott Williams & Wilkins
351 W. Camden Street
Baltimore, MD 21201

410 528 4000 tel
www.LWW.com

DATE: 2/23/11

Abid A. Kazi
Cellular and Molecular Physiology, Mail Code H-166
Rm C4765, Hershey Medical Center
500 University Dr,
Hershey, PA 17033

Fee: $0.00

Re: ***SHOCK***
Spec Mat: SHK, 2011; 35(2):117-25
Non-Commercial Request / To use in a PhD thesis

CONDITIONS

Permission is granted for your requested use. Retain this copy for your records. This permission is subject to the following conditions:

1) A credit line will be prominently placed and included: for books – the author(s), title of book, editor, copyright holder, year of publication; for journals – the author(s), title of article, title of journal, volume number, issue number and inclusive pages.

2) The requestor warrants that the material shall not be used in any manner which may be considered derogatory to the title, content, or author(s) of the material or to Wolters Kluwer Health.

3) Permission is granted for one time use only as specified in your correspondence. Rights herein do not apply to future reproductions, editions, revisions, or other derivative works.

4) Permission granted is non-exclusive, and is valid throughout the world in the English language only.

5) Wolters Kluwer Health cannot supply the requestor with the original artwork or a "clean copy."

6) The requestor agrees to secure written permission from the author (for book material only).

7) Permission is valid if the borrowed material is original to a Wolters Kluwer Health imprint (Lippincott, Williams & Wilkins, Lippincott-Raven Publishers, Williams & Wilkins, Lea & Febiger, Harwal, Igaku-Shoin, Rapid Science, Little Brown and Company, Harper & Row Medical American Journal of Nursing Co, and Urban & Schwarzenberg – English Language).

Molecular Medicine

The Feinstein Institute for Medical Research
350 Community Drive
Manhasset, NY 11030 USA
Phone: 516.562.2114
Fax: 516.562.1022

January 24, 2011

Tobias A. Rupprecht
Department of Cellular and Molecular Physiology
Pennsylvania State University College of Medicine
Hershey, PA 17033

RE: Permission to reprint manuscript

Dear Dr. Kazi:

We are in receipt of your request to reprint the manuscript entitled "PRAS40 Regulates Protein Synthesis and Cell Cycle in C2C12 Myoblasts," published in *Molecular Medicine* 16: 359-371, for your PhD dissertation.

Permission is granted on the condition that you properly cite the article.

Sincerely,

Margot Puerta

Margot Puerta
Managing Editor, *Molecular Medicine*

VITA
Abid A. Kazi

CONTACT INFORMATION
Phone: (717) 531 - 5346
Email: aak3@psu.edu

EDUCATIONAL BACKGROUND

Doctor of Philosophy in Cellular and Molecular Physiology, Aug 2011
The Pennsylvania State University, University Park, PA
Dissertation: Role of PRAS40 and DEPTOR – two mTOR binding proteins in C2C12 myocytes
(Laboratory of Dr. Charles Lang, Ph.D.)

PEER-REVIEWED PUBLICATIONS (IN CHRONOLOGICAL ORDER)

Kazi AA, Hong-Brown LQ, Lang SM, Lang CH. *DEPTOR knockdown enhances mTOR activity and protein synthesis in myocytes and ameliorates disuse muscle atrophy*. **Mol Med. 2011** May 19. doi: 10.2119/molmed.2011.00070. PMID: 21607293.

Kazi AA, Pruznak AM, Frost RA, Lang CH. *Sepsis-Induced Alterations in Protein-Protein Interactions within mTOR Complex 1 in Skeletal Muscle*. **Shock 2011 Feb;35(2):117-25.** PMID: 20577146.

Kazi, AA and CH. Lang, *PRAS40 regulates protein synthesis and cell cycle in C2C12 myoblasts*. **Mol Med, 2010**. **16(9-10): p**. **359-71.** PMID: 20464060.

Hong-Brown LQ, Brown CR, **Kazi AA**, Huber DS, Pruznak AM, Lang CH. *Alcohol and PRAS40 knockdown decrease mTOR activity and protein synthesis via AMPK signaling and changes in mTORC1 interaction*. **J Cell Biochem**. **2010 Apr 15;109(6):1172-84.** PMID: 20127721.

Pruznak AM, **Kazi AA**, Frost RA, Vary TC, Lang CH. *Activation of AMP-activated protein kinase by 5-aminoimidazole-4-carboxamide-1-beta-D-ribonucleoside prevents leucine-stimulated protein synthesis in rat skeletal muscle*. **J Nutr**. **2008 Oct; 138 (10):1887-94.** PMID: 18806097.

AWARDS AND HONORS

2008 PA DOH/Tobacco Settlement Funds, Graduate Research Supplemental Award
2010 Mead Johnson Young Investigator Award for Outstanding Research, Experimental Biology 2010 Endocrinology and Metabolism Section of the American Physiology Society
2011 Nominated for the Alumni Association Dissertation Award, The Pennsylvania State University
2011 Young Investigator Award for Outstanding Research, Experimental Biology 2011 Endocrinology and Metabolism Section of the American Physiology Society